Studies of the scale-up of production and recovery of recombinant proteins formed as inclusion bodies

A thesis submitted to the University of London
for the degree of DOCTOR OF PHILOSOPHY
by

Kai JIN B.Sc. (Eng.)

January, 1992

Department of Chemical and Biochemical Engineering
University College London
Torrington Place
London WC1E 7JE

ProQuest LLC.
789 East Eisenhower Parkway
P.O. Box 1346
Ann Arbor, MI 48106 – 1346

ACKNOWLEDGEMENTS

I would like to thank my supervisor, Professor Peter Dunnill, for his patient, kind and invaluable supervision throughout the course of this study. Without his encouragement and advice, the production of this thesis would not have been possible.

I also wish to thank Professor Mike Hoare for giving me the benefit of his experience and knowledge, and Dr Owen Thomas for his initiating impetus and valuable ideas which helped me find the way forward.

Thanks are also due to Dave Allen, who helped me to get familiar with the research group in a short time; Dr David Salt, who helped me in the early stage of my project; Billy Doyle and Clive Orsborn for training and assisting me to operate pilot plant equipment; Ralf Tinnes for his kind help in my final experimental work and Drs John Ward and Andy Ison for their valuable criticism during the writing of this thesis.

Finally, I would like to offer my thanks to the British Council for its financial support and to Drs H. Field and G.T. Yarranton for providing materials.

To my grandparents

ABSTRACT

This is a study of the production of two recombinant proteins, prochymosin and a mini-antibody (formed as inclusion bodies) and the subsequent recovery of the former at pilot plant scale. Recombinant *E.coli* strains which contain temperature-sensitive multicopy plasmids carrying foreign genes have been employed in this study. The scale-up work involved fermentations, up to 100 litre in capacity, and recovery of expressed prochymosin inclusion bodies.

A number of different scales of fermentations (20L, 42L & 100L) were examined to determine the fermentation process suitable for large-scale production of recombinant prochymosin in *E.coli* HB101 pMG168. Fermentations at 20L scale were also performed for expression of recombinant mini-antibody in *E.coli* CAG629 pMG LF9. Fermentation media were defined to allow scale-up of production of recombinant prochymosin: a cheap nutrient source was evolved and antibiotic was removed, allowing low costs and facilitating safety while retaining plasmid stability. Thermal induction of cells at different stages during growth was examined. Expression of recombinant prochymosin was only achieved when cells were induced during the exponential growth phase. Furthermore, higher yields of prochymosin were obtained by inducing cells at later stages in the growth phase.

An industrial high pressure homogeniser was employed to examine the disruption of recombinant *E.coli* cells. Repeated homogenisation resulted in the reduction of cell debris size without significantly affecting inclusion body particle size, thus easing subsequent separation of the inclusion body fraction from cell debris by centrifugation.

The separation of prochymosin inclusion bodies from cell debris was studied in an industrial disc stack centrifuge. Deviations were found between real performance of an industrial disc centrifuge and theoretically predicted performance. A method has been developed to monitor disc centrifuge performance by turbidimetric ratio measurements at two wavelengths, and this method has potential application in developing an automatic controlling system for optimal recovery of inclusion bodies.

A variety of techniques for protein analysis have been applied to investigations on the productivity of expression of recombinant prochymosin from fermentations, on the disruption of recombinant cells in an industrial high pressure homogeniser and on the separation of prochymosin inclusion bodies from cell debris in an industrial disc stack centrifuge. These techniques include high performance liquid chromatography (HPLC), particle analysis and protein gel electrophoretic techniques. In addition, various gel elution methods for purification and direct quantitation of protein species, in addition to scanning densitometry, have been employed.

CONTENTS

LIST OF FIGURES

LIST OF TABLES

1. INTRODUCTION

1.1 The importance of recombinant DNA techniques

The advent of recombinant DNA techniques has contributed more strongly to the development of biotechnology than any other single development. This new technology allows the transfer and the expression of genes between species. One leading application of recombinant DNA techniques is the production of eukaryotic proteins in prokaryotic hosts. Heterologous expression is already leading to potential clinical and industrial uses by providing a new source of improved, previously scarce or unavailable products.

A number of recombinant proteins have been produced for therapeutic use. For instance, human insulin, obtained from genes cloned in *E. coli* (Crea *et al.*, 1978; Goeddell *et al.*, 1979a), meets the need of many diabetic patients; human growth hormone, also made by *E. coli* cells (Goeddel *et al.*, 1979b; Szoka *et al.*, 1986), is safer than that derived by extraction of human cadavers; alpha interferon, again synthesized in *E. coli* (Staehelin *et al.*, 1981), provides an abundant source in contrast to its low natural availability.

Some recombinant proteins have potential therapeutic advantages. Recombinant vaccines cannot cause the problem of infection which may be associated with attenuated viruses. The use of gene cloning in this field is based on the fact that the immune response may be stimulated not only by the whole viral particle, but also by the proteins present in the virus coat. Thus recombinant virus coat proteins produced in bacteria cells may be used as vaccines instead of attenuated virus (Valuenzuela *et al.*, 1985; Patzer *et al.*, 1986; Tartaglia *et al.*, 1988).

The ability of making recombinant antibodies in mammalian cell culture extends the usefulness of monoclonal antibodies originally derived by Köhler and Milstein (1975). Recombinant antibodies can be specially designed to give new effector functions or to be less immunogenic with regard to humans (reviewed by Williams, 1988). An example of the former is the production of antibodies with both antigen-binding specificity and enzyme activity (Neuberger *et al.*, 1984), while an example of the latter is the production of antibodies which have a variable region from a rodent source but a human constant region

(Morrison *et al.*, 1984). Recombinant antibodies can also be used as immunoreagents to image tumours. However, mammalian cell culture at large scale is expensive and labour intensive. The use of bacterial cells such as *E. coli* to produce antibodies provides a cheap way for large-scale production. Recently, there is a strong interest in producing miniantibodies (Ward *et al.*, 1989; Skerra and Plückthun, 1988; Field, 1988). Miniantibodies may provide an alternative to whole antibodies. They are smaller than whole antibodies and may be ideal for making immunotoxins because they penetrate tumours readily (Klausner, 1986). Antibody fragments have already been used for constructing of second generation ricin immunotoxins (Vitetta *et al.*, 1987). The production of miniantibodies and their potential applications will be further discussed in section 1.5.

In addition to the application of recombinant DNA technology in the pharmaceutical industry, other areas such as the food industry also could benefit from the ability to engineer microorganisms to produce valuable proteins. One example of this is the production of calf prochymosin. Prochymosin is the precursor of the milk-clotting enzyme, called chymosin. Chymosin is of commercial importance in cheese making. Because the supply of chymosin from the natural source, young calf stomach, is limited, one alternative is to use bacterial cells such as *E. coli* for prochymosin synthesis, from which chymosin may be derived. Chymosin made via recombinant prochymosin (produced in *E. coli* K12 strain) is the first food ingredient which has been approved by the FDA (Flamm, 1991). This will be discussed in details in section 1.6.

1.2 Particular features of fermentation with recombinant *E. coli*

1.2.1 Why *E. coli* has been chosen as host cell

A wide range of microbial hosts have been used for the production of recombinant proteins. These include primarily *Escherichia coli*, the yeast *Saccharomyces cerevisiae* and various strains of bacilli (Klotz, 1983).

E. coli is by far the most commonly used host strain for the expression of heterologous proteins, owing to its well-defined genetic structure and subsequent ease of genetic manipulation. There are also a variety of promoters available for construction of expression vectors (Zabriskie and Arcuri, 1986). They are either constitutive or regulated type. An example of constitutive promoters is the β-lactamase promoter (Bernard and Helinski, 1980). More commonly used promoters are regulated ones which include the *lac* promoter (Goeddel *et al.*, 1979b), the *trp* promoter (Goeddel *et al.*, 1980; Nugent *et al.*, 1983), the *tac* promoter (deBoer *et al.*, 1983) and the bacteriophage λ promoters: λP_L and λP_R (Murooka and Mitani, 1985).

From a fermentation process standpoint, there are also some advantages for choosing *E. coli* as host cell. Compared to yeast and bacilli cells, *E. coli* has a high specific growth rate, and high cell densities can be achieved. These properties combined with the high expression level of heterologous proteins in *E. coli* result in high fermenter productivities (Fieschko, 1989). The high specific growth rate may also reduce the degree of asepsis required in the fermenter operation and reduce the potential for contamination.

However, there are a number of problems associated with the production of proteins from foreign genes cloned in *E. coli*. For example, the recombinant proteins often form as inclusion bodies in many *E. coli* expression system (Schoner *et al.*, 1985) and the proteins in these inclusion body forms are frequently found non-biologically active (This will be further discussed in section 1.2.2); the post-translational modifications between eukaryotes and prokaryotes are different, in particular, many eukaryotic proteins undergo glycosylation, which may be essential for the correct functioning of the proteins, but this process does not occur in *E. coli*; rapid degradation of foreign proteins may occur because the bacterium

contains a group of proteolytic enzymes (Baker *et al.*, 1984); high expression of a cloned foreign gene has been found to affect cell viability (Wright *et al.*, 1986).

1.2.2 Protein overproduction in *E. coli*

With the ability of gene manipulation, it has been possible to get high expression of eukaryotic gene in prokaryotic cells. A characteristic of many *E. coli* systems with the over production of heterologous proteins intracellularly is the formation of highly refractile aggregates, known as inclusion bodies (Schoner *et al.*, 1985). The proteins in these inclusion bodies are frequently found in a non-biologically active form. In order to obtain an active product from these systems, a number of relatively complicated procedures including disruption of the cells, purification of the inclusion bodies, solubilisation and refolding of the product protein are required. This will be dealt with in section 1.4. The exact mechanism of inclusion body formation is still not clear, although Mitraki and King (1989) have suggested that most inclusion bodies are derived from intermediates in intracellular protein folding pathways, and not from the native or fully unfolded proteins. The process of aggregate formation is strongly dependent on environmental conditions such as temperature and pH value.

It might seem that the inclusion body formation of heterologous protein in *E. coli* systems is a major disadvantage. However, there are also several advantages with the inclusion body derived material. The protein in inclusion body seems to be more resistant to proteolysis during the fermentation process (Cheng *et al.*, 1981) although Goff and Goldberg (1985) have found that proteolytic attack on inclusion bodies does occur in some instances. The first stage of product recovery, involving a relatively simple step of cell disruption, yields a product that is much purer than would be obtained by using a non-inclusion body producing system (Thatcher, 1990). The processing volumes are also smaller. This will be discussed in details in section 1.4.2.

1.2.3 Stability of recombinant plasmids in the scale-up of a fermentation

One crucial problem which occurs with the scale-up of a fermentation using recombinant microorganisms is plasmid instability (Ryu and Siegel, 1986; Zabriskie and Arcuri, 1986).

There are two categories of plasmid instability: segregational instability and structural instability (Nugent *et al.*, 1983). Segregational instability is defined as the loss of the complete plasmid from the host cells. Structural instability is defined as a change in plasmid structure due to insertion, deletion or rearrangement of DNA, which can result in phenotypic loss of plasmid function.

There are several published reports dealing with plasmid stability at lab-scale fermentations. Some of these reports have stated that environmental conditions in fermentations influenced plasmid stability. For example, Jone and Melling (1984) found that the chosen nutrient limitation affected plasmid stability in chemostat studies of plasmid pBR322 in *E. coli.* Plasmid stability was relatively higher under glucose and magnesium limitation compared to phosphate limitation. Structural instability was observed by Godwin and Slater (1979) in a chemostat study of *E. coli* with a plasmid coding for ampicillin, streptomycin, sulfonamide and tetracycline resistance. Glucose limited growth led to the loss of tetracycline resistance only, whereas one or more antibiotic resistances lost by phosphorus limited growth. Specific growth rate also affects the stability of plasmids in terms of plasmid copy number. Seo and Bailey (1985) reported that the copy number of plasmid decreased with increasing specific growth rate for a recombinant *E. coli* HB101 strain in batch fermentations, thus resulting in reduced recombinant product level. Since the different growth rates in these batch experiments were achieved by employing different growth media, the change in plasmid copy number and recombinant product yield could be due to the change of growth rate or the result of nutrient effect or both.

In contrast to these investigations on the relationship between environmental fermentation conditions and the stability of plasmids, Caulcott *et al.* (1985) studied the reasons which result in the instability of plasmid. They concluded that the instability of plasmid was related to the expression level of recombinant product in their systems studied (see section 3.2.2.2). Therefore, the expression of recombinant protein should be repressed in the cell growth phase and derepressed during the production phase in order to avoid the loss of plasmids. This leads to the development of dual-origin plasmids with inducible promoters to maintain low plasmid copy number during the growth phase and to amplify copy number during the production phase (Yarranton *et al.*, 1984; Wright *et al.*, 1986).

The use of selective pressure (antibiotic for example) during cell growth can enhance the stability of plasmid. In some cases, the period of maintenance of antibiotic selection is short because of the attack from the antibiotic resistant gene product and this leads to the development of the low inoculum method (Pierce and Gutteridge, 1985). By using tiny inoculum, cells grow for a number of generations before exhausting antibiotic. Therefore, the takeover by plasmid-free cells can be delayed to such an extent that the cells may be harvested at high density after a period of foreign protein production. It has also been proved by Pierce Gutteridge (1985) that the low inoculum method is more effective than using high concentration of antibiotic, which is also expensive. However, the use of selective pressure (antibiotic) may not be feasible on a large scale because of high cost and safety problems. Furthermore, the use of antibiotic selection may not solve structural instability problem. The dual-origin plasmids mentioned earlier seem to provide a suitable system for large-scale fermentation process development (see section 1.7.1). However, research work need to be carried out to verify the stability of this type of dual-origin plasmids when not employing antibiotic selection (section 3.2.2.2).

It is also important to select a proper fermentation strategy for a recombinant system, which favour plasmid maintenance. This will be discussed in the next section (section 1.2.4).

1.2.4 Fermentation methods for recombinant *E.coli*

It is important to choose a proper fermentation strategy to achieve high productivity of recombinant products. The three fermentation methods that are most commonly used with microorganisms are batch, fed-batch and single-stage continuous.

The use of continuous fermentation has been industrially limited to the production of cell mass, *i.e.*, single cell protein for use as an animal feed or human food supplement and to the biological treatment of wastes, *e.g.*, in the activated sludge process (Fieschko, 1989). Continuous culture is not applied for recombinant strains so far although it is often used to investigate recombinant systems as discussed in the last section. The main reason is that continuous culture can open up the possibility of plasmid loss (Dwivedi *et al.*, 1982). This is because recombinant organisms generally tend to have lower growth rates than their plasmid-free forms. If the plasmid is lost from some of the cells, these cells will divide at

a much faster rate than the plasmid-bearing cells. In the case of continuous fermentation, the plasmid-free cells will quickly dominate the culture because of the continuous washing out of cells. Therefore, little or no product would be obtained. Continuous culture will not be chosen for use of recombinant strains until very stable plasmid/host systems have been developed.

A batch process is the simplest operation to run. It has been successfully used for the production of recombinant proteins (prochymosin) in *E. coli* by Marston *et al.* (1984) and Gardiner (1988) and this batch mode was chosen in this study. However, because the cells in a batch are always in a dynamic environment, these fermentations are arguably the least controlled and least predictable (Fieschko, 1989). In the case of batch fermentation of *E. coli*, unrestricted growth on excess glucose under aerobic conditions, causes the formation of acidic by-products, of which acetate is the most predominant (Holms, 1986). The production of acidic by-products, especially acetate, is a major factor in the limitation of high cell density growth (Allen *et al.*, 1987; Anderson *et al.*, 1984). Moreover, the accumulation of acetate during recombinant *E.coli* fermentations has been correlated with a reduced production of recombinant protein (Brown *et al.*, 1985).

Fed-batch fermentation may be the preferred strategy in growing recombinant microorganisms. During a fed-batch fermentation, one or more of the nutrients such as glucose are added incrementally to the fermenter. In this way, the formation of partially oxidized by-products such as acetate in the case of *E.coli*, may be avoided. Catabolic repression by glucose or other substrates also could be prevented. In addition, the specific growth rate may be controlled at a desired constant value. Regulation of the specific growth rate makes it possible to optimize the growth rate with respect to expression level and cell density. The fed-batch system also allows regulation of the rate at which the cells consume oxygen and evolve heat. This is of critical importance in fermentations with high cell density of recombinant microorganisms (Fieschko, 1989). Fieschko and Ritch (1986) used a fed-batch system (in a sixteen litre stirred fermenter) for the production of human alpha consensus interferon. Glucose feeding rates were adjusted periodically to give specific growth rates in the range 0.10 - 0.14h^{-1} to prevent acetate formation. The maximum feeding rate was restricted to the level at which no oxygen limitation occurred. The culture was induced by shifting the temperature to 42^{0}C when a cell density of 30 g/L was reached. A

final density of 65 g/L of *E. coli* and 5.5g/L of interferon were obtained without measurable quantities of acetate. Muth (1984) concluded from high-density fermentations for the production of human insulin fusion protein in *E. coli* that regulation of temperature or glucose feeding rates to avoid oxygen limitation was equally effective with respect to growth and yield of the insulin A chain.

1.3 Downstream processing of proteins

For large-scale production of recombinant products, a number of microbiological and process engineering criteria must be satisfied. In the last section (1.2), the microbiological aspect has been discussed, as well as fermentation process design. Downstream processing is another important area with respect to process engineering criteria. Its efficiency will have a great effect on the recovery of desired recombinant proteins.

The recovery of recombinant proteins has its own particular features, for example, products are formed as inclusion bodies in many cases. This will be discussed in the next section (1.4). However, a number of general downstream processing operations are applied to the recovery of both native and recombinant proteins. There are several reviews on protein recovery methods (Lambert and Meers, 1983; Becker *et al.*, 1983; Kula, 1985). Some basic unit operations involved in the recovery of native proteins are briefly reviewed here (a simplified general scheme of downstream processing is presented in Fig 1.3.1).

1.3.1 Cell separation

The separation of cells from fermentation broth is a solid-liquid separation process. Centrifugation is often employed for cell separation, which relies on the density difference between the solid and the liquid phase. Filtration, which does not depend on density difference, is an alternative unit operation for cell harvest. It is especially attractive when dealing with the fermentation broth in which the density difference between microorganism and broth is fairly small. Cross-flow membrane filtration has been used to harvest bacterial cells (Dostalek and Häggstrom, 1982; Nagata *et al.*, 1989). However, centrifugation is most favoured for recovery of bacterial cells at present.

1.3.1.1 Solids recovery by centrifugal separation

Four principal designs of centrifuge are used : the tubular, multichamber, scroll and disc stack centrifuges (Kula, 1985; Bell *et al.*, 1983). These four different designs are based on the bowl conformation and the means by which solids are removed. Figure 1.3.2 shows a classification scheme of these machines in terms of the way of solids discharge.

Figure 1.3.1 Process flowsheet for downstream processing of proteins

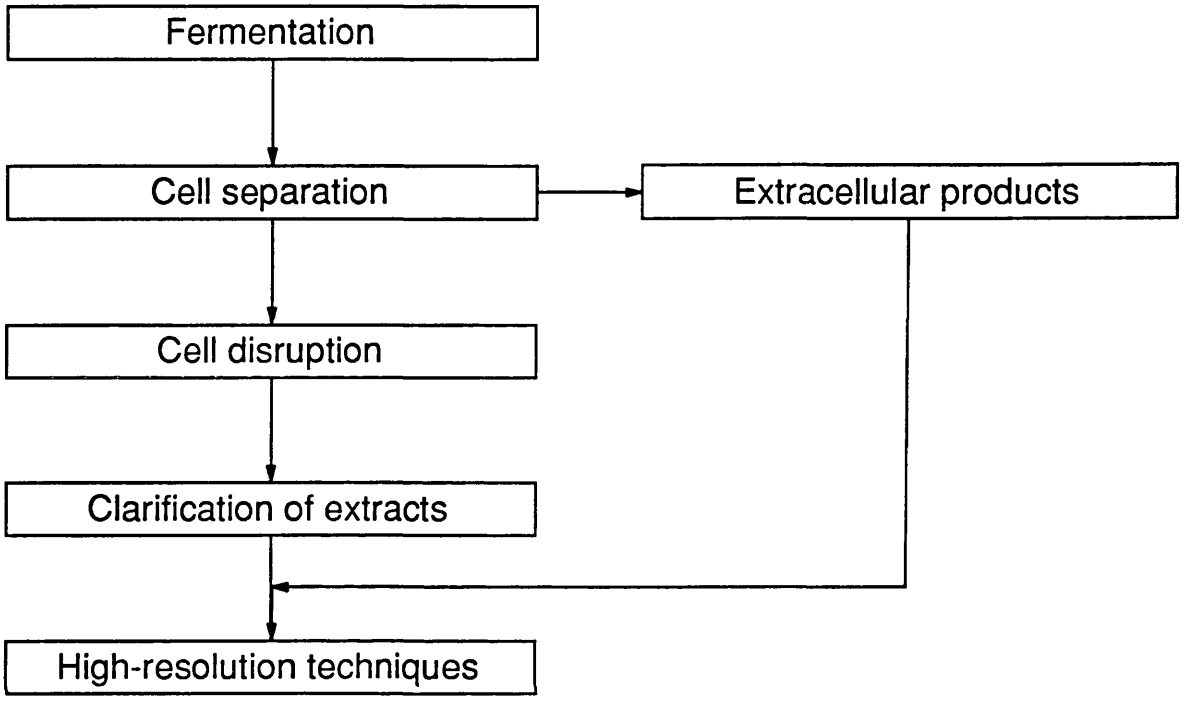

Figure 1.3.2 Classification of centrifugal separation equipments

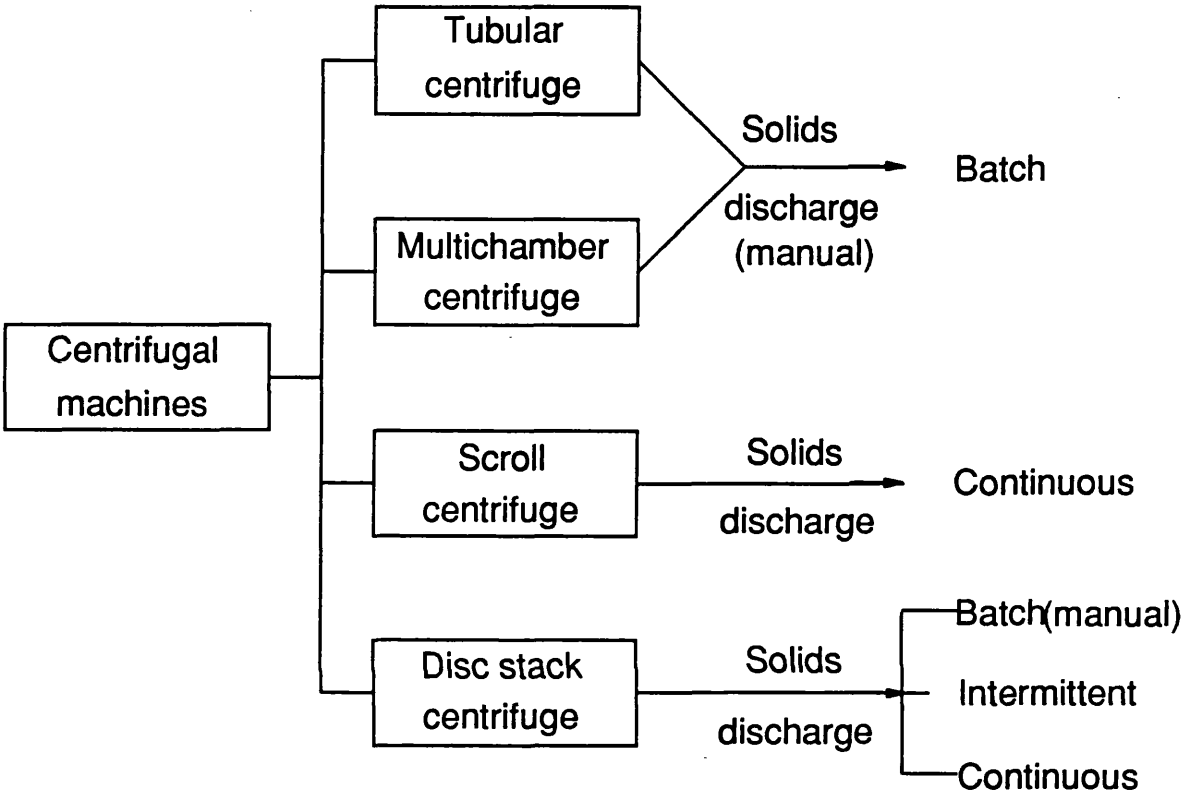

The tubular centrifuge has a relatively simple design and an excellent separation capability due to its high centrifugal force. Its down-time can be reduced by using a plastic liner which can be pulled out with solids after each run. Despite these advantages, a tubular centrifuge can only be operated in a batch mode and its application is limited to small volumes of process suspensions with low solid concentrations owing to its low solid collection capacity.

In a multichamber centrifuge, several concentric cylinders are installed within a bowl. Each chamber thus operates like a tubular centrifuge. So the equivalent clarifying surface is enlarged. The sequential flow through the chambers also increases the residence time within the centrifuge. A higher volumetric flow (up to 15000 l/h) is possible (Kula, 1985). In addition, since the centrifugal forces are increasing with radius, a certain classification of larger and smaller particles within the chambers is possible. However, like a tubular centrifuge, a multichamber centrifuge cannot be operated continuously. Furthermore, the down-time of a multichamber centrifuge is much greater, as it would have to be dismantled and each cylinder cleaned by scraping solids from the surface after each run.

The scroll centrifuge allows continuous solids discharge. Its centrifugal force is generally not as high as the other types of centrifuges. However, it can operate with feed suspensions containing up to 60% solids.

The disk stack centrifuge is a distinct type of centrifuges (Brunner and Molerus, 1979). A large number of conical, superimposed discs are installed within the bowl. The disc interspaces are as small as 0.3 mm. The liquid stream is divided into many thin layers in the disc stack and the settling path for solids is considerably shortened. There are three ways for solids discharge as follows:

(1) batch operation

Solids can be retained in the bowl and removed manually when the centrifuge is stopped and the bowl dismantled. This method is only practical in the case of low solids concentration in the feed. For feeds containing high solids concentration, the other two modes of solids discharge are widely used.

(2) intermittent discharge

A disc stack centrifuge with the mode of intermittent solids discharge is also termed a self-cleaning separator. In this solids discharge method, solids are ejected by

hydraulically opening ports in the periphery of the bowl while keeping full bowl speed and sustaining feed supply. The self-cleaning separator can deal with feeds containing a wet solids content up to 10% by volume. A feed with higher solids content needs frequent solids ejection, requiring continual bowl opening mechanism. This may lead to drive motor failure. In this case, a design with the mode of continuous solids discharge is required.

(3) continuous discharge

A nozzle disc stack separator discharges solids continuously through nozzles located at the outer diameter of the bowl. A feed with a wet solids concentration up to 20% by volume can be handled in this type of separator. However, attention should be paid to the design and operation to minimize the plugging and erosion of nozzles.

In the process of separation of cells from fermentation broth, tubular and multichamber centrifuges are normally used to meet the demand of high degree of dewatering. The application of disc stack centrifuges will be discussed in details in section 1.4.2.3.

1.3.1.2 Some theoretical aspects of centrifugal separation

If a spherical particle of diameter d and density of ρ_S is placed in a centrifugal field with an angular speed ω and liquid phase of density ρ_L and viscosity μ, it will accelerate in the r direction (normal to the gravity force) with a velocity of v_r at the centrifugal radius of r. According Newton's law of motion, the mass of the partial ($1/6\pi d^3\rho_S$) times acceleration at position r (dv_r/dt) is equal to the sum of the forces, in this centrifugal field, the centrifugal force acts on the sphere in the r direction, while the buoyant force and the drag force act in the opposite direction:

$(1/6\pi d^3\rho_S)(dv_r/dt)$ = F(centrifugal force) - F(buoyant force) - F(drag force) (1.3.1)

where F(centrifugal force) = $1/6\pi d^3\rho_S\omega^2 r$

F(buoyant force) = $1/6\pi d^3\rho_L\omega^2 r$

F(drag force) = $3\pi\mu dv_r$ according to Stokes' law

Within milliseconds, the acceleration (dv_r/dt) is practically zero, and equation (1.3.1) is thus written as:

$$\frac{1}{6}\pi d^3\rho_S\omega^2 r - \frac{1}{6}\pi d^3\rho_L\omega^2 r - 3\pi\mu dv_r = 0 \qquad (1.3.2)$$

rearrange equation (1.3.2), we get

$$v_r = \frac{d^2(\rho_S - \rho_L)\omega^2 r}{18\mu} \qquad (1.3.3)$$

The force of gravity is not appeared in equation (1.3.1) because its direction is normal to r direction. In practice, the centrifugal acceleration $\omega^2 r$ is usually many times larger than the acceleration of gravity g ($\omega^2 r$ = 600 - 600,000g).

It can be seen that equation (1.3.3) is a highly idealized one. Stokes' law is applied to describe the sedimentation process of a solid particle. Stokes' law assumes that solid particles are small, inert spheres in diluted dispersion and that laminar flow condition should be met with a Reynold number no more than 0.1 (i.e. $Re = v_r \rho_L d/\mu < 0.1$). Although these conditions are hardly met in practice, equation (1.3.3) is still the starting point to understand centrifugal sedimentation theoretically. The theory of centrifugal separation in an ideal disc stack centrifuge and the discussion of separation in a real disc stack centrifuge will be dealt with in details in section 1.4.2.3.1 and 1.4.2.3.2 respectively.

1.3.2 Cell disruption

The internal contents of a microbial cell is protected from the external environment by a complex wall and membrane structure. The cell wall has to be disintegrated or made permeable in order to isolate intracellular proteins. The methods available for cell disruption have been reviewed in several literatures (Coakley *et al.*, 1977; Engler, 1985; Chisti and Moo-Young, 1986). These methods can be divided into two categories: mechanical and non-mechanical methods.

Disruption methods for large-scale applications have been mainly concentrated on mechanical techniques, especially high speed bead milling and high pressure homogenisations, because non-mechanical methods are either hard to scale up or highly specific to one cell type and product. The use of high pressure homogenization is more common for cell disruption at large-scale than high speed bead milling (Scawen *et al.*, 1980).

Hetherington *et al.*(1971) presented a kinetic model for the disruption of yeast cells, which

gave a relationship between protein release and the number of passes (N) and the operating pressure:

$$\log\frac{R_m}{R_m-R} = KNP^a \qquad (1.3.4)$$

where R_m - the maximum soluble protein available for release

R - the soluble protein release

K - a dimensional disruption constant

a - a measure of cell-specific resistance to disruption

For bakers' yeast, 'a' was found to have a value of 2.9. Engler and Robinson (1979, 1981) also were able to correlate their results for the yeast *Candida utilis* using equation (1.3.4). In their results, the value of 'a' was 1.77. The disruption kinetics of *E. coli* cells (a constitutive mutant) for β-galactosidase and protein release have been examined (Gray *et al.*, 1972). It was found that both enzyme and protein release fitted this first order kinetics model with respect to the number of passes, 'a' was reported to be 2.2 for β-galactosidase release.

The disruption process described by equation (1.3.4) has been found to be independent of yeast cell concentration over the range of 100 - 600 gDW/L, and for a pressure range of 196 - 1180 barg (Hetherington *et al.*, 1979). Dunnill and Lilly (1975) examined the disruption of commercial bakers' yeast in a Manton-Gaulin homogenizer capable of operating at pressures up to 1180 barg. They found their results for pressures above 690 barg deviated from the dependency on operating pressure previously observed by Hetherington *et al.*(1971). This deviation was attributed to a non-optimal design of the homogenizing valve for higher operating pressure.

Keshavarz *et al.* (1990) recently studied the mechanism of disruption of Bakers' yeast in a high pressure homogenizer, and indicated that the main disruption mechanism was impingement, the rate of cell breakage being related to the stagnation pressure or maximum wall stress of the fluid jet. Decreased gap width and decreased impact distance both contribute to an increased cell disruption rate.

The objective of the homogenisation unit operation is to break cells and release intracellular protein products, while the size of cell debris has to be considered for the subsequent

clarification unit operation where larger particles are more desirable as they are easer to remove. Although homogenisation with multiple passes result in complete protein release, a reduction in cell debris size has been observed (Keshavarz, 1990; Olbrich, 1989). Keshavarz (1990) has studied the effect of valve geometry on the cell debris formation and stated that although it might be possible to reduce the number of passes by replacing the valve geometry while releasing the same quantity of soluble proteins, the particle size distribution did not shift towards larger sizes.

Little research work has applied the high pressure homogenization to the recombinant organisms. This will be discussed in section 1.4.2.2.

1.3.3 Clarification of crude extracts

The separation of insoluble fragments such as cell debris from soluble proteins after cell disruption is a very difficult task. In principle, solid-liquid separation techniques, *e.g.*, centrifugation, can be employed. However, the centrifugation operation is difficult to perform because of the fact that cell fragments are smaller than intact microorganisms, the range of particle sizes is much wider, the density difference is small between fragment and liquid, and the viscosity increases during homogenization. Therefore, during centrifugation the throughput has to be decreased considerably compared with cells, which results in a longer operating time. In consequence, separators with direct bowl cooling are required to prevent a pronounced temperature rise.

As mentioned in the last section, it is difficult to optimise homogenisation conditions such as choosing more efficient valve geometry, thus reducing the number of passes to give larger particle sizes. One of the solutions to enhance cell debris separation is to use selective flocculation. Polyethyleneimine (PEI), which is a cationic polymer, has been used as a flocculant of cell debris (Milburn *et al.*, 1990; Bentham, 1990). The extent of sedimentation achieved will be influenced by a number of factors: the flocculant itself, the flocculant concentration, cell concentration, dilution and pH value of cell suspension, and stirrer speed during flocculation.

1.3.4 High-resolution techniques

Chromatography is a high resolution technique and therefore preferred if proteins of high purity are required. Ion-exchange , affinity, and gel filtration chromatography have found many applications in protein purification. Recently, a growing number of research reports on purification of proteins have been in the area of high performance liquid chromatography (HPLC). HPLC is not a separate technique in itself, but rather a means for improving the speed and resolution of existing forms of chromatography (Kennedy *et al.*, 1989).

Howard and Martin (1950) first introduced reverse-phase high performance liquid chromatography (RP-HPLC). RP-HPLC is a rapid technique with a very high selectivity and has been used widely for the separation of polar molecules including peptides and proteins. The basic principle for the RP-HPLC system is the relative hydrophobicity of the stationary and mobile phase which determine the mobility of the solute molecule on the column. As the solute molecules interact with the stationary phase through hydrophobic interactions, for small molecules, these interactions are relatively simple, *i.e.*, their mobility increases with the increase of hydrophobicity in the mobile phase. There are two running modes for RP-HPLC, isocratic and gradient elution (Alm *et al.*, 1952). During isocratic elution the solute can be thought of as partitioning between the mobile phase and the stationary phase. The elution time will depend on the partition coefficient of the solute in the two phases (Meek, 1980), and separation will occur throughout the length of the column. During gradient elution, the loading condition for the solute is such that the stationary phase strongly adsorbs the solute, *i.e.*, the solute completely partitions in the stationary phase. Then, by increasing the hydrophobicity of the mobile phase, a point is reached at which the solute is desorbed from the stationary phase and passes to the mobile phase. If the hydrophobicity of the mobile phase continues to be raised, the solute will completely partition into the mobile phase. In gradient elution, separation is a function of the applied solvent gradient rather than of column length (Pearson *et al.*, 1982).

Proteins are complex molecules composed of large numbers of both hydrophobic and hydrophillic amino acids. Therefore, protein separation on RP-HPLC is more complex than for small molecules. For example, it was observed that small changes of the organic modifier concentration in the mobile phase dramatically affected adsorption of bovine serum albumin

to a reverse-phase support (Lewis *et al.*, 1980). Thus gradient elution of proteins is a preferred choice rather than the isocratic elution. Because of the fact that proteins are both hydrophobic and hydrophillic, they will interact with a reverse-phase support under conditions of both high and low hydrophobicity in mobile phase. Thus, as the hydrophobicity is developing in mobile phase, there will be a discrete point existing at which an adsorbed protein on support will be desorbed, but above and below that point desorption will not occur.

A number of problems exist with the RP-HPLC of proteins. These include: fouling of the column, poor peak shape, multiple peaks, low recoveries and the loss of biological activity. The main reason for such problems is the structural complexity of proteins and subsequent presence of multiple configurations of proteins during chromatography. Correct selection of stationary and mobile phase may overcome these problems. Protein structural change on binding to a reverse-phase support was observed by Katzenstein *et al.*(1986). Pearson *et al.*(1982) stated that the silica support was the determinant of resolution. In this case of a silica reverse phase support, proteins will interact with exposed silanol groups (SiOH), which are not 100% covered by silanizing reagents. In consequence, modification and irreversible binding of proteins could be caused leading to fouling of column and low recovery of proteins. The use of polymer based reverse phase materials may avoid this problem. Poor peak shape and multiple peaks can be caused by the conformational changes of proteins on reverse-phase supports (Cohen *et al.*, 1984; Bendek *et al.*, 1984) although they may also be caused by poor diffusional kinetics of proteins (Lewis *et al.*, 1980). Conformational changes of proteins may lead to loss of biological activity, agglomeration of proteins with subsequent fouling and low recovery, and lead to peak distortion and multiple peaks.

From the discussion above, it can be seen that in order to obtain good separation of proteins on RP-HPLC column, not only should the proper stationary and mobile phase be chosen, but the prevention of conformational changes of proteins should be considered as well. The deliberate denaturation of protein before loading on the reverse-phase column can sidestep the denaturing effect of the reverse-phase support and the problem of poor peak shape again caused by conformational changes of proteins can be solved. Cohen *et al.*(1985) provided an excellent example of this. They demonstrated that at 37^{0}C, when ribonuclease was fully denatured, it gave a narrow well-shaped peak while the peak deteriorated when the

temperature was decreased. However, the protein must be subsequently renatured and this may lead to substantial activity loss. This will be further discussed when dealing with processing of recombinant proteins formed as inclusion bodies in section 1.4.4.

1.4 Particular features of recovery of recombinant proteins

As mentioned at the beginning of the last section (1.3), the downstream processing of recombinant proteins is a crucial part of the production of the final product of interest. In many cases, the expression of the heterologous protein is in the form of insoluble protein aggregates known as inclusion bodies, which develop in the cytoplasm of microorganisms such as *E. coli*. Because of the particular characteristic of recombinant inclusion body proteins (see section 1.2.2), the recovery of recombinant proteins has to have extra steps adapted to the situation. In other words, the recovery process does not just involve the unit operations discussed in the last section (1.3) for soluble protein products, but involves extra steps such as solubilisation and renaturation for recovering active, soluble products from insoluble non-active forms (reviewed by Marston, 1986; Thatcher, 1990). It is advantageous that the inclusion bodies are separated from other bacterial cell constituents such as cell debris before solubilisation. As earlier discussed in section 1.2.2, the initial recovery of product in the form of inclusion bodies has many attractive process features. The inclusion body product, which is in dense granules of tight size distribution, may be recovered at high purities by cell disruption followed by centrifugation (Taylor *et al.*, 1986; Fish and Hoare, 1988; Hoare and Dunnill, 1989).

In contrast to Fig 1.3.1 for soluble protein recovery, the process scheme for inclusion body recovery is shown in Fig 1.4.1.

1.4.1 Cell separation

The unit operation for cell recovery discussed in section 1.3.1 basically applies here for the recovery of cells containing inclusion bodies. It has been reported that inclusion body producing cells have a greater buoyant density than natural cells (Cheng, 1983). In Cheng's study, *E. coli* cells producing the β-galactosidase protein or its nonsense promoter X90, had cell buoyant densities 1.11 - 1.13 g/l, while wild type cells had cell buoyant densities 1.08 - 1.09 g/l. This would enhance the centrifugal sedimentation of the recombinant cells (see equation 1.3.3 in section 1.3.1.2).

Figure 1.4.1 Process flowsheet for downstream processing of recombinant proteins formed as inclusion bodies

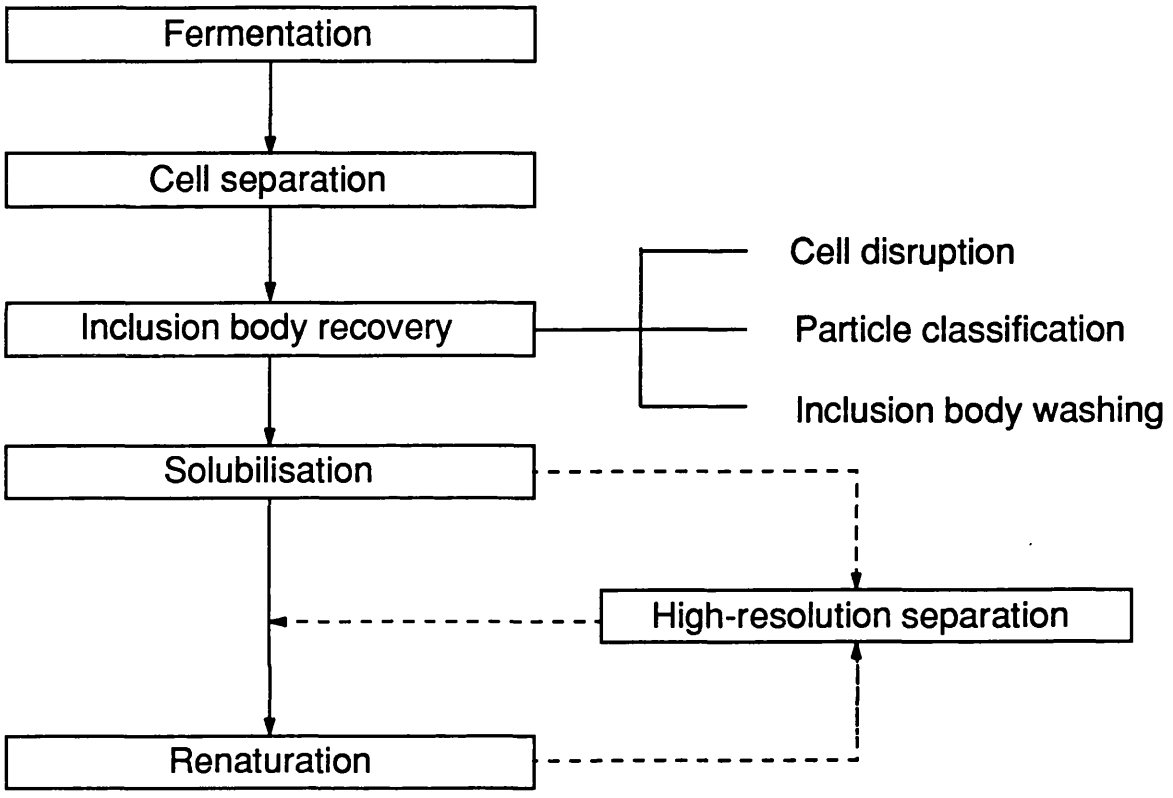

1.4.2 Inclusion body recovery

The unit operations involved in this stage include (Fish and Hoare, 1988):

(1) cell disruption

(2) particle classification

(3) inclusion body washing

All these operations are designed to give optimal cell disruption, hence ensure complete inclusion body release with significant size difference between inclusion bodies and cell debris and ease subsequent separation of inclusion bodies from cell debris. In order to achieve this purpose, the systematic analysis of particle size of both inclusion bodies and cell debris is desirable. This information is a prerequisite for optimizing both homogenization and subsequent centrifugation conditions. Therefore, it is necessary to briefly review methods of characterising biological particles before further discussion of these inclusion body recovery operations (a detailed review see Olbrich (1989)).

1.4.2.1 Characterisation of biological particles

1.4.2.1.1 Photon correlation spectroscopy (PCS)

Photon correlation spectroscopy (PCS) appeared as a method of particle analysis in 1970's. The basic principle of this technique is that a suspension of particles is illuminated by a coherent monochromatic light source (laser), a pattern of interference is obtained and is sent to a detector for analysis (Weiner, 1984). The main advantages of this method is that its speed of analysis is high and the instrumentation is sensitive for over the range from 0.003 μm to 3 μm, thus making it suitable for measurement of both cell debris and inclusion body particles. However, it suffers several disadvantages: the theory assumes rigid compact spherical particles which is rarely met practically; dust can cause noisy background.

1.4.2.1.2 Electrical sensing zone measurement (ESZ)

In contrast to PCS, the technique of electrical sensing zone measurement (ESZ) employs a different principle. This method is based on a change in resistance caused by a particle passing through an orifice because of a different electrical conductivity between the particle

and the electrolyte (Allen, 1981). The change in resistance is converted into a voltage change due to a constant current, and the voltage change which is picked up by a signal amplifier is proportional to the particle volume. The lower and upper size limit of particles is determined by the diameter of orifice. For example, a 18 μm orifice tube gives a measurable particle size range between 0.6 to 6 μm. While the ESZ method is well developed, there are still several potential error sources associated with the particle material, particle porosity and particle shape.

1.4.2.1.3 Centrifugal disc photosedimentation (CPS)

The theory of CPS method can be referred to section 1.3.1.2. The equation 1.3.3 which can describes the sedimentation process is repeated here for further discussion:

$$v_r = \frac{d^2(\rho_S - \rho_L)\omega^2 r}{18\mu} \qquad (1.3.3)$$

where v_r - sedimentation speed of the particle

ρ_S - density of the particle

d - diameter of the particle

ρ_L - density of the spin fluid

μ - viscosity of the spin fluid

ω - rotational speed of the disc

If we use dr/dt, where r is the radial position with respect to the centre of rotation of the disc, to replace v_r in equation 1.3.3 and integrate it from the initial radius of injected sample, R_o, at time t=0, to the radius of the detector, R_d, at time t, we get equation 1.4.1:

$$d = \sqrt{\frac{18\mu}{(\rho_S - \rho_L)\omega^2 t}\ln\left(\frac{R_d}{R_0}\right)} \qquad (1.4.1)$$

As discussed in section 1.3.1.2, this is the fundamental relationship between time of appearance at the detector and particle size because Stokes' law is applied. Therefore, all the limitations of Stokes' law are applicable, i.e. the solid particles are small, inert spheres in diluted dispersion and laminar flow condition should be met with a Reynold number no more than 0.1 (i.e. $Re = v_r\rho_L d/\mu < 0.1$). For non-spherical particles an equivalent Stokes diameter can be calculated from the appearance time. Although centrifugal analysis is convenient for sizes up to about 10 μm, from equation 1.4.1, this limit can be extended by selecting a more viscous spin fluid and so as to match the particles' density more closely, and a slower rotational speed can also be used. However, the minimum size is limited by diffusion.

There are several techniques available for carrying out the centrifugal disc photosedimentation (CPS) method. In the line-start method, a sample is simply layered onto the spin fluid. The serious problem in this method is the occurrence of unstable sedimentation (Scarlett *et al.*, 1967). A gradient spin fluid is applied to solve this problem. There are three ways to form the gradient: the buffered line-start (BLS) and two external gradient techniques (EG).

The BLS technique consists of injecting a small volume of liquid, called spin fluid buffer, with a lighter density and lower viscosity onto the spin fluid while the disc is rotating. Then the rotation is changed, either decelerated or accelerated briefly (Scarlett *et al.*, 1967). This causes the two liquids to mix partially and form the gradient. The older of the two external gradient techniques (Coll and Searles, 1986) requires two cylinders of liquid, a precise pump and patience. This method has been extensively used by Olbrich (1989). In a new and simpler external gradient technique, the gradient is formed by sucking in spin fluid and spin fluid buffer to a syringe and injecting them into the spinning disc before they are completely mixed (see section 2.6.5.2).

The above discussion listed the common methods which are used for characterising biological particles. However, before Olbrich (1989) carried out systematic work to characterize inclusion body and cell debris particles, very little work had been carried out on sizing inclusion bodies and cell debris. Paul *et al.* (1983) and Kawaguchi *et al.* (1984) gave a value of 1 μm for proinsulin inclusion bodies and a value of 0.5 μm for prochymosin

inclusion bodies by using transmission electron microscopy, respectively. However, theseresults were not statistically meaningful due to the small sample size. Taylor *et al.* (1986) examined the physical properties of frozen prochymosin and γ-interferon inclusion bodies. They obtained a mean value of 0.81μm for the γ-interferon inclusion bodies and 1.28 μm for the prochymosin inclusion bodies by using a combination of centrifugal disc photosedimentation (CPS) and electrical sensing zone measurement (ESZ). But no examination of size distribution of cell debris was made. Olbrich (1989) systematically examined the characteristics of both the inclusion bodies and cell debris of calf-prochymosin producing *E. coli* cells (HB101 pCT70) and cell debris of the relevant host cells (*E. coli* HB101). The results of his study, which will be discussed in details in subsequent sections, led to a greater understanding of the inclusion body recovery unit operation. Olbrich (1989) also predicted the theoretical sedimentation of inclusion bodies and cell debris in an industrial disc stack centrifuge by using the results from particle sizing, which will be discussed in section 1.4.2.3.

1.4.2.2 Cell disruption

It was noted in section 1.3.2 that mechanical methods are generally more suitable for large-scale disruption of cells than non-mechanical methods. Most previous studies of cell disruption employed the high pressure homogenization method, and were mainly concerned with various non-recombinant microorganisms for soluble protein products. When this unit operation of cell disruption is applied to recombinant cells containing foreign proteins formed as inclusion bodies, it becomes even more complex than for non-recombinant cells. For a non-recombinant system, which contains intracellular soluble protein products, the objective of the homogenisation unit operation is to break the cells and release the proteins into solution. A subsequent centrifugation must be able to remove the insoluble contaminants such as cell debris. This demands minimal micronisation of the debris. For a recombinant system, which contains insoluble products in the form of inclusion bodies, the objective of cell disruption is to ensure a sufficient size difference between the cell debris and inclusion bodies, and to allow subsequent separation of inclusion bodies from cell debris efficiently.

Therefore, in the first unit operation for inclusion body recovery, *i.e.* cell disruption using homogenisation, the study of the effect of repeated homogenisation on size reduction in cell

debris and inclusion body particles is important. There have been no published detailed studies apart from Olbrich's (1989) work. Even homogenisation studies employing recombinant strains are very rare so far (discussed in section 4.3).

Olbrich (1989) studied the effect of repeated homogenisation on recombinant *E. coli* HB101 pCT70 and host *E. coli* HB101 with the particle sizing techniques discussed in section 1.4.2.1. For example, he did a batch fermentation at 42L scale and carried out repeated homogenisation (550 barg) of 1, 3 and 5 passes for the cells without intermediate cell freezing. He used post-homogenisation purification conditions of 2000xg (RCF) for 26 minutes in a lab-centrifuge for samples from 1,3 and 5 passes and characterised the inclusion bodies obtained and also the cell debris. The relevant results are summarised in Table 1.4.1.

It can be seen from the value of D_{50} (see note of Table 1.4.1) that the size of the cell debris is significantly reduced after repeated homogenisation of 1, 3 and 5 passes while there is no measurable breakage of inclusion bodies.

Table 1.4.1 Inclusion body and cell debris size distribution from 1/3/5 passes (adapted from Olbrich (1989))

Homogenisation passes	Inclusion bodies		Cell debris	
	D_{50}(μm)*	Size range	D_{50}(μm)*	Size range
1	-	-	0.43±0.02	0.22-0.80
3	0.85	0.50-1.30	0.37±0.02	0.21-0.70
5	0.84	0.50-1.30	0.28±0.02	0.21-0.70

*D_{50}: value of particle size at which 50% of the population is greater than that diameter.

In order to check whether further homogenisation, i.e. above 5 passes, would break down the inclusion bodies and cell debris, Olbrich (1989) did another batch fermentation at 20L scale, applied the same homogenisation conditions to the cells obtained and used the same conditions of post-homogenisation purification, i.e. 2000xg (RCF) for 26 min. in a lab-

centrifuge, to obtain inclusion bodies and cell debris from homogenate of 5 and 7 passes. The key results are shown in Table 1.4.2.

Table 1.4.2 Inclusion body and cell debris size distribution from 5/7 passes (adapted from Olbrich (1989))

Homogenisation passes	Inclusion bodies		Cell debris	
	D_{50}(μm)*	Size range	D_{50}(μm)*	Size range
5	0.79	0.50-1.16	0.29±0.02	0.20-0.70
7	0.77	0.46-1.21	0.29±0.02	0.20-0.70

*D_{50}: value of particle size at which 50% of the population is greater than that diameter

The results show that there is no further reduction to the size of cell debris in terms of D_{50}, but inclusion body breakage occurs to some extent above 5 passes.

From these results and the measurement of protein release (results not shown here), Olbrich (1989) concluded that although cell breakage was completed at 3 discrete passes (550 barg) for recombinant *E. coli* HB101 pCT70, the homogenate benefited from 5 discrete passes to effect greater cell debris particle size reduction.

A comparison of recombinant *E. coli* HB101 pCT70 cell debris and its relevant host *E. coli* HB101 cell debris was performed by Olbrich (1989) under the same homogenisation conditions (550 barg, 5 passes). He applied post-homogenisation purification conditions [4000xg (RCF) for 33 min. in a lab-centrifuge] to recombinant homogenate to obtain cell debris. For host homogenate, he did not apply this process. The particle size of these two cell debris is shown in Table 1.4.3.

It is easy to see the difference between these two types of cells from the value of D_{50}, *i.e.* recombinant cell debris shows smaller size compared with host cell debris. This difference could indicate that recombinant cell wall is weaker because of differences between recombinant and wild type cells. However, this difference could be caused by other reasons. For example, because the recombinant homogenate was processed via a post-homogenisation

purification step, the large cell debris could be sedimented with inclusion bodies. The results in Table 1.4.3 suggest that this was not the case because there is a "gap" between the size range of recombinant cell debris and that of inclusion bodies.

Table 1.4.3 Comparison of recombinant cell debris and its relevant host cell debris (adapted from Olbrich (1989))

Cell type	Cell debris		Inclusion bodies	
	D_{50}(μm)*	Size range	D_{50}(μm)*	Size range
Recombinant	0.21±0.02	0.18-0.32	0.82	0.40-1.30
Host	0.25±0.01	0.10-0.60	-	-

*D_{50}: value of particle size at which 50% of the population is greater than that diameter

Nevertheless, results from Table 1.4.1 and Table 1.4.2 show that there is no size "gap" between inclusion bodies and cell debris, and that indeed "overlap" in size distribution appears. Furthermore, the existence of the "gap" of size distribution of inclusion bodies and that of cell debris in Table 1.4.3 could be due to analytical problems. As stated by Olbrich (1989), "owing to the relatively large particle sizes of inclusion bodies compared to the cell debris, the inclusion body samples for CPS sedimentation (see section 1.4.2.1.3) had to be diluted to such an extent in order to ensure stable CPS sedimentation, that significant cell debris detection within these inclusion body samples was not possible with the CPS."

Olbrich (1989) also managed to measure the densities of inclusion bodies and cell debris with a combination of CPS, ESZ and PCS techniques. The results which are summarised in Table 1.4.4 show inclusion bodies are slightly more dense than cell debris.

From Olbrich's (1989) results, it is difficult to be certain that recombinant cells (*E. coli* HB101 pCT70) are easier to break compared with the relevant host cells although this is the conclusion drawn. Confirmation requires protein release assay of both recombinant and host homogenate for the same homogenisation conditions, and this will be further discussed in section 4.3.

Table 1.4.4 Apparent densities for *E. coli* HB101 pCT70 cell debris and inclusion bodies from different runs (adapted from Olbrich (1989))

Run No.	Cell debris ρ (Kg/m^3)	Inclusion bodies ρ (Kg/m^3)
1	1061 ± 32	1141 ± 3.5
2	1061 ± 32	1160 ± 3.5
3	1068 ± 20	1152 ± 3.5
4	1068 ± 20	1154 ± 3.5
5	1085 ± 14	1177 ± 3.0

The positive aspects of the recombinant cell disruption have been mentioned above, *i.e.*, the inclusion bodies are relatively stable for repeated homogenisation up to 5 passes, and recombinant cells are readily disrupted according to Olbrich (1989). The fact that inclusion bodies have larger sizes and are more dense provides the possibility of separating them from cell debris to some extent in a subsequent centrifugation process at large scale (Hoare and Dunnill, 1989; Thatcher *et al.*, 1990). However, this cannot be taken to be general until further comparative studies are made.

There has been no published work about the application of flocculation techniques to the homogenisation of recombinant cells, although there are quite a few successful applications of flocculation to non-recombinant systems (see section 1.3.3). Future work is needed in applying flocculation to recombinant system. For instance, it is interesting to find out whether inclusion bodies could be flocculated to ease subsequent particle classification.

1.4.2.3 Particle classification

Particle classification is the next unit operation for inclusion body recovery. As mentioned in the last section (1.4.2.2), the homogenisation of recombinant cells (*E. coli* HB101 pCT70) results in some attractive features for subsequent separation of inclusion bodies from cell debris by employing centrifugation.

Various methods have been quoted for employing centrifugation at the stage of particle classification, but no systematic studies have been carried out. Builder (1986) used a low speed centrifugation (1000 *g*) for a time range from 10 minutes to 1 hour (depending on process volume), which was sufficient to pellet the inclusion body material and to leave the cell debris in the supernatant. Marston *et al.* (1984), Schoemaker *et al.* (1985) and Lowe *et al.* (1984) reported that a 12000 *g* centrifugation for 5 minutes was sufficient for the separation of prochymosin inclusion bodies. Gribskov and Burgess (1983) used 8000 *g* for 30 minutes to isolate the sigma sub-unit of RNA polymerase. Olbrich (1989) determined the centrifugal conditions of 2000 *g* for 26 minutes, which were sufficient to separate calf-prochymosin inclusion bodies from cell debris where the homogenate was obtained after 5 discrete passes at 550 barg.

To recover inclusion bodies from cell debris on a large scale requires operation of industrial disc stack centrifuges (Hoare and Dunnill, 1989). However, the difference of size distribution of inclusion bodies and cell debris overlaps. This will make it difficult to achieve high purity of inclusion bodies free from cell debris while retaining high recovery rate in a single stage of centrifugation. Olbrich (1989) predicted theoretically the recovery of inclusion bodies from cell debris and this will be further discussed in section 1.4.2.3.3. The prediction was based on the data obtained from particle analysis of cell debris and inclusion bodies for *E. coli* HB101 pCT70. One problem about this prediction is that the data used to build this model might not be correct because of the way by which the samples of cell debris and inclusion bodies were obtained. Olbrich (1989) obtained the cell debris and inclusion bodies by applying a centrifugal condition of 2000xg for 26 minutes to the homogenate, and took the supernatant as the cell debris sample and the pellet as inclusion body sample. The problem about this method is that some cell debris may co-sediment with inclusion bodies and some inclusion bodies may still remain in the supernatant. Gel electrophoretic analysis of the material is needed. The theoretical disc-stack separation model also needs to be experimentally checked in future studies.

Little experimental work has been done so far to study the process of particle classification by employing industrial disc stack centrifuges for inclusion body recovery. Recently, Thomas *et al.* (1991) used an Alfa-Laval BTPX-205 continuous discharge disc stack centrifuge to develop particle size analysis method (CPS) for process control. They employed cell

homogenate from recombinant *E. coli* which produced porcine somatotropin (pST) inclusion bodies and they monitored inclusion body recovery in the disc centrifuge. Because their study was only concerned with developing assay method, no work was carried out to study the centrifugal conditions for optimal recovery of inclusion bodies. Their work will be discussed again in section 4.4.2.

In order to study the performance of an industrial disc stack centrifuge for inclusion body recovery, the basic theory of separation in an ideal disc stack centrifuge is worth reviewing.

1.4.2.3.1 Theory of centrifugal separation in an ideal disc stack centrifuge

In section 1.3.1.2, the basic theory has been described. The derived fundamental equation, 1.3.3, is repeated here because it will be used for the description of sedimentation of particles in an ideal disc stack centrifuge.

$$v_r = \frac{d^2(\rho_S - \rho_L)\omega^2 r}{18\mu} \qquad (1.3.3)$$

where v_r - sedimentation speed of the particle

ρ_S - density of the particle

d - diameter of the particle

ρ_L - density of the spin fluid

μ - viscosity of the spin fluid

ω - rotational speed in the centrifugal field

As discussed in section 1.3.1.2, the derivation of this fundamental relationship applies Stokes' law. Further assumptions must be made for separation in an ideal disc stack centrifuge. They include:

(1) the feed is assumed to be divided evenly between all disc spaces

(2) particles are evenly distributed in the feed and particle separation is irreversible, i.e. separated particles do not re-enter the liquid phase

(3) the feed is directed in a radial plane, and parallel to the disc surface without tangential flow, i.e. the feed has the same angular velocity as the discs

Under these assumptions, supposing a feed with a flow rate of Q enter a disc stack centrifuge with the number of discs, z, the flow in each disc space, q, is thus equal to Q/z. A spherical particle is supposed to have a critical diameter of d_c which means this particle will just be separated from the feed when starting at the upper surface of the lower of the two discs at the outer disc radius R_a and reaching the settling wall which is the lower surface of the upper of the two discs at the inner disc radius R_0 before the feed leaves the disc space (see Figure 1.4.2). The particle's trajectory is the results of three partial velocities, namely the radial settling velocity v_r, the particle velocity v_p and the gravity settling velocity which can be neglected (not shown in Fig 1.4.2) compared with the other two velocities.

The radial setting velocity v_r can be expressed as

$$v_r = \frac{dh}{dt\ \cos\theta} \qquad (1.4.2)$$

where h is the gap width between two discs, θ is the disc angle as defined in Fig. 1.4.2. The particle velocity v_p is parallel to the disc surface, and can be expressed as

$$v_p = \frac{dr}{dt\ \sin\theta} \qquad (1.4.3)$$

Solving equation 1.4.2 and 1.4.3 for dt, we get

$$\frac{v_r}{v_p} = \frac{dh}{dr}\tan\theta \qquad (1.4.4)$$

The particle velocity v_p is approximately equal to the velocity of the feed v(h), i.e. $v_p \approx v(h)$. Replacing v_p in equation 1.4.4 with v(h) and rearrange it, we get

$$v(h)dh = \frac{1}{tg\theta}v_r dr \qquad (1.4.5)$$

Figure 1.4.2 Flow through the disc space of an ideal disc centrifuge

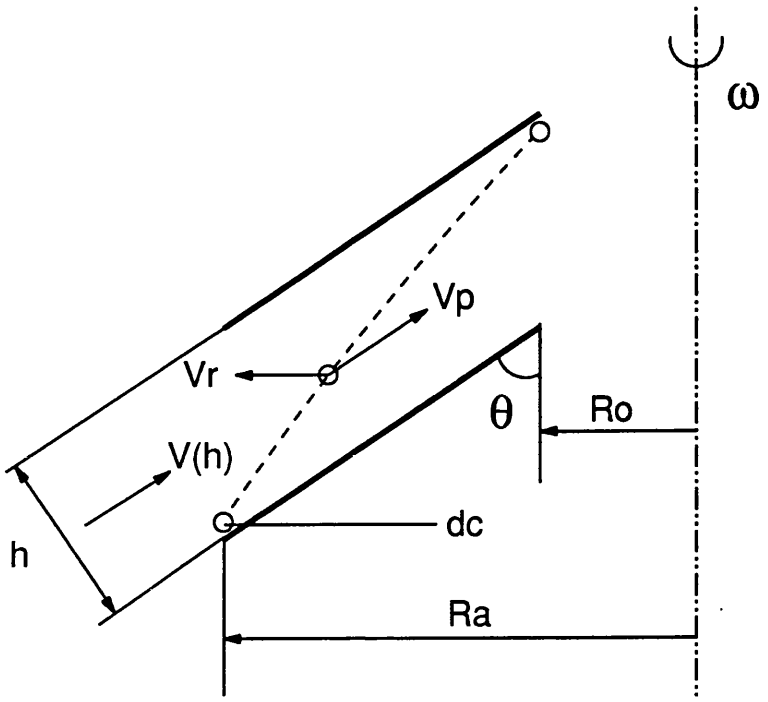

Because the particle has the critical diameter as defined before, we integrate equation 1.4.5 on both sides, the left side is from 0 to h, the right side is from inner radius R_0 to outer radius R_a correspondently.

$$\int_0^h v(h)dh = \int_{R_0}^{R_a} \frac{1}{tg\theta} v_r dr \qquad (1.4.6)$$

Equation 1.4.6 can be modified as equation 1.4.7, by adding "2πr" on both sides.

$$\int_0^h 2\pi r\, v(h)dh = \int_{R_0}^{R_a} \frac{2\pi r}{tg\theta} v_r dr \qquad (1.4.7)$$

The velocity of feed v(h) is given by:

$$v(h) = \frac{1}{2\pi r}\frac{dq}{dh} \qquad (1.4.8)$$

where q is the flow in each disc space, i.e. q = Q/z.
Equation 1.4.8 can be integrated as

$$q = \int_0^h 2\pi r\, v(h)dh \qquad (1.4.9)$$

Replacing equation 1.4.7 with equation 1.4.9, we obtain

$$q = \int_{R_0}^{R_a} \frac{2\pi r}{tg\theta} v_r dr \qquad (1.4.10)$$

Now we use equation 1.3.3 to replace v_r in equation 1.4.10. The particle we discussed so far is the particle with the critical diameter d_c. Integrating equation 1.4.10 gives

$$q = \frac{d_c^2(\rho_S - \rho_L)g}{18\mu}\frac{2\pi\omega^2}{3gtan\theta}(R_a^3 - R_0^3) \qquad (1.4.11)$$

Replacing q with Q/z in equation 1.4.11, gives

$$Q = \frac{d_c^2(\rho_S-\rho_L)g}{18\mu}\frac{2\pi\omega^2 z}{3g\tan\theta}(R_a^3-R_0^3) \qquad (1.4.12)$$

Equation 1.4.12 can be written as

$$Q = \frac{d_c^2(\rho_S-\rho_L)g}{18\mu}A_e \qquad (1.4.13)$$

where

$$A_e = \frac{2\pi\omega^2 z}{3g\tan\theta}(R_a^3-R_0^3) \qquad (1.4.14)$$

A_e is called equivalent separation area, which has the dimension of a length squared and corresponds to the area of a gravity setting tank capable of the same separation performance. From equation 1.4.13, we obtain

$$d_c = \sqrt{\frac{18\mu Q}{(\rho_S-\rho_L)A_e\, g}} \qquad (1.4.15)$$

Particles which have a diameter $d \geq d_c$ will be recovered in this ideal disc centrifuge. Some particles with a smaller diameter than d_c may also be recovered. This is because not all the particles in a single disc space start from the upper surface of the lower of the two discs. Instead, some of them may start from somewhere between the two discs. In this situation, even some of them which are smaller than d_c may still be recovered.

The grade efficiency, T, is used to describe the probability of a particle with smaller diameter than d_c being recovered from feed. In an ideal disc centrifuge, T is given by:

$$T = \left(\frac{d}{d_c}\right)^2 \qquad for \quad d<d_c$$
$$T = 1 \qquad for \quad d \geq d_c \qquad (1.4.16)$$

Spacer ribs are often used to separate the discs from each other. Therefore, a correction factor, f_L, is introduced to account for the small reduction of separation area. The equivalent separation area is then given by:

$$A_e = \frac{2\pi\omega^2 z}{3g\tan\theta}\left(R_a^3 - R_0^3\right) f_L \qquad (1.4.17)$$

where

$$f_L = 1 - \frac{3 z_L b_L}{4\pi R_a} \frac{1-(R_0/R_a)^2}{1-(R_0/R_a)^3} \qquad (1.4.18)$$

where z_L is the number of spacer ribs on a single disc and b_L is the width of spacer ribs. If point spacer are used, then $f_L = 1$.

1.4.2.3.2 Separation in a real disc stack centrifuge

Prediction of the separation performance of a real disc stack centrifuge based on the equations introduced in the last section often results in deviation from observation. The reason for the deviation is the highly idealised assumptions made for an ideal centrifuge. In practice, there are at least three aspects which do not follow the assumptions and thus result in reduced separation efficiency in a real disc centrifuge (see Fig. 1.4.3). They are:

(1) the feed in the disc space is not necessarily in a laminar flow pattern.

(2) particle sedimentation is reversible, i.e. particles which have already settled on the underside of the disc may be remixed into the feed.

(3) solids are not evenly distributed at the entrance to the discs and neither is the feed loading in each disc space.

Figure 1.4.3 Grade efficiency, T, of an ideal and real disc stack separator

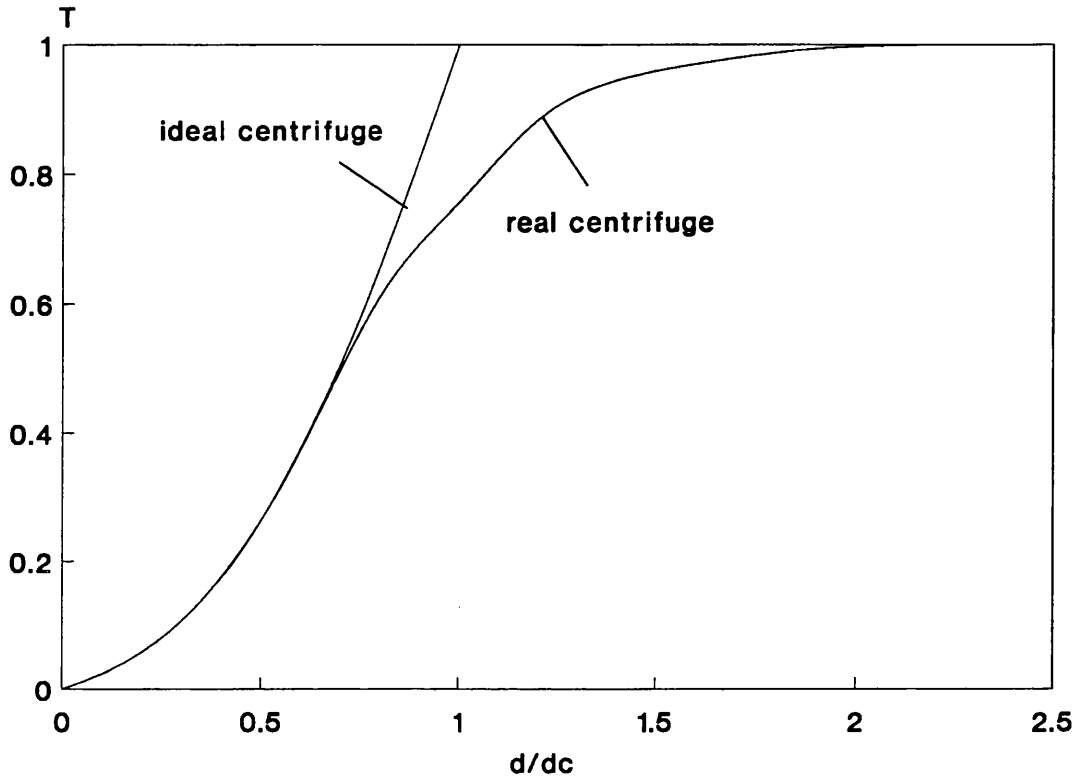

Investigation of separation efficiency of disc centrifuges has been performed. The existence of large vortices in the flow was established by photography by Willus and Fitch (1973). Coarse particles are remixed by vortexing resulting in a reduced separation efficiency. Brunner and Molerus (1979) reported that long radial spacer rids proved beneficial as they suppressed fluid flow in the circumferential direction and hence vortex formation. Point spacers were found unsuitable because of the premature transition from laminar to turbulent flow in the disc spaces. In advanced centrifuges, the discs have feed channels. By using the distribution holes, the sliding solids are able to bypass the incoming suspension thus the degree of back-mixing of sliding solids can be limited. In contrast, feeding suspension from the periphery into the disc spaces gives rise to crossflow between the sliding solids and the fresh feed. Skvortsov (1984) examined the influence of the sediment holding space on the separation efficiency. He showed that there is a non-uniform distribution of solids particles entering the disc stack because coarse particles may already settle down in the outer disc space.

Sokolov and Dolzhanova (1972) reported that the separation performance of a disc stack centrifuge is a function of the angular velocity of the form ω^{2k}, where k = 0.6 - 0.9. Based on this result, Zastrow (1976) used equation 1.4.19 as an expression for the sedimentation velocity of a particle in a centrifugal field

$$v_r = v_g\left(\frac{r\omega^2}{g}\right)^k \qquad (1.4.19)$$

instead of equation 1.4.20 applied in an ideal centrifuge

$$v_r = v_g\left(\frac{r\omega^2}{g}\right) \qquad (1.4.20)$$

where v_g is the gravitational sedimentation velocity.

The corresponding equivalent separation area in equation 1.4.14 can be modified as:

$$A_e = \frac{2\pi z}{(2+k)\tan\theta}\left(\frac{\omega^2}{g}\right)^k \left(Ra^{2+k} - R_0^{2+k}\right) \qquad (1.4.21)$$

When k = 1, equation 1.4.14 and 1.4.21 coincide. Good agreement between theoretical and experimental results was obtained for the separation of a polyvinylacetate/water suspension if k = 0.71 is used in equation 1.4.21.

Mannweiler (1989) developed a two-parameter model equation to describe the grade efficiency curve of an industrial disc stack centrifuge by using a non-linear curve-fitting algorithm. This model was used by Olbrich (1989) to predict the separation of inclusion bodies from cell debris for *E. coli* HB101 pCT70 in an industrial disc stack centrifuge. This will be further discussed in the next section 1.4.2.3.3.

1.4.2.3.3 Theoretical prediction for separation of inclusion bodies from cell debris in an industrial disc stack centrifuge

The performance of a centrifuge is affected by a number of factors which can be divided into two categories, i.e. the machine parameters and the features of the feed, as can be seen in the equations given in section 1.4.2.3.1 and 1.4.2.3.2. The mass yield, E_T , is used to describe the separation performance in a given system. It is defined as:

$$E_T = 1 - \frac{m_1}{m_0} \qquad (1.4.22)$$

where m_1 is the mass of solids in the supernatant and m_0 is the mass of solids in the feed. In order to describe the relationship between the separation performance and the property of solids (assume the viscosity and density of the liquid phase is constant), the grade efficiency, T(x), is defined as: (Mannweiler, 1989)

$$T(x) = 1 - \frac{m_1(x)}{m_0(x)} \qquad (1.4.23)$$

where $m_1(x)$ is the mass of solids of property x in the supernatant, $m_0(x)$ is the mass of solids of separation property x in the feed.

Since the particle density is usually assumed to be constant for a given system, the grade efficiency may be specified as:

$$T(d) = 1 - \frac{m_1(d)}{m_0(d)} \qquad (1.4.24)$$

where d the Stokes' diameter of the particles.

If the size distribution F(d), which is the cumulative volume distribution expressed as the % in-range on a volume basis, is introduced, the equation 1.4.24 can be rewritten as:

$$T(d) = 1-(1-E_T)\frac{\Delta F_1(d)}{\Delta F_0(d)} \qquad (1.4.25)$$

where $\Delta F_1(d)$ is the particle size distribution in the supernatant, and $\Delta F_0(d)$ is the particle size distribution in the feed.

It is easy to find out the relationship between $\Delta F(d)$ and F(d), i.e.

$$\Delta F(d) = F(d+\Delta d) - F(d) \qquad (1.4.26)$$

which is on the mean particle size $d+\Delta d/2$.

According the definition of F(d), the sum of all size fractions ($\Delta F(d)$) making up the particle size distribution is 100%. It can be expressed as:

$$\sum_{d_{min}}^{d_{max}} \Delta F(d) = 1 \qquad (1.4.27)$$

On integrating equation 1.4.25 and applying equation 1.4.27, we get,

$$E_T = \sum_{d_{min}}^{d_{max}} T(d)\Delta F(d) \qquad (1.4.28)$$

If the chosen size interval Δd is small enough, equation 1.4.28 can be expressed as:

$$E_T = \int_{d_{min}}^{d_{max}} T(d)dF(d) \qquad (1.4.29)$$

Mannweiler (1989) used a two parameter model equation to describe the grade efficiency T(d) in equation 1.4.29. The model equation is expressed as:

$$T(d) = 1 - \exp[- k (d/d_c)^n] \qquad (1.4.30)$$

These two parameters, k and n, were determined by experimentally (Mannweiler, 1989), and they were specific for a given system, i.e. the machine parameters and the features of the feed including the flow rate Q.

Olbrich (1989) predicted the separation performance of the same separator as Mannweiler (1989) for the recombinant homogenate from *E. coli* HB101 pCT70 basing on equation 1.4.29. He used the model of the grade efficiency T(d) (equation 1.4.30), developed by Mannweiler (1989), and applied his own results from particle sizing [F(d)] to calculate mass yield E_T for both inclusion bodies and cell debris. His calculation results showed the viscosity of the feed greatly affected the recovery rate (discussed in section 4.4.1). However, his calculation results should be checked by experiments because there is a great difference between the feed property on which Mannweiler's model was based and that Olbrich (1989) used for calculation.

1.4.2.4 Inclusion body washing

The inclusion bodies obtained from the particle classification step will still contain a number of types of contaminants. They may include: cell debris, bacterial proteins which are weakly or strongly associated with the inclusion body particles, lipids, ribosomes and DNA components such as plasmids. Therefore, a secondary purification (washing) of the inclusion bodies is normally employed (Marston, 1986).

The weakly associated proteins, i.e. some membrane proteins, may be removed by using mild denaturing conditions such as non-ionic detergents which do not effect the solubilisation of inclusion bodies. Triton X-100 (0.5 v/v %) combined with 10^{-3} M EDTA was used to remove protein contaminants from a prochymosin inclusion body preparation (Marston *et al.*, 1984). Schoner *et al.* (1985) used 2M urea, even 5M urea at pH 8.5 to remove major contaminants from a bovine growth hormone inclusion body preparation, without significant

solubilisation of the inclusion body product. Gardiner (1988) found that buffer containing 0.5 v/v % Triton-100 detergent was not significantly more effective in removing the protein contaminants from prochymosin inclusion bodies than buffer alone. He also showed that urea concentrations as low as 2M gave a maximal solubilisation of prochymosin inclusion bodies, and even 1M urea reached 50% solubilisation of prochymosin inclusion bodies. Clearly, washing buffer can affect various inclusion bodies in different ways, and its effectiveness appears highly specific to particular inclusion body types.

It is thought that proteins, which are strongly associated with inclusion bodies, and other contaminants such as cell debris, lipids, nucleic acids, will dissolve under extreme conditions which also cause inclusion bodies to be solubilized. It may be possible to apply high-resolution techniques such as chromatography (section 1.4.4) to remove most of these contaminants as well as some detergents after the stage of solubilisation of inclusion bodies. In addition, these contaminants are often poorly soluble under renaturing conditions, and will precipitate without influencing the refolding of the recombinant product (Thatcher, 1990).

1.4.3 Inclusion body solubilisation

In order to recover biologically active material from inclusion bodies, the washed pellet from the last unit operation (washing) must be solubilized to some extent by using denaturants. Then by modifying the environmental conditions, *e.g.*, removing the denaturants, the solubilized protein is allowed to refold into its proper conformation.

It is necessary to understand the structure of inclusion bodies before adopting inclusion body processing strategies. The stabilising forces involved in inclusion body structure are analogous to those involved in protein structure. In an aqueous system, those interactions which are responsible for protein stability can be divided into five types:

(1) covalent bonds
(2) hydrogen bonds
(3) Van der Waals forces
(4) electrostatic interactions
(5) hydrophobic interactions

The peptide bond is the most fundamental covalent bond in proteins. Another important covalent bond in proteins is the disulphide bond (S-S), which is formed between two cysteine side-chains and is used to stabilise the tertiary structure of proteins. Hydrogen bonding contributes to the maintenance of secondary structure such as the α-helix and the β-pleated sheet. Van der waals forces exist between all molecules. Electrostatic interactions occur between charged side chain groups and the solvent. Hydrophobic interactions are a result of the low solubility of non-polar side chains in water.

Inclusion bodies are held together by the same forces described above. Although disulphide bonds are not considered to be structural stabilisers *in vivo* due to the reduced state in the cytoplasm of *E. coli* (Fahey *et al.*, 1977; Kane and Hartley, 1988), they are formed upon exposure to an oxidising environment during cell disruption (Tsuji *et al.*, 1987; Langley *et al.*, 1987; Schoemaker *et al.*, 1985).

The objective of solubilisation is to solubilise and unfold the product protein to a structural state from which the maximum yield of renatured product can be obtained. This objective is based on a model proposed by Gardiner (1988), which indicates solubilisation of inclusion

bodies as distinct from unfolding. By employing partially denaturing conditions, leading just to solubilisation, the renaturation rates were increased.

Prior to the work of Gardiner (1988), little systematic work had been carried out on the solubilisation of inclusion bodies. In most of the studies, extreme denaturing conditions were used routinely. For example, Shoemaker *et al.*(1985) used 8M urea at pH10.7 to solubilise prochymosin inclusion bodies, while Builder (1986) used 6M guanidine hydrochloride (GuHCl) at pH 8 to solubilise prochymosin inclusion bodies. The solubilized inclusion bodies were then sulphonated by adding sodium sulphite and sodium tetrathionate to break any incorrect disulphide linkages.

Gardiner (1988) systematically studied the inclusion body solubilisation process. He examined a number of factors which affected the inclusion body solubilisation process, such as the denaturant types, the concentration of denaturants, pH values, temperatures, *etc.*

Among a number of denaturants, urea and GuHCl are widely used to solubilise inclusion bodies. This is due to the requirement for reversibility of the denaturation/ renaturation process. However, urea and GuHCl do in certain cases lead to irreversible denaturation. This is known to occur when employing low concentrations of urea or GuHCl for protein denaturation. It is thought to be due to partially unfolded intermediates interacting and forming stable structures (Ghelis and Yon, 1982).

A large number of inclusion body proteins have disulphide bonds. The disruption of disulphide bonds in inclusion bodies is not a prerequisite for solubilisation, but they must be broken to allow correct refolding to take place. However, urea and GuHCl alone cannot break these disulphide linkages. Thiol reagents such as dithiothreitol and 2-mercaptoethanol can be used to reduce disulphide bonds.

Alternatively, by using high pH values, disulphide bond breakage will also be effected. High alkalinity in solubilisation also permits the use of a lower denaturant concentration without decreasing the extent of solubilisation (Gardiner, 1988). However, the consequences of irreversible denaturation at high pH, due to side-chain modification, must be considered in designing high pH inclusion body solubilisation operations. Gardiner (1988) managed to

effect complete solubilisation of prochymosin inclusion bodies using a high pH value of 10.7 and very low urea concentration of 2M. No disulphide reducing reagent was required.

The concentration of denaturant during solubilisation stage will strongly affect the renaturation rate. As mentioned earlier, Gardiner (1988) found the renaturation rate of prochymosin was increased by using partially denaturing conditions, *i.e.*, employing low urea concentrations or reducing the solubilisation reaction time at high urea concentrations. High urea concentration were preferred in order to obtain an acceptable yield of product. Because there was the danger of irreversible denaturation occurring at less severe denaturing conditions, which led to decrease in yield, as already mentioned earlier in this section.

1.4.4 High-resolution separation

There are two strategies in the purification of proteins obtained from inclusion bodies. One is to purify the protein product in its native formation after the refolding stage. When this route is chosen, the purification techniques will be limited to those which will not damage the native conformation of the product, *e.g.*, precipitation, ion-exchange chromatography *etc.* Reverse phase chromatography may pose problems because of denaturation effect induced by the stationary phase support (see section 1.3.4).

When the other strategy is chosen, *i.e.*, to purify the protein product in its denatured state before refolding, then other purification techniques such as reverse or normal phase chromatography are available.

Salt and Turner (1990) has examined the separation of denatured prochymosin standard from synthetic mixtures of pure proteins on a polymeric reverse phase HPLC support with gradient elution, in order to develop a quantitative assay method for monitoring the production and recovery of prochymosin. In future work, this system will be verified by applying samples of the prochymosin inclusion body fraction, obtained by centrifugal separation of the recombinant cell homogenate (refer to section 1.4.2.3)

1.4.5 Inclusion body renaturation

The objective of the renaturation process is to maximize the recovery of active product while minimizing the processing scale and time.

The protein renaturation can occur only under the conditions such that:

(1) the aqueous environment is changed such that the unfolded state is unstable relative to the native state;

(2) the polypeptide has not undergone any irreversible chemical modification;

(3) the aqueous environment is suitably oxidising for the formation of native disulphides;

A number of factors will influence the renaturation rate and yield. These include: the denaturation conditions; the environmental conditions; the formation of native disulphide bonds.

The denaturation conditions, whose most important component is the denaturant concentration, will determine the extent of unfolding and side-chain modification. The renaturation rate and yields will be greatly affected by the state of inclusion body protein, *i.e.*, fully or partially unfolded, prior to refolding (see section 1.4.3)

Environmental conditions for protein renaturation are important. First, the concentration of the denaturants must be reduced to make the transfer from an unfolded state to a native structure energetically favourable. If the denaturant concentration is not reduced sufficiently to allow complete refolding, the protein may be maintained in a loose conformation in which intermolecular interactions can occur. This results in specific activity reduction (Brems *et al.*, 1987). Secondly, the protein concentration employed during renaturation are also crucial. High protein concentration leads to low cost processing. However, this will result in irreversible protein aggregation and thus low yield due to intermolecular interactions. Thirdly, the pH during renaturation will determine the reactivities of the various side-chain groups. One of the most important groups is the cysteine side-chains. The rate of disulphide bond formation will be highest at pH values close to the pKa (8.33) of the cysteine group. Renaturation under more acidic conditions leads to reduced rates due to the greater stability of the cysteine thiol. Under high pH condition, intermolecular interaction is thought unlikely

due to the effects of charge repulsion. This may enhance renaturation. However, high pH leading to modification of side-chain must be considered as mentioned in section 1.4.3. Fourthly, the protein purity during renaturation should be considered although Weir and Sparks (1987) have indicated that aggregation during renaturation of a protein product is not a function of the overall protein concentration but of the protein product concentration. This result implies that protein contaminants do not have a deleterious effect on product renaturation yield. However, further examination of this aspect is necessary. Other factors involved in renaturation conditions such as inorganic salts, renaturation temperature and time, also influence this process with respect to rate and yield.

During renaturation, proteins which contain disulphide bond in the native state must be permitted to undergo thiol-disulphide interchange to correct any mismatching of cysteine thiol groups. Experiments have shown that optimum renaturation rate and yield are obtained with redox mixtures using a molar ratio of 10 to 1 reducing agent to oxidising agent (Ahmed *et al.*, 1975).

Gardiner (1988) studied diafiltration for constant volume renaturation, which avoided the potential problem of unacceptable increase in processing volume when using dilution to remove the denaturing environment. He showed that by using diafiltration, renaturation yields were increased and processing volume reduced.

1.5 The use of recombinant DNA techniques to produce fragments of antibodies and the potential application of such fragments

1.5.1 The structure of immunoglobulin

The adaptive immune system is responsible for recognition and reaction to antigens. Immunoglobulins or antibodies are a type of protein molecules which play a key role in the immune response. They are produced by B cells and are readily adapted for specific recognition and binding to an invading antigen.

Each antibody molecule such as IgG class (immunoglobulins of gamma class) consists of two identical heavy chains of about 440 amino acids and two identical light chains of about 220 amino acids, and shares in a Y-shape structure (see Figure 1.5.1).

Figure 1.5.1 The structure of an antibody molecule

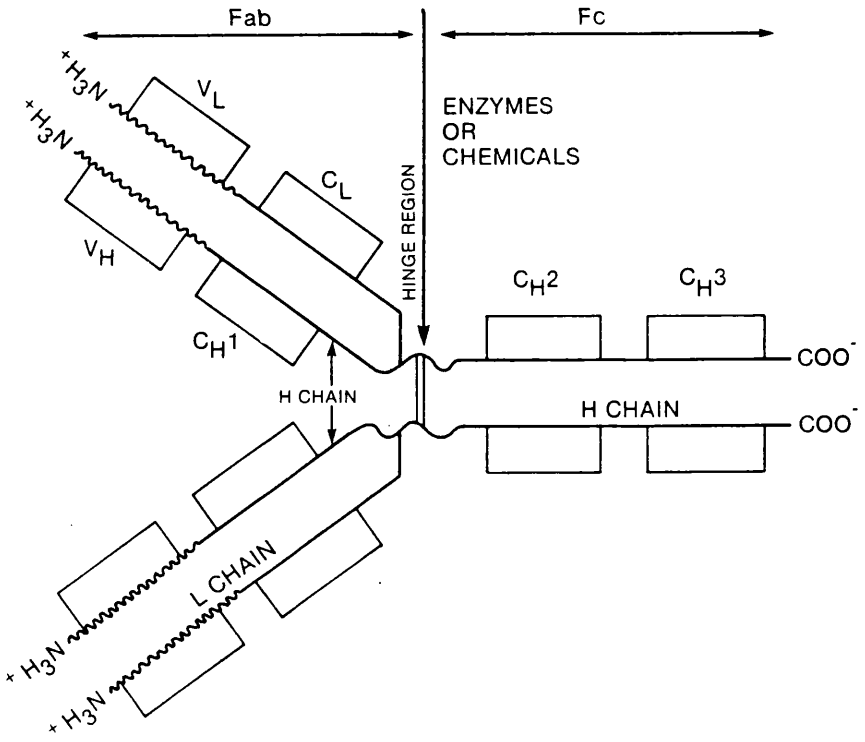

The molecule can be fragmented into Fab arms and the Fc region containing effector functions (a number of cells in the body have receptors for the Fc region). Each arm (Fab) is composed of a light chain and the first two hundred and twenty residues of the heavy chain. The N-terminal half of the Fab is called Fv variable domain or variable region, which is composed of V_H and V_L subdomains. The rest of domains of a heavy and a light chain forms the constant domains or constant region. The Fv consists of two parts, namely complementary determining region (CDR) and framework region (FR). CDRs form the antigen combining site (ACS) and are composed of six hypervariable loops, three from the heavy and three from the light chain, which are supported by a conserved FR. Variability of the ACS is generated by the large number of variable region genes and by alternative combinations of variable region genes and other gene segments - the D and J segments which make up the third CDR. The constant region (Fc) is responsible for effector functions such as complement fixation and binding to other receptors (Davies and Metzger, 1983).

1.5.2 Expression of antibodies in mammalian cells and problems of this system

Monoclonal antibodies obtained by hybridoma technology (Köhler and Milstein, 1975) have many applications. For examples, they have been used as diagnostic reagents (reviewed by Scott, 1985) and in constructing first-generation ricin immunotoxins (Vitetta *et al.*, 1987). However, there are limitations: it is not always possible to generate antibodies with the precise specificity desired or with the appropriate combination of specificity and effector function; human hybridoma antibodies, which have the advantage of being less immunogenic than rodent antibodies like mouse monoclonals, are difficult to obtain (Morrison, 1985; Brunt, 1986). As mentioned in section 1.1, recombinant antibodies have been made to possess hapten-specificity and a nuclease activity (Neuberger *et al.*, 1984) and the so-called chimeric antibodies have also been made in several laboratories, which have a variable region from a rodent source but a human constant region and may be less immunogenic when used *in vivo* because the constant domains of rodent source are likely to be antigenic with regard to humans (Morrison *et al.*, 1984; Neuberger *et al.*, 1985; Liu *et al.*, 1987). Although mammalian cell culture is capable of large-scale production of secreted, complete and active antibody molecules, it is expensive and labour intensive.

Large quantities of antibodies are required not only in therapeutic use but in some antibody-

antigen binding studies, the aim of which is to discover the rules governing combining site structure for efficient design of antibody and vaccines. Computer modelling of the antigen combining site (ACS) (de la Paz *et al.*, 1986; Smith-Gill *et al.*, 1987) is desirable because the formation of protein antigen-antibody crystals has proved difficult and few crystallographic structures of combining site have been obtained. All computer models require a system by which they can be tested. A rapid model testing procedure (compared with crystallography) was developed, which employed site-directed mutagenesis (SDM) of residues in those heavy and light chain variable genes thought to be critical for binding, and the subsequent antibody cDNAs were cloned and an expression system (frog oocytes) was used to produce intact antibody material for direct binding analysis (Roberts and Rees, 1986; Rees and de la Paz, 1986). When crystals can be grown, SDM combined with X-ray crystallography is an approach for verification of computer models of ACS and it has been used by Alber *et al.* (1987). However, testing and verification methods are valuable only if a large quantities of mutated antibodies can be obtained. Therefore, there is an additional interest in large-scale production of recombinant antibodies in bacterial cells such as *E. coli* for low cost and easy manipulation.

1.5.3 Production of antibody fragments in *E. coli*

A major consideration for antibody component production in bacterial cells such as *E. coli* is the manner of expression of the foreign genes. Proteins secreted by cells into the medium or periplasmic space are frequently found to be in their native forms. However, In the case of a cytoplasmic expression in *E. coli* cells, foreign proteins are formed as inclusion bodies and a refolding process of insoluble products is required. At the time when this study began, only the latter option was available for biochemical engineering study.

1.5.3.1 Choosing Fv for cytoplasmic expression in *E. coli*

Cabilly *et al.* (1984) and Boss *et al.* (1984) reported producing heavy and light chain (cloned in separate plasmids) of IgG and IgM in cytoplasm of *E. coli* respectively, and renaturing the mixture of crude extracts containing heavy and light chains leading to the reconstitution of functional four-chain antibodies *in vitro*. However, the reconstitution of whole active antibody molecules was inefficient. This was explained by the differences between *in vivo*

and *in vitro* refolding. Refolding *in vitro* is complicated by aggregating pathways which compete for folding. The existence of interchain disulphides in antibody molecules may lead to incorrect folding when chemically renatured (Field, 1990). The absence of some proteins which act as catalysts *in vitro*, e.g. disulphide isomerase and proline isomerase (Lang and Schmid, 1988), heavy chain binding protein (BiP) (Kassenbrock *et al.*, 1988; Pelham, 1988), may account, in part, for the lack of efficiency of whole antibody molecules assembly.

Recombinant Fv produced in the cytoplasm of *E. coli* should be refolded more efficiently. Because Fv contains low numbers of intrachain disulphide, and there is no interchain disulphide in Fv (Field, 1988). Fv has been shown to exist in isolation after being proteolytically cleaved from the rest of the rest of the antibody (Hochman *et al.*, 1973; Sharon and Givol, 1976; Sen and Beychok, 1986). This indicates that a stable association exists in Fv. Indeed, a novel mode of packing at the V_H and V_L interface has been observed by Chothia *et al.* (1985), which shows the stable association between V_H and V_L is a consequence of extensive hydrophobic interactions. Efficient refolding of Fv from denatured V_H and V_L subdomains was demonstrated by Hochman *et al.*, (1973). They found that 87% of the original binding was recovered, although it should be noted that in their study proteolytically derived Fv from monoclonal antibody was used.

There were two ways to produce Fv in the cytoplasm of *E. coli* at the time this study commenced. One was the production of so called "single-chain Fv". Single-chain Fv consisting of V_H and V_L tethered by a short polypeptide linker can be expressed from one recombinant gene. It was proposed that the presence of a linker gave the single-chain Fv a lot of flexibility, e.g. the linker could be designed to have toxin properties or to allow drug to bind to it (Klausner, 1986). However, the linker itself could be highly immunogenic. Huston *et al.* (1988) reported the production of a single-chain Fv formed as inclusion bodies in *E. coli*. Renatured single-chain Fv had an association constant $K_a = 3.2 \times 10^7/M$, a 6-fold decrease in binding affinity compared with its Fab ($K_a = 1.9 \times 10^8/M$). Three other single-chain Fvs were produced, one of which had a $K_a = 1.1 \times 10^9/M$, a 7-fold decrease in binding affinity compared with its Fab ($K_a = 8 \times 10^9/M$) (Bird *et al.*, 1988). Interference from the linker polypeptide itself may account for the reduced binding.

Another way of achieving cytoplasmic expression of Fv in *E. coli* is to produce subdomains of V_H and V_L individually, then to partially purify and reconstitute V_H and V_L into Fv (Field, 1988). Studies of the V_H - V_L association will benefit from the availability of purified V_H and V_L. The V_H and V_L of Gloop2 antibody, one of five monoclonal antibodies (Gloop1-5) specific for the so called "loop" region of hen egg lysozyme residues, were produced in severely protease-deficient *E. coli* strains (Field, 1988). Solubilisation and reconstitution of V_H and V_L resulted in an Fv with the same binding affinity for a peptide antigen (dissociation constant $K_d = 9 \times 10^{-9}$ M) as that for the Fab ($K_d = 1.7 \times 10^{-8}$ M) or whole antibody ($K_d = 2.1 \times 10^{-8}$ M), within experimental error. Although Gloop2 Fv was produced at an average yield of 42 mg/litre, purification resulted in an average yield of 0.75 mg/litre. In this system, there is the additional advantage, that both V_H and V_L can be examined structurally by nuclear magnetic resonance studies because of their small size (only about 14 KDa each).

1.5.3.2 Secreted expression of antibody fragments in *E. coli*

A secretion route into the periplasm has been chosen for a light chain expressed in *E.coli* (Zemel-Dreasen and Zamir, 1984). They showed that *E. coli* could refold the two subdomains (V_L and C_L) upon secretion. It should be possible to apply the same secretion route for Fv expression. This was accomplished during the present study by Skerra and Plückthun (1988). They described the secretion of an Fv into the periplasmic space of *E. coli*. The secreted Fv was functional with an identical K_a (1.21×10^5/M) to that of the native antibody (1.6×10^5/M). However, low yields of 0.2 mg/litre were obtained after purification. The low yield may be caused by concentration effects; because of a finite volume in periplasmic space, much of the material remained in the cytoplasm. Great progress was made with the secretion route in *E. coli* by expressing an Fab which was secreted through the external cell wall of *E. coli* into the medium (Better *et al.*, 1988). Ward *et al.* (1989) also reported an expression of V_H subdomains in *E. coli*, which were secreted into the medium. Isolated V_H subdomains had a similar binding affinity ($K_a = 5 \times 10^7$/M) to that of native antibodies. This secretion system can bypass the problem of limited product accumulation in the periplasmic space. Interest in V_H subdomains stems from reports that they bind antigen with good affinity in the absence of their partner V_L subdomains (Austin, 1989). Future production of antibody fragments may lie in this direction and this will be further discussed

in section 4.1.

1.5.4 The potential application of antibody fragments

The first generation of antibodies (monoclonals) have found application mainly in diagnosing and treating disease but for the latter there has been the limitation of high cost and high immunogenicity, which has been mentioned in section 1.5.2. The potential advantage of the second-generation antibodies lies in lower cost, smaller size, less immunogenicity and greater stability (Klausner, 1986). The lower cost would make large-scale uses like immunoaffinity columns particularly attractive (Klausner, 1986). The production of antibody fragments (Fv) in an economical system (using bacterial cells such as *E. coli*) potentially allows scale-up (Field, 1988; Skerra and Plückthun, 1988). Recombinant Fv offers potential advantages in crystallographic analysis of antibody combining sites due to its small size and the elimination of the flexible elbow joining variable and constant domains (Huber, 1986). The small size is also a critical advantage in structural studies of ACS by nuclear magnetic resonance (Redfield and Dobson, 1988). The treatment of viral diseases may also benefit from the availability of smaller size of antibody fragments. Many viruses hide the binding sites (to host cells) in a deep crevasse on their surfaces. Normal antibodies are too big to enter these so called "canyon sites". Antibody fragments might be small enough to slip in and block these binding sites (Rossman *et al.*, 1985; Weis *et al.*, 1988). Antibody fragments may be a more suitable candidate for making immunotoxins also because of their smaller size. It was found that the efficacy of first generation ricin immunotoxin (made with whole monoclonal antibody) was reduced by the inaccessibility of the target cell to the circulation. Fab-immunotoxins have been used in second generation ricin immunotoxins to achieve more efficient penetration into the tumour and internalisation of the toxin into target cells (Vitetta *et al.*, 1987). Finally, it has been proposed that antibody fragments (e.g. Fv) are less immunogenic than whole antibodies, but this should be examined (Klausner, 1986; Field, 1990).

1.6 The use of recombinant DNA techniques to produce prochymosin and the potential application of this material

Traditionally, most commercial cheeses and other protease-dependent dairy products have been made using chymosin isolated from the fourth stomachs of unweaned calves (Burgess and Shaw, 1983). Therefore, the availability and price of chymosin depends on the consumption of veal. The production of prochymosin from *E. coli* or other organisms may provide an alternative and cheap source of chymosin for the cheese-making industry.

The prochymosin gene has been cloned into several microorganisms where prochymosin is produced and acid-hydrolysed into active chymosin. Chymosin (rennin) is the active enzyme present in rennet, which is responsible for proteolysis of κ-casein in milk (Foltmann, 1970). K-casein normally stabilizes micelles in milk, but when it is cleaved, the micelles precipitate into curds. After the liquid whey is removed, the curds may be processed into cheese or other dairy products.

As discussed in section 1.2.1, there is an interest in employing bacteria like *E. coli* as host strain for production of recombinant proteins. Expression of calf prochymosin in *E. coli* was first reported by Emtage *et al.* (1983). In their system, the plasmid pCT70, an intermediate copy number plasmid carrying prochymosin gene was transformed in *E. coli* K-12 HB101, and prochymosin was expressed at a level up to 5% of total proteins in the cytoplasm of *E. coli* and formed as inclusion bodies. There are some advantages in inclusion body formation (see section 1.2.2) and particularly an advantage at the stage of particle classification, where prochymosin inclusion bodies were separated from cell debris by employing centrifugation (detailed in section 1.4.2.3). The derived product, chymosin, from prochymosin produced in *E. coli* K-12 strain is the first food ingredient approved by the FDA (Flamm, 1991). Because of the instability problem of plasmid pCT70 (Caulcott, 1985), a dual-origin plasmid, plasmid pMG168 carrying the prochymosin gene, was developed and an expression level of 10-13% of total cellular proteins was achieved (Wright *et al.*, 1986, detailed in section 1.7.2).

Obtaining an active product from a protein expressed as inclusion bodies requires that the protein be denatured and then refolded to the native form (section 1.4.3 & 1.4.5). This is a slow, difficult procedure which greatly reduces the net yield. Therefore, efforts have always

been made to develop systems which are capable of secreting recombinant proteins, because proteins secreted by cells are frequently found to be in their native forms. Secreted expression of prochymosin in *E. coli* was achieved in the form of fusion protein (Holland, 1989). Other bacterial strains such as *B. subtilis* and *S. cremoris* have also been exploited for secreted expression of prochymosin (Brunt, 1987). In addition to bacterial cells, the yeast *S. cerevisiae* and *K. lactis* have been developed as host organisms for expression and secretion of prochymosin (Smith *et al.*, 1985; van den Berg *et al.*, 1990), as well as the fungus *A. niger* for secreted expression of prochymosin in a fusion protein form (Ward *et al.*, 1990). However, the expression level of recombinant prochymosin was low in the secreted expression systems. This problem will not be solved until the molecular and biochemical principals of secretion are better understood.

1.7 The systems selected and the proposed studies

1.7.1 The expression systems

From the discussion in section 1.2.3 and section 1.2.4, it is important to choose an effective expression system (vector/host) prior to scale-up of fermentation and subsequent downstream processing. As discussed in section 1.2.1, *E. coli* is by far the most commonly used host strain for the expression of heterologous proteins, owing to its well-defined genetic structure and subsequent ease of genetic manipulation. Furthermore, *E. coli* has several advantages such as a high specific growth rate, high expression level of heterologous proteins and the availability of well characterised promoters. It has been widely used for expression of valuable recombinant proteins (section 1.5 and 1.6). In this study, different *E.coli* strains were employed for expression of antibody fragments, and later for prochymosin (section 2.1.1).

As stated in section 1.2.3, plasmid stability is crucial for recombinant fermentation process. Therefore, the type of plasmid chosen should retain stability to allow scale-up of production of recombinant proteins.

The dual-origin plasmid pMG411 (see Figure 1.7.1) developed by Yarranton *et al.* (1984) carries a temperature-sensitive derivative of the pSC101 *ori* (Hashimoto-Gotoh *et al.*, 1981) which is a low copy number origin, and a 'hybrid' ColE1-based *ori* which is a high copy number origin whose function is controlled by the λp_L (λ leftward promoter). λp_L promoter is repressed by the product of *c*Its gene, which is temperature-sensitive. It will be destroyed by raising temperature to 42°C. At 30°C, the plasmid replication will use low copy number *ori*, derived pSC101. When temperature is shifted to 42°C, promoter λp_L is derepressed, and the replication of plasmid using high copy number 'hybrid' ColE1-based *ori* occurs. The vector confers ampicillin resistance to the host.

The advent of dual-origin plasmids may pave the way to large-scale production of foreign proteins in bacterial cells because there are a number of advantages to the dual-origin plasmids. They can be stably maintained at approximately four copies per chromosome at 30°C and readily amplified by thermal induction of strains carrying a thermolabile λ

repressor. This characteristic makes it a suitable vector for cloning foreign genes because the stability of the plasmid carrying foreign gene can be retained during the growth phase by controlling temperature, and induced during production phase. In addition, it provides a cheap procedure for induction. Such physical induction eliminates the problems caused by chemical induction which is normally expensive and could contaminate the product, thus increasing the downstream processing requirements.

Figure 1.7.1 Physical maps of the dual-origin plasmid pMG411
(Adapted from Yarranton *et al.*, 1984)

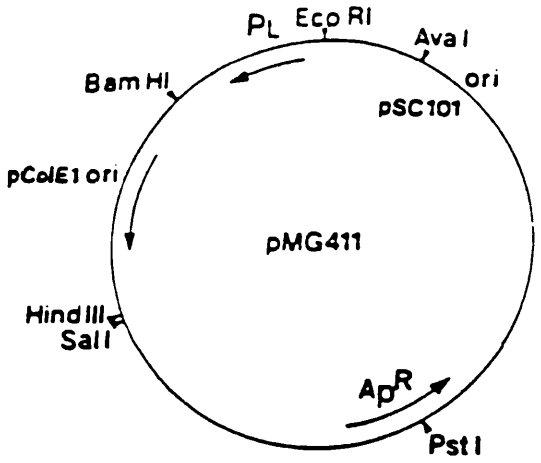

However, plasmid pMG411 has several limitations when used for cloning foreign genes: it can only be used as a controllable copy-number vector in host cells carrying *c*Its gene, whose product represses λp_L promoter; under growth conditions lacking selection for plasmid-bearing cells (antibiotics in this case), there is a significant plasmid loss. To overcome these limitations, some modifications has been made for pMG411, *i.e.* the λp_L (λ leftward promoter) has been replaced with λp_R (λ rightward promoter) and the *c*Its857 gene. Thus its copy-number is controllable in *E. coli* strains with or without the *c*Its857 gene. In order to solve the problem of segregational instability of plasmid, the temperature-sensitive pSC101 derived *ori* in plasmid pMG411 has been replaced by a non-mutant pSC101 *ori* and its associated *par*, the *par* ensures segregational stability in the absence of antibiotic selection (Meacock and Cohen, 1980). This modified dual-origin plasmid has been used for cloning foreign genes (Wright, *et al.*, 1986; Field, 1988).

1.7.1.1 The vector/host for expression of antibody Gloop2 fragments (V_H and V_L)

The plasmids for expression of antibody fragments in this project were pMG LF9 and pPW HF2, which were constructed by Field (1988). Plasmids pMG LF9 and pPW HF2 carry V_L gene and V_H gene, respectively. V_L and V_H are light chain variable subdomain and heavy chain variable subdomain of antibody Gloop2, which is one of the five monoclonal antibodies, Gloop1-5, raised for the so called 'loop' region of hen egg lysozyme (Field, 1988). Plasmid pMG939 (See Figure 1.7.2), a dual-origin plasmid derived from the modified vector pMG411 as described in the last section, was used as the parent plasmid for construction of plasmids pMG LF9 and pPW HF2.

Figure 1.7.2 A computer generated map of the expression vector pMG939 (adapted from Field, 1988)

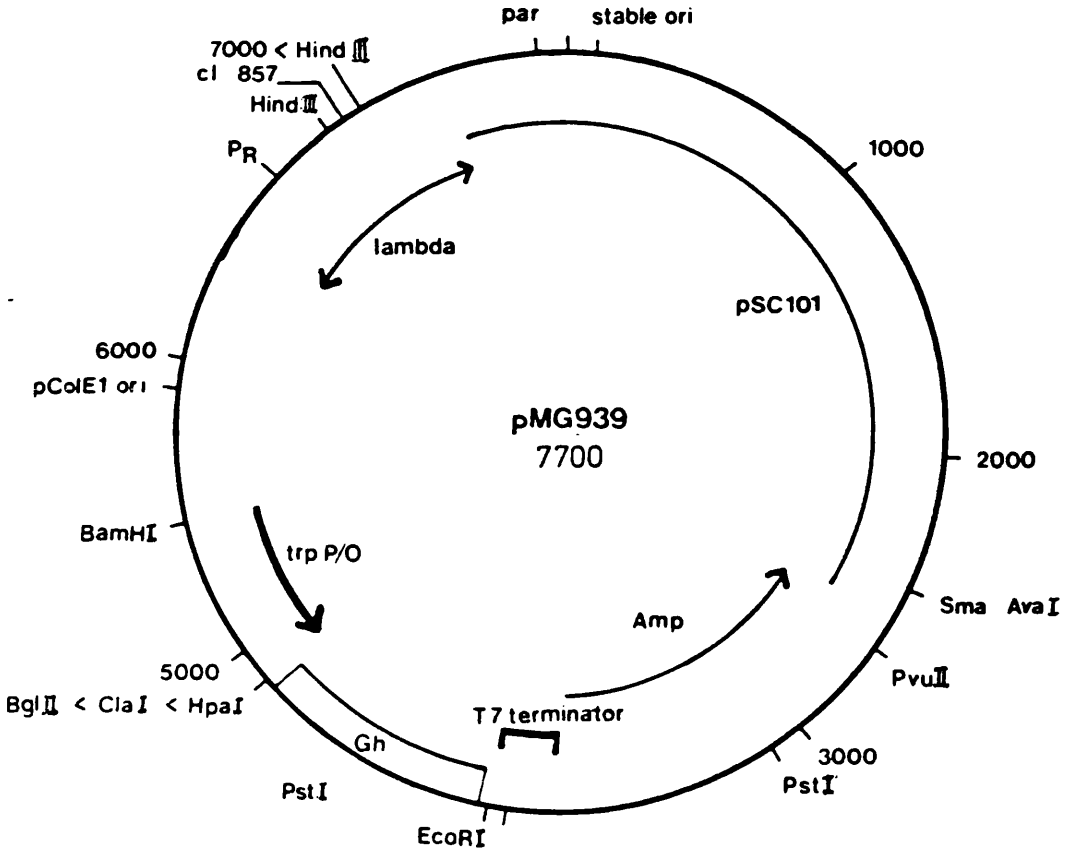

In plasmid pMG939, the expression of the cloned mammalian growth hormone gene is under control of the tryptophan promoter-operator, whose attenuator region is removed. A consequence of attenuation is that complete derepression cannot be achieved naturally even under tryptophan-starvation conditions, unless an inducer such as indole acrylic acid is added (Tacon *et al.*, 1983). The construction of plasmids pMG LF9 and pMG HF2 was performed by replacing the mammalian growth hormone gene in plasmid pMG939 with V_L and V_H gene respectively (Figure 1.7.3).

The construction of plasmid pPW HF2 was the same as for pMG HF2 except that plasmid pPW1 was used instead of pMG939 presented in Figure 1.7.3. Vector pPW1 was essentially the same as pMG939, but contained a longer Shine-Dalgarno sequence (physical map of pPW1 not shown). A higher expression level of V_H from plasmid pPW HF2 has been achieved compared with that from pMG HF2 (Field, 1988).

The transcription of V_H and V_L genes should be repressed by the *trp* repressor protein which is expressed from the chromosomal *trpR* gene in the presence of tryptophan when plasmid pPW HF2 and pMG LF9 are at low copy number. Even in tryptophan-starvation conditions, the expression level of V_H and V_L should be very low because of the low copy number of plasmid. However, when the cells are induced, synthesis of V_H and V_L will occur even in the presence tryptophan because the copy number is increased and the *trp* promoter cannot be tightly controlled (Caulcott *et al.*, 1985).

Figure 1.7.3 Construction of expression vectors pMG HF2 and pMG LF9 containing the heavy and light Fv genes respectively (adapted from Field, 1988)

Dual-origin vector sequences are shown with thin lines, and other DNA vectors with thick lines. The filled arc shows the GH sequences, and open arcs represent Gloop2 DNA. Some of the features of the dual origin vector are shown. The novel *Bgl*II - *Eco*RI fragments containing V_H and V_L were isolated from pHF2 and VLG2.9 and ligated into the vector which had been similarly isolated, generating the constructs pMG HF2 and pMG LF9.

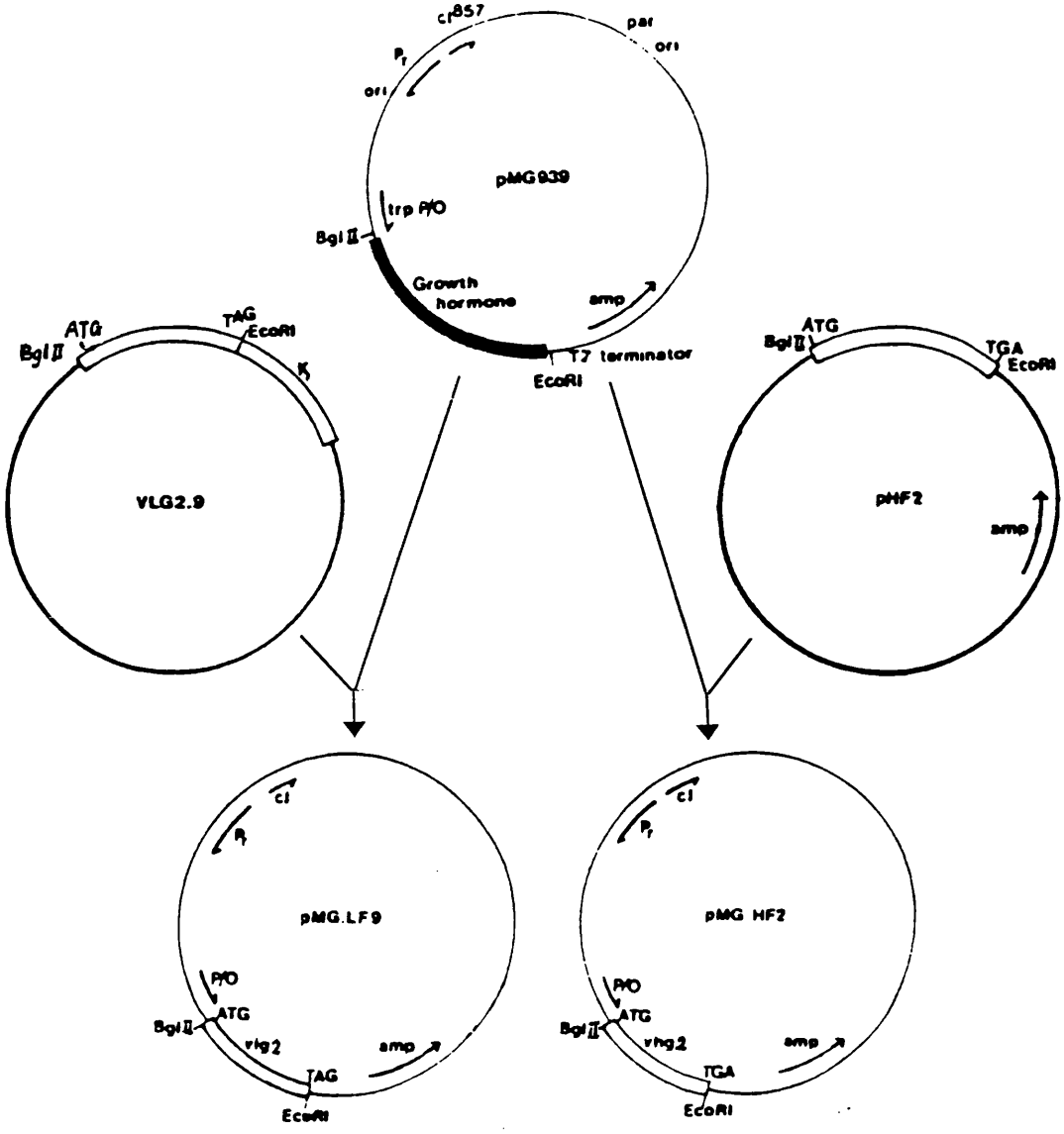

Plasmid pMG LF9 or pPW HF2 were transformed into *E. coli* CAG629 strain. This *E. coli* strain is heat shock protease and *La* protease deficient (*htpR*$^-$, *lon*$^-$). The reason for choosing this strain is to eliminate the production of proteolytic enzymes which are responsible for degradation of recombinant proteins. Because many of these proteases are formed in response to heat-shock, they become a particular problem in the temperature-inducible expression system. Protease La, encoded by the gene *lon*, hydrolyses abnormal proteins in an ATP-dependent fashion (Waxman and Goldberg, 1982). The *htpR* locus controls expression of heat shock genes (Grossman *et al.*, 1984). The proteolytic capacity of the cell declines to a great extent in the case of *htpR*$^-$ strains (Baker *et al.*, 1984).

At the first stage of this study, plasmid pMG LF9 in *E. coli* CAG629 and pPW HF2 in *E. coli* CAG629 were chosen and they were donated by Dr H. Field (University of Oxford). In this system, antibody fragments (V_L and V_H) are expressed in the cytoplasm of *E. coli*, forming as inclusion bodies.

1.7.1.2 The vector/host for expression of calf met-prochymosin

The plasmid used for expression of prochymosin in this study was also a dual-origin plasmid, called pMG168 (Figure 1.7.4). The modified vector pMG411 (described in section 1.7.1) was also used as the parent plasmid for the construction of plasmid pMG168 (Wright *et al.*, 1986). This was performed by insertion of a 2.2-kb *Hind*III - *Sal*I fragment carrying the prochymosin gene, isolated from plasmid pCT70 (Emtage *et al.*, 1983). Because plasmid pMG168 belongs to the same family as for plasmid pMG939, plasmids pMG LF9 and pPW HF2, it has the same characteristics as those which have been discussed above, in terms of the induction method, the change of plasmid copy number before and after induction and *trp* promoter control of the foreign gene. Furthermore, prochymosin is also expressed in the cytoplasm of *E. coli*, forming as inclusion bodies.

Figure 1.7.4 Physical map of plasmid pMG168 (adapted from Wright *et al.*, 1986)

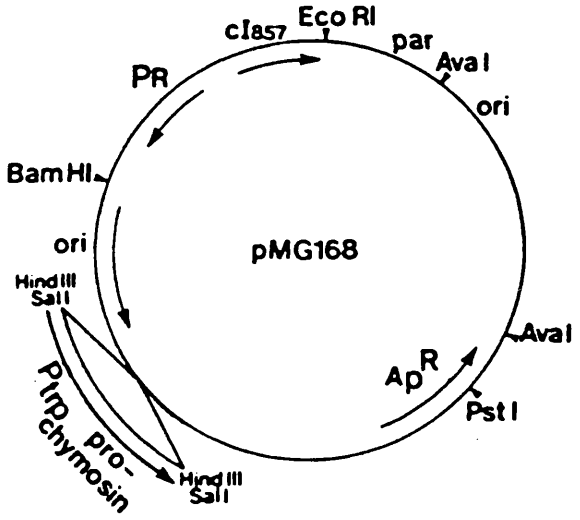

Plasmid pMG168 was transformed into *E. coli* K-12 HB101 strain, which is nonpathogenic and has been widely used as a laboratory organism (reviewed by Flamm, 1991). The safety of host cells is extremely important for the production of recombinant proteins such as prochymosin, whose derivative, chymosin, is used in the food industry (section 1.6).

1.7.2 The proposed studies

1.7.2.1 Scale-up of production of recombinant proteins

The first task of this project was to study the large-scale production of recombinant proteins formed as inclusion bodies by employing *E. coli* strains containing dual-origin plasmids (section 1.7.1). For this investigation, the following aspects were considered:

(1) the stability of dual-origin plasmids during fermentations;

(2) the efficiency of thermal induction of dual-origin plasmids during fermentations;

(3) the possibility of medium changes to allow scale-up (for low cost and safety).

(4) the effect of induction at different cell growth stages on the yields of recombinant proteins;

A series of fermentations at different scales were planned in order to obtain this information and to produce cell material for downstream processing study.

1.7.2.2 Scale-up of recovery of recombinant proteins

Cell disruption in an industrial homogeniser was planned to examine the effect of repeated homogenisation on particle size distribution of cell debris and inclusion bodies. This research was to extent a previous study (Olbrich, 1989) of the characteristics of cell debris and inclusion body particle sizes, and to verify the homogenisation conditions for achieving reduction in cell debris size without significantly reducing inclusion body size. The optimized homogenisation conditions would ease subsequent separation of inclusion bodies from cell debris by centrifugation.

As discussed in section 1.2.2 and section 1.4.2.3, the inclusion body formation of heterologous protein in *E. coli* system is an advantage in the first stage of product recovery, *i.e.* a much purer product can be obtained than that from a non-inclusion body producing system. The processing volumes are also smaller. Operation of an industrial disc stack centrifuge is required for large-scale recovery of inclusion bodies. Theoretical prediction of the performance of an industrial disc stack centrifuge has been made (Olbrich, 1989). In order to verify the theoretical model, experiments for the recovery of inclusion bodies in an industrial disc centrifuge were planned.

2. MATERIAL AND METHODS

Table 2.1 Suppliers of special chemicals

Chemical	Supplier
Polypropylene glycol 2025 (2025) Urea DTT Protein markers	BDH Ltd.
Acrylamide N, N'-methylene bisacrylamide Ammonium persulphate Coomassie G-250 Bromophenol blue TEMED SDS TRIS	BioRad Laboratories Ltd.
Acetic acid (acetate) assay kit	Boehringer Mannheim
Standard Yeatex	Bovril Foods Ltd.
Casamino acids Bacto-tryptone Bacto-yeast extract powder Bacto-agar	Difco
Phenyl methyl sulphonyl fluoride (PMSF) 2-mercaptoethanol Lysozyme	Sigma Chemical Co. Ltd.
BCA protein assay reagent	Pierce and Warriner (UK) Ltd.

All other chemicals were obtained from Fison's Scientific Apparatus (FSA), BDH Ltd., or Sigma Chemical Co. Ltd. Unless otherwise stated, all chemicals were of AnalaR grade. The addresses of all the equipment and chemical suppliers are listed in Appendix 2.

2.1 Strain and strain maintenance

2.1.1 Microorganisms

Two kinds of *E. coli* strain were used in this project.
E. coli CAG629 is heat shock protease and *La* protease deficient (*htpR*$^-$, *lon*$^-$) strain.
E. coli K12 HB101 is *Pro*$^-$, *Leu*$^-$, *Thi*$^-$, *Str*^{r}, *RecA*$^-$ strain.

2.1.2 Plasmids

(1) Plasmid pMG LF9 and pPW HF2 in *E. coli* CAG629 respectively were kindly donated by Dr. H. Field (University of Oxford).

The plasmid pMG LF9 in *E. coli* CAG629 contains the Gloop2 V_L gene, which is the variable light chain subdomain gene of the Gloop2 antibody raised for the so called 'loop' region of hen egg lysozyme. It is maintained at low copy number at 30^{0}C, and its copy number will be greatly increased when the temperature is shifted to 42^{0}C.

The plasmid pPW HF2 in *E. coli* CAG629 contains the Gloop2 V_H gene, which is the variable heavy chain subdomain of the Gloop2 antibody raised for the so called 'loop' region of hen egg lysozyme. Its copy number is also temperature amplifiable.

Both of the two plasmids make use of the tryptophan promoter/operator sequence. They confer ampicillin resistance on the host.

(2) Plasmid pMG168 in *E. coli* K12 HB101 was kindly donated by Dr G.T. Yarranton (Celltech Ltd., Slough, U.K).

The plasmid pMG168 in *E. coli* K12 HB101 contains the calf-intestinal met-prochymosin gene. It is maintained four copies per chromosome at 30^{0}C, and is readily amplifiable by thermal induction. It makes use of the tryptophan promoter/operator sequence for transcriptional control of the structural gene and confers ampicillin resistance on the host.

2.1.3 Strain maintenance

2.1.3.1 Glycerol stock culture

Strains were stored in 80 v/v % glycerol at -70^{0}C. Stocks were prepared by transferring single colonies from a LB agar plate (section 2.2.3) to 10 ml of starter cultures (section 2.2.4) using a flame-sterilised nichrome loop. After these starter cultures were incubated at 30^{0}C and 200 rpm for 24 hours in an orbital shaker (New Brunswick, Scientific Ltd.), 1 ml of these cultures was aseptically transferred to a 7 ml bijou bottle containing 1 ml of sterile glycerol (the sterile glycerol was obtained by sterilising for 20 minutes at 121^{0}C and cooled). These glycerol stocks were stored at -70^{0}C.

2.1.3.2 Plasmid reselection

Due to the problem of plasmid instability, it was necessary to reselect the recombinant stocks periodically. A loop of the glycerol stock was plated out on the LB agar plates, and was incubated at 30^{0}C for 24 hours. Single colonies were aseptically transferred to universal bottles containing starter cultures (section 2.2.4). Immediately after inoculation, 0.05 ml of the culture from each universal bottle was transferred aseptically to each of 400 ml shake flasks containing 50 ml of sterile LB medium (see section 2.2.5.2). Each flask was marked to correspond to each universal bottle. Both the universal bottles and flasks were incubated at 200 rpm and 30^{0}C for 16 hours in an orbital shaker. The universal bottles were used to prepare glycerol stock cultures (section 2.1.3.1), and each bijou bottle was marked to correspond to each universal bottle. Therefore, each bijou bottle containing glycerol stock corresponded to a particular flask. Shake flask cultures were induced, and samples were taken from each flask 6 hours after induction (see section 2.2.5.2). These samples were analyzed by SDS-PAGE (see section 2.6.6). The glycerol stock corresponding to the maximum expression of foreign gene was chosen for the inoculum.

2.2 Production of recombinant proteins formed as inclusion bodies

2.2.1 Medium formulation

Table 2.1.1 LB Medium (Miller, 1972)

Component	Concentration (g/L)	
	E.coli CAG629 (pMG LF9 & pPW HF2)	*E. coli* K12 HB101 (pMG168)
Bacto-yeast extract powder	5	5
Bacto-tryptone	10	10
NaCl	10	10
Ampicillin	0.1	0.1
Tetracycline	0.01	-

Table 2.2.2 LB agar plates

Component	Concentration (g/L)	
	E.coli CAG629 (pMG LF9 & pPW HF2)	*E. coli* K12 HB101 (pMG168)
Bacto-agar	15	15
Bacto-yeast extract powder	5	5
Bacto-tryptone	10	10
NaCl	10	10
Ampicillin	0.1	0.1
Tetracycline	0.01	-

Table 2.2.3 Seed and fermentation medium 1 for *E. coli* CAG629 pMG LF9

Component		Concentration (g/L)	Sterilisation method
Bacto-yeast extract powder	A	20	*in situ (1)*
KH_2PO_4		3.8	
Na_2HPO_4		2.5	
$(NH_4)_2SO_4$		3.3	
NaCl		1.5	
$(NH_4)_3C_6H_5O_7$		1.88	
Polypropylene glycol 2025 (PPG)		0.1 ml/L	
Glucose	B	20 / 10 (for seed)	heat (2)
$MgSO_4 \cdot 7H_2O$	C	1.3	heat(3)
$CaCl_2 \cdot 6H_2O$	D	0.14	filter (4)
$FeCl_3 \cdot 6H_2O$		75 mg/L	
$ZnSO_4 \cdot 7H_2O$		18.8 mg/L	
$CoSO_4 \cdot 7H_2O$		7.5 mg/L	
$MnCl_2 \cdot 4H_2O$		2.5 mg/L	
$CuSO_4 \cdot 5H_2O$		3.13 mg/L	
H_3BO_4		0.75 mg/L	
$Na_2MoO_4 \cdot 2H_2O$		62.5 µg/L	
Ampicillin	E	0.1	filter(5)
Tetracycline		0.01	

(1) Sterilisation *in situ* of Components A was performed in the fermenter as described in section 2.3.3.

(2) Component B was separately sterilised at 121°C for 20 minutes.

(3) Component C was separately sterilised at 121°C for 20 minutes.

(4) Component D was separately filter-sterilised using a 0.2 µm Acrodisc (Gelman Science Ltd.).

(5) Component E was separately filter-sterilised using a 0.2 μm Acrodisc (Gelman Science Ltd.).

Table 2.2.4 Fermentation medium 2 for *E. coli* K12 HB101 pMG168

Component		Concentration (g/L)	Sterilisation method
KH_2PO_4 A.R. grade	A	3.0	*in situ(1)*
Na_2HPO_4 A.R. grade		6.0	
NaCl A.R. grade		0.5	
Casamino acids		30.0	
NH_4Cl A.R. grade		4.0	
Glycerol A.R. grade		16.0	
Bacto-yeast extract powder		1.0	
Polypropylene glycol 2025 (PPG) A.R. grade		0.1 ml/L	
$MgSO_4 \cdot 7H_2O$ A.R. grade	B	0.25	heat(2)
$CaCl_2 \cdot 6H_2O$ A.R. grade	C	0.022	filter(3)
L-Proline		0.5	
Thiamine hydrochloride		0.01	
Ampicillin		0.1	

(1) Sterilisation *in situ* of Components A was performed in the fermenter as described in section 2.3.3.

(2) Component B was separately sterilised at 121°C for 20 minutes.

(3) Components C was filter-sterilised using a 0.2 μm Acrodisc (Gelman Science Ltd.).

Table 2.2.5 Seed and fermentation medium 3 and 4 for *E. coli* K12 HB101 pMG168

Component		Concentration			Sterilisation method
		Seed	Fermentation medium		
			3	4	
KH_2PO_4 G.P.R. grade	A	3.0	3.0	3.0	*in situ(1)*
Na_2HPO_4 G.P.R. grade		6.0	6.0	6.0	
NaCl G.P.R. grade		0.5	0.5	0.5	
Standard Yeatex		15.0	20.0	30.0	
NH_4Cl Technical grade		4.0	4.0	4.0	
Glycerol Technical grade		8.0	16.0	16.0	
Polypropylene glycol 2025 (PPG) A.R. grade		-	0.1 ml/L	0.1 ml/L	
$MgSO_4 \cdot 7H_2O$ G.P.R. grade	B	0.25	0.25	0.25	heat(2)
$CaCl_2 \cdot 6H_2O$ A.R. grade	C	0.022	0.022	0.022	filter(3)
L-Proline		0.5	0.5	0.5	
Thiamine hydrochloride		0.01	0.01	0.01	
Ampicillin		0.1	0.1	-	

(1) Sterilisation *in situ* of Components A was performed in the fermenter as described in section 2.3.3.

(2) Component B was separately sterilised at 121°C for 20 minutes.

(3) Components C was filter-sterilised using a 0.2 μm Acrodisc (Gelman Science Ltd.).

2.2.2 Inoculum/seed strategies

Two types of inoculum/seed strategy were used. They were: (1) the low inoculum method; (2) the standard inoculum method.

2.2.2.1 The low inoculum method

Because of the plasmid instability problem resulting from the removal of antibiotic selective pressure by β-lactamase attack early in the fermentation, Pierce and Gutteridge (1985) introduced a so called "tiny inoculum" method (see section 1.2.3). It was decided to apply the low inoculum method to the *E. coli* K12 HB101 pMG 168 system initially in this study where fermentation medium 2 was used (Table 2.2.4). A 10^{-4} - 10^{-3} (v/v) inoculum was used at all scales in this case.

2.2.2.2 The standard inoculum method

The low inoculum method proved to be unsuitable when using fermentation medium 3 and 4 (Table 2.2.5) because of the long lag phase, caused by the introduction of a cheap chemical like Standard Yeatex. The low inoculum method was not applicable when antibiotic was removed in the case of medium 4. Therefore, the standard inoculum method was applied to imitate more closely an industrial scale fermentation. An inoculum size of 3% (v/v %) was used for inoculation at all scales.

2.2.3 Agar plates preparation

LB medium containing bacto-agar (Table 2.2.2 in section 2.2.1) was sterilised in a flask for 20 minutes at 121°C in an autoclave. After autoclaving, and when cooled (below 48°C), quantities of antibiotic for corresponding LB medium volume were made up in deionised water and were added aseptically to the flask through a 0.2 μm sterile filter (Acrodisc, Gelman Science). Plates were made by pouring approximately 20 ml of LB agar medium into each Petri dish.

2.2.4 Starter culture

Starter cultures (10 ml in each Universal) were prepared by making up quantities of components except antibiotic in LB medium (Table 2.1.1 in section 2.2.1) for 10 ml cultures in separate 25 ml universal bottles containing 9 ml of deionised water. The universal bottles were sealed and sterilised for 20 minutes at 121°C in an autoclave. After autoclaving, and when cooled (below 48°C), quantities of antibiotic for 10 ml cultures were made up in 1 ml of deionised water and were added aseptically to each universal bottle through a 0.2 μm sterile filter (Acrodisc, Gelman Science). The low inoculum method was used for inoculation of starter culture in all the cases. The procedure was as follows:

> The glycerol stock culture (0.1 ml, section 2.1.3.1) was used to inoculate a LB starter culture (section 2.2.4), and 0.1 ml of this starter culture was used to inoculate the second starter culture, which was then incubated at 30°C and 200 rpm for 20 hours. This developed culture was then used to inoculate flask culture or fermenters.

2.2.5 Shake flask culture

Shake flask culture experiments were performed for seed culture preparation. They were also used for expression of the recombinant protein whose gene was cloned in a plasmid to check whether the recombinant strains were functional, which was the prerequisite for large scale fermentation, and to reselect recombinant strains (section 2.1.3.2).

2.2.5.1 Shake flask culture used as seed cultures for fermentations

Seed cultures were prepared by making up solution of the components whose sterilisation method is "*in situ*" (Table 2.2.3 and 2.2.5 in section 2.2.1). The medium solution was made more concentrated to account for dilution, i. e. 230 ml of the solution contained the quantities of the "*in situ*" sterilising components for 250 ml of the culture. Two or more of 2L flasks were used (the number of flasks used depended on the size of seed inoculum needed, see section 2.2.2), one of which has a side arm, connecting tubing and needle for inoculation of the fermenter. Each flask containing 230 ml of medium was sealed for sterilisation (121°C, 20 minutes). After autoclaving, and when cooled (below 48°C), quantities of other separately sterilised components (Table 2.2.3 and 2.2.5 in section 2.2.1)

in concentrated solution, 20 ml for 250 ml of culture, were added aseptically to each flask through a 0.2 μm sterile filter (Acrodisc, Gelman Science). The low inoculum method was applied (section 2.2.2.1) and the procedure was as follows:

> Each flask containing seed culture was inoculated from the developed starter culture (section 2.2.4) at an inoculum size of 10^{-3} (v/v), and incubated for 18 hours in an orbital shaker at 30°C and 200 rpm. The developed seed culture was then used to inoculate the fermenter.

2.2.5.2 Shake flask culture for expression of recombinant proteins

Both LB medium and fermentation medium were used (Table 2.2.1, 2.2.3 - 2.2.5 in section 2.2.1) when shake flask culture was performed for expression of recombinant proteins. Both the low inoculum and the standard inoculum methods were used (stated in results section 3 for each experiment). Flask cultures at 50 ml scale (in 400 ml flasks) were performed in most cases. Culture incubation was the same as for seed culture except that a further induction step was carried out. The procedure was as follows:

> Flask cultures were inoculated from the developed starter culture (section 2.2.4) at an inoculum size of 10^{-3} (v/v) in the case of the low inoculum method, or 3% (v/v) in the case of the standard inoculum method. Cultures were grown at 30°C, shaking at 200 rpm to an OD_{600nm} range of 0.2-2, then the culture was induced by heat shock, i.e. the flask was immersed in a 45°C water bath with a sterile thermometer (cleaned with 70% ethanol) monitoring this process and with frequent shaking, until the culture reached 42°C. Induced cells were subsequently grown at 37°C, shaking at 200 rpm.

Cell culture samples were taken before induction and 6 hours after induction. Samples were analyzed by 12.5% - 15% SDS-PAGE (section 2.6.6) and visualised by Coomassie staining (section 2.6.6.2).

2.2.6 Fermentation

Fermentations were performed at a working volume of 14L for the 20L fermenter, 30L for the 42L fermenter and 100L for the 150L fermenter. respectively (LH Fermentation Ltd).

The sterilisation of fermentation medium, Component A (see Table 2.2.2 - Table 2.2.5 in section 2.2.1), was performed in the fermenter at 121^{0}C for 20 minutes with a steam line pressure of 2 barg. The other components of the fermentation medium were sterilised separately (see Table 2.2.2 - Table 2.2.5 in section 2.2.1) and transferred into the fermenter aseptically when the fermenter was cooled.

All ancillaries of the 20L and 42L fermenters, including air inlet filter line, base and antifoam reservoirs and sampling system were separately sterilised in an autoclave at 121^{0}C for 60 minutes with a steam line pressure 2 barg. Inlet air was filtered through a 0.2 μm Pall depth-filter and outlet gas was filtered through a 0.2 μm Pall cartridge filter (Pall Process Filtration Ltd.), which was sterilised with the fermenter. In the case of the 150L fermenter, all these ancillaries were connected to the fermenter and sterilised with the fermentation medium, Component A (see Table 2.2.2 - Table 2.2.5 in section 2.2.1).

Both the low inoculum and standard inoculum methods (section 2.2.2.1 & 2.2.2.2) were used to inoculate the fermenter. The low inoculum method was used in two cases: (1) when fermentation medium 2 (Table 2.2.4) was used, the fermenter was directly inoculated from the developed starter cultures (section 2.2.4) at an inoculum size of 10^{-4} (v/v); (2) when fermentation medium 3 (Table 2.2.5) was used, the fermenter was inoculated from the developed seed cultures (section 2.2.5.1) at an inoculum size of 10^{-3} (v/v). The standard inoculum method was applied when using medium 4 (Table 2.2.5). The starter and seed cultures prepared as inocula still contained antibiotic and applied the low inoculum method in order to retain plasmid stability. The fermenter was inoculated from the developed seed cultures prepared in flasks (section 2.2.5.1) except the 150L fermenter, which was inoculated from the developed seed culture prepared in a 20L fermenter. The inoculum size was 3% (v/v) in all these cases.

The variable set-points given in Table 2.2.6 for different scales of fermentations were used.

Table 2.2.6 Fermentation set-points

Parameters	Fermenters		
	LH 20L	LH 42L	LH 150L
Temperature before induction (^{0}C)	30.0±0.5	30.0±0.5	30±0.5
Temperature at induction point (^{0}C)	41.5-42.0	41.5-42	41.5-42
Temperature after induction (^{0}C)	37.0±0.5	37.0±0.5	37±0.5
Stirrer speed (rpm)	600-1200	400-700	400-475
pH	7.0±0.2	7.0±0.2	7.0±0.2
DOT (%)	≥25	≥25	≥25
Gas flow rate (slpm)	7-12	15-20	50-70

rpm: revolutions per minute.

DOT: dissolved oxygen tension measured as % of air saturation at the fermentation temperature and pressure.

slpm: standard litres per minute.

The induction of cells were carried out as follows: when cell growth (at 30^{0}C) reached an defined induction point (in terms of OD_{600nm}), the stirrer speed was increased to the maximum set point to keep the DOT above 25% at the induction temperature, and steam was introduced through the steam line inside the fermenter in the case of 20L fermenter or through the steam jacket in the case of 42L and 150L fermenters. When the temperature reached 41^{0}C, the steam valve was turned off quickly and the automatic cooling and heating system were turned on. Then temperature set point was changed from 30^{0}C to 37^{0}C. The temperature dropped to 37^{0}C after first increasing to 41.5^{0}C - 42^{0}C, depending on the size of fermenter.

The value of pH was maintained at its setpoint with 4M-NaOH. Sterile polypropylene glycol 2025 (sterilised at 121^{0}C for 20 minutes) was used as an antifoaming agent. The key fermentation environmental variables were monitored and controlled by i3000 series instrumentation on the 20L and 42L fermenters and by i2000 series instrumentation on the 150L fermenter.

The fermentation exit gas was analyzed by a VG MM8-80 scanning magnetic mass spectrometer (VG Gas Analysis Systems Ltd.) for O_2, CO_2, N_2 and Ar concentrations. Oxygen uptake rates, carbon dioxide evolution rates and respiratory quotients were derived from these data. All the data were logged by Bio-I software (BCS Ltd.).

Samples of culture broth were aseptically removed from the fermenter through a sample line for dry weight, optical density, plasmid stability measurements (sections 2.6.1 & 2.6.2) and for SDS-PAGE analysis (section 2.2.6).

2.3 Cell recovery

Cells from a 14L fermentation (in a 20L fermenter) was recovered by centrifugation at 25,000 xg (30,000 rpm) using a Sharples 1P tubular centrifuge (Pennwalt Ltd) with a feed rate of 30 L/h. Ethylene glycol was used for centrifuge cooling.

Cells from a 30L fermentation (in a 42L fermenter) was recovered by centrifugation at 9,500 xg (10,000 rpm) using a Westfalia KDD 605 multichamber centrifuge (Westfalia Separators (U.K.) Ltd), with a feed rate of 60 L/h.

Cells from a 100L fermentation (in a 150L fermenter) was harvested by centrifugation at 20,000 xg (17,000 rpm) using an AS26 tubular centrifuge (Pennwalt Ltd.) with a feed rate of 200 L/h. Ethylene glycol was used for centrifuge cooling.

Cell pastes were frozen at -20^{0}C for homogenisation (section 2.4).

2.4 Cell disruption

An APV Manton Gaulin Lab60 high pressure homogeniser (APV Ltd.) with ethylene glycol cooling was used to disrupt *E. coli* HB101 pMG168. The frozen cell paste, thawed from -20^{0}C overnight, was resuspended to a concentration of 100 g ww (wet weight)/L in homogenisation buffer (see Table 2.4.1 below) using a Silverson mixer-emulsifier (Silverson Machines Ltd.).

Table 2.4.1 Homogenisation buffer

Component	Concentration (M)
Tris-HCl pH 8.0	$5x10^{-2}$
EDTA	10^{-3}
NaCl	$5x10^{-2}$

The cell suspension was subjected to 3 and 5 discrete passes through the homogeniser, with a cell disruption valve assembly, at 550 barg and 5°C. The homogenate was then processed in a lab (3 & 5 passes) or industrial disc stack centrifuge (5 passes) for separation of the inclusion body fraction from cell debris (section 2.5). Samples taken after each pass were centrifuged at 13,400 xg (13,000 rpm) in a Microcentaur centrifuge (MSE Scientific Instruments Ltd.) for 10 minutes at room temperature using a 16x1.5 ml rotor. The supernatant was recovered and stored at -20°C for the measurement of protein concentration to determine the degree of cell disruption.

2.5 Separation of the inclusion body fraction from homogenate of *E. coli* HB101 pMG168

Centrifugation was used to process homogenate **of *E. coli*** HB101 pMG168 obtained from cell disruption step (section 2.4) for separation of inclusion bodies from cell debris. A lab centrifuge or an industrial disc stack centrifuge were employed for this study according to the scale.

2.5.1 Inclusion body separation in a lab centrifuge

The homogenate obtained from 3 and 5 discrete passes through the Lab60 homogeniser (section 2.4) was centrifuged in a MSE 21 centrifuge (MSE Scientific Instruments Ltd) using a 6 x 300 ml rotor with the conditions determined by Olbrich (1989) which were: 2000 xg (4400 rpm) for 26 minutes at 5°C. Highly diluted homogenate (35-fold dilution) was also applied to the lab centrifuge in order to mimic the feed material used in an industrial disc centrifuge (see the next section). The supernatant was collected for SDS-PAGE analysis (section 2.6.6) together with cell homogenate to examine the recovery rate of prochymosin

inclusion body for comparison with the performance in the industrial disc centrifuge (section 2.5.2). The solid fraction, which was washed and solubilised, was applied to a polymeric reverse phase HPLC column (section 2.6.4).

2.5.2 Inclusion body separation in an industrial disc stack centrifuge

In order to study the separation of inclusion bodies from cell debris by centrifugation at a large scale, a Westfalia CSA 8-06-476 high speed stainless steel disc stack centrifuge (Westfalia Separator AG) equipped with a full-hermetic feed zone was employed. Some important centrifuge specifications are listed in Table 2.5.1, and referred to Figure 1.4.2 and Equation 1.4.18 in section 1.4.2.3.1.

Table 2.5.1 Disc stack centrifuge design specifications

Parameter	Value
Feed type	hermetic
Bowl speed, n (rpm)	9350
Number of discs, z	71
Half disc opening angle, θ	38^0
Outer disc radius, R_a (m)	0.076
Inner disc radius, R_0 (m)	0.036
Caulk type	long
Number of caulks, z_L	8
Caulk width, b_L (m)	0.006
Caulk height (gap width), h (mm)	0.5

rpm : revolutions per minute, $\omega = \pi n/30$

The experimental procedure, illustrated in Figure 2.5.1, was summarised as follows:
Cells of *E. coli* HB101 pMG168 (2.4 kg) were suspended in 22L homogenisation buffer and subjected to 5 discrete passes through the homogeniser (section 2.4). The homogenate obtained was diluted to give a volume of 700L in a 1000 Litre Chemap fermenter used as a feed vessel (Chemap AG). The final concentration of particle in terms of optical density

Figure 2.5.1 Schematic diagram for recovery of inclusion bodies by an industrial disc stack centrifuge

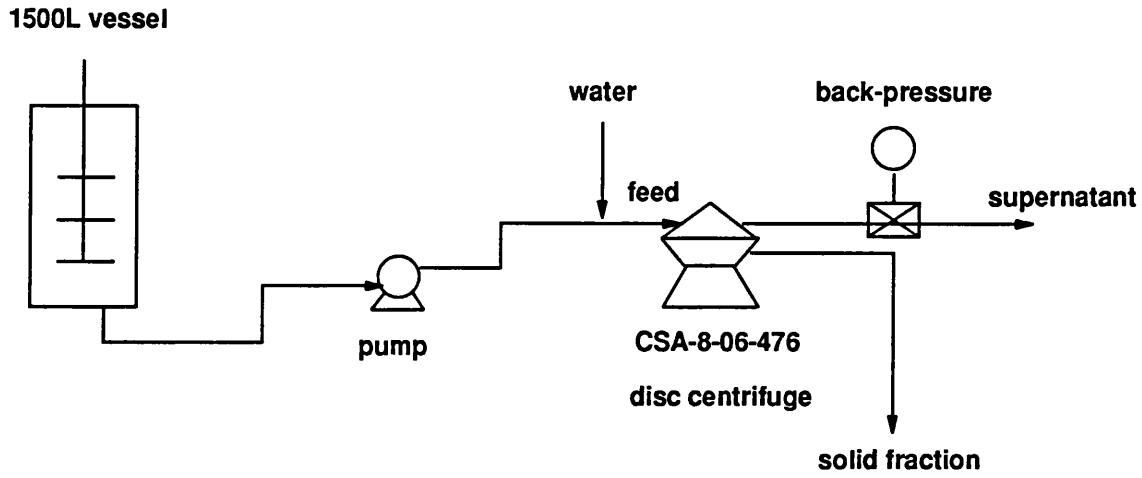

was: OD_{600nm} = 0.965; OD_{420nm} = 1.497. The stirrer was run to give a homogeneous feed to the centrifuge, and when the volume of homogenate was below 300L, air was introduced to sustain mixing. A magnetic-inductive flowmeter (Turbo AG, Germany) was used for measuring the feed rate. Because of measurement limit of the flowmeter (maximum 600 L/h), flow rates beyond 600 L/h were calibrated by weighing the supernatant per unit time. The flow rates below 600 L/h were also calibrated in the same way for comparison. A gear pump, on-line controlled by the inductive flowmeter and manual calibration, was used to provide accurate and constant flow rates. Seven throughput settings in the range of 200 - 1100 L/h were examined. The order of these throughputs to avoid time-depend errors was: 228 L/h, 518 L/h, 760 L/h, 1100 L/h, 920 L/h, 460 L/h and 540 L/h. For each throughput, the first sample of supernatant was taken when the feed volume, which was carried through the separator, was 10 times as much as the bowl volume (3L), i.e. 30 L in volume. The subsequent samples were taken when 45L, 60L, 75L and 90L of the feed had passed through the separator. In order to avoid cross contamination, the separator was discharged and clean water passed after each throughput. Samples from the supernatant were subjected to optical measurement at two wavelengths (600nm and 420nm), and were analyzed by gel electrophoresis to determine the recovery rate of inclusion body proteins and the removal of cell debris proteins.

2.6 Assay material and methods

2.6.1 Biomass measurements

2.6.1.1 Optical density measurements

Cell growth during shake flask culture or fermentation was determined by measuring the optical density of the culture at 600 nm against a water blank through a Perspex cuvette (1 cm path length) in an UV/visible spectrophotometer. Culture broth was diluted with a 0.7 w/v % NaCl solution to give an OD_{600nm} reading in the range of 0-0.5 OD. All measurements were duplicated.

2.6.1.2 Dry weight measurements

Micro-test tubes (1.5 ml) were placed in an oven at 105°C for at least 24 hours before being transferred to a desiccator to cool and then weighed. Samples (1.5 ml) from a shake flask culture or a fermentation were placed in a preweighed tube, then centrifuged at 13,400 xg (13,000 rpm) for 10 minutes at room temperature in a Microcentaur centrifuge (MSE Scientific Instruments Ltd.) using a 16 x 1.5 ml rotor. The tube was then removed and the supernatant was carefully withdrawn using a plastic Pasteur pipette. A solution (1 ml) of 0.7 w/v % NaCl was added to the tube and the pellets were resuspended. The tube was centrifuged as before and the supernatant was again withdrawn. The tube was then dried for at least 24 hours before being reweighed. All measurements were duplicated.

2.6.2 Measurement of plasmid stability

Samples from a shake flask culture or a fermentation were diluted with sterile LB medium (Table 2.2.1) and plated onto a LB agar plate (section 2.2.3) without antibiotic. After incubating at 30°C for 24 hours, 100 single colonies were picked onto both LB agar plates containing antibiotic and LB agar plates without antibiotic as control. The number of colonies resistant to the antibiotic was expressed as a percentage of the number growing on the LB agar plate without antibiotics, and was taken to represent the proportion of the population which carried the plasmid.

2.6.3 Protein concentration measurement

The assay for protein concentration was performed by using BCA protein assay reagent (Pierce and Warriner (U.K.) Ltd.). The reason for choosing BCA protein assay reagent is its great tolerance towards some detergents like SDS (up to 1%). Therefore, it is suitable to be used for measurement of insoluble protein concentration, where insoluble proteins are dissolved in some strong detergents like SDS (no more than 1%).

The BCA protein assay reagent includes:

(1) Reagent A solution which contains sodium carbonate, sodium bicarbonate, BCA detection reagent and sodium tartrate in 0.2N NaOH

(2) Reagent B solution which is 4% copper sulphate

The Working Reagent are made by mixing 50 parts of Reagent A and 1 part of Reagent B before assay. The protein standard used is the supplied 2mg/ml solution of purified Bovine Serum Albumin (BSA).

2.6.3.1 Soluble protein assay

The soluble protein samples were the supernatants of homogenate obtained from different passes through the homogeniser(section 2.4). They were assayed to determine the degree of cell disruption. The procedure was as follows:

(1) A set of protein standards of known concentration (0.2 mg/ml - 1.2 mg/ml) was prepared by diluting the BSA standard solution with 15-20 fold diluted homogenisation buffer (Table 2.4.1 in section 2.4) to maintain the same diluent as the samples. The samples (in homogenisation buffer) were 15-20 fold diluted with water to fall in the range of the standard protein concentration.

(2) 0.15 ml of each standard or sample was pipetted into each cuvette, (for blank, 0.15 ml of 15-20 fold diluted homogenisation buffer was used), and 3 ml of working reagent (50 part of Reagent A, 1 part of Reagent B) was added to each cuvette and mixed well.

(3) All cuvettes were incubated at 37^{0}C for 30 minutes.

(4) After incubation, when all cuvettes were cooled to room temperature, the absorbance at 562 nm of each cuvette was measured against water.

(5) The absorbance of the blank was subtracted from each value of standard or sample.

(6) A standard curve was made by plotting the net (blank corrected) absorbance at 562 nm vs. known protein concentrations. The protein concentration of samples was determined by using this standard curve.

2.6.3.2 Insoluble protein assay

The procedure for measuring insoluble protein concentration was the same as for soluble protein (see last section), except that the insoluble protein samples had to be dissolved in sample buffer (1% SDS/50 mM Tris-HCl pH 7.9), and the sample buffer was used as diluent for preparation of standard protein of known concentration.

2.6.4 Chromatography of the inclusion body fraction

2.6.4.1 Chromatography equipments

Experiments were performed using a Perkin Elmer binary pump 250, Perkin Elmer LC1 Laboratory Computing Integrator (Perkin Elmer), LKB Bromma 2510 Uvicord SD UV detector (Pharmacia Ltd.) and Rheodyne 7125 injector valve (Rheodyne). Columns were packed using a Shandon HPLC packing pump (Shandon Southern Products Ltd.).

2.6.4.2 Reverse phase HPLC system and operation conditions

The stationary phase material was PLRP-S 300, 15-25 μm, obtained from Polymer Laboratories Ltd., Church Stretton, Shropshire, U.K. It was packed into a 50x4.6 mm analytical column and a 50x10.8 semi-preparative column by slurring the material in a solution of acetonitrile:water = 4:1, sonicated for 5 minutes and packed at a pressure of 4000 psi. Gradient elution was used with the mobile phase of 25 mM KH_2PO_4/2M urea as solvent A, and 40 mM KH_2PO_4/50% acetonitrile as solvent B, with a gradient of 60% solvent B to 100% solvent B over 15 minutes, 100% solvent B for 15 minutes.

Chromatography was performed at 60°C in a water bath. Solvents were filtered using 0.45 μm nitrocellulose filters (Whatman Labsales Ltd.) and were degassed with helium for 10 minutes. Sample was applied to the column via a 100 μl injection loop and eluted with a solvent gradient. Solute elution was monitored at 226 nm and the UV signal was processed using the integrator mentioned in section 2.6.4.1.

2.6.4.3 Sample preparation

Samples for the reverse phase HPLC analytical and semi-preparative column were prepared by dissolving prochymosin inclusion bodies (obtained from cell homogenisation followed by centrifugation in a lab centrifuge, see section 2.5.1) in a solubilisation buffer at room temperature for 8 hours. The solubilisation buffer was 8M urea/50 mM KH_2PO_4 with pH 10.7. Samples were filtered using Millipore type HV 0.45 μm filters (Millipore).

The prochymosin standard was a gift from Celltech. It was diluted into the same solubilisation buffer, 8M urea/50 mM KH_2PO_4 of pH 10.7 and filtered as for samples.

2.6.5 Characterisation of prochymosin inclusion bodies and cell debris

2.6.5.1 Photon correlation spectroscopy (PCS)

A Malvern P4700 sub-micron particle size analyser (Malvern Instruments) was used to characterise prochymosin inclusion bodies and cell debris obtained from section 2.5.1, i.e. samples were obtained after particle classification step in a lab centrifuge (MSE 21). Samples of cell debris and inclusion bodies (a few drops) were analyzed by PCS in a 3 ml glass cuvette. The scattered light was detected by a photomultiplier and the signal was sent to a correlator. The data was analyzed using a computing accessory software system (autosizer, Malvern instruments). Each sample was analyzed at least 5 times. The actual type of distribution obtained from the PCS measurement was a scattered intensity distribution which was measured at 90°. This intensity distribution can be converted to a number distribution and the volume distribution can be obtained from the number distribution. All these conversions were done by the software system.

2.6.5.2 Centrifugal disc photosedimentation (CPS)

A centrifugal disc photosedimentometer BI-DCP (Brookhaven Instruments Corporation) was used to characterise the whole homogenate (5 passes through homogeniser, see section 2.4) and cell debris from centrifugation in a lab centrifuge (MSE 21).

The samples were run in a spin fluid of 15 ml of 10% sucrose with a buffer fluid of 1 ml of water by the external gradient (EG) method, recommended in the "Instruction Manual" for this instrument, in order to avoid unstable sedimentation. This new EG method was much simpler compared with the older one which was used by Olbrich (1989). The procedure of EG method was as follows:

> First, 15 ml of spin fluid was drawn up into a syringe. With the syringe pointed down, the buffer liquid was drawn, and partial mixing took place forming the gradient when the lighter buffer rose up through the denser spin fluid. The partially mixed liquids in the syringe were injected simultaneously into the disc which was spinning at a constant speed. The gradient was maintained by the centrifugal force. Then 0.25 ml of sample was injected onto the surface of the spin fluid.

As particles passed through the light beam (white light from a tungsten/halogen lamp), the light intensity was extinguished due to scattering and absorption. The transmitted light was measured by a photodiode and recorded by the computer as a function of time. The data were analyzed by the DCP data system.

2.6.6 Sodium dodecyl sulphate-polyacrylamide gel electrophoresis (SDS-PAGE)

2.6.6.1 Materials for SDS-PAGE analysis

A Bio-Rad PROTEAN II slab cell and a Bio-Rad Mini PROTEAN II slab cell (Bio-Rad Laboratories Ltd.), vertical slab electrophoresis instrument, were used with an EPS 400/500 power unit (Pharmacia Ltd.). Discontinuous gels which consist of a resolving gel and a stacking gel were used in all gel analysis. The formulation for discontinuous gels (Creighton, 1990) is listed in Table 2.6.1. The formulation of running buffer, staining and destaining solution is given in Table 2.6.2.

Table 2.6.1 Formulation of resolving and stacking gels

Component	Resolving gel*			Stacking gel
	12.5%	13.5%	15%	4%
Acrylamide/Bis(30%)[1]	12.5 ml	13.5 ml	15 ml	2.7 ml
1.5M Tris-HCl pH 8.8[2]	7.5 ml	7.5 ml	7.5 ml	-
0.5M Tris-HCl pH6.8[3]	-	-	-	5 ml
10% SDS[4]	0.3 ml	0.3 ml	0.3 ml	0.2 ml
10% Ammonium persulfate[5]	0.1 ml	0.1	0.1 ml	0.1 ml
TEMED[6]	0.02 ml	0.02 ml	0.02 ml	0.02 ml
Deionised water	9.6 ml	8.6 ml	7.1 ml	12 ml
Total volume[7]	30 ml	30 ml	30 ml	20 ml

* Resolving gel with 12.5%, 13.5% and 15% of acrylamide/bis were used for comparison of the resolution of protein species of interest.

1. Acrylamide/Bis(30%): 29.2 g acrylamide and 0.8 g bisacrylamide were dissolved into deionised water and made up to 100 ml. The solution was then filtered through Whatman No.1 filter paper (Whatman Labsales Ltd.) and stored at 4^{0}C in a bottle wrapped with aluminium foil.
2. 1.5M Tris-HCl pH 8.8: 18.2 g of Tris was dissolved in about 80 ml of water and adjusted to pH 8.8 with 6M HCl, made up to 100 ml. This buffer was then filtered through Whatman No.1 filter paper and stored at 4^{0}C.
3. 0.5M Tris-HCl pH 6.8: 6.1 g of Tris was dissolved in about 80 ml of water and adjusted to pH 6.8 with 6M HCl, calibrated to 100 ml. This buffer was then filtered through Whatman No.1 filter paper and stored at 4^{0}C.
4. 10% SDS: 10 g of SDS was dissolved in water and brought to 100 ml, and stored at room temperature.
5. 10% Ammonium persulfate: This solution was freshly made before casting gels.
6. TEMED: N, N, N', N'- tetramethylethylenediamine was stored at 4^{0}C.
7. Total volume: 30 ml of resolving gel and 20 ml of stacking gel were for one gel with size of 20x16x0.075 cm (length x breadth x width) or for six mini gels with the size of 7.3x8x0.075 cm (length x breadth x width) each.

Table 2.6.2 Formulation of running buffer, staining and destaining solutions

5X Running buffer stock pH 8.3 *	1 L solution containing: 15g Tris base 72g Glycine 5g SDS
Staining solution	1 L solution containing: 417 ml water 417 ml methanol 167 ml acetic acid 1 g Coomassie blue G-250
Destaining solution	1 L solution containing: 600 ml water 300 ml methanol 100 ml acetic acid

* Running buffer stock was 5-fold diluted before use.

2.6.6.2 Operation of SDS-PAGE

As mentioned earlier, discontinuous gels, consisting of a resolving gel (lower) and a stacking gel (upper) were used for all analysis in this study. The stacking gel acted to concentrate large sample volumes, resulting in better band resolution than was possible using the same volume on a gel without a stack. The procedure of operating SDS-PAGE with the gel size of 20x16x0.075 cm (length x breadth x width) and with the mini-gel size of 7.3x8x0.075 cm (length x breadth x width) were the same, as follows:

(1) The stock solutions listed below Table 2.6.1 were prepared.

(2) Glass plates were cleaned with ethanol or methanol, and assembled.

(3) A comb was completely placed into the assembled gel sandwich, and a mark was made on the glass plate 2 cm below the teeth of the comb for the big gel, and 1 cm below the teeth of the comb in the case of a mini-gel. The comb was then removed. This was the level to which the resolving gel was poured.

(4) Resolving gel solution was made according to the formulation in Table 2.6.1 using all the stock solutions except 10% Ammonium persulfate (APS) and TEMED, and the solution was degassed for 10 minutes by a water vacuum pump.

(5) APS(10%) and TEMED were added to the degassed resolving solution, gently mixed and the solution was slowly poured into the assembled gel sandwich until to the mark. For a mini-gel, a glass pipette and bulb was used to pour the gel solution.
(6) Water was immediately overlaid on the top of resolving gel with a glass pipette and bulb and it was done with great care, i.e. using a steady , even rate of delivery to prevent mixing.
(7) The resolving gel was allowed to polymerize for at least 40 minutes for a large gel, and 20 minutes for mini gel before the stacking gel solution was poured.
(8) The stacking gel solution was prepared in the same way as for the resolving gel, i.e. step (4) and (5) were repeated.
(9) The top of the polymerized resolving gel was rinsed with deionised water and the area above the resolving gel was dried completely with filter paper before the stacking gel solution was poured.
(10) A comb was placed in the gel sandwich at a slight angle (~ 10^0) to prevent air from being trapped under the comb teeth while pouring the stacking gel.
(11) Stacking gel solution was poured from the upturned comb side until all the teeth were covered by the solution. Then the comb was properly aligned and more stacking gel solution was added to fill the space completely.
(12) The stacking gel was allowed to polymerize for 30 minutes, and the comb was pulled out gently, the wells were rinsed with running buffer (Table 2.6.2) immediately.
(13) The gels were then ready and were attached to the central water-cooling core. Running buffer were filled into the upper reservoir.
(14) Prepared samples (see section 2.6.6.3) were loaded into the wells using a 100 µl microsyringe which was washed with the running buffer between samples.
(15) After sample loading, the core was quickly placed in the electrophoresis tank with the running buffer. An EPS 400/500 power unit provided a constant current of 20 mA to the gels.
(16) On completion of electrophoresis, the gels were removed and the stacking gel was cut away. The resolving gel was placed in staining solution (Table 2.6.2) for at least 1 hour. The gel then was destained with destaining solution (Table 2.6.2) and the developed gel was subjected to subsequent analysis (section 2.6.6.4- 2.6.6.5).

2.6.6.3 Sample preparation for SDS-PAGE

The sample buffer used for preparation of samples for gel loading was given in Table 2.6.3.

Table 2.6.3 Formulation of sample buffer for SDS-PAGE

Component	Concentration
Tris-HCl pH6.8	62.5 mM
Glycerol	10%
2-mercaptoethanol	5%
or DTT	10 mM
SDS	2.5%
Bromophenol blue	0.05%

The sample buffer was stored at -20°C.

In the initial study, the procedure of sample preparation was as follows:

(1) 1 OD_{600nm} cells were removed from a culture and placed into 1.5 ml microfuge tubes. Cells were spun at 13,400 xg (13,000 rpm) for 10 minutes at room temperature in a Microcentaur centrifuge (MSE Scientific Instruments Ltd.) using a 16 x 1.5 ml rotor. Supernatant was removed.

(2) The pellets were resuspended in 1 ml deionised water, and the centrifuged repeated as in step (1), Supernatant was discarded.

(3) The washed pellets were suspended in 50 µl sample buffer (Table 2.6.3), and were boiled in 100°C water for 10 minutes.

(4) Boiled samples were spun for 2-3 minutes, the supernatant was transferred to a clean microfuge tube, and the supernatant was loaded on the gel after cooling down to room temperature.

Inclusion body preparation (Field, 1988) was also carried out to enhance the visibility of expressed recombinant foreign protein band. The procedure of inclusion body preparation was as follows:

(1) Cells (1 OD_{600nm}) were removed from a culture, harvested and resuspended in 45

μl of cold lysis buffer (100 mM Tris-HCl pH 7.5/ 5 mM EDTA/ 270 $\mu g.ml^{-1}$ lysozyme) with 2 μl of 5 mM phenylmethylsulphonyl fluoride (PMSF, Made fresh in 90% methanol)

(2) Incubation was on ice for 5 minutes.

(3) 2.5 μl of 4% deoxycholic acid (sodium salt) in lysis buffer were added to a final concentration of 0.2%, and incubated for 10 minutes on ice.

(4) 2 μl of 1 $mg.ml^{-1}$ DNase I (in 0.15 M NaCl + glycerol solution) and 0.5 μl 1M magnesium chloride were added, mixed and incubated for 10 minutes on ice.

(5) The insoluble material was separated from the soluble material by centrifugation at 13,400 xg (13,000 rpm) for 10 minutes in a Microcentaur centrifuge (MSE Scientific Instruments Ltd.) using a 16 x 1.5 ml rotor.

(6) The pellets were washed with 45 μl of 2% Triton X-100 in Tris-EDTA solution (100 mM Tris-HCl pH 7.5/ 5 mM EDTA), and then washed with 45 μl of water.

(7) The insoluble material was then ready for gel analysis (dissolved in sample buffer, Table 2.6.3) or for applying to the reverse phase HPLC analytical column (section 2.6.4.3).

In the initial gel analysis, samples obtained by the above two methods always resulted in a problem of gel streaking. This could be caused by several factors, for example, the existence of some salts like potassium ions (Hames and Rickwood,1987) in the samples, which precipitating SDS. Lipid and DNA in the samples also interfered with electrophoresis.

It was decided to apply the method of TCA (trichloroacetic acid) precipitation of proteins (Creighton, 1990) to solve the streaking problem. The procedure of this method was as follows:

(1) Cells (0.5 mg) in culture broth contained in a 1.5 ml microfuge tubes were spun down and resuspended in 1 ml of deionised water, 333 μl of 100% TCA solution was added to give final concentration of 25% TCA, then incubated at 4^0C for at least 2 hours.

(2) The precipitated proteins were obtained by centrifugation at 13,400 xg (13,000 rpm) for 7 minutes. The supernatant was discarded.

(3) 1 ml of acetone/5 mM HCl solution was added to the pellets, which were then resuspended by vortex mixing.

(4) Pellets were spun down as in step (2), the supernatant was discarded, and 1 ml

of acetone was added. The pellets were resuspended by vortex mixing again and recovered as in step (2).

(5) The pellets were dried in a speed vacuum desiccator (Savant, Speed vac sc 100) for 15 minutes, and were ready to be dissolved in sample buffer (Table 2.6.3) for gel analysis.

2.6.6.4 Quantitation of protein species on SDS-gels

Developed gels were either scanned using an LKB XL laser densitometer (Pharmacia Ltd.), which measured Coomassie Blue absorbance at 660 nm or the method of elution of Commassie Blue from stained protein bands for spectrophotometric measurement was applied (Ball, 1986).

The method of quantitation of protein by elution of dye from stained bands is described below:

The standard protein in a BCA reagent kit (BSA) (section 2.6.3) was used for creating standard curve of absorbance vs. protein quantities. A set of known amounts of standard protein (BSA) in the range of 0.25 μg - 10 μg were loaded on a gel (section 2.6.6.2). After the gel was developed, this set of protein bands corresponding to known protein quantities were cut out and each gel piece containing one band was put into a 1.5 ml microfuge tube respectively, then 1 ml of an extracting solution (3% SDS in 50% iso-propanol) was added to each microfuge tube. These microfuge tubes were incubated in a 37^{0}C water bath for 24 hours without agitation. After incubation, and when cooled to room temperature, the liquid in each microfuge tube was recovered and put in a 1 ml cuvette, the optical density was then measured at a wavelength of 595 nm against water. The extracting solution was used as a blank. The absorbance of the blank was subtracted from each value of the standard. A standard curve was made by plotting the net (blank corrected) absorbance at 595 nm vs. known protein quantities.

Unknown bands (in terms of quantity) were cut out and subjected to exactly the same procedure as for standard protein bands as described above, then the protein quantity of each band was determined by using the standard curve.

2.6.6.5 Gel elution method for purification of protein species

The method of elution of proteins from SDS-polyacrylamide gels was developed by Hager and Burgess (1980). It was applied in this study for purification of prochymosin standard obtained from Celltech. The procedure was as follows: prochymosin standard (2 ml at 1 mg/ml) was diluted with 2 ml of sample buffer (Table 2.6.2), and mixed and 3 ml of this sample was loaded into a single well on a preparative gel with dimensions 20x16x0.15 cm. After the gel was developed (section 2.6.6.2), the major band was cut out and chopped into small pieces with a razor blade and placed in four 0.5 ml microfuge tubes. The bottom of each microfuge tubes was punctured with a needle (3 holes was made for each one). Each microfuge tube was placed inside a 2 ml eppendorf vial, which was then spun for 2 minutes at 13,400 xg (13,000 rpm) in a Microcentrifuge. The disintegrated gel particles in each eppendorf vial were then resuspended with 1.5 ml protein elution buffer (see Table 2.6.4), which was vortexed and incubated overnight at 25°C.

Table 2.6.4 Protein elution buffer

Component	Concentration
SDS	0.1%
Tris-HCl pH 7.9	0.05 M
EDTA	0.1 mM
DTT	5 mM
NaCl	0.15 M

After incubation, the vials were spun for 10 minutes at 13,400 xg (13,000 rpm) in a Microcentrifuge and the supernatants removed and placed in four fresh 1.5 ml Eppendorf tubes. The rest of the supernatant remaining in the disintegrated gel pieces was recovered in the following way: the gel slurry was decanted into a syringe, which had been plugged at the outlet with a small glass ballotini beads and piece of glass wool, then the syringe plunger was forced down onto the gel and the supernatant collected. the collected supernatant was added to the supernatant obtained earlier and the total supernatant was subjected to TCA precipitation (section 2.6.6.3). The eluted prochymosin was analyzed by SDS-PAGE for purity, and subsequently used as the standard in electrophoresis.

2.6.7 Determination of acetate concentration

Acetate concentration in the fermentation broth was determined using a test kit supplied by Boehringer Mannheim following their recommended procedure.

The determination of acetate is based on the formation of NADH measured by an increase in absorbance at 340nm produced during the series of 'coupled' reactions presented below:

(1) $Acetate + ATP + CoA \xrightarrow{ACS} acetyl\text{-}CoA + AMP + pyrophosphate$

where ACS = acetyl-CoA synthetase

(2) $Acetyl\text{-}CoA + oxaloacetate + H_2O \xrightarrow{CS} citrate + CoA$

where CS = citrate synthase

(3) $Malate + NAD^+ \overset{MDH}{\rightleftharpoons} oxaloacetate + NADH + H^+$

where MDH = malate dehydrogenase

3. RESULTS

3.1 Shake flask culture and fermentation with antibody fragments expression system

3.1.1 Shake flask culture for expression of antibody Gloop2 fragments

3.1.1.1 Expression of antibody Gloop2 V_L in *E. coli* CAG629 pMG LF9 at 50ml and 1L scale using LB medium

In order to check whether the plasmid pMG LF9 in *E. coli* CAG629 was functional, shake flask cultures at 50ml and 1L scale were performed. This was a prerequisite of scale-up work. These two shake flask cultures were inoculated from developed starter cultures using the standard inoculum method, detailed in section 2.2.5.2. The induction points and final cell densities (6 hours after induction) are shown in Table 3.1.1.

Table 3.1.1 Induction points and final OD readings for shake flask cultures of *E. coli* CAG629 pMG LF9 using LB medium

Culture scale	OD_{600} (induction)	*Final OD_{600}
50ml	0.8	2.92
1L	0.96	2.52

*Final OD_{600} : OD reading 6 hours after induction

Samples were taken before induction and 6 hours after induction and applied to SDS-PAGE analysis (section 2.6.6). SDS-PAGE (12.5%) of cell samples were visualised by Coomassie staining (section 2.6.6.2). Gloop2 V_L protein was visible at 9 KDa (see Figure 3.1.1).

This experiment demonstrated that the Gloop2 V_L gene was expressed when LB medium was used. However, the cell density achieved was very low (Table 3.1.1). In order to achieve high cell density, seed and fermentation medium 1 (Table 2.2.3 in section 2.2.1) was chosen for cell growth. Before carrying out fermentation, it was necessary to perform shake flask

Figure 3.1.1 Expression of V_L from pMG LF9 in *E. coli* CAG629 at 50ml and 1L scale using LB medium

Samples were taken before induction and 6 hours after induction, and analyzed by 12.5% SDS-PAGE and visualised by Coomassie staining.

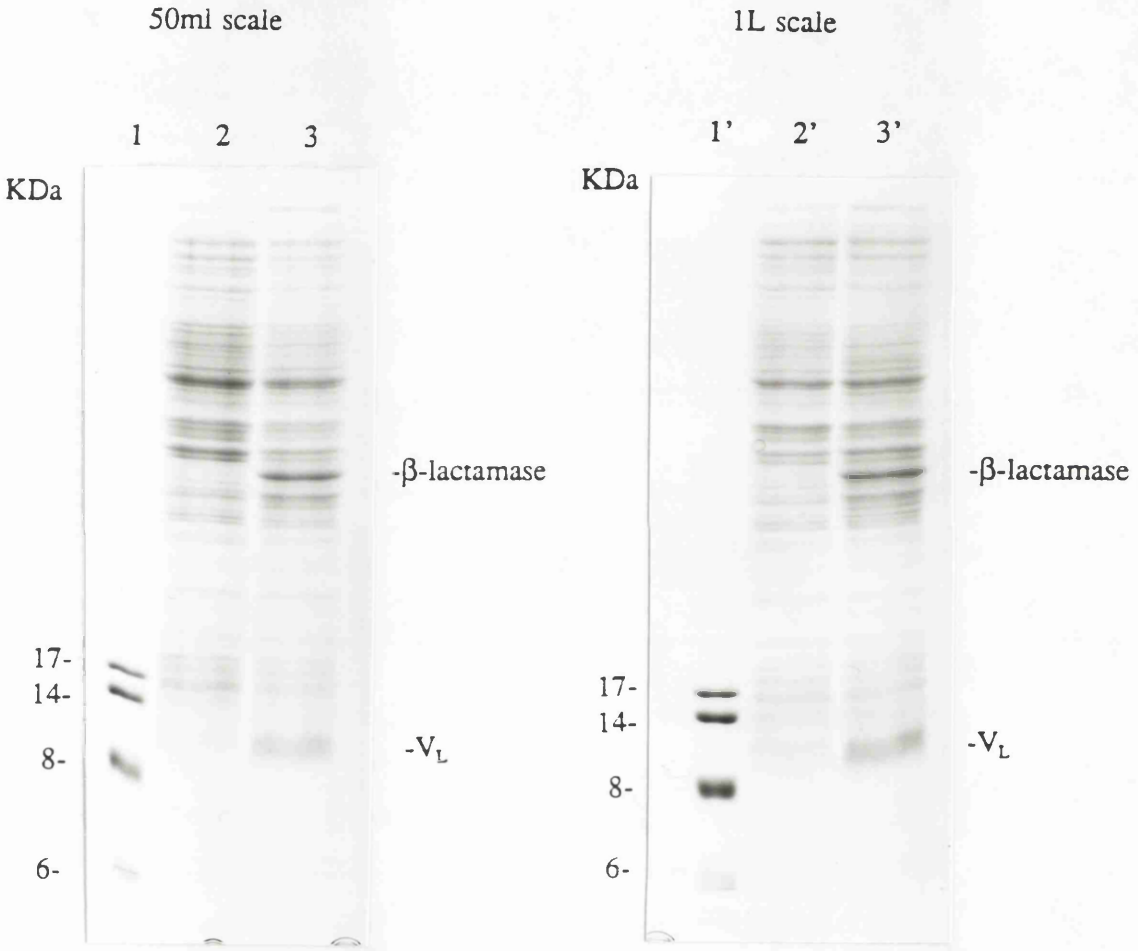

Lane 1 and Lane 1': Protein Marker

Lane 2 and Lane 2': Cells before induction

Lane 3 and Lane 3': Cells 6 hours after induction

culture to check whether the expression of V_L gene in plasmid pMG LF9 can be achieved by using seed medium 1.

3.1.1.2 Expression of antibody Gloop2 V_L in *E. coli* CAG629 pMG LF9 at 50ml scale using seed medium 1

In this experiment, seed medium 1 (Table 2.2.3 in section 2.2.1) was used for shake flask culture at 50 ml scale. The objective was mentioned in the last section. A set of shake flask cultures was run at 50ml scale, where the standard inoculum method were applied (section 2.2.5.2) and shake flask culture with LB medium was used as control in all cases. The expression of V_L gene was achieved in all control flask cultures with LB medium, but only one shake flask culture with seed medium 1 showed expression of V_L. The results are summarised in Table 3.1.2.

Table 3.1.2 Induction points, final OD readings and expression for shake flask cultures of *E. coli* CAG629 pMG LF9 using seed medium 1, with LB medium as control

Run No.	Culture medium	Induction point OD_{600}	*Final OD_{600}	Expression
1	Seed medium 1	5.5	8.5	NO
	Seed medium 1	No induction	11.7	-
	LB medium	0.9	3.6	YES
2	Seed medium 1	0.9	7.0	NO
	Seed medium 1	No induction	12.0	-
	LB medium	0.8	2.6	YES
3	Seed medium 1	0.8	5.6	YES
	LB medium	0.7	2.9	YES

*Final OD_{600} : OD reading 6 hours after induction. In Run 1 & 2, where one flask culture was not induced in each case, OD reading was at the same time as for induced cells.

In run 1, cells were induced at an OD_{600} of 5.5, about half of the final OD reading. The reason for choosing a later stage during growth for induction was to get high cell density, because the thermal induction would kill some cells and expression of a foreign protein would affect cell viability (Wright *et al.*, 1986). However, it was hard to see any V_L expressed, while the control flask culture with LB medium exhibited expression of V_L (SDS-PAGE picture not shown). The lack of expression in medium 1 might be the result of poor oxygen transfer in shake flask culture especially when the cell density was high. It might also be a consequence of the induction point. When the cell density was high (OD_{600} of 5.5 in seed medium 1 compared with OD_{600} of 0.9 in LB medium), heat transfer might be not efficient when using water bath for induction by temperature change (section 2.2.5.2). So it was decided to carry out the shake flask culture of Run 2 (see Table 3.1.2), in which cells were induced at approximately the same OD_{600} (0.9) as for control flask culture with LB medium. However, there was still no expression of V_L for seed medium 1 but expression was obtained for LB medium (SDS-PAGE picture not shown). Surprisingly, the final OD_{600} for seed medium 1 was still high, only a little bit lower than that induced at an OD_{600} of 5.5 in Run 1 (Table 3.1.2). This might meant that the temperature shift (residence time at 42^0C) for induction was not long enough.

Therefore, the shake flask culture of Run 3 was performed, where heat induction was carried out in such a way that culture of seed medium 1 remained at 42^0C longer than the previous ones. This time, expression of V_L in both of LB medium and seed medium 1 was achieved (see Figure 3.1.2). However, this could not be repeated in subsequent flask cultures, which indicated that there were more complicated reasons behind these results.

Figure 3.1.2 Expression of V_L from pMG LF9 in *E. coli* CAG629 at 50ml scale using seed medium 1 and using LB medium as control

Samples were taken before induction and 6 hours after induction, and analyzed by 12.5% SDS-PAGE and visualised by Coomassie staining. The inclusion body preparation (section 2.6.6.3) was applied to samples from LB medium (lane 3 - Lane 6).

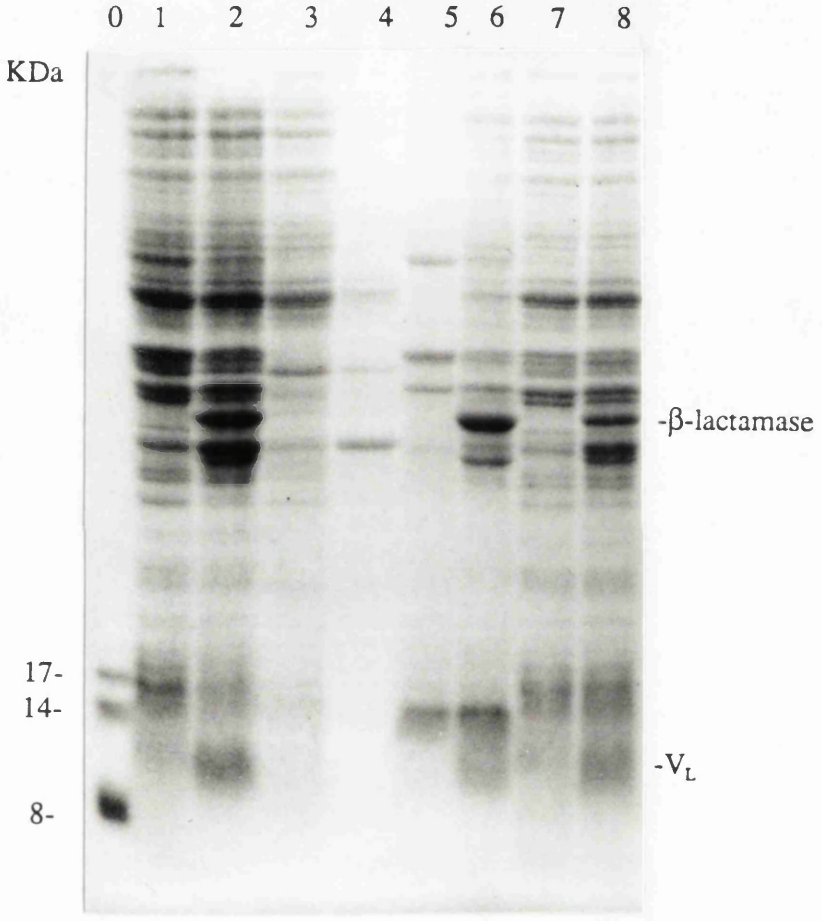

Lane 0 : Protein Marker

Lane 1 : Cells before induction (from LB medium)

Lane 2 : Cells 6 hours after induction (from LB medium)

Lane 3 : Soluble fraction of uninduced cells (from LB medium)

Lane 4 : Soluble fraction of induced cells (from LB medium)

Lane 5 : Insoluble fraction of uninduced cells (from LB medium)

Lane 6 : Insoluble fraction of induced cells (from LB medium)

Lane 7 : Cells before induction (from seed medium 1)

Lane 8 : Cells 6 hours after induction (from seed medium 1)

3.1.1.3 Expression of antibody Gloop2 V_H in *E. coli* CAG629 pPW HF2 at 50 ml scale using LB medium

In the antibody fragment expression system, Gloop2 V_H was cloned in plasmid pPW HF2. Shake flask cultures of *E. coli* CAG629 pPW HF2 were carried out using LB medium at the first step for the same purpose as that for the V_L.

The procedure of flask culture and sampling was exact the same as for V_L. The results are summarised in Table 3.1.3.

Table 3.1.3 Induction points and final OD readings for shake flask cultures of *E. coli* CAG629 pPW HF2 at 50ml scale using LB medium

Flask No.	OD_{600} (induction)	*Final OD_{600}
1	0.86	2.50
2	0.80	2.20

*Final OD_{600} : OD reading 6 hours after induction

Samples were taken before induction and 6 hours after induction and applied to 12.5% SDS-PAGE analysis (2.6.6). Because of the low expression level of V_H, it was difficult to see the V_H band in the whole cell protein (Lane 2 and Lane 2' in Figure 3.1.3). Inclusion body purification was carried out by the method called inclusion body preparation, fractionating cells into soluble and insoluble phases (section 2.6.6.3). V_H was then seen in the insoluble fraction of the induced cells at 11 KDa (Lane 4 and Lane 4' in Figure 3.1.3).

Because of the problem of expression of V_L in seed medium 1 as discussed in the last section, there was no point in performing shake flask cultures for expression of V_H gene by using seed medium 1 at this stage. The next step was to study fermentations of V_L gene expression system.

Figure 3.1.3 Expression of V_H from pPW HF2 in *E. coli* CAG629 at 50ml scale using using LB medium

Samples were taken before induction and 6 hours after induction, and analyzed by 12.5% SDS-PAGE and visualised by Coomassie staining. The inclusion body preparation (section 2.6.6.3) was applied to samples because of the low expression level of V_H. V_H band is hardly visible in the induced whole cell proteins (Lane 2 & Lane 2'), but it is visible in the insoluble fraction of induced cells (Lane 4 & Lane 4'), obtained by the inclusion body preparation.

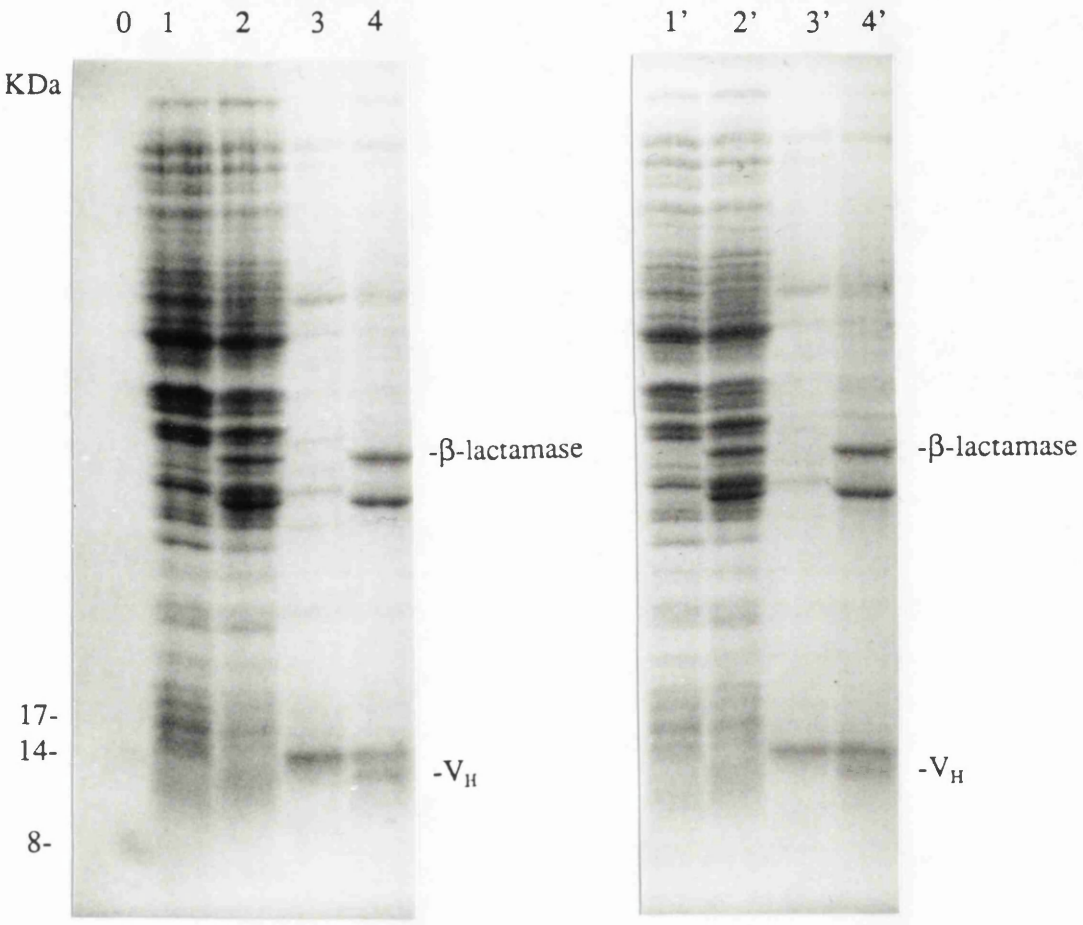

Lane 0 : Protein Marker

Lane 1 and Lane 1': Cells before induction

Lane 2 and Lane 2': Cells 6 hours after induction

Lane 3 and Lane 3': Insoluble fraction of uninduced cells

Lane 4 and Lane 4': Insoluble fraction of induced cells

3.1.2 Fermentation of *E. coli* CAG629 pMG LF9 at 20L scale

It seemed still worthwhile effort being put into fermentation despite the problem of achieving expression of V_L in seed medium 1 by shake flask cultures. Because parameters such as pH value, dissolved oxygen tension were able to be controlled during fermentation, while they were difficult to be controlled in shake flask culture, and this could affect expression of V_L. Fermentations of *E. coli* CAG629 pMG LF9 were carried out at 20L scale. In order to examine the efficiency of thermal induction in the 20L fermenter, LB medium was used in the first fermentation rather than fermentation medium 1. The reason for this was that all shake flask cultures with LB medium achieved expression of V_L and all factors influencing expression from the medium thus could be eliminated when using LB medium as fermentation medium.

3.1.2.1 The fermentation of *E. coli* CAG629 pMG LF9 at 20L scale using LB medium

The fermentation method was detailed in section 2.2.6. The standard inoculum method was used to inoculate fermenter (section 2.2.2.2). The growth curve, measured by OD_{600nm}, is shown in Figure 3.1.4. The corresponding induction point, final OD reading and average specific growth rate μ in the growth phase is shown in Table 3.1.4.

Samples for SDS-PAGE (12.5%) analysis (section 2.6.6) were taken before induction and at 1 hour intervals after induction (until 6 hours later). SDS-PAGE (12.5%) of cell samples was visualised by Coomassie staining. Gloop2 V_L was visible at about 9 KDa, 4 hours after induction (see Figure 3.1.5).

This experiment demonstrated that the cells of *E. coli* CAG629 pMG LF9 were efficiently induced in 20L fermenter. However, because of the limitation of nutrition in LB medium, final cell density was very low (OD_{600nm} = 2.86). The next step was to use fermentation medium 1 (Table 2.2.3 in section 2.2.1) to find out whether expression of V_L could be achieved.

Figure 3.1.4 *E. coli* CAG629 pMG LF9 fermentation growth curve at 20L scale using LB medium

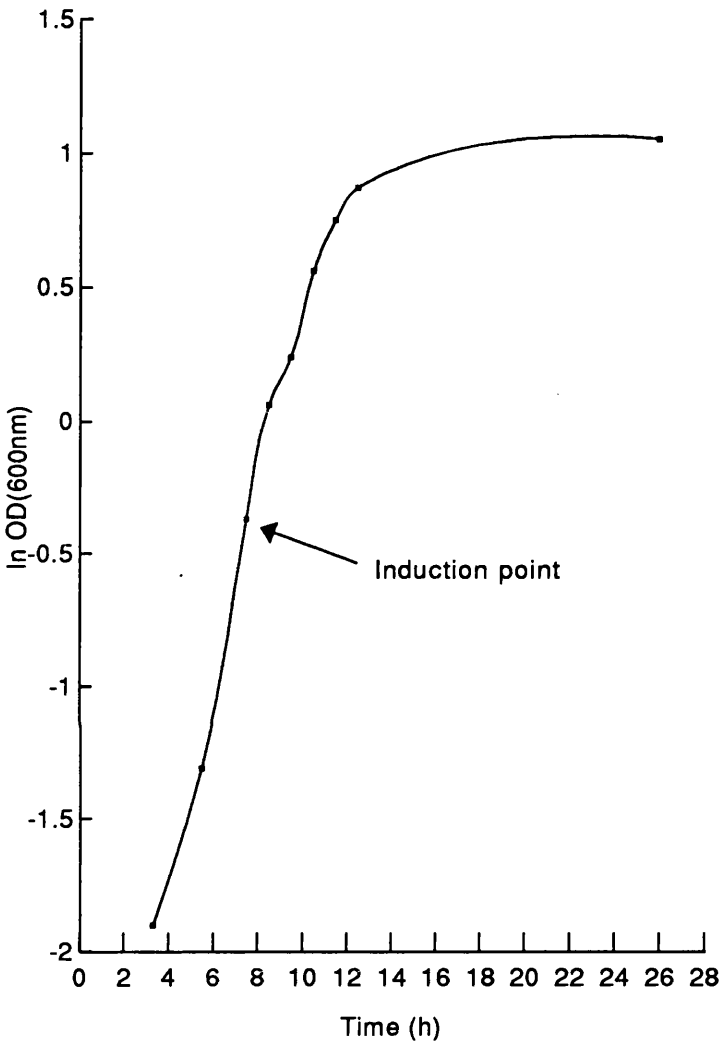

Table 3.1.4 Induction point, final OD reading and average specific growth rate in growth phase of *E. coli* CAG629 pMG LF9 fermentation at 20L scale using LB medium

Induction point (OD_{600nm})	Final OD_{600nm}	μ (average) (h^{-1})
0.69	2.86	0.35

Figure 3.1.5 Expression of V_L from pMG LF9 in *E. coli* CAG629 at 20L scale fermentation using LB medium

Samples were taken before induction and 1,2,3,..., and 6 hours after induction, and analyzed by 12.5% SDS-PAGE and visualised by Coomassie staining. Gloop2 V_L was visible at about 9 KDa 4 hours after induction.

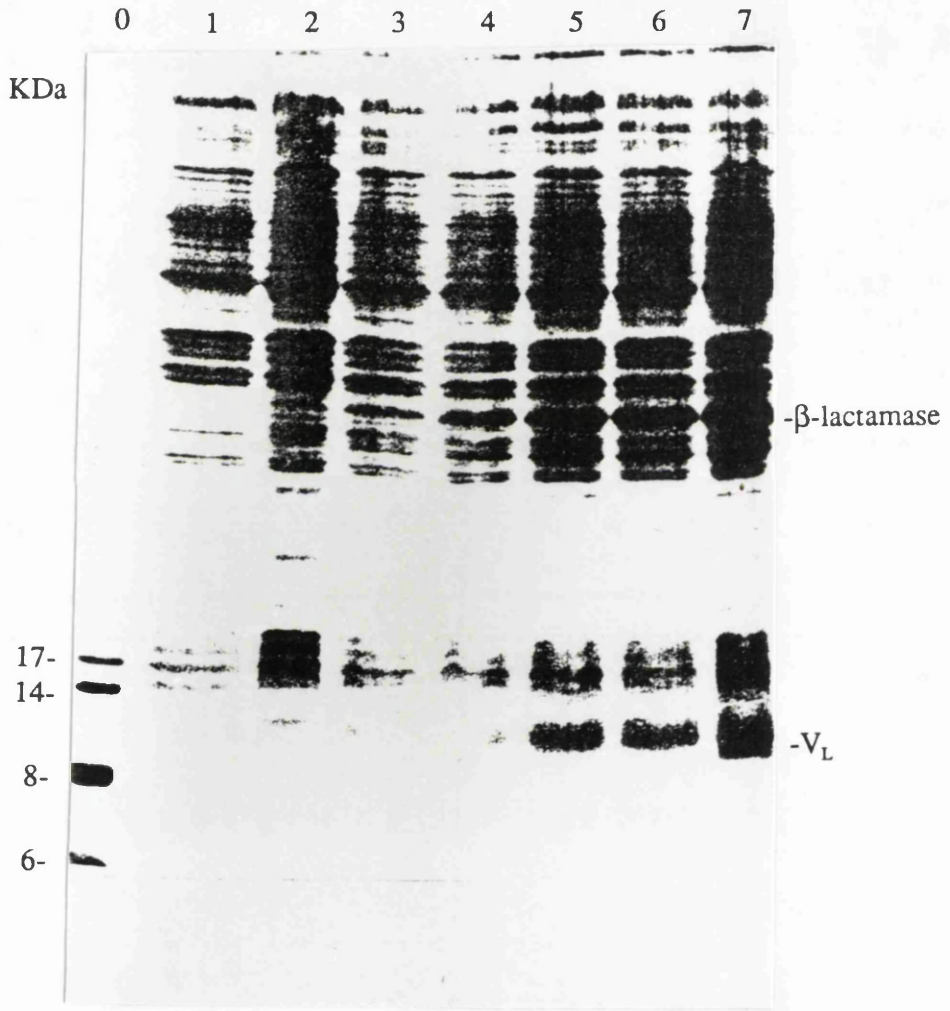

Lane 0 : Protein Marker

Lane 1 : Cells before induction

Lane 2 - Lane 7 : Cells 1,2,...,6 hours after induction

3.1.2.2 The fermentation of *E. coli* CAG629 pMG LF9 at 20L scale using fermentation medium 1

Before studying the induction of *E. coli* cells with plasmid pMG LF9 during fermentation using fermentation medium 1 (Table 2.2.3 in section 2.2.1), it was necessary to carry out a fermentation without induction of the cells. From the growth curve without induction, some basic parameters such as specific growth rate and the final cell density can be obtained and would help to define the induction point. One 20L scale fermentation was performed using fermentation medium 1 without induction. The fermentation method was detailed in section 2.2.6. The standard inoculum method was used to inoculate fermenter (section 2.2.2.2). The growth curve, measured by OD_{600nm}, is shown in Figure 3.1.6. The corresponding final OD reading and average specific growth rate μ in the growth phase is shown in Table 3.1.5.

From this growth curve, it was decided to try to induce cells at an OD_{600nm} of about 10, half way to the final OD reading of about 20 (Table 3.1.5). The purpose of choosing the induction point at an early stage in the stationary phase was to find out whether cells would be properly induced when the density was fairy high during the fermentation, although no expression was achieved for shake flask culture induced at fairy high cell density (section 3.1.1.2). The fermentation was carried out under the same conditions as previously except that cells were induced at an OD_{600nm} of 10. The growth curve is also shown in Figure 3.1.6, and the corresponding induction point, final OD reading and average specific growth rate μ in growth phase are shown in Table 3.1.5. Samples for SDS-PAGE (12.5%) analysis (section 2.6.6) were taken before induction and 1.5 hours after induction and subsequent 1 hour intervals (last sample was 5.5 hours after induction). However, expression of Gloop2 V_L was not achieved (SDS-PAGE picture not shown).

The reasons for not achieving expression of V_L might be:

(1) the medium composition

The specific growth rates for fermentation medium 1 were 0.8 h^{-1} (Table 3.1.5). They were much higher than the specific growth rate when LB medium was used (0.35 h^{-1}, see Table 3.1.4). It was reported that the copy number of plasmid and recombinant product level increased with decreasing μ (Seo and Bailey, 1985). In

Figure 3.1.6 *E. coli* CAG629 pMG LF9 fermentation growth curves at 20L scale with or without induction using fermentation medium 1

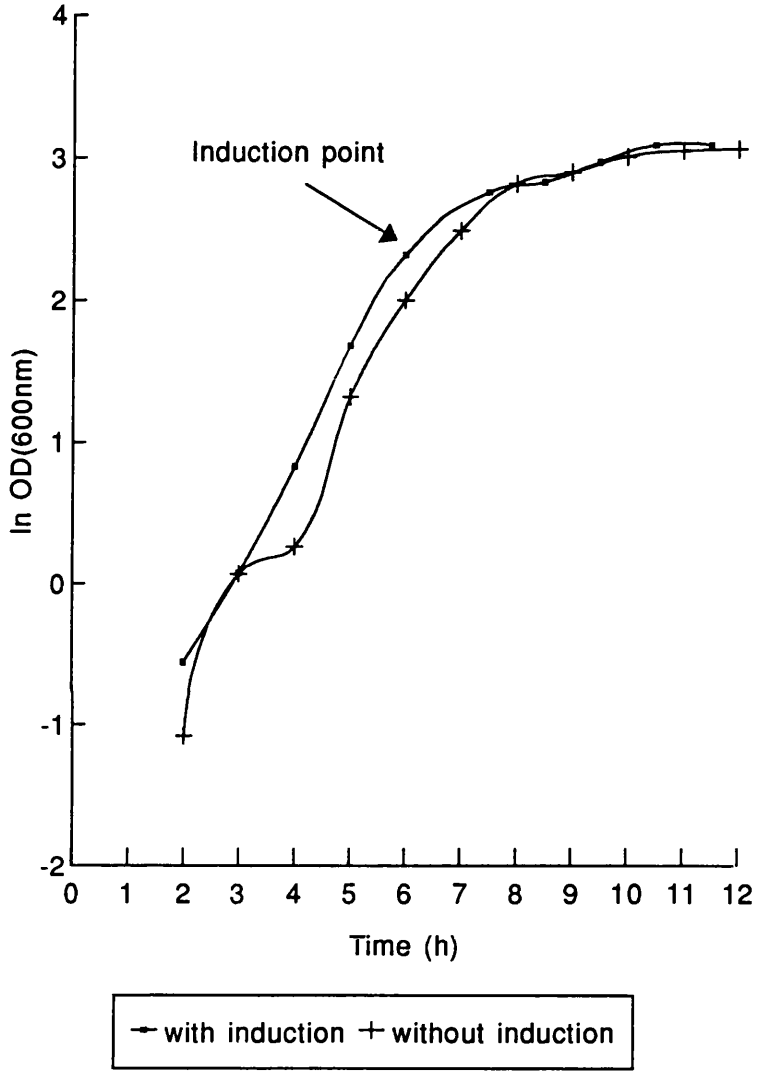

Table 3.1.5 Induction point, final OD readings and average specific growth rates in growth phase of *E. coli* CAG629 pMG LF9 fermentations at 20L scale with or without induction using fermentation medium 1

Fermentation	Induction point (OD_{600nm})	Final OD_{600nm}	μ (average) (h^{-1})
no induction	-	21.2	0.81
induction	10.2	20.2	0.80

the future studies, the medium composition should be changed to give low specific growth rate while provide enough nutrition for reaching high cell density.

(2) the induction point

The induction point of the fermentation using fermentation medium 1 was at an early stage in the stationary phase (shown in Figure 3.1.6). In contrast, the induction point for fermentation using LB medium was at a middle stage of the growth phase, mimicking the induction during shake flask cultures (using LB medium) performed in section 3.1.1 and by Field (1988). In future experiments, it was necessary to study inductions at different point of growth phase.

(3) the stability of the plasmid

In all the shake flask cultures and fermentations so far, standard inoculum method was used (section 2.2.2.2). This could result in the removal of antibiotic selection pressure by β-lactamase attack at an early stage of fermentation. The low inoculum method (section 2.2.2.1) might improve the stability of plasmids (Pierce and Gutteridge, 1985) and it appeared worthwhile to try this in the case of fermentation medium 1, although the expression of V_L was achieved by using standard inoculum method when LB medium was used.

It was decided to change the expression system and the target protein in this study at this stage. A prochymosin expression system was chosen for subsequent studies (see section 1.7). This was because the expression level of V_H was too low. This would cause the difficulty in subsequent downstream processing studies such as recovery of each fragment and construct of Fv. In the prochymosin expression system, the plasmid was of the same family as the previous ones, and expression strategy was similar, *i.e.* cytoplasmic expression where inclusion bodies were formed. Therefore, the research experience from the previous studies would help studies of the new system. Realistic expression levels were especially important because of the intention to pursue pilot plant downstream processing studies as part of the doctoral training programme.

3.2 Studies of the scale-up of production of recombinant protein with calf met-prochymosin expression system

3.2.1 Initial scale-up study on the production of calf met-prochymosin using fermentation medium 2 (casamino acids as nitrogen source and with antibiotics)

Fermentation medium 2 (Table 2.2.4) has been used for growing *E. coli* K12 HB101 strain transformed with plasmid pCT70, which is an intermediate copy number plasmid (40 - 60 copies each chromosome) carrying prochymosin gene, up to 400L scale (Marston *et al.*, 1984) and 100L scale (Gardiner, 1988). The prochymosin expression system in this project used the same strain and produced the same recombinant protein (prochymosin), although the plasmid pMG168, a dual-origin plasmid, was a different type (section 1.7.1.2). Therefore, it was decided to use medium 2 in the initial scale-up work.

3.2.1.1 Expression of calf met-prochymosin in *E. coli* HB101 pMG168 at 50ml scale using LB medium

A prerequisite of scale-up work was to make sure that the plasmid pMG168 in *E. coli* HB101 was functional. Before employing fermentation medium 2, LB medium (Table 2.2.1) was used for initial shake flask culture because it was usually used at lab-scale.

Three shake flask cultures at 50ml scale using LB medium were performed for this purpose (section 2.2.5.2). In contrast to the antibody fragments expression system where the standard inoculum method was used (section 2.2.2.2), the low inoculum method was chosen in this experiment (section 2.2.2.1). The induction point of one flask culture (No. 1) was chosen according to the published report, *i.e.* about an OD_{600nm} of 0.4 (Wright *et al.*, 1986), No. 2 flask culture was induced at an earlier stage to examine the influence on final OD reading. Flask culture No. 3 was not induced. (see Table 3.2.1).

Table 3.2.1 Induction points and final OD readings for shake flask cultures of *E. coli* HB101 pMG168 using LB medium

Culture No.	OD_{600} (induction point)	*Final OD_{600}
1	0.36	2.60
2	0.18	1.08
3	-	5.86

*Final OD_{600} : for culture No. 1 and No. 2, OD readings 6 hours after induction and 13 hours after inoculation; for culture No. 3, OD reading 24 hours after inoculation.

Samples were taken before induction and 6 hours after induction and applied to SDS-PAGE analysis (section 2.6.6). SDS-PAGE (12.5%) of cell samples were visualised by Coomassie staining (section 2.6.6.2). As seen from Figure 3.2.1, prochymosin protein bands are visible at about 40 KDa (Lane 4 and Lane 6), but the prochymosin bands in the whole cell extracts are doublets, as well as the prochymosin standard whose major portion matches the lower band, while a tiny portion matches the upper band of each doublet in the whole cell extracts. The upper band of each doublet probably represented the reduced form while the lower one represented the oxidised form. In the oxidised state, the prochymosin molecule has a more compact structure because of the formation of intramolecular disulfides, leading to a noticeably faster mobility. The reason for the presence of doublets might be the improper storage of sample buffer (stored at 4^0C) for SDS-PAGE analysis (see Table 2.6.3) in the initial study. The proper storage temperature should be -20^0C. Thus the reducing agent dithiothreitol (DTT) in sample buffer would be less effective after keeping at 4^0C for a long period. Another explanation for the formation of the doublets was that the lower band of each doublet might be the degradation product of prochymosin.

Figure 3.2.1 Expression of calf met-prochymosin in *E. coli* HB101 pMG168 at 50ml scale using LB medium

Samples were taken before induction and 6 hours after induction, and analyzed by 12.5% SDS-PAGE and visualised by Coomassie staining. The formation of prochymosin doublets was explained in the text. The presence of β-lactamase indicated readthrough of the ampicillin resistance gene.

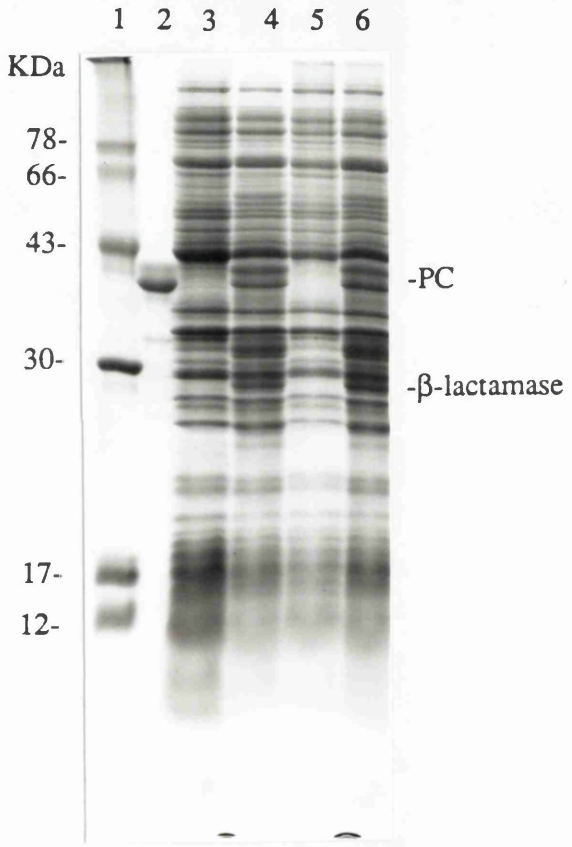

Lane 1 : Protein marker

Lane 2 : Prochymosin marker

Lane 3 and Lane 5 : Cells before induction

Lane 4 and Lane 6 : Cells 6 hours after induction

In order to find out the reason for the existence of prochymosin doublets, SDS-gel analysis was repeated for the same cell samples obtained in these two shake flask cultures. This time, sample buffer for SDS-PAGE was freshly made and used for preparation of cell samples. The previous prochymosin standard for SDS-PAGE was still used because pure prochymosin was not available for making new standard at that time. The inclusion body preparation for purification of insoluble proteins was performed to improve the visibility of prochymosin band (section 2.6.6.3). The picture of the SDS-gel is shown in Figure 3.2.2. The prochymosin doublets disappeared in the whole induced cell extracts (Lane 2 and Lane 3) and in the insoluble fraction of induced cell proteins (Lane 6). This confirmed that the lower band in each doublet observed from the previous SDS-gel results (Figure 3.2.1) was the oxidised form, not the degradation products. Not surprising, the major portion of the "old" prochymosin standard still presents as oxidised form, although the pattern of band was different from that in Figure 3.2.1. This result indicated that the doublets were associated with the reducing agent (DTT) in the sample buffer, which should be stored properly in the following study. From Figure 3.2.2, it was found that there was little difference between the whole cell extracts and the insoluble fractions, which indicated uncomplete breakage of cells in this inclusion body preparation. The new bands appearing in the insoluble fractions (Lane 5 and Lane 6) at about 12 KDa were lysozyme, which was used to break cells during inclusion body preparation (marked in Figure 3.2.2).

This shake flask culture experiment demonstrated that the prochymosin gene was expressed when LB medium was used. The problem was the low cell density achieved (Table 3.2.1) as for expression of antibody fragments in the previous study (section 3.1). In order to achieve high cell density, fermentation medium 2 (Table 2.2.4 in section 2.2.1) was chosen for cell growth. Before carrying out fermentation, it was necessary to perform a shake flask culture.

Figure 3.2.2 Expression of calf met-prochymosin from pMG168 in *E. coli* HB101 at 50ml scale using LB medium (using fresh sample buffer for preparation of cell extracts)

Samples were taken before induction and 6 hours after induction, applied inclusion body preparation was applied and analyzed by 12.5% SDS-PAGE. The whole cell extracts for SDS-gel were prepared with freshly made sample buffer, while the prochymosin standard was still the previous one which was made with improper stored sample buffer (4^{0}C). The presence of β-lactamase indicated readthrough of the ampicillin resistance gene. The lysozyme appeared in Lane 5 and Lane 6, because it was used to break cells during inclusion body preparation.

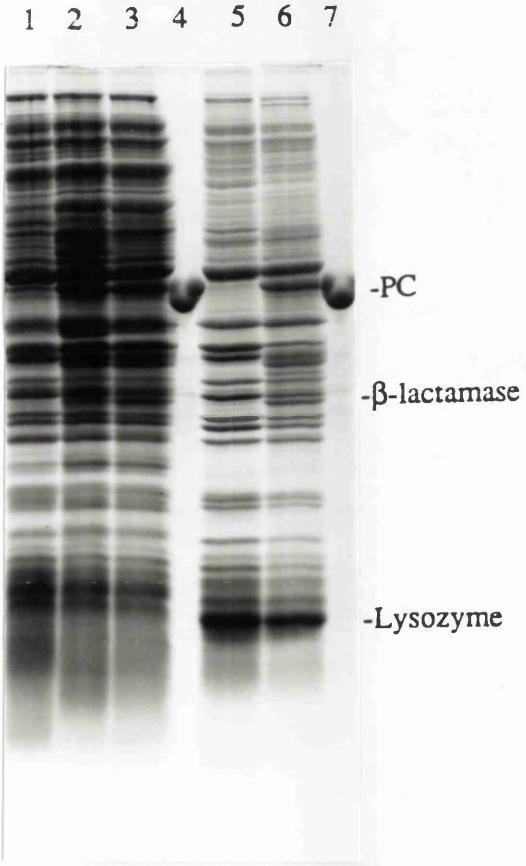

Lane 1 : Cells before induction

Lane 2 and Lane 3 : Cells 6 hours after induction

Lane 4 and Lane 7 : Prochymosin standard

Lane 5 : Insoluble fraction of uninduced cells

Lane 6 : Insoluble fraction of induced cells

3.2.1.2 Expression of calf met-prochymosin in *E. coli* HB101 pMG168 at 50ml scale using fermentation medium 2

In this experiment, fermentation medium 2 (Table 2.2.4 in section 2.2.1) was used for shake flask culture at 50 ml scale. The objective was to check whether expression of prochymosin would be achieved before carrying out any fermentations. A set of three shake flask cultures was performed at 50ml scale, where the low inoculum method was used (section 2.2.5.2). Two cultures (No.1 & No.2) were induced, while one flask culture (No.3) was used to grow cells without induction as a control in order to compare the one using LB medium without induction (No.3 culture in the last section). The results of OD reading at different stage of sampling are summarised in Table 3.2.2.

Table 3.2.2 Induction points and final OD readings for shake flask cultures of *E. coli* HB101 pMG168 using fermentation medium 2

Culture No.	Induction point (OD_{600})	*Final OD_{600}
1	0.94	4.0
2	0.92	5.7
3	-	13.4

*Final OD_{600} : for culture No. 1 and No. 2, OD readings 6 hours after induction and 19 hours after inoculation; for culture No. 3, OD reading 24 hours after inoculation.

Expression of prochymosin in flask culture No 1 and No 2 are shown in Figure 3.2.3. Although in flask culture No 1 and No 2, cells were induced at about OD_{600nm} of 1, higher than that when employing LB medium (Table 3.2.1), expression of prochymosin was still achieved (Lane 6 and Lane 7 in Figure 3.2.3). Comparing those two uninduced flask cultures (No.3, see Table 3.2.1 and Table 3.2.2), the final cell density achieved with fermentation medium 2 (OD_{600nm} = 13.4) was much high than that with LB medium (OD_{600nm} = 5.86).

The major portion of prochymosin standard presented as oxidised form because it was still the one used in the previous gel analysis (Figure 3.2.2). It was necessary to prepare new

Figure 3.2.3 Expression of prochymosin from pMG168 in *E. coli* HB101 at 50ml scale using fermentation medium 2

Samples were taken before induction and 6 hours after induction, and analyzed by 12.5% SDS-PAGE and visualised by Coomassie staining. The whole cell extracts for SDS-gel were prepared with proper stored sample buffer (-20^{0}C), while the prochymosin standard was still the previous one which was made with improper stored sample buffer (4^{0}C).

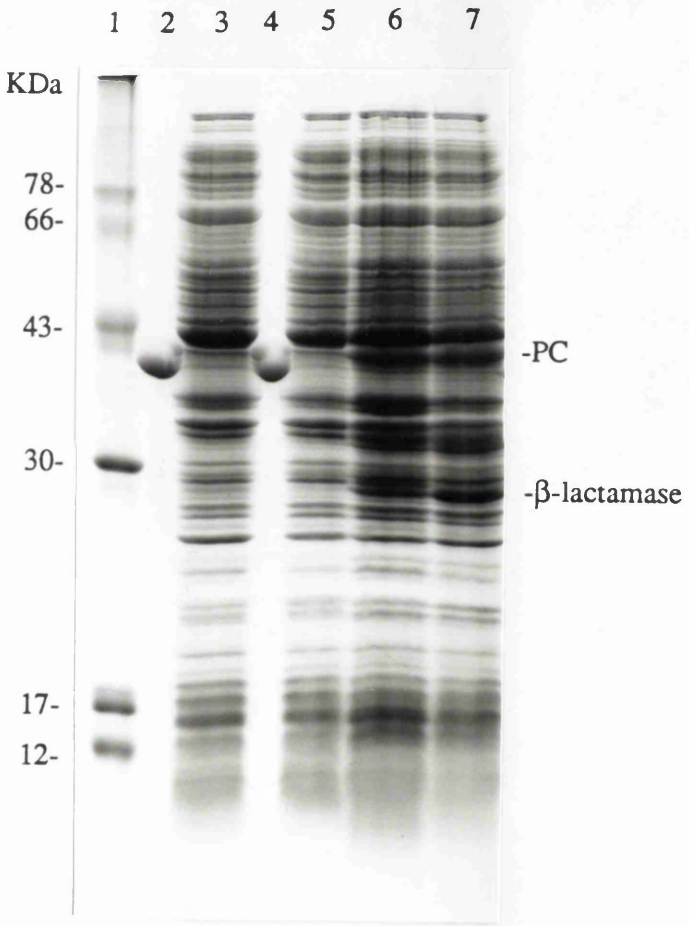

Lane 1 : Protein Marker

Lane 2 and Lane 4 : Prochymosin standard

Lane 3 and Lane 5 : Cells before induction

Lane 6 and Lane 7 : Cells 6 hours after induction

prochymosin standard for SDS-PAGE from pure prochymosin using correctly stored sample buffer. The results of SDS-gel analysis of the freshly made prochymosin standard and the previous used one are shown in Figure 3.2.4, which shows that the freshly made prochymosin standard presents as reduced form while the previous used one presents as oxidised form. In this picture, it is hard to see the presence of reduced form in the "old" standard (upper band of the doublet) observed in the previous gel pictures. This was probably because the "old" prochymosin standard was further oxidised after repeated heating required for each loading.

In order to confirm that the prochymosin band in the induced cell extracts matched the prochymosin standard, samples from shake flask cultures employing both LB medium (see the last section) and fermentation medium 2 (this section) were re-analyzed by SDS-gel, in which both the cell extracts and prochymosin standard were prepared with the same source of sample buffer stored at -20^{0}C at the same time. Inclusion body preparation was also carried out with cell samples from fermentation medium 2, the results are shown in Figure 3.2.5. As seen from Figure 3.2.5, the prochymosin standard matches the prochymosin bands both in whole cell extracts (Lane 3,4,and 5) and in insoluble fraction (Lane 8), although there was a tiny band just below the major band in the prochymosin standard, which might be degradation products or contaminants, but not oxidised form because further purification of prochymosin standard by gel elution method (section 2.6.6.5) gives one single band, the results of which are presented in Appendix 1. This tiny band was not observed in the previous gel pictures which have the "old" prochymosin standard, this might because of its similar molecular mobility with the oxidised form of prochymosin. However, this tiny band did not appear in prochymosin standard in Lane 2 of Figure 3.2.4 either, which was also freshly made, indicating a difference between pure prochymosin stored in different microtubes.

In the following SDS-analysis, prochymosin standard was always freshly prepared using the same source of sample buffer (stored at -20^{0}C) as for cell samples.

Figure 3.2.4 Comparison of freshly-made prochymosin standard in properly stored SDS-PAGE sample buffer with that used in the previous SDS-gel analysis

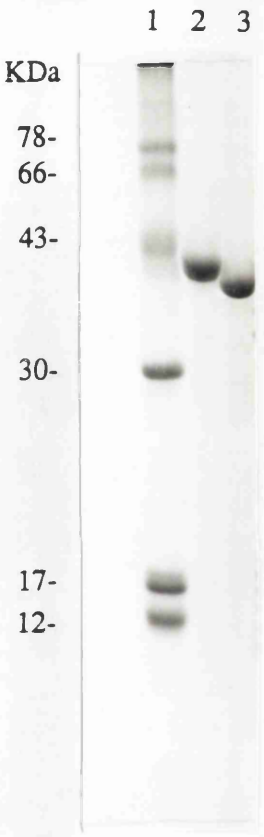

Lane 1 : Protein marker

Lane 2 : Prochymosin standard made with proper stored sample buffer (-20^{0}C)

Lane 3 : Prochymosin standard used in the previous gel analysis

Figure 3.2.5 Expression of prochymosin from pMG168 in *E. coli* HB101 at 50ml scale using both LB medium and fermentation medium 2

Cell samples were from the previous shake flask cultures both using LB medium and fermentation medium 2, and both cell extracts and prochymosin standard were prepared with the sample buffer of the same storage (stored at -20^{0}C). Inclusion body preparation were carried out for cells from fermentation medium 2. SDS-PAGE of 12.5% was applied. The presence of lysozyme in insoluble fraction was explained in Figure 3.2.2.

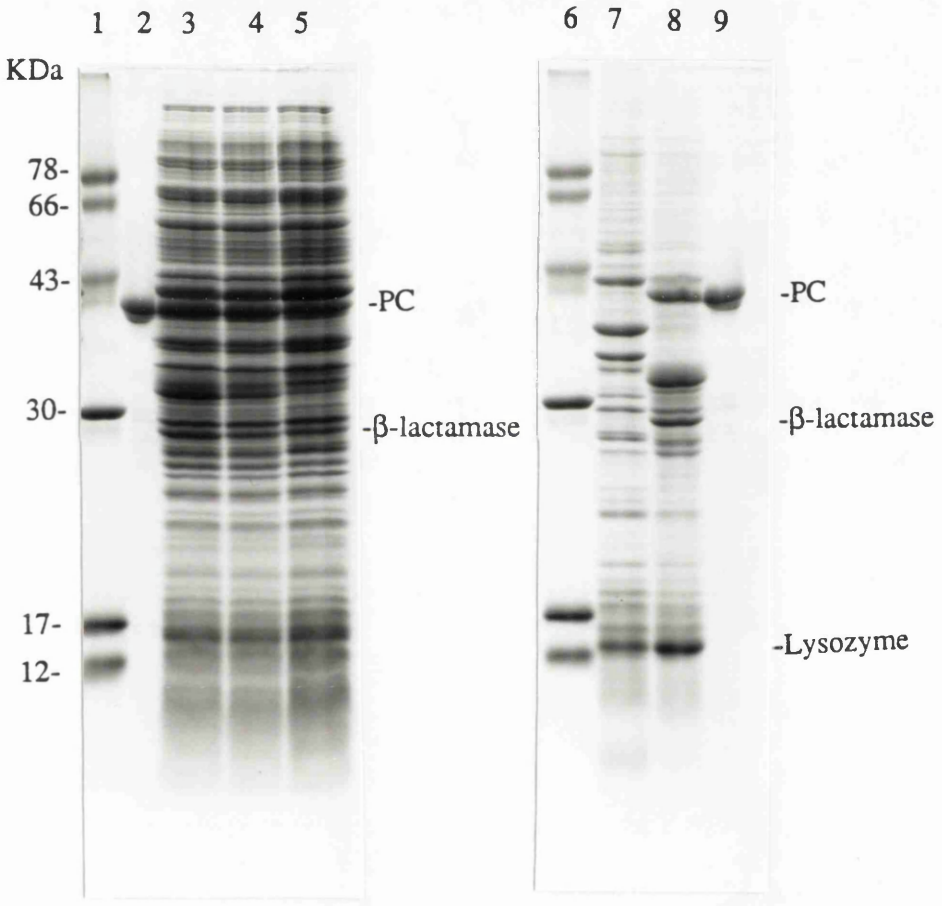

Lane 1 and Lane 6 : Protein Marker

Lane 2 and Lane 9 : prochymosin standard

Lane 3 : Cells 6 hours after induction (from LB medium)

Lane 4 and Lane 5 : cells 6 hours after induction (from medium 2)

Lane 7 : Insoluble fraction of uninduced cells (from medium 2)

Lane 8 : Insoluble fraction of induced cells (from medium 2)

3.2.1.3 Fermentation for production of calf met-prochymosin at different scales using fermentation medium 2

Because of the expression of prochymosin achieved in shake flask cultures using fermentation medium 2, it was decided to carry out fermentations.

One fermentation of *E. coli* HB101 pMG168 at 42L scale was carried out without induction. The objective of this experiment was to obtain the cell growth curve in fermentation medium 2 (Table 2.2.4), which was helpful for defining the induction point. The fermentation method was detailed in section 2.2.6. The low inoculum method was used to inoculate the fermenter (section 2.2.2.1). The growth curve, measured by OD_{600nm} and cell dry weight, is shown in Figure 3.2.6. The corresponding final OD reading and average specific growth rate μ in the growth phase is listed in Table 3.2.3.

From this growth curve, it was decided to induce cells at an OD_{600nm} range of 6 - 8, about one third of the final OD reading of 23 (Table 3.2.3), in the subsequent fermentations. This induction range was after the mid-point of the growth phase but not at the very late stage of the growth phase. The reason for choosing this induction range was to give effective thermal induction while cell density was reasonably high but cells were still metabolically active, thus to achieve reasonably high cell density. It was thought that if cells were induced at high density (at a very late stage of growth phase or in stationary phase), they would not be properly induced to produce prochymosin because of not being metabolically active (from the results of the antibody fragments expression system). This was also confirmed by the results obtained in later experiments (section 3.2.2.2.3). However, if cells were induced at low cell density, the final cell mass achieved would be low because of the temperature shift resulting in the death of some cells, which would account for a large proportion in the case of low cell density, and the induction of cells resulting in expression of foreign proteins, which would affect cell viability (from the results of shake flask cultures). This was also confirmed by later fermentation results (section 3.2.2.2.3).

Fermentations at 20L and 100L scale were carried out under the same condition as 42L one except that cells were induced. The growth curves of 20L and 100L fermentation, measured by OD_{600nm} and cell dry weight, are also shown in Figure 3.2.6. The corresponding induction

Figure 3.2.6 *E. coli* HB101 pMG168 fermentation growth curves in terms of OD_{600nm} and cell dry weight (CDW) at 42L scale without induction and at 20L and 100L scales with induction using fermentation medium 2

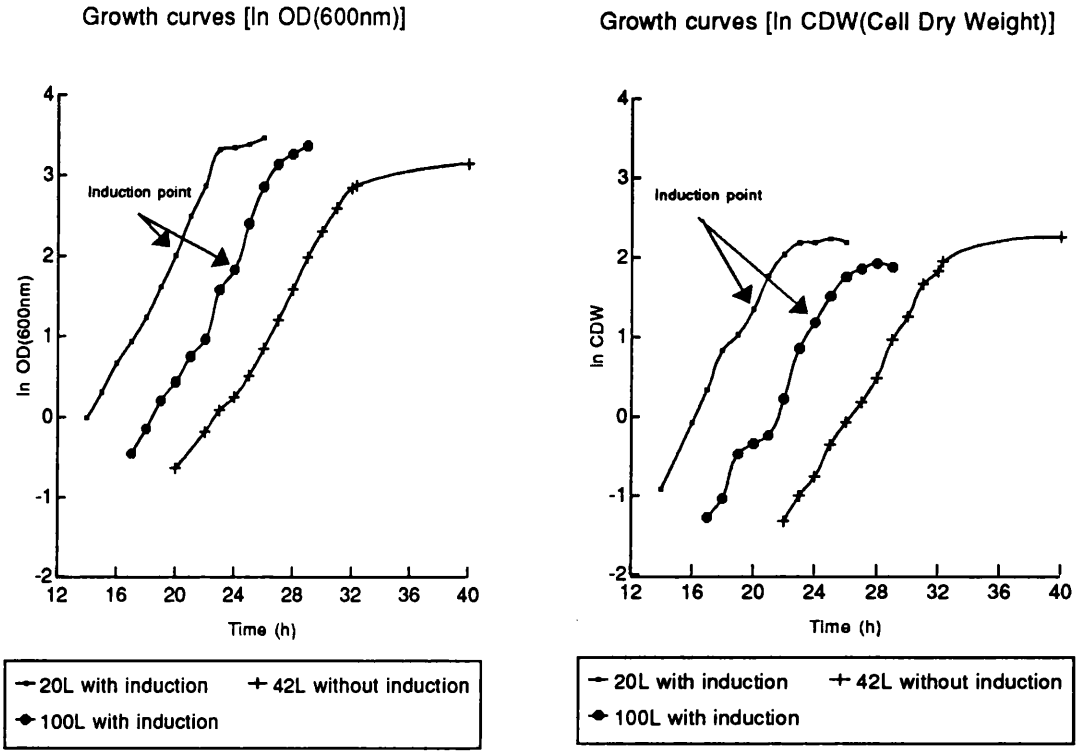

Table 3.2.3 Induction points, final OD readings, final cell dry weights (CDW) and average specific growth rates in the growth phase of *E. coli* HB101 pMG168 fermentations at 20L, 100L and 42L scale (without induction) using fermentation medium 2

Batch	Induction point (OD_{600nm})	*Final OD_{600nm}	*Final CDW ($g.L^{-1}$)	μ (average) (h^{-1})
20L	7.4	31.8	8.9	0.38
100L	6.2	29.0	6.5	0.37
42L	-	23.2	9.5	0.37

*Final OD_{600nm} and Final CDW : cell density of the last sample of each fermentation.

point, final OD reading and average specific growth rate μ in growth phase are listed in Table 3.2.3.

As seen from Figure 3.2.6, the 42L fermentation had a longer lag phase than the other two batches. The reason for this was the heater control failure during the lag phase, the temperature dropped from set point (see section 2.2.6). The final OD readings of the two batches with induction (20L and 100L scale) were higher than that without induction (42L scale), while the final cell dry weight (CDW) of the induced batches were lower than the uninduced one (Table 3.2.3). The higher turbidity of induced cells indicated the formation of inclusion bodies which were highly refractile. The relationship between the optical density and cell dry weight is further discussed in section 3.2.3. By comparing the two induced batches, the 20L fermentation reached a higher cell density than the 100L one. This was probably because the 20L batch was induced at higher cell density than that for the 100L one as explained earlier.

Samples for SDS-PAGE (12.5%) analysis (section 2.6.6) were taken before induction and subsequent 1 hour interval after induction for these two fermentations with induction (20L and 100L). The results of SDS-gel analysis for 20L and 100L fermentation are shown in Figure 3.2.7 and Figure 3.2.8, respectively. Prochymosin bands are visible at about 40 KDa 2 hours after induction. The developed SDS-gel for samples from 100L fermentation was subjected to gel scanning (section 2.6.6.4) to determine the expression level of prochymosin (percentage of total cell proteins) at different period after induction. The results are summarised in Table 3.2.4.

Because of the inaccuracy of gel scanning, the prochymosin percentage of total cell proteins only represent approximate expression levels. However, it was observed that in the 100L fermentation, the expression level reached a maximum 3 hours after cell induction.

Figure 3.2.7 Expression of calf met-prochymosin from pMG168 in *E. coli* HB101 at 20L scale fermentation using medium 2

Samples were taken before induction and 1,2,3,..., and 6 hours after induction, and analyzed by 12.5% SDS-PAGE and visualised by Coomassie staining. The presence of β-lactamase indicated readthrough of ampicillin resistance gene. Prochymosin bands are visible at about 40 KDa.

The method of TCA precipitation of proteins for sample preparation was not applied.

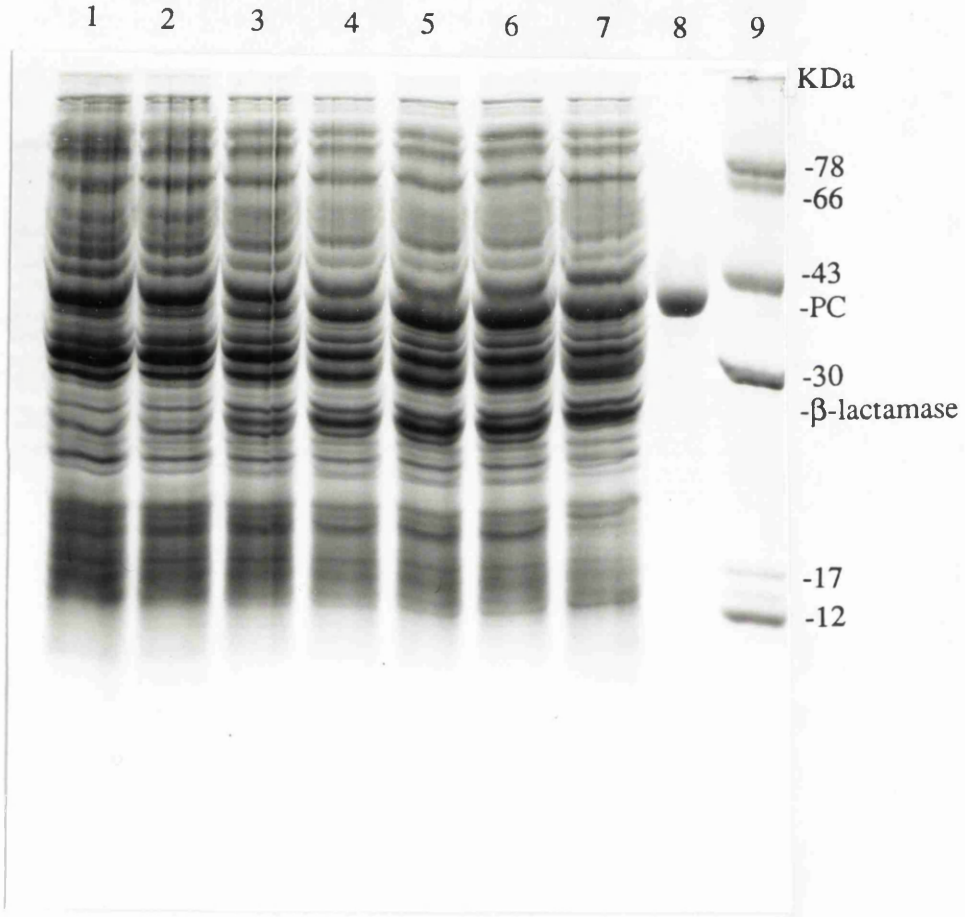

Lane 1 : Cells before induction

Lane 2 - Lane 7 : Cells 1,2,...,6 hours after induction

Lane 8 : Prochymosin standard

Lane 9 : Protein Marker

Figure 3.2.8 Expression of calf met-prochymosin from pMG168 in *E. coli* HB101 at 100L scale fermentation using medium 2

Samples were taken before induction and 1,2,..., and 5 hours after induction, and analyzed by 12.5% SDS-PAGE and visualised by Coomassie staining. Prochymosin bands are visible at about 40 KDa.

The method of TCA precipitation of proteins for sample preparation was applied.

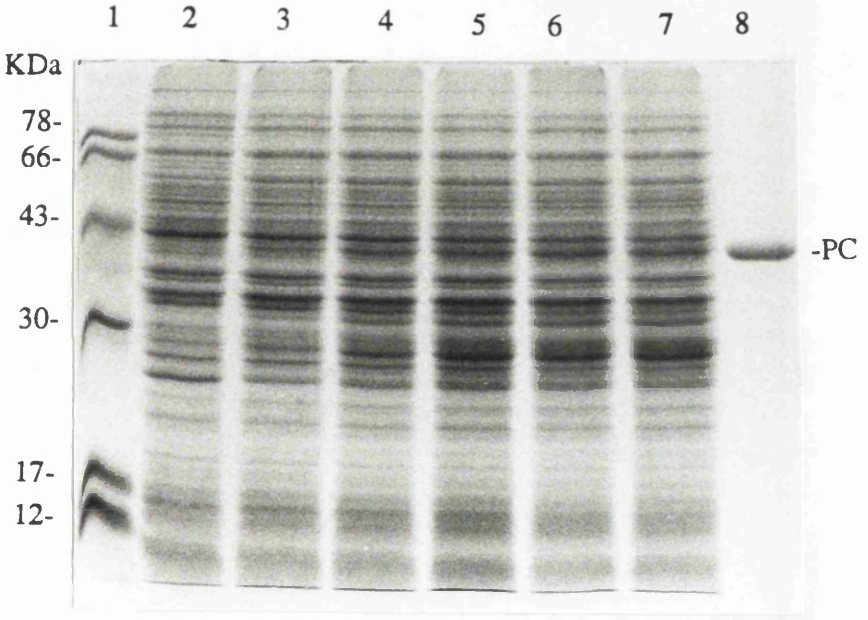

Lane 1 : Protein Marker

Lane 2 : Cells before induction

Lane 3 - Lane 7 : Cells 1,2,...,5 hours after induction

Lane 8 : Prochymosin standard

Table 3.2.4 Expression level of prochymosin at 100L scale fermentation using medium 2

Time (h)[1]	0	1	2	3	4	5
Expression level (%)[2]	-	3.2	7.2	7.8	7.8	7.6

1. Time (h): 0 represents the moment just before cell induction, and 1,2,...,5 means 1,2,...,5 hours after induction.
2. Expression levels (%): the percentage of total cell proteins.

3.2.1.4 The formation of acetate during the 100L fermentation using medium 2

It was interesting to know the quantity of acetate produced during the 100L fermentation. As discussed in section 1.2.4, acetate is a major factor in the limitation of achieving high cell density (Allen *et al.*, 1987), and is correlated with a reduced production of recombinant protein (Brown *et al.*, 1985). It was expected that the production level of acetate would be low because glycerol was used as carbon source rather than glucose.

Acetate concentration was determined using a test kit (section 2.6.7). It was found that the concentration of acetate was low before cell induction (below 0.5 g/L), but acetate production was significantly increased after induction (reached 2 g/L five hours after induction), as shown in Figure 3.2.9.

Figure 3.2.9 Acetate concentration during 100L fermentation using medium 2

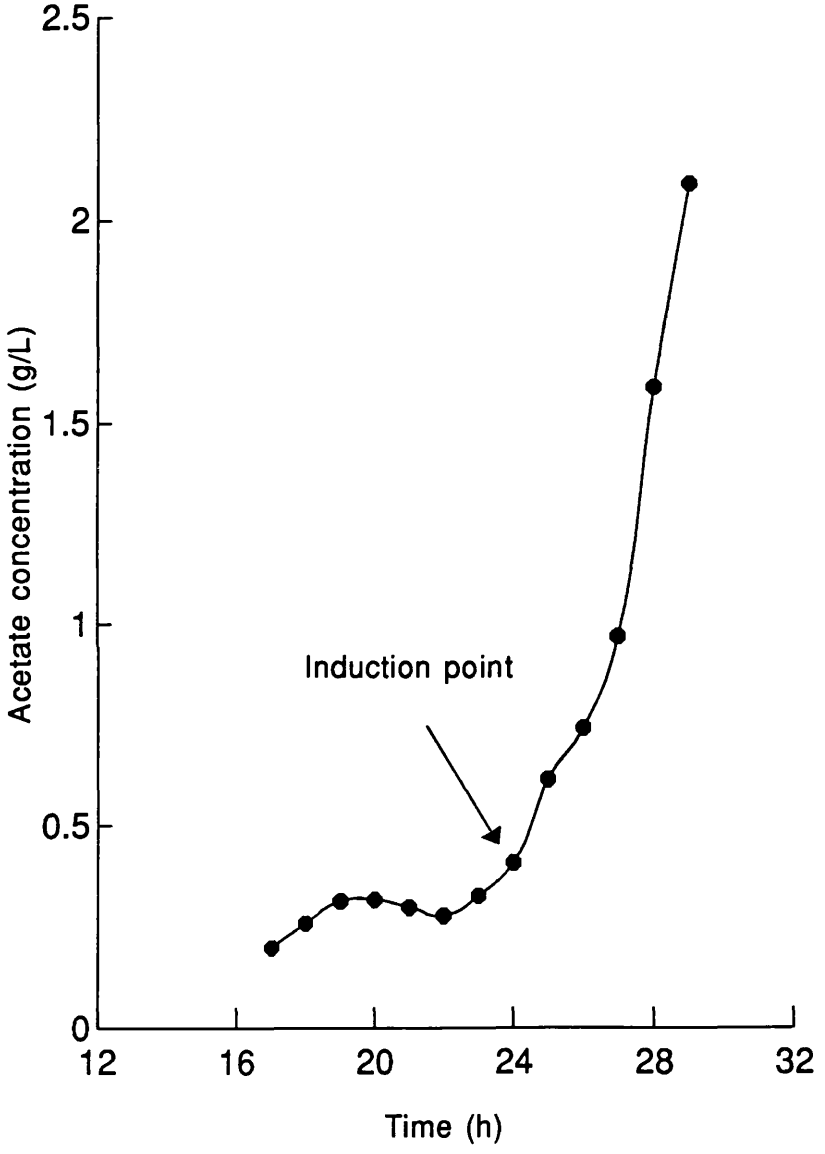

3.2.2 Studies of medium changes to allow scale-up of production of calf met-prochymosin

Although the fermentation of *E. coli* HB101 pMG168 has been scaled up to 100L, there are two main disadvantages with the fermentation medium 2 (Table 2.2.4) employed. First, the medium is expensive because of using casamino acids and antibiotic the cost of which is also high. In addition, all chemicals used are AnalaR grade which cost more and are not practical in large scale fermentation. Thirdly, the use of antibiotic (ampicillin in this case), although it plays the role in retaining plasmid stability, not only increases the cost but causes safety problems especially at large scale. In order to overcome these drawbacks of fermentation medium 2 for large scale production, cheap chemicals needed to be introduced and the possibility of avoiding antibiotic sought.

3.2.2.1 Fermentation medium 3, Standard Yeatex used as nitrogen source instead of casamino acids and G.P.R. grade chemicals used for replacement of A.R. grade

Casamino acids account for the major part of the medium cost because of its high cost per unit and large quantity needed (total cost of medium 2 listed in Table 3.2.13, section 3.2.4). The material is an acid-hydrolysed casein and its composition is listed in Table 3.2.5. There is no tryptophan in the amino nitrogen source, resulting in tryptophan-starvation conditions in fermentation medium 2.

Table 3.2.5 Components of casamino acids

Component	Percentage (%)
Sodium Chloride	25 - 35
Ash	30 - 40
Total Nitrogen	7 - 10
(Amino Nitrogen)	(4.8)
including 17 amino acids: Ala, Arg, Asn, Cys, Gln, Gly, His, Ile, Leu, Lys, Met, Phe, Pro, Ser, Thr, Tyr, Val.	

As mentioned at the beginning of section 3.2.1, fermentation medium 2 was originally used for growing the *E. coli* K12 HB101 strain transformed with plasmid pCT70, which is an intermediate copy number plasmid (40 - 60 copies each chromosome) carrying the prochymosin gene (Marston *et al.*, 1984). The prochymosin gene is under the control of tryptophan promoter, requiring tryptophan-starvation conditions in the growing medium for expression. However, Caulcott *et al.* (1985) found that even when tryptophan was added to the medium (100 mg/L), the prochymosin gene in plasmid pCT70 was still efficiently expressed from the tryptophan promoter. This suggested that the *trp* promoter cannot be tightly controlled on a multi-copy plasmid like pCT70 (40 - 60 copies each chromosome). One positive outcome from this result is that the tryptophan-starvation conditions need not be met and other nitrogen sources may be used besides casamino acids for plasmid pCT70. The plasmid pMG168 used in this project can reach 100 - 150 copies per chromosome after induction (Wright *et al.*, 1986), and the *trp* promoter is more difficult to control even with the presence of tryptophan compared with plasmid pCT70. Therefore, the tryptophan-starvation conditions for a nitrogen source need not be met either for plasmid pMG168.

Casamino acids can be replaced by inorganic nitrogen sources or other organic ones in order to reduce cost. However, the use of an inorganic source was found to cause the problem of plasmid instability though the reason was not clear (Caulcott *et al.*, 1985). Therefore, it was unwise to try inorganic sources before a full understanding of the recombinant system. It was decided to try Standard Yeatex (Bovril Foods Ltd.) to replace casamino acids because of its low cost (Table 3.2. in section 3.2.3). The composition is listed in Table 3.2.6. The AnalaR grade chemicals in fermentation medium 2 were also replaced by G.P.R grade (General Purpose Reagent) to achieve a further cut in cost. A concentration of 20 g/L was used for Standard Yeatex instead of 30 g/L for casamino acids because there was a concern about the solubility of Standard Yeatex. This resulted in medium 3 (Table 2.2.5). Although small quantities of insoluble materials were found in the medium solution, it was shown that these insoluble materials from Standard Yeatex existed regardless of concentration.

Shake flask cultures and one fermentation at 42L scale were carried out to explore fermentation medium 3.

Table 3.2.6 Components of Standard Yeatex

Component	Percentage (%)
Moisture	27
Ash	18.3
Fat	0.1
Carbohydrate	10.8
Protein	43.8

3.2.2.1.1 Expression of calf met-prochymosin in *E. coli* HB101 pMG168 at 50ml scale using fermentation medium 3

In this experiment, three shake flask cultures were performed at 50ml scale, two of which (No.1 without induction and No.2 with induction) employed fermentation medium 3 (Table 2.2.5 in section 2.2.1), while the remaining one (No.3) used fermentation medium 2 as control (Table 2.2.4). The low inoculum method was used. The results of OD reading at different stages of sampling are listed in Table 3.2.7. No.2 flask culture with fermentation medium 3 was induced at a higher OD compared with No.3 using fermentation medium 2, resulting in a higher final cell density. The final cell density achieved for No.1 flask without induction was lower than the previous shake flask culture without induction but using fermentation medium 2 (Table 3.2.2). This may be due to the low concentration of Standard Yeatex used. The lag phase for the cultures using fermentation medium 3 was longer than for that using medium 2 (see the notes of Table 3.2.7). The reason for this may be the existence of insoluble materials in Standard Yeatex, so that cells need to produce solubilizing agents to take up these insoluble nutrients.

The expression of prochymosin in flask cultures No. 2 and No. 3 is shown in Figure 3.2.10. Prochymosin bands are visible in Lane 3 and Lane 6 at about 40 KDa. The presence of prochymosin bands in cell extracts before induction (Lane 2 and 7) indicated the *trp* promoter could not be tightly repressed even at low plasmid copy number in these flask cultures. For all the previous SDS-gel analysis, prochymosin bands in cell extracts before induction were much more faint, indicating the *trp* promoter was tightly controlled (refer to

all the gel pictures above).

Table 3.2.7 Induction point and final OD reading for shake flask cultures of *E. coli* HB101 pMG168 using fermentation medium 3

Culture No.	Induction point (OD_{600})	*Final OD_{600}
1	-	8.8
2	1.9	6.8
3	0.9	5.8

*Final OD_{600} : for culture No. 1, final OD_{600nm} means OD reading 35 hours after inoculation; for culture No. 2, final OD_{600nm} means OD reading 6 hours after induction and 30 hours after inoculation; for culture No.3, final OD_{600nm} means OD reading 6 hours after induction and 20 hours after inoculation.

Figure 3.2.10 Expression of prochymosin from pMG168 in *E. coli* HB101 at 50ml scale using fermentation medium 3

Samples were taken before induction and 6 hours after induction, and analyzed by 12.5% SDS-PAGE and visualised by Coomassie staining.

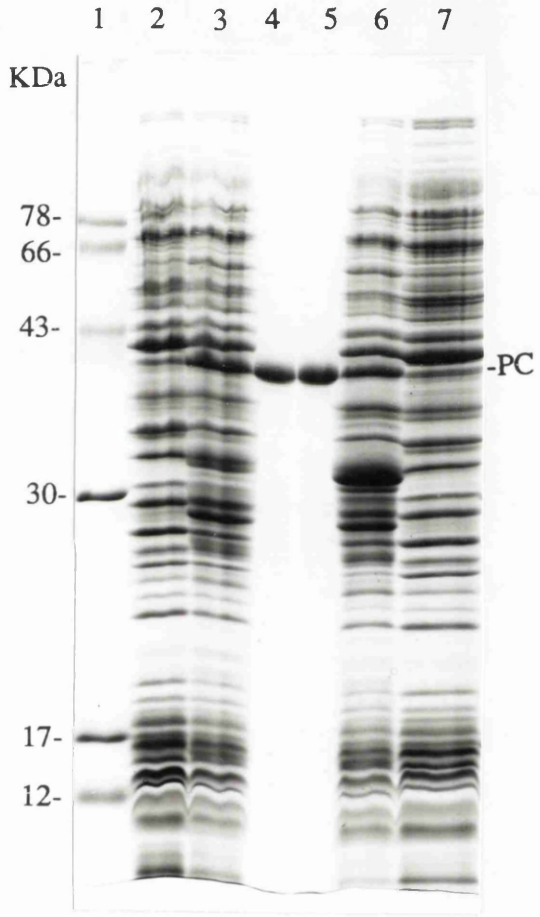

Lane 1 : Protein Marker

Lane 2 : Cell extracts before induction (from medium 3)

Lane 3 : Cell extracts 6 hour after induction (from medium 3)

Lane 4 and Lane 5 : Prochymosin standard

Lane 6 : Cell extracts 6 hours after induction (from medium 2)

Lane 7 : Cell extracts before induction (from medium 2)

3.2.2.1.2 Fermentation of calf met-prochymosin in *E. coli* HB101 pMG168 at 42L scale using fermentation medium 3

It was decided to carry out a 42L scale fermentation to further verify fermentation medium 3. The low inoculum method was still used (section 2.2.2.1), However, an extra seed culture step was used for cell adaptation before inoculating the fermenter in order to reduce the long lag phase observed in shake flask cultures (section 2.2.6).

The growth curve, measured by OD_{600nm} and cell dry weight, is shown in Figure 3.2.11. The corresponding induction point, final OD reading and average specific growth rate μ is shown in Table 3.2.8. The induction point (OD_{600nm} of 7) was still in the same range as using fermentation medium 2 at OD_{600nm} of 6 - 8. It was observed that the cell density achieved was lower than that using fermentation medium 2 (Table 3.2.3). The reason may be the low concentration of nitrogen source, as mentioned in the last section for shake flask cultures. The specific growth rate (0.41 h^{-1}) was slightly higher than that for using fermentation medium 2 (0.37 - 0.38 h^{-1}). However, the lag phase was still much longer than that for using fermentation medium 2 (Figure 3.2.6).

The relationship between the optical density and cell dry weight will be discussed in section 3.2.3.

Table 3.2.8 Induction point, final OD readings, final cell dry weight (CDW) and average specific growth rates of *E. coli* HB101 pMG168 fermentations at 42L scale using fermentation medium 3

Induction point (OD_{600nm})	Final OD_{600nm}	Final CDW ($g.L^{-1}$)	μ (average) (h^{-1})
7.3	14.4	4.8	0.41

From the results of SDS-gel analysis (Figure 3.2.12 & Figure 3.2.13), the expression of prochymosin was achieved, although expression level (6% of total cell proteins) was slightly lower than that obtained from the 100L fermentation using medium 2 (7.6%).
(The expression level from each batch used for comparison was referred to that of the final sample, see Table 3.2.4. The scanning results of the batch using medium 3 not shown.)

Figure 3.2.11 *E. coli* HB101 pMG168 fermentation growth curves at 42L scale using fermentation medium 3

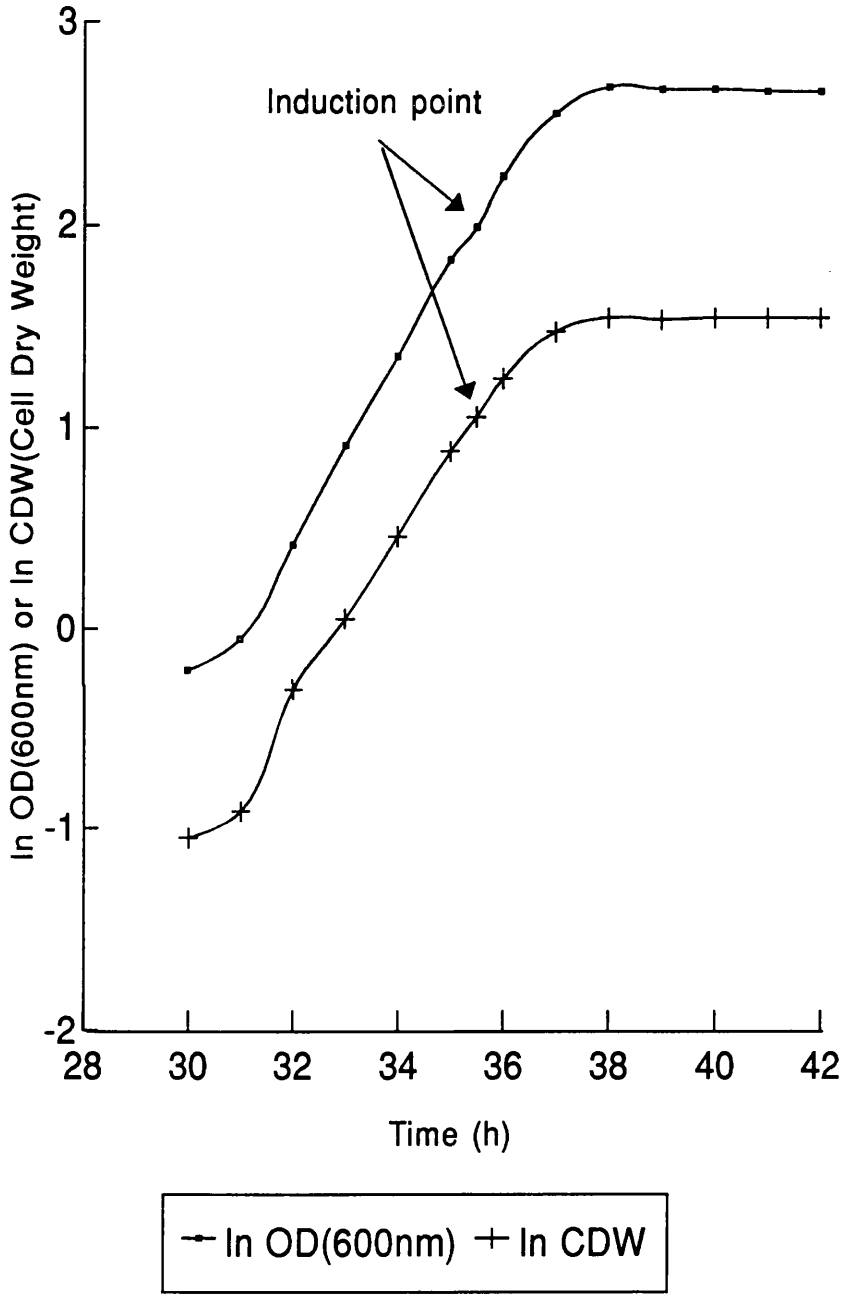

Figure 3.2.12 Expression of calf met-prochymosin from pMG168 in *E. coli* HB101 at 42L scale fermentation using medium 3

Samples were taken before induction and 6 hours after induction, and analyzed by 12.5% SDS-PAGE and visualised by Coomassie staining. Not being satisfied with the gel streaking, the method of TCA precipitation of protein was used for samples preparation (section2.6.6.3), and re-analyzed by 13.5% SDS-gel (mini-gel), whose picture is shown in Figure 3.2.13.

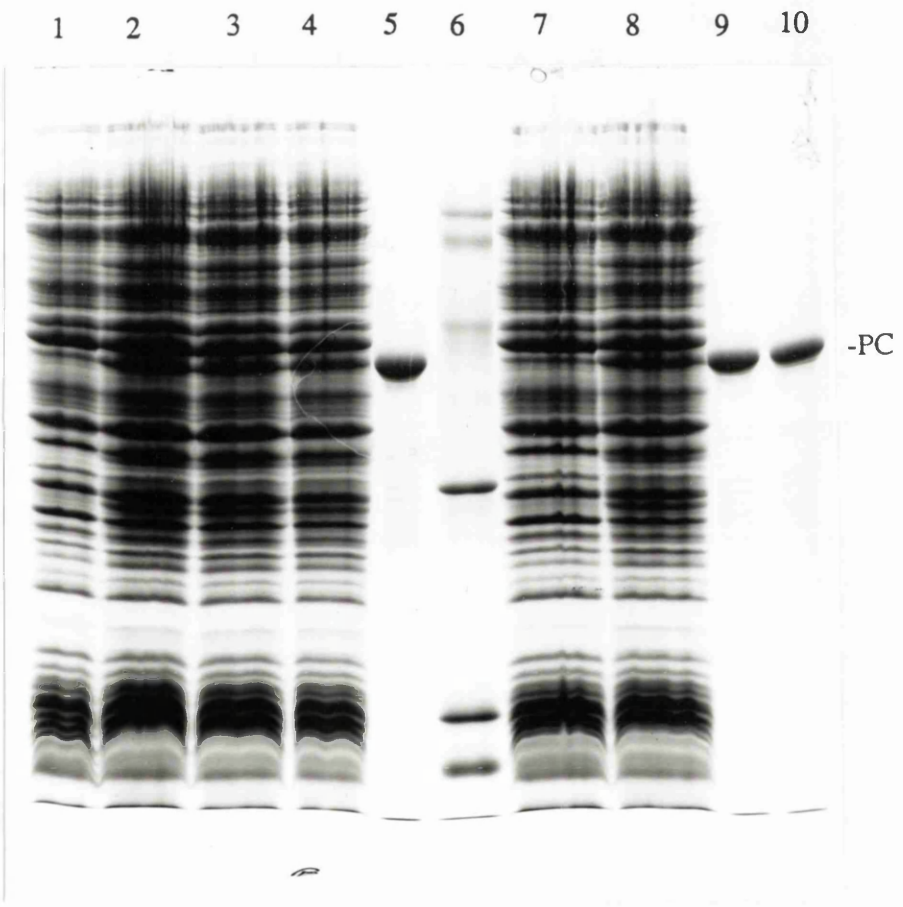

Lane 1 & Lane 7: Cell extracts before induction

Lane 2 - Lane 4: Cell extracts 3, 4, 5 hours after induction

Lane 8: Cell extracts 6 hours after induction

Lane 5, Lane 9 & lane 10: Prochymosin standard

Lane 6: Protein marker

Figure 3.2.13 Re-analysis of the samples from the 42L fermentation using medium 3 (using the method of TCA precipitation of proteins for sample preparation)

Samples were analyzed by 13.5% SDS-PAGE (mini-gel) and visualised by Coomassie staining. Prochymosin bands are visible at about 40 KDa. Because of the limit of protein loading in the mini-gel, all the bands are faint. Because running mini-gel is cheap and time-saving, it is applied to the subsequent SDS-gel analysis (in most cases).

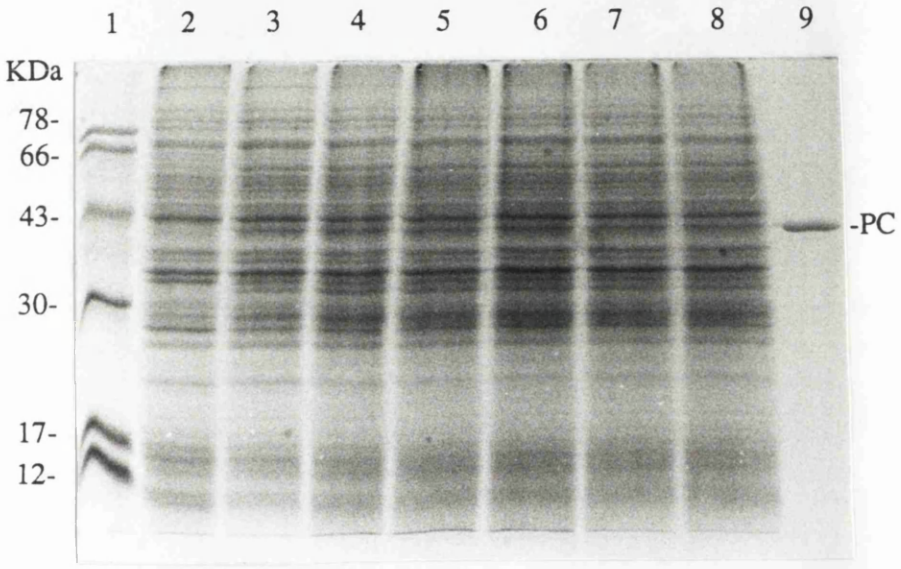

Lane 1 : Protein Marker

Lane 2 : Cells before induction

Lane 3 - Lane 8 : Cells 1,2,...,6 hours after induction

Lane 9 : Prochymosin standard

3.2.2.2 Fermentation medium 4, removal of antibiotic

As mentioned at the beginning of section 3.2.2, the use of antibiotic (ampicillin in this case) is not only expensive but potentially hazardous for industrial scale fermentations. It would be valuable if antibiotic could be avoided.

Caulcott *et al.* (1985) investigated the reason for the instability of plasmids. They employed three different plasmids, pCT70, pCT66 and pCT54. The first one (pCT70) is an intermediate copy number plasmid (40 - 60 copies each chromosome) carrying the prochymosin gene, having a high expression level of prochymosin. The second one (pCT66) is similar to the first (pCT70) but with low expression level of prochymosin. The third one (pCT54) is the parent plasmid of pCT70 and pCT66, not carrying the prochymosin gene. By performing chemostat and shake flask culture (without antibiotic selection), they found that plasmid pCT66 and pCT54 were stable, while plasmid pCT70 was rapidly lost from the host cells. They concluded that the loss of plasmids was related to the expression level of prochymosin gene, because the expression level for pCT70 was higher than for pCT66, and no expression for pCT54. From their results, it was thought that plasmid pMG168 in this project might be stable without antibiotic selection before induction, because of the low copy number of plasmid and thus the low expression level of prochymosin gene. After induction, there is a substantial increase of plasmid copy number so that high level expression of the prochymosin gene results in loss of plasmids. However, cells may possibly be harvested at high density after a period of prochymosin production before the takeover of plasmid-free cells.

Therefore, it was decided to remove antibiotic from fermentation medium 3. Because of the lower cell density achieved by using medium 3 compared with using medium 2, the concentration of Standard Yeatex was increased from 20 g/L to 30 g/L. This resulted in fermentation medium 4 (Table 2.2.6). The initial concern about the solubility of Standard Yeatex proved groundless despite the existence of small quantities of insoluble materials from Standard Yeatex. They were concentration independent as mentioned in the last section. Shake flask culture and fermentation were carried out to verify fermentation 4.

The low inoculum method, whose function was to give long period of maintenance of antibiotic selection, was countered by resulting in long lag phase. In the case of medium 4

where antibiotic was removed, the low inoculum method was not applied because it would not only result in long lag phase but increase the possibility of the loss of plasmids during an increased number of cell generations. In addition, there was a longer lag phase caused by the replacement of casamino acids with Standard Yeatex as observed when using medium 3. Therefore, the standard inoculum method was applied in the subsequent shake flask cultures and fermentations when using medium 4 without antibiotic selection.

3.2.2.2.1 Shake flask culture for expression of calf met-prochymosin in *E. coli* HB101 pMG168 at 50ml scale using fermentation medium 4

Two shake flask cultures were performed at 50ml scale using medium 4 (Table 2.2.6), detailed in section 2.2.5.2. The standard inoculum method was used for inoculation of flask cultures (section 2.2.2.2). The induction points and final OD reading are listed in Table 3.2.9. No.2 flask culture was induced at a higher OD compared with No.1, resulting in higher final cell density. The final cell density achieved for this culture was higher than that for the previous shake flask culture with a similar induction point but using fermentation medium 3 (refer to Table 3.2.7). This might be due to the higher concentration of Standard Yeatex used in medium 4. The lag phase was reduced because of the large inoculum size. The time required for achieving similar induction points was 14 hours for medium 4 compared with 24 hours for medium 3 (see the notes of Table 3.2.9 and Table 3.2.7).

Table 3.2.9 Induction points and final OD readings for shake flask cultures of *E. coli* HB101 pMG168 using fermentation medium 4

Culture No.	Induction point (OD_{600})	*Final OD_{600}
1	1.8	10.5
2	2.0	11.4

*Final OD_{600} : final OD_{600nm} means OD reading 6 hours after induction and 20 hours after inoculation.

Expression of prochymosin in flask cultures of No. 1 and No. 2 was achieved (analyzed by 12.5% SDS-gel, gel picture not shown).

3.2.2.2.2 Fermentation for the production of calf met-prochymosin using medium 4

The standard inoculum method was used to inoculate the fermenter. In order to ensure no plasmid-free cells in the inoculum, antibiotic was still used in the starter and seed cultures, thus the low inoculum method was still applied for their preparation (section 2.2.6). The plasmid stability measurement (section 2.6.2) was performed in all the following fermentations to monitor the presence of plasmids in cells. It was crucial in the case of fermentation medium 4 which lacks antibiotic selection.

One fermentation of *E. coli* HB101 pMG168 at 20L scale was carried out without induction, the objective of which was the same as when carrying out the initial scale-up work using medium 2, *i.e.* to obtain the cell growth curve which was helpful to define the induction point. The growth curve, measured by OD_{600nm}, is shown in Figure 3.2.14 (A). The corresponding final OD reading and average specific growth rate μ in the growth phase are shown in Table 3.2.10. The measurement of plasmid stability was carried out during the fermentation, and the assay result showed that it was 100% stable (Figure 3.2.15).

From this growth curve, it was observed that the cell density achieved was higher than that using medium 3 (Figure 3.2.11) but lower than that using medium 2 (Figure 3.2.6). The growth curve (measured by OD_{600nm}) of the uninduced batch using medium 2 is shown in Figure 3.2.14 (B) again for the convenience of comparison. In initial scale-up study on production of prochymosin using fermentation medium 2, two different induction points, *i.e.* an OD_{600nm} of 7.4 and 6.2 corresponding to 20L and 100L fermentations, were defined in a narrow range in the growth phase (marked with arrows in Figure 3.2.14 (B)). Because the objective of scale-up work is to achieve both maximum expression level of prochymosin and maximum cell density, *i.e.* maximum yield of prochymosin, it is crucial to find out the effect of different induction points on prochymosin yield. It was decided to carry out fermentations with different induction points in a wider range on the growth curve compared with the previous scale-up work. Four induction points, an OD_{600nm} of 11.0, 7.8, 5.2 and 3.0 (marked with arrows in Figure 3.2.14 (1)), were used in four fermentations. Three fermentations at 20L scale were carried out with the induction point of an OD_{600nm} of 5.2, 7.8 and 11.0 respectively, while one fermentation at 100L scale was performed with the induction point of an OD_{600nm} of 3.0. The reason for choosing these induction points is dealt with in the next

section 3.2.2.2.3.

These four fermentations were carried out under the same conditions as for the uninduced batch except that cells were induced. The growth curves of the fermentations at 20L scale, measured by OD_{600nm} and cell dry weight, are shown in Figure 3.2.16, which includes the growth curve of the previous uninduced batch using medium 4 for comparison. The cell growth curve for the 100L batch is shown in Figure 3.2.17. The corresponding induction points, final OD reading and average specific growth rate μ in the growth phase for all these batches are listed in Table 3.2.10. The measurement of plasmid stability was carried for each batch just before cell induction and the results showed the plasmid was 100% stable in these four induced batches (Figure 3.2.15). The relationship between OD_{600nm} and CDW (Cell Dry Weight) for all the batches using medium 4 will be discussed in section 3.2.3. The expression level for each induced batch from SDS-gel analysis is listed in Table 3.2.11, and the relevant yield of prochymosin shown in Table 3.2.12. The fermentation results are discussed in the next section 3.2.2.2.3.

Figure 3.2.14 The *E. coli* HB101 pMG168 fermentation growth curves from uninduced batches employing medium 4 and medium 2

(A) cell growth curve without induction (medium 4)
the arrowed points indicate where subsequent inductions are to be carried out

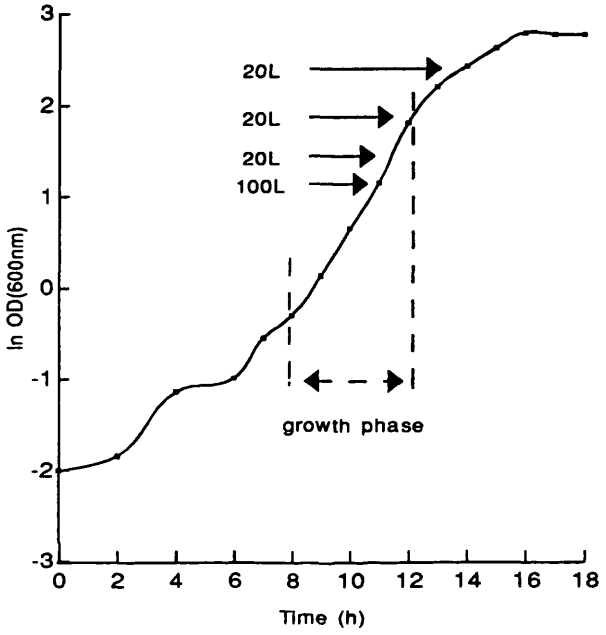

(B) cell growth curve without induction (medium 2)
the arrowed points indicate where previous inductions were carried out

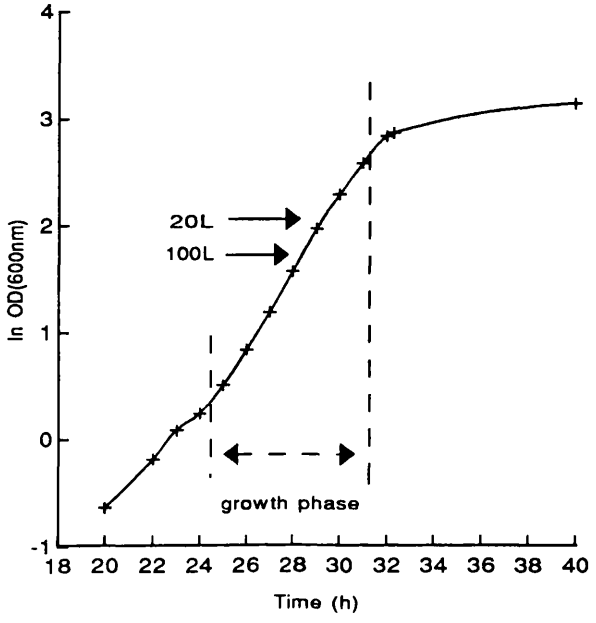

Figure 3.2.15 Plasmid stability during fermentations using medium 4

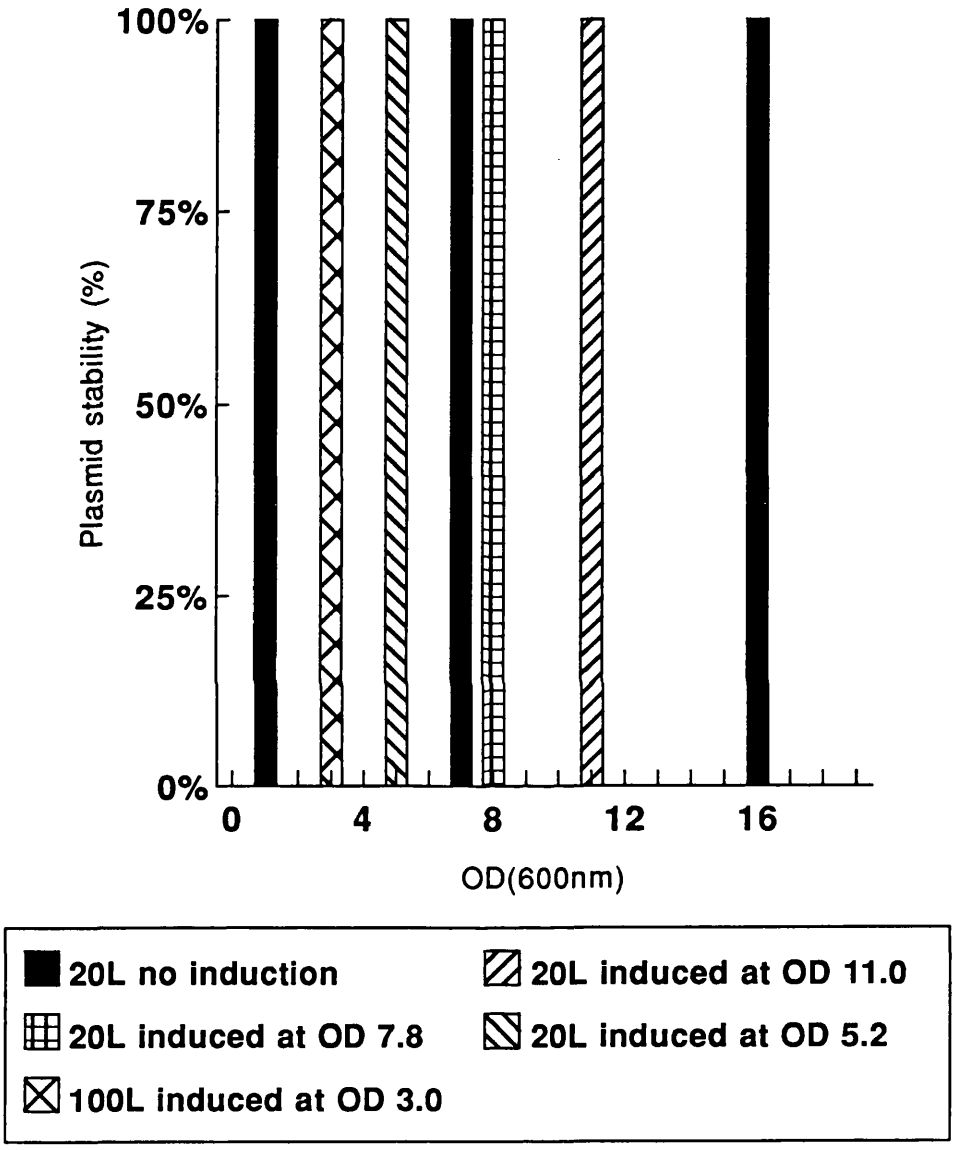

Figure 3.2.16 Growth curves for 20L fermentations using medium 4

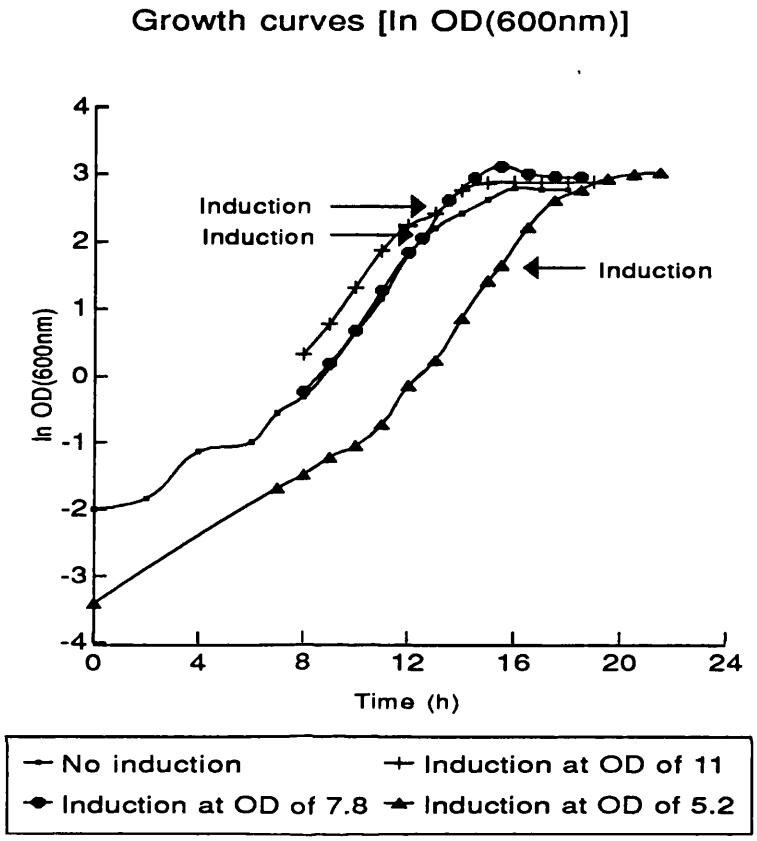

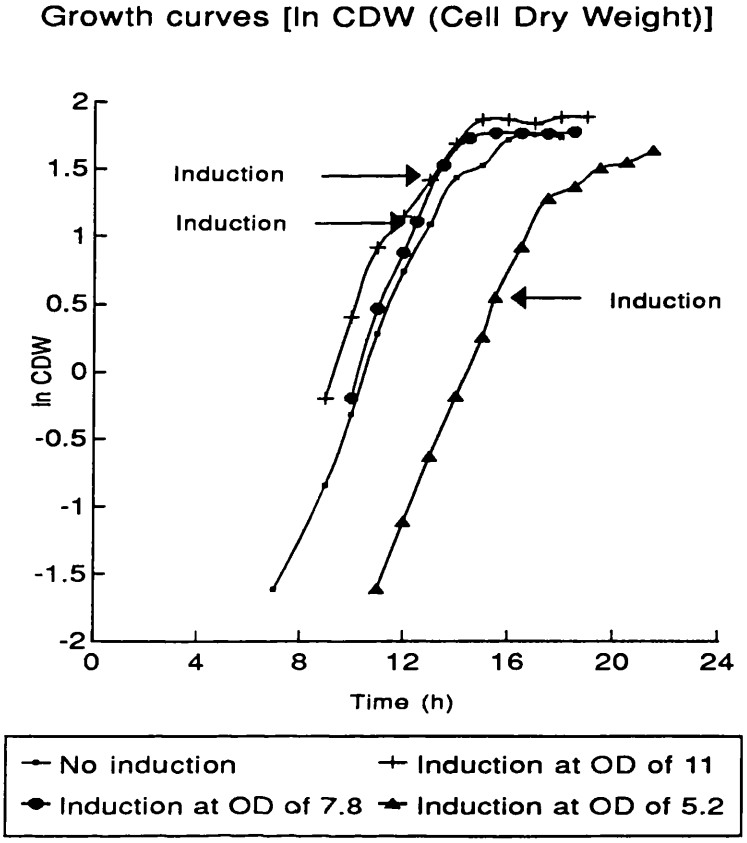

Figure 3.2.17 Growth curve for the 100L fermentation using medium 4

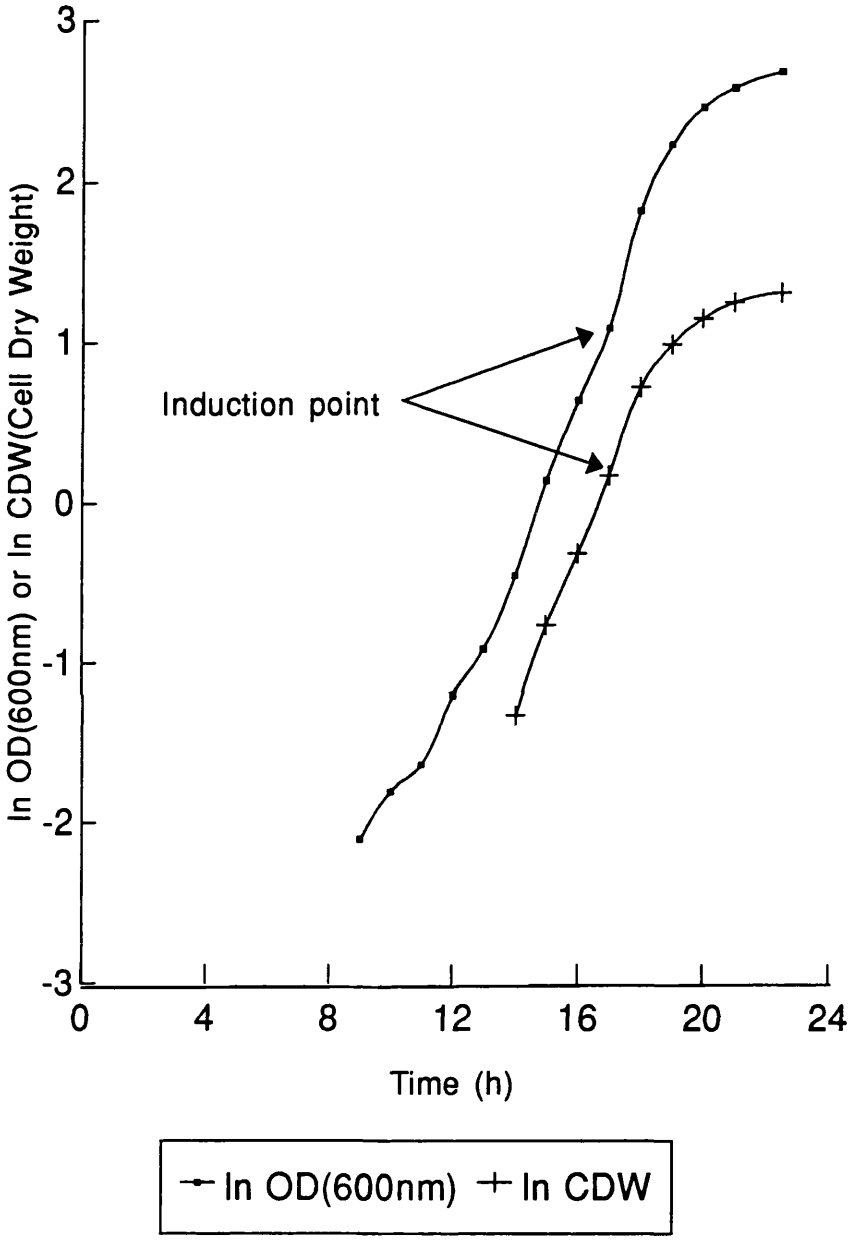

Table 3.2.10 Induction point, final OD readings, final cell dry weights(CDW) and average specific growth rates of *E. coli* HB101 pMG168 fermentations at 20L and 100L scales using medium 4

Batch		Induction point (OD_{600nm})	*Final OD_{600nm}	*Final CDW ($g.L^{-1}$)	μ (average) (h^{-1})
20L	Uninduced	-	16.3	5.8	0.55
	Induced	11.0	17.8	6.6	0.51
	Induced	7.8	19.1	5.9	0.52
	Induced	5.2	20.6	5.1	0.54
100L	Induced	3.0	14.6	3.7	0.52

*Final OD_{600nm} and Final CDW : cell density of the last sample of each fermentation.

Table 3.2.11 Expression level of prochymosin (percentage of total cell proteins) at 20L and 100 scales fermentations using medium 4

Expression level (%) for each batch		Time (h)[1]						
		0	1	2	3	4	5	6
20L	Induced at OD 11.0	-	-	-	-	-	-	-
	Induced at OD 7.8	-	1.8	3.5	4.2	4.4	5.7	5.4
	Induced at OD 5.2	-	1.8	2.9	3.8	4.4	6.5	6.2
100L	Induced at OD 3.0	-	2.0	3.8	4.3	4.8	5.7	/

1. Time (h): 0 represents the moment just before cell induction, and 1,2,...,5 means 1,2,...,5 hours after induction.

Table 3.2.12 Prochymosin yields achieved by different batches using medium 4

Batch	20L induced at OD 5.2	20L induced at OD 7.8	100L induced at OD 3.0
Yield (g/L)	0.3	0.3	0.2

*The calculation procedure of prochymosin yield see overleaf:

The prochymosin yield $Y = C_c \times C_p \times A$

where C_c - Final cell dry weight (CDW) of each batch [g/L] (Table 3.2.10)

C_p - Total protein concentration [g protein/g CDW] (soluble protein + insoluble protein, see Table 3.5.1)

A - Prochymosin expression level of each batch [%] (Table 3.2.11, the expression level from the final example was used)

3.2.2.2.3 The effect of induction point on the yield of prochymosin when using fermentation medium 4

The induction point for the first 20L fermentation using medium 4 was defined as an OD_{600nm} of about 5 - 5.5 from the growth curve without induction, one third of the final OD_{600nm} of 16, to mimic the 20L fermentation using medium 2 which was induced at an OD_{600nm} of 7.4, one third of the final OD_{600nm} of 23 (see Figure 3.2.14). The cell density achieved (5.1 g/L) was lower than with the uninduced batch (5.8 g/L) in terms of cell dry weight (Table 3.2.10), and this was also observed in the case of the 20L fermentation using medium 2 (Table 3.2.3). The expression level of prochymosin (percentage of total cell protein) was 6.5% (Table 3.2.11) from SDS-gel analysis, shown in Figure 3.2.18(B) and Figure 3.2.19 (repeated analysis for better resolution).

Induction of cells at a later stage in the growth phase (an OD_{600nm} of 7.8) and an early stage in the stationary phase (an OD_{600nm} of 11.0) was carried out in two 20L batches respectively. The objective was to find out whether expression of prochymosin could be achieved and cell density improved.

The batch which was induced at an OD_{600nm} of 7.8 achieved higher cell density (5.9 g/L CDW) but compensated by exhibiting lower expression level (5.7%), compared with the previous batch induced at an OD_{600nm} of 5.2. The SDS-gel picture is shown in Figure 3.2.18(A).

The batch induced in the stationary phase (an OD_{600nm} of 11.0) achieved highest cell density (6.6 g/L CDW) but no prochymosin was produced (Figure 3.2.20). The reason for not achieving expression of prochymosin when induced in the stationary phase might be: cells in the stationary phase were not metabolically active thus resulted in the structural instability of plasmid when induced, *i.e.* the loss of prochymosin gene. In the gel picture (Figure 3.2.20), β-lactamase bands are visible after induction (not before induction), indicating the existence of a high copy number of plasmids in the cells because the antibiotic resistance gene is on the plasmid. The presence of plasmids in the cells was also confirmed by the plasmid stability measurement (Figure 3.2.15).

The results obtained from 20L scale fermentations showed that the induction point should be in the growth phase. The expression level of prochymosin decreased but the cell density increased with induction in the later stage of the growth phase. A definition of yield was required for comparison of different batches. The prochymosin yields (g per unit volume of medium) of the two 20L fermentations induced in the growth phase (an OD_{600nm} of 5.2 and 7.8 respectively) were the same (0.3 g/L), and are listed in Table 3.2.12.

With these results, a fermentation at 100L scale was carried out to produce recombinant cell materials for downstream processing studies. The induction point for the 100L batch could be defined in an OD_{600nm} range of 5 - 8, because the two 20L batches had the same yield of prochymosin (Table 3.2.12). However, in order to find out whether cell induction at an earlier stage in the growth phase, *i.e.* before an OD_{600nm} of 5.2, would achieve a higher expression level of prochymosin, an OD_{600nm} of 3.0 was defined as the induction point. Because this induction point was at the relative same position in the growth phase as in the case of the 100L fermentation using medium 2 (see Figure 3.2.14), in which the highest expression level (7.6%) was achieved so far (Table 3.2.4). The 100L fermentation growth curve using medium 4 (Figure 3.2.17) showed that the cell density achieved (3.7 g/L) was lower than for the two 20L batches (5.9 g/L & 5.1 g/L respectively). There was a one third reduction compared with the uninduced batch with cell density of 5.8 g/L, as seen from Table 3.2.10 (The extent of reduction in cell density was the same as in the case of medium 2. A level of 6.9 g/L was achieved in the 100L batch compared with 9.5 g/L achieved in the uninduced batch, see Table 3.2.3). The SDS-gel analysis results suggested that expression of prochymosin in the 100L batch using medium 4 was not improved (Figure 3.2.18(C) & Figure 3.2.19, repeated analysis for better resolution). The expression level (5.7%) was the same as that achieved in the 20L batch induced at an OD_{600nm} of 7.8, but lower than that obtained in the 20L batch induced at an OD_{600nm} of 5.2 (6.5%) (Table 3.2.11). The lower cell density and not improved expression in this 100L batch resulted in a lower yield of prochymosin (Table 3.2.12). The comparison of prochymosin yields achieved by using medium 4 and medium 2 will be discussed in section 3.2.4.

Figure 3.2.18 Expression of calf met-prochymosin from fermentations of *E. coli* HB101 pMG168 using medium 4: (A) & (B), 20L batches induced at an OD_{600nm} of 7.8 & 5.2 respectively; (C), 100L batch induced at an OD_{600nm} of 3.0

Samples were analyzed by 13.5% SDS-PAGE and visualised by Coomassie staining. Prochymosin bands are visible at about 40 KDa. Not being satisfied with the resolution, samples from the 20L batch (induced at an OD_{600nm} of 5.2) and the 100L batch (induced at an OD_{600nm} of 3.0) were re-analyzed and shown in Figure 3.2.19.

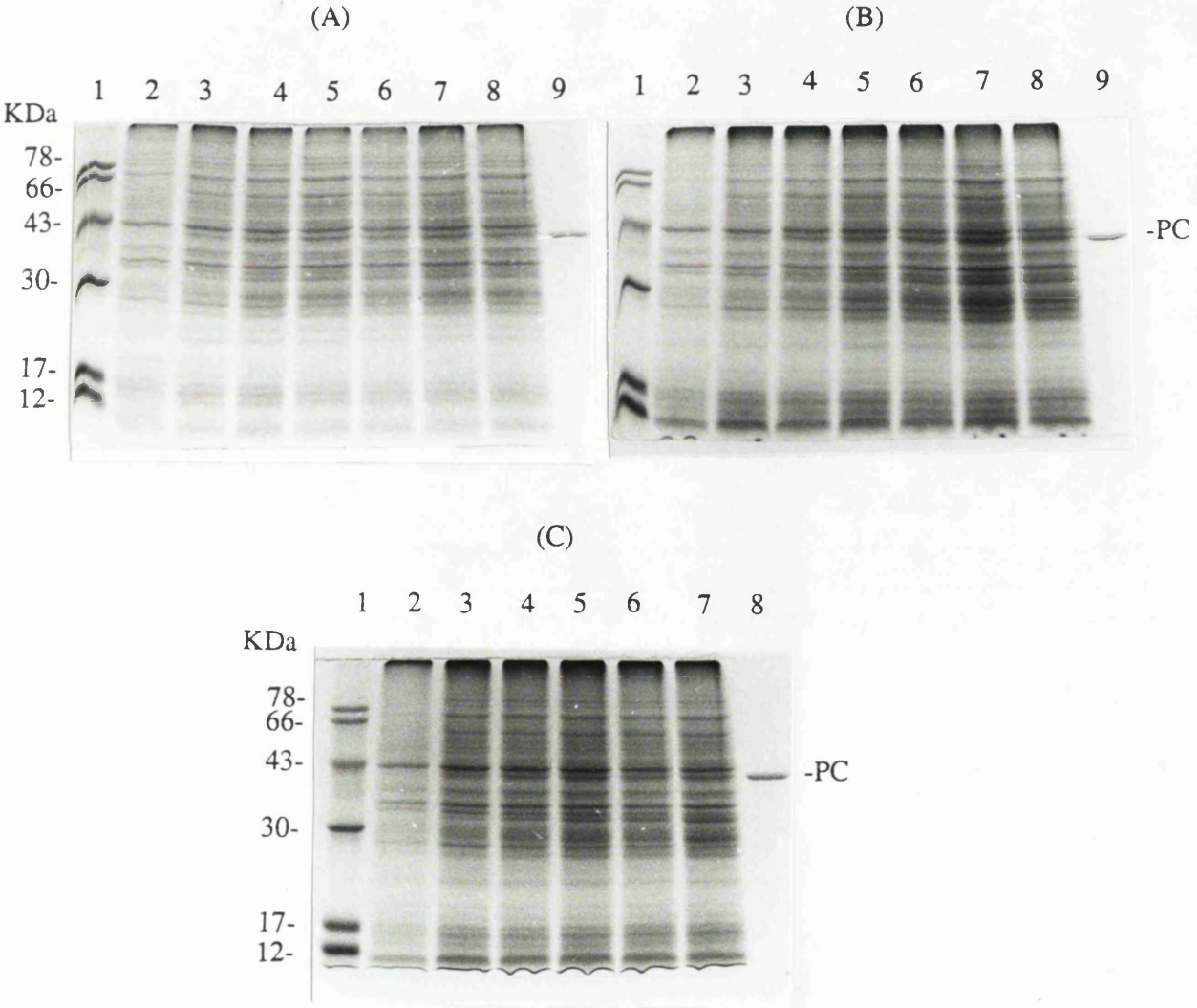

Lane 1 in each picture : Protein Marker; Lane 2 in each picture : Cells before induction; Lane 3 - Lane 7 in each picture : Cells 1,2,...,5 hours after induction; Lane 8 in pictures (A) & (B): cells 6 hours after induction; Lane 9 in pictures (A) & (B) and Lane 8 in picture (C): Prochymosin standard.

Figure 3.2.19 Re-analysis of samples from the 20l batch induced at an OD_{600nm} of 5.2 and the 100L batch induced at an OD_{600nm} of 3.0 (using medium 4)

Samples were analyzed by 15% SDS-PAGE and visualised by Coomassie staining. Prochymosin bands are visible at about 40 KDa.

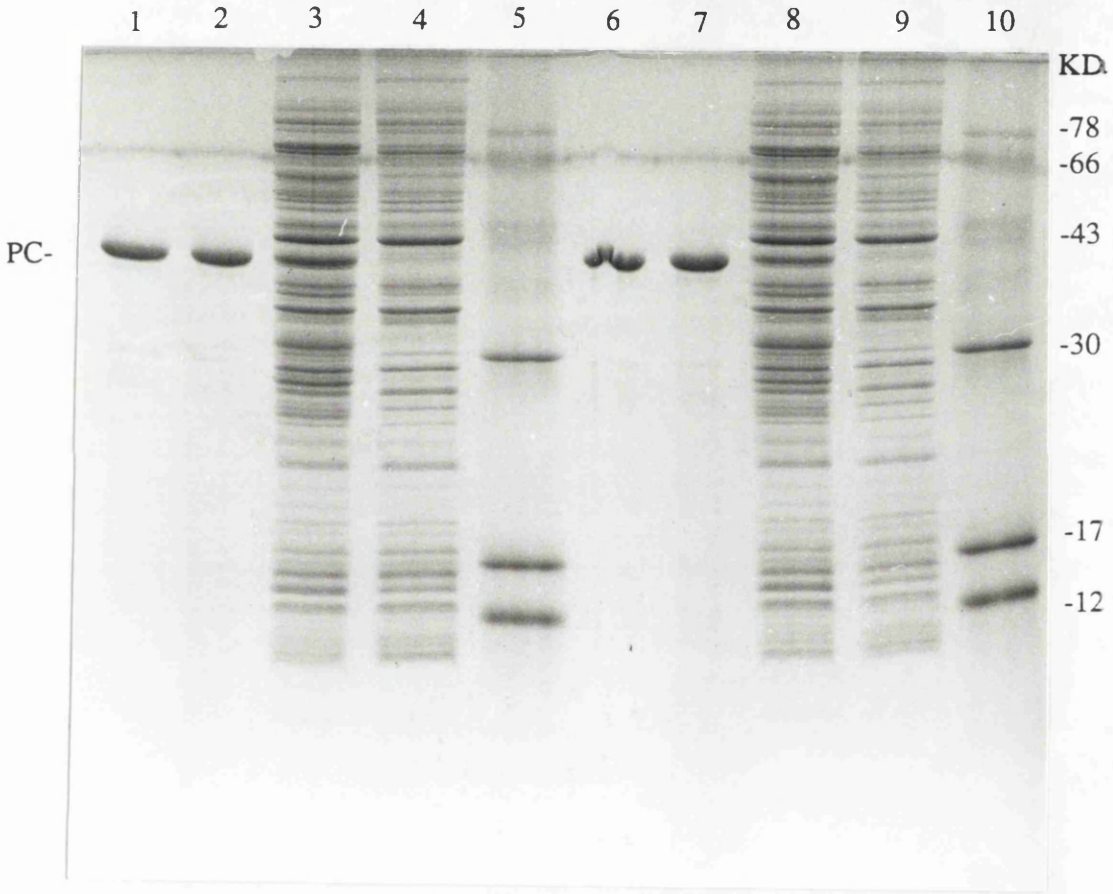

Lane 1, lane 2, lane 6 & Lane 7: Prochymosin standard;

Lane 5 & Lane 10: Protein marker;

Lane 4 & Lane 9: Cells before induction for the 20L and the 100L batch respectively;

Lane 3 & Lane 8 : Cells 6 hours after induction for the 20L and the 100L batch respectively.

Figure 3.2.20 Expression of calf met-prochymosin from pMG168 in *E. coli* HB101 at 20L scale fermentation induced at an OD_{600nm} of 11.0 using medium 4

Samples were taken before induction and 1,2,3,..., and 6 hours after induction, and analyzed by 13.5% SDS-PAGE and visualised by Coomassie staining. Pochymosin bands are not visible. However, the presence of β-lactamase bands at about 29 KDa indicated readthrough of ampicillin resistance gene in the plasmid, thus confirmed the existence of plasmids in cells. The possible reason for poor expression is detailed in the text.

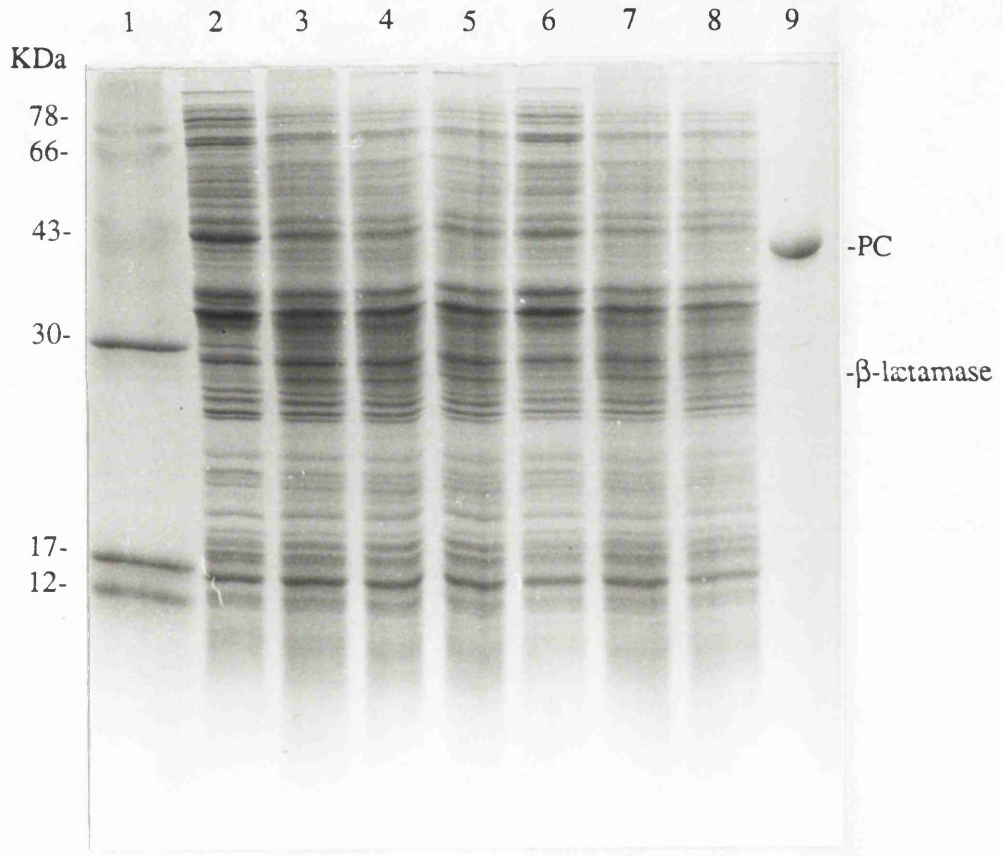

Lane 1 : Protein Marker

Lane 2 : Cells before induction

Lane 3 - Lane 8 : Cells 1,2,...,6 hours after induction

Lane 9 : Prochymosin standard

3.2.2.2.4 The effect of inclusion body formation on the respiratory quotient (RQ) in the batches using fermentation medium 4

It was expected that the respiratory quotient (RQ) would increase after cell induction compared with uninduced cells at the same stage in the growth phase. However, it is difficult to see any change of the RQ from Figure 3.2.21, which contains the parameter RQ for the uninduced 20L batch and the batch induced at an OD_{600nm} of 5.2 using medium 4 (see the last section 3.2.2.2.3). The value of RQ remained at 0.75 - 0.85 in the late stage of growth phase. The same value of RQ was observed for the other batches using medium 4 (results not shown). Thus, it was not possible to find any correlation between the expression level of prochymosin and the value of RQ in this system.

Figure 3.2.21 Respiratory quotients for *E. coli* HB101 pMG168 (using fermentation medium 4)

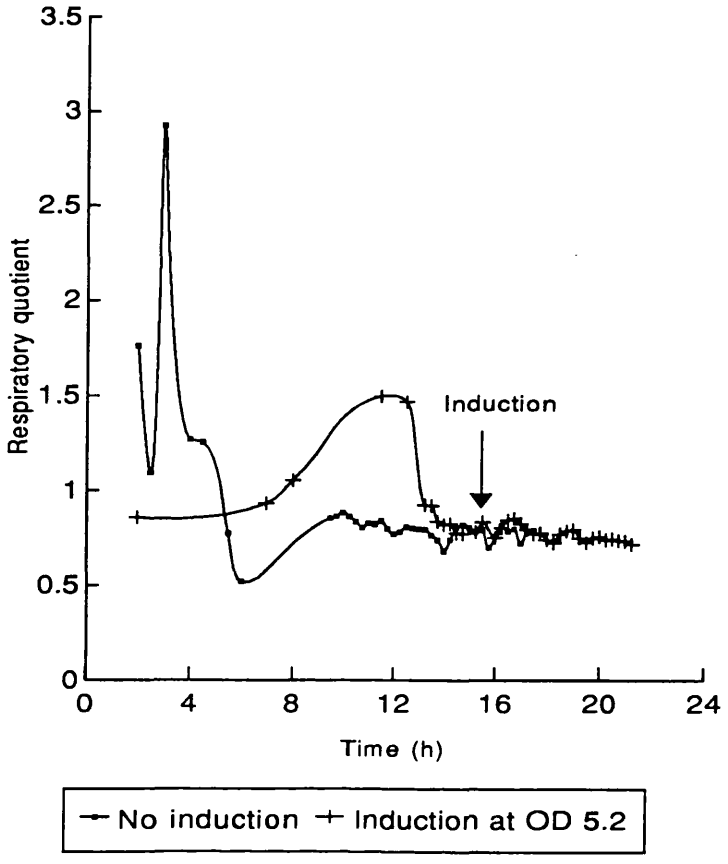

3.2.3 The effect of inclusion body formation on the ratio of OD_{600nm}/CDW(cell dry weight) for *E. coli* HB101 pMG168

Figure 3.2.22 gives the change of ratio of OD_{600nm}/CDW (cell dry weight) via time for the three batches using fermentation medium 2 (section 3.2.1.3). Figure 3.2.23 and Figure 3.2.24 present the same plot for the fermentation using medium 3 (section 3.2.2.1.2) and those using fermentation 4 (section 3.2.2.2.2).

The usually linear relationship between optical density and cell dry weight for bacteria in dilute suspensions is invalid in this recombinant system. It was observed that the ratio of OD_{600nm}/CDW increased after induction in all the batches except the 20L one induced at an OD_{600nm} of 11.0 shown in Figure 3.2.24, which did not achieve expression of prochymosin (discussed in section 3.2.2.2.3). In contrast, all the other induced batches achieved prochymosin expression. It was also observed that there was no such change for the batches without induction. It seemed that the increased ratio of OD_{600nm} /CDW was different for each batch, and to be corresponded to the expression level of prochymosin (presented in each graph). The increase of the ratio reached the greatest extent in the 100L batch using medium 2 where the highest expression level was achieved (7.8%) among all the induced batches (Figure 3.2.22). However, it was difficult to give a quantitative correlation between the ratio of OD_{600nm}/CDW and the expression level of prochymosin.

The increase of the ratio of OD_{600nm}/CDW after induction is a good indicator of the formation of recombinant inclusion bodies, although SDS-gel analysis is still needed for confirmation. The divergence of OD and cell dry weight for inclusion body producing cells has also been observed by Fieschko *et al.* (1985). Hwang and Feldberg (1990) also reported that induction affected turbidity to a greater extent than cell dry weight in their inclusion body producing system, and a new constant value for the relationship of turbidity and cell dry weight was achieved after an initial transition phase (lasting for three hours).

In this study, it was difficult to find a constant ratio of OD_{600nm}/CDW at the early stage of cell growth for the uninduced batches and the batches before induction. The constant ratio was achieved at the late stage of cell growth for the uninduced batches. However, only one induced batch seemed to achieved a constant ratio three hours after induction (Figure 3.2.23).

Figure 3.2.22 The relationship between culture turbidity (OD_{600nm}) and cell dry weight for fermentations at 20L, 100L and 42L scales using medium 2

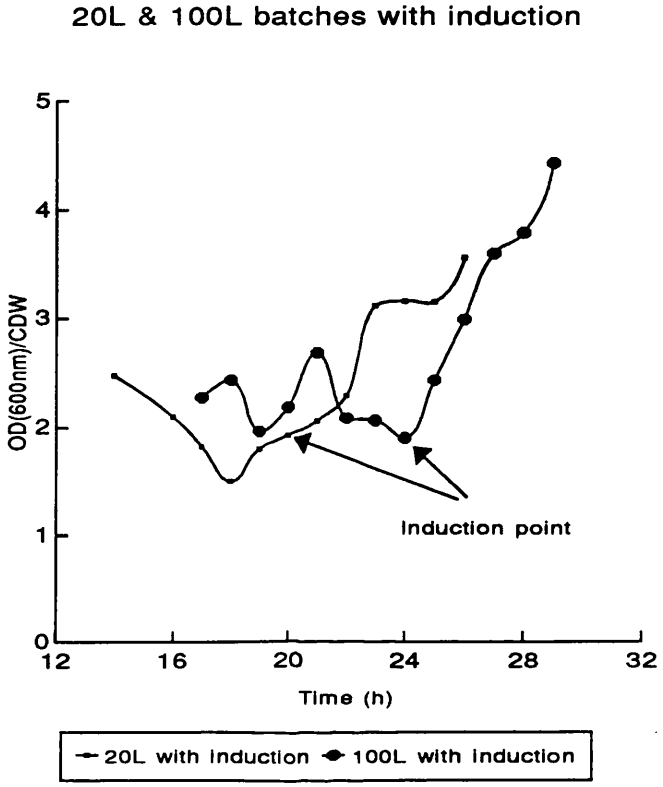

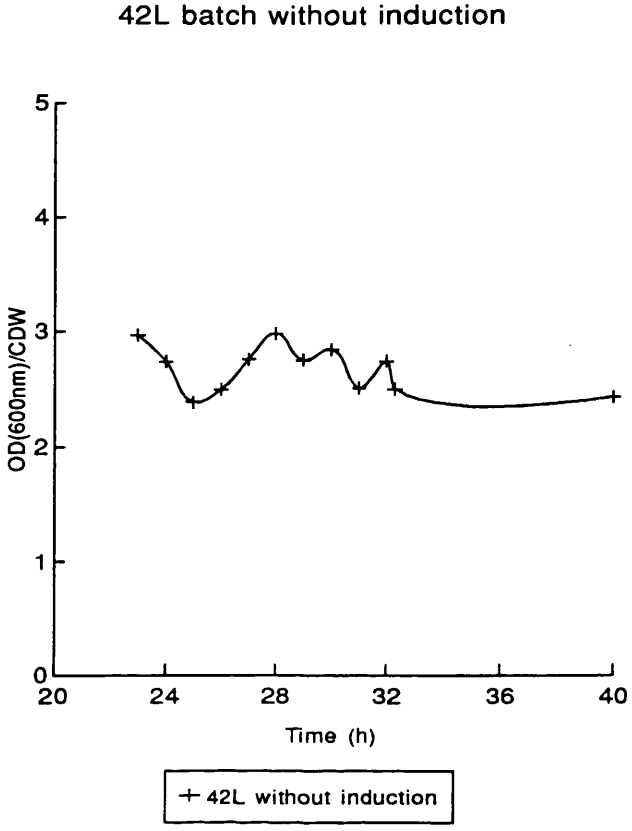

Figure 3.2.23 The relationship between culture turbidity (OD_{600nm}) and cell dry weight for the 42L scale fermentation using medium 3

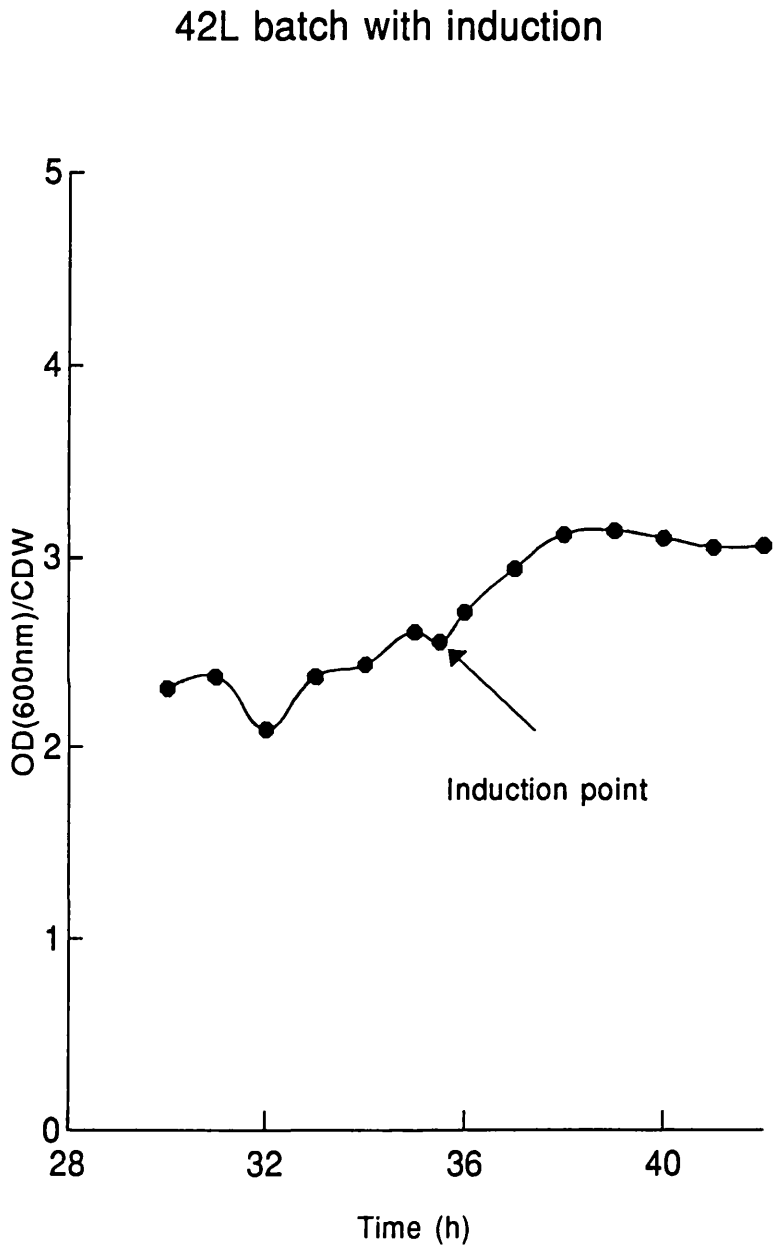

Figure 3.2.24 The relationship between turbidity (OD_{600nm}) and cell dry weight (CDW) for fermentations at 20L and 100L scales using medium 4

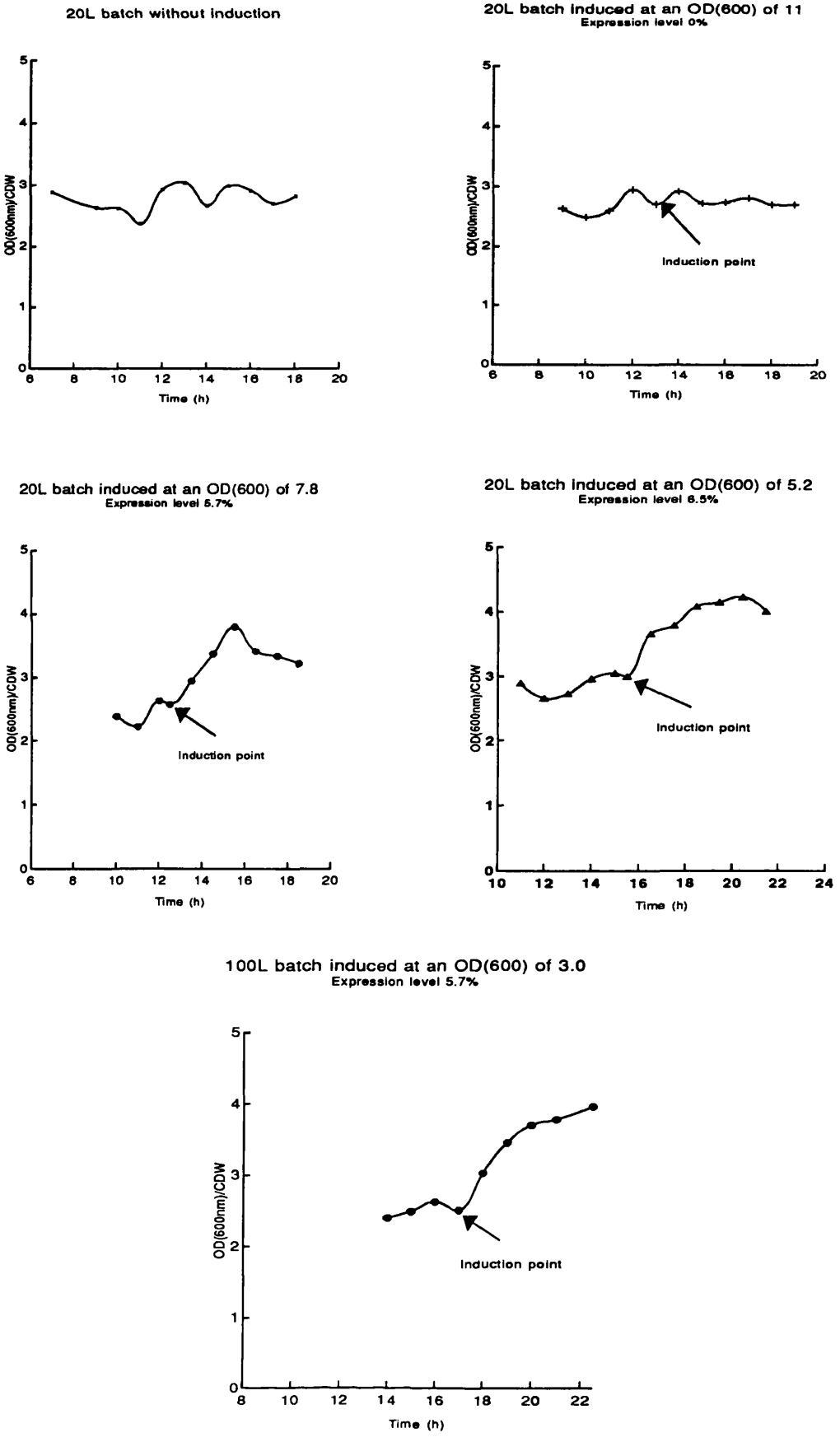

3.2.4 Comparison of medium 2 and medium 4

The costs for chemicals in fermentation medium 2 (Table 2.2.4) and in fermentation medium 4 (Table 2.2.5) for running a 1000L fermentation are listed in Table 3.2.13. As can be seen from Table 3.2.13, the cost is substantially reduced by replacing medium 2 with medium 4. However, this comparison is not accurate because the fermentation results have shown that the expression level of prochymosin and the cell density achieved in batches using medium 4 (Table 3.2.10 and Table 3.2.11) were different from those using medium 2 (Table 3.2.3, Table 3.2.4), thus giving different yields. The yields of prochymosin in batches using medium 4 are shown in Table 3.2.12, and listed in Table 3.2.13 again for comparing with the yield achieved in the 100L fermentation using medium 2. Therefore, the costs for producing the same quantities of prochymosin (100 g) by using medium 2 and medium 4 are calculated, shown in Table 3.2.13.

Table 3.2.13 Cost comparison for production of prochymosin using medium 2 and medium 4

Medium	Cost (1000L)	Yield (g/L)	Cost (per 100 g)
medium 2	Ł2260	0.4	Ł600
medium 4	Ł360	0.3/0.2	Ł120/Ł180

Because of the poorer yield of prochymosin achieved in the 100L batch (0.2 g/L) using medium 4 compared with the 20L batches (0.3 g/L), the cost is raised substantially, but is still less than one third of the cost when using medium 2. However, the yield can be improved by changing the induction point to that used in the 20L batches (section 3.2.2.2.2), thus further reducing the cost to only one fifth of the cost for using medium 2. Furthermore, medium 4 is favoured for large scale production because of the removal of antibiotic, solving the safety issue.

* The calculation procedure of the prochymosin yield see the notes of Table 3.2.12

3.3 Cell disruption

The method for cell disruption was detailed in section 2.4. The relationship between the number of homogenisation passes (N) and soluble protein release (R) for the disruption of *E. coli* HB101 pMG168 at constant pressure (550 barg) is shown in Figure 3.3.1.

It was observed that the cell disruption was almost complete after 3 passes. Although the increase in the number of homogenisation passes from 3 to 5 did not lead to further release of soluble protein, it was previously shown that the size of cell debris was reduced while the size of inclusion bodies was not affected, and this eases the subsequent separation of inclusion bodies from cell debris (Olbrich, 1989). This was confirmed by the particle sizing results (section 3.4.1). Therefore, the cell homogenate used for studies of the inclusion body recovery in an industrial disc centrifuge (section 3.5) was subjected to 5 discrete passes.

The variation in the protein release values (Figure 3.3.1) may due to the variation of cells from different batches or to protein assay errors.

Figure 3.3.1 High pressure homogenisation of *E. coli* HB101 pMG168: soluble protein release

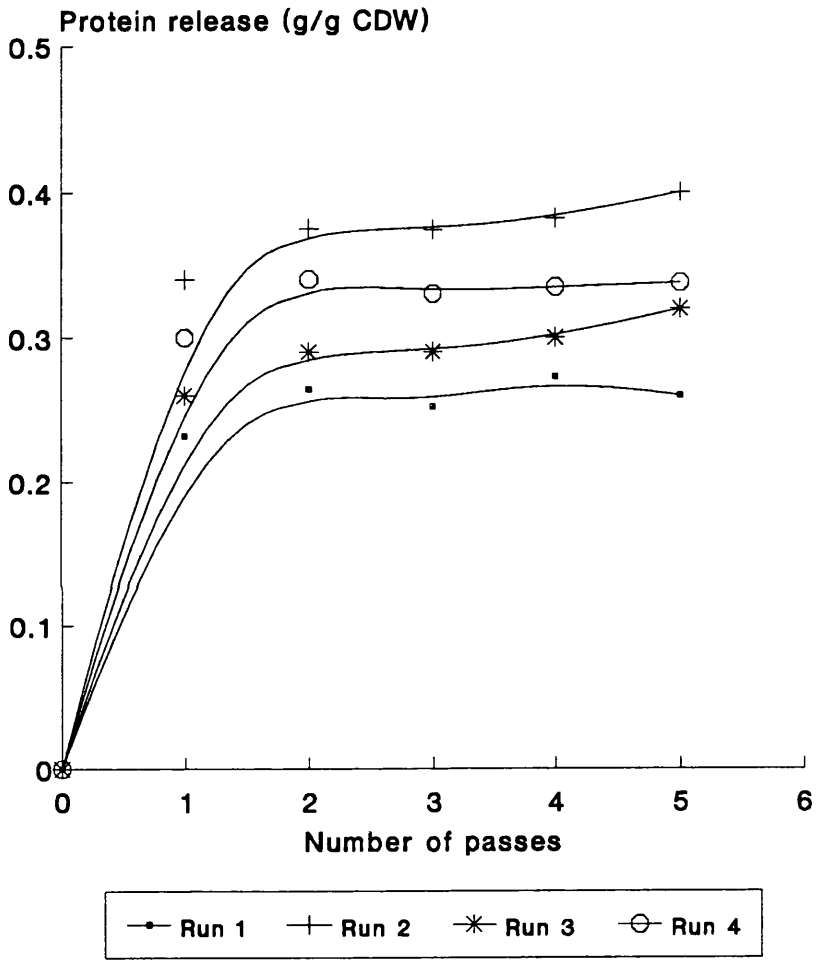

Run 1: Cells from the 100L fermentation batch using medium 2 (section 3.2.1.3), Rm = 0.27 (g/g CDW)

Run 2: Cells from the 100L fermentation batch using medium 4 (section 3.2.2.2.2), Rm = 0.40 (g/g CDW)

Run 3: Cells from the same source as for Run 2, but with a different storage time, Rm = 0.32 (g/g CDW)

Run 4: A mixture of cells from the above two 100L batches, Rm = 0.34 (g/g CDW)

As discussed in section 1.3.2, a disruption model was established by Hetherington *et al.* (1971).

$$\log[Rm/(Rm - R)] = KNP^a$$

where R = soluble protein release

Rm = maximum soluble protein release

K = a dimensional disruption constant

N = number of passes

P = pressure drop

a = a measure of cell-specific resistance to disruption

The disruption of *E. coli* HB101 pMG168 in this study does not seem to have a first-order dependency on the number of passes. However, it may be described by the modified form of the model above (Sauer *et al.*, 1989).

$$\log[Rm/(Rm - R)] = KN^bP^a \qquad (3.3.1)$$

where b = an exponent constant

Because a constant disruption pressure of 550 barg was used in this study, therefore, the above equation can be written as

$$\log[Rm/(Rm - R)] = K'N^b \qquad (3.3.2)$$

where $K' = KP^a$

The value of b is not constant for each run (see Figure 3.3.2), but an average value is obtained as 0.43. The value of K' is also found to vary from 0.72 to 0.93 for these four runs, thus gives an average value of 0.83.

Figure 3.3.2 Relationship between ln [log (Rm/(Rm - R))] and ln N

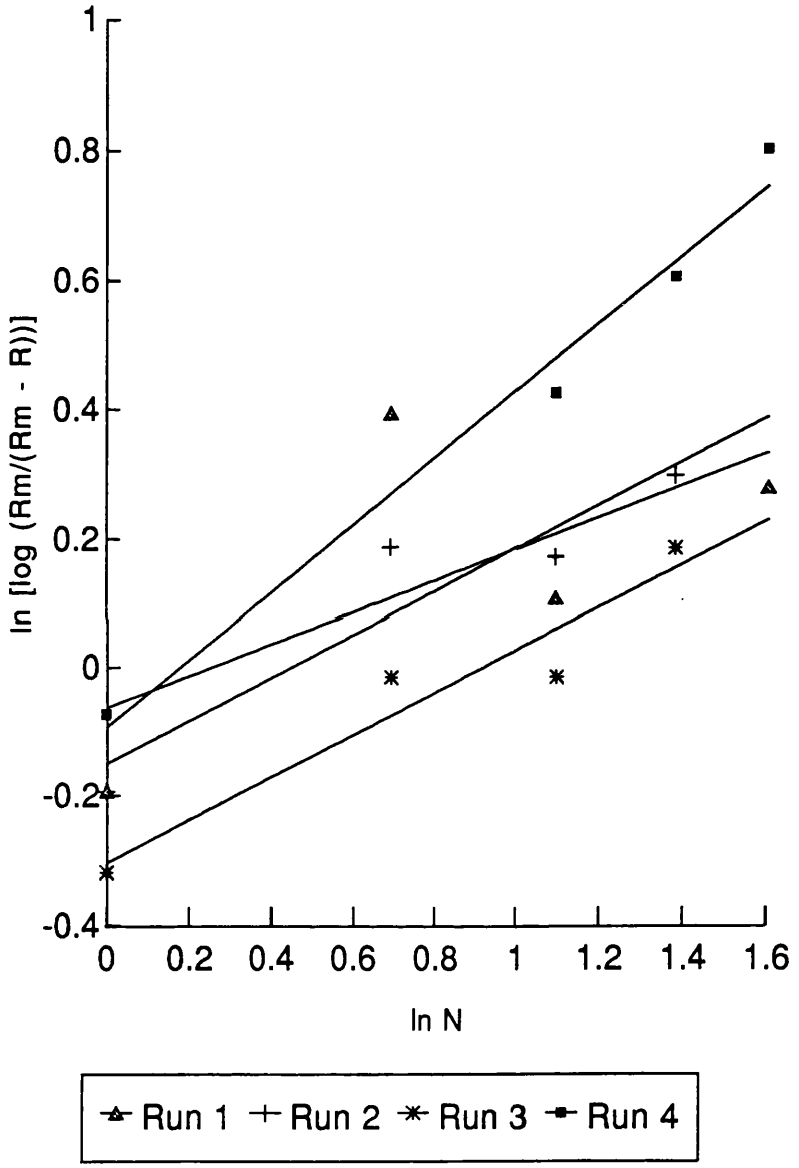

3.4 Inclusion body fraction recovery for *E. coli* HB101 pMG168 at lab-scale

Prior to large-scale separation and recovery of inclusion bodies employing an industrial disc stack centrifuge, preliminary work using a lab centrifuge was undertaken. Various methods were employed for analyzing inclusion body separation and recovery. These included measurements of particle size distribution, turbidity at different wavelengths, protein content and SDS-polyacrylamide gel electrophoretic analysis followed by scanning laser densitometry. In the large scale recovery study, highly-diluted homogenate had to be used because the requirement for a very large amount of cell material could not be met. Hence, lab-scale separations of inclusion bodies were performed with the same highly-diluted homogenate. However, measurements of particle size distribution using centrifugal disc photosedimentation (CPS) with highly diluted homogenate were technically difficult to achieve. Consequently, the cell debris supernatant derived from the undiluted cell homogenate (100 g/L, wet weight) were used for CPS measurements (2.6.5.2).

Homogenates from different passes were centrifuged using conditions (2000 xg, 26 minutes, 5^{0}C) previously determined by Olbrich (1989), a procedure detailed in section 2.5.1). The supernatant fraction contained cell debris free of inclusion bodies while the pellet contained the inclusion body fraction.

3.4.1 Particle sizing of cell debris and inclusion bodies of *E.coli* HB101 pMG168

3.4.1.1 The effect of repeated homogenisation on the particle sizes of cell debris and the inclusion body fraction measured by photon correlation spectroscopy (PCS)

Samples of cell debris in suspension (hence forward referred to as cell debris) and the inclusion body fraction obtained from homogenate with 3 and 5 discrete passes were characterised by PCS, a technique detailed in section 2.6.5.1. Three analyses were carried out for each sample and an average intensity distribution was calculated. The results are shown in Figure 3.4.1.

It was observed that the size of cell debris was reduced to some extent by repeated homogenisation, *i.e.* from 3 to 5 discrete passes, with 50% of particles by intensity greater

than 0.26 and 0.23 μm respectively (termed as D_{50} in figure 3.4.1 and used in the subsequent discussion). In the case of the inclusion body fraction, it was difficult to observe the size difference between 3 and 5 passes, with approximately an identical D_{50} of 0.98 μm. This confirmed that the subsequent separation of the inclusion body fraction from cell debris might benefit from repeated homogenisation although the cell breakage was complete after 3 passes (section 3.3).

3.4.1.2 Particle size analysis of cell debris and the inclusion body fraction by centrifugal disc photosedimentation (CPS)

It was thought that the CPS data would allow a much more accurate measurement of particle sizes (Olbrich, 1989). The samples of cell debris and the inclusion body fraction from homogenate with 5 discrete passes (undiluted) were applied to CPS analysis, a procedure described in section 2.6.5.2. The densities of cell debris and the inclusion body fraction which were required to obtain size distributions were taken from Olbrich's thesis (1989). However, it was not possible to obtain the size distribution of cell debris and only that of inclusion body fraction was measured. The possible reason was the insensitivity of light source in the CPS instrument used to small particles such as *E. coli* cell debris in this study. The results from the optical density readings of the cell debris with different wave lengths support this explanation to some extent (section 3.4.2). The CPS measurement results for the inclusion body fraction are shown in Fig 3.4.2, with the PCS data for cell debris (intensity in Figure 3.4.1 was transferred into cumulative volume oversize) for comparison.

It was observed that CPS analysis gave an average D_{50} of 0.94 μm for the inclusion body fraction in contrast to a D_{50} of 0.23 μm for cell debris obtained by PCS analysis. The size distribution of both the cell debris and the inclusion body fraction obtained in this study matched the data obtained by Olbrich (1989), indicating that his theoretical prediction for separation of prochymosin inclusion bodies from *E.coli* cell debris in an industrial disc stack centrifuge might be the basis for the following study (see section 1.4.2.3.3).

Figure 3.4.1 Particle size analysis (PCS) of *E. coli* HB101 pMG168 cell debris and the inclusion body fraction after homogenisation with 3 and 5 discrete passes

Three runs were carried out for each sample and only an average size distribution is shown for each. In (A), cell debris from 3 passes has a D_{50} = 0.26 ± 0.02 μm, while cell debris from 5 passes has a D_{50} = 0.23 ± 0.02 μm. In (B), the inclusion body fraction from 3 and 5 passes has an identical D_{50} = 0.98 μm.

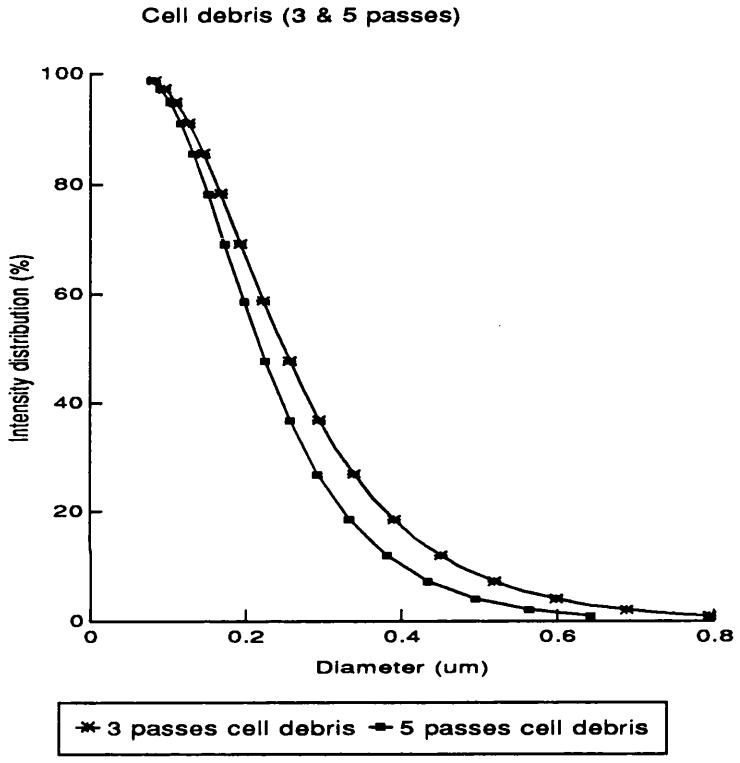

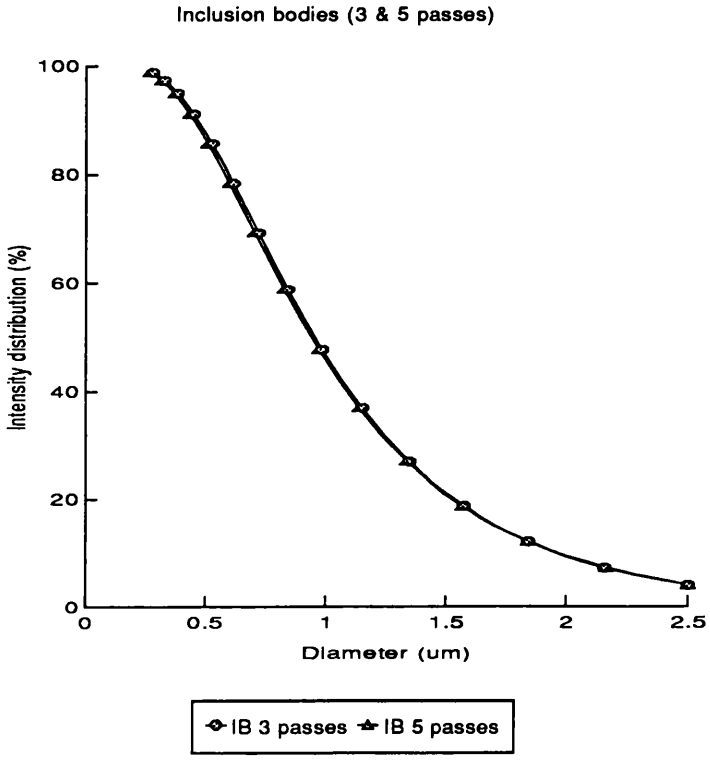

Figure 3.4.2 Particle size analysis (CPS) of the inclusion body fraction together with the PCS data of cell debris (obtained from 5 discrete passes)

Two sets of data were plotted for both the inclusion body fraction and cell debris and the solid lines indicate the average size distributions, with a D_{50} = 0.94 μm for the inclusion bodies and a D_{50} = 0.23 ± 0.02 μm for cell debris.

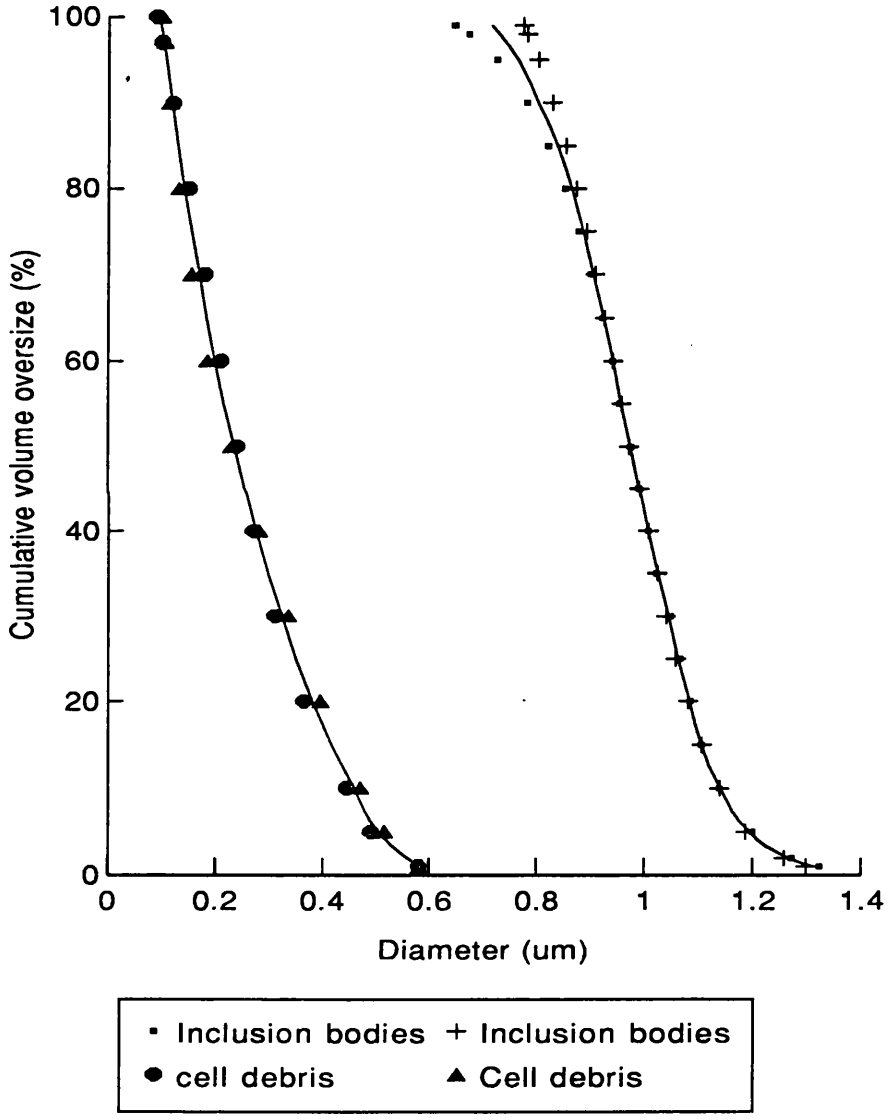

3.4.2 A difference in turbidity ratio (OD_{600nm}/OD_{420nm}) for cell debris and cell homogenate

Following centrifugal separation of the inclusion body fraction described above (using homogenate after 5 passes), turbidimetric measurements of the cell debris supernatants and cell homogenate were made at two wavelengths, 600nm and 420nm. Comparison of measurements made at these two wavelengths for the supernatant fraction containing cell debris and cell homogenate revealed an interesting finding. When the optical densities at 600nm and 420nm were expressed as the ratio of OD_{600nm}/OD_{420nm}, the figure obtained for homogenate was 0.64. Following centrifugation, this ratio changed to 0.38 for the supernatant cell debris (Table 3.4.1). It was possible that dilution could affect particle aggregation/disaggregation characteristics and therefore effect a change in the ratio (OD_{600nm}/OD_{420nm}) on dilution. However, these ratios remained unchanged on dilution of both cell homogenate and supernatant cell debris. The change in the ratio of OD_{600nm}/OD_{420nm} is presumably related to the composition of particles in terms of their sizes and reflectance in suspension. The most likely explanation is that the larger refractile inclusion body particles in cell homogenate scattered light at 600nm more effectively than smaller cell debris particles in the supernatant. (This might also explain in part the failure to detect cell debris in CPS analysis, see section 3.4.1.2). As described later in section 3.5.2, the relationship between the ratio of OD_{600nm}/OD_{420nm} and the particle composition in the suspension was confirmed in a large-scale inclusion body recovery study.

Table 3.4.1 OD_{600nm}, OD_{420nm}, and OD_{600}/OD_{420nm} for the cell debris supernatant and cell homogenate

	OD_{600}	OD_{420nm}	OD_{600nm}/OD_{420nm}
cell debris supernatant	0.065	0.17	0.38
cell homogenate	0.96	1.50	0.64

Homogenate containing inclusion bodies and supernatant containing cell debris were analyzed further by scanning between wavelengths 300nm and 700nm, in order to detect differences in their absorption spectra. No greater differences were observed and consequently "better" wavelengths, which could enhance the differences between cell debris and whole homogenate, in terms of a ratio using two wavelengths, could not be found.

3.4.3 SDS-PAGE analysis of proteins from whole cell homogenate and cell debris fraction

The conditions for lab-scale separation of inclusion body fraction from cell debris previously determined by Olbrich (1989) required verification by SDS-PAGE analysis because there was the possibility that some inclusion bodies might remain in the supernatant.

SDS-PAGE analysis enabled identification of typical soluble proteins, insoluble cell debris proteins and inclusion body proteins. In addition, co-sedimenting proteinaceous contaminants in the inclusion body fraction could be identified.

Figure 3.4.3(A) shows a typical SDS-PAGE analysis of proteins from whole cells before and after induction. Three intense bands appear in cells after induction (Lane 1). They are 41 KDa and 29 KDa bands - corresponding to inclusion body proteins, prochymosin and β-lactamase respectively, and an unidentified 31 KDa protein species. These three proteins are only weakly represented in uninduced cells as evidenced by the presence of extremely feint bands (Lane 2).

Sedimented materials from supernatant containing cell debris and whole cell homogenate were obtained by high speed centrifugation in a microcentrifuge at 13,400 xg (13,000 rpm) for 10 minutes. Results of SDS-PAGE analysis on sedimented cell debris and total insoluble materials from induced cell homogenate (*i.e.* sedimented cell debris and inclusion bodies) are presented in Figure 3.4.3(B).

The sedimented cell debris fraction (Lane 2) contains very faint bands of prochymosin (41 KDa), β-lactamase and the 31 KDa protein. On the basis of two pieces of evidence the 31 KDa protein can be identified as an inclusion body protein - these are (1) that it only appears after induction and (2) that it is absent from the sedimented cell debris fraction.

The sedimented cell debris fraction (Lane 2 in Figure 3.4.3(B)) contains only two major protein species, migrating with apparent molecular weights of 37 and 35 KDa. These two species will be referred to as class I cell debris proteins.

Figure 3.4.3 SDS-PAGE analyses for identifying soluble, cell debris and inclusion body protein species from *E. coli* HB101 pMG168 (quantities of protein loading in each well were based on the same sample volume)

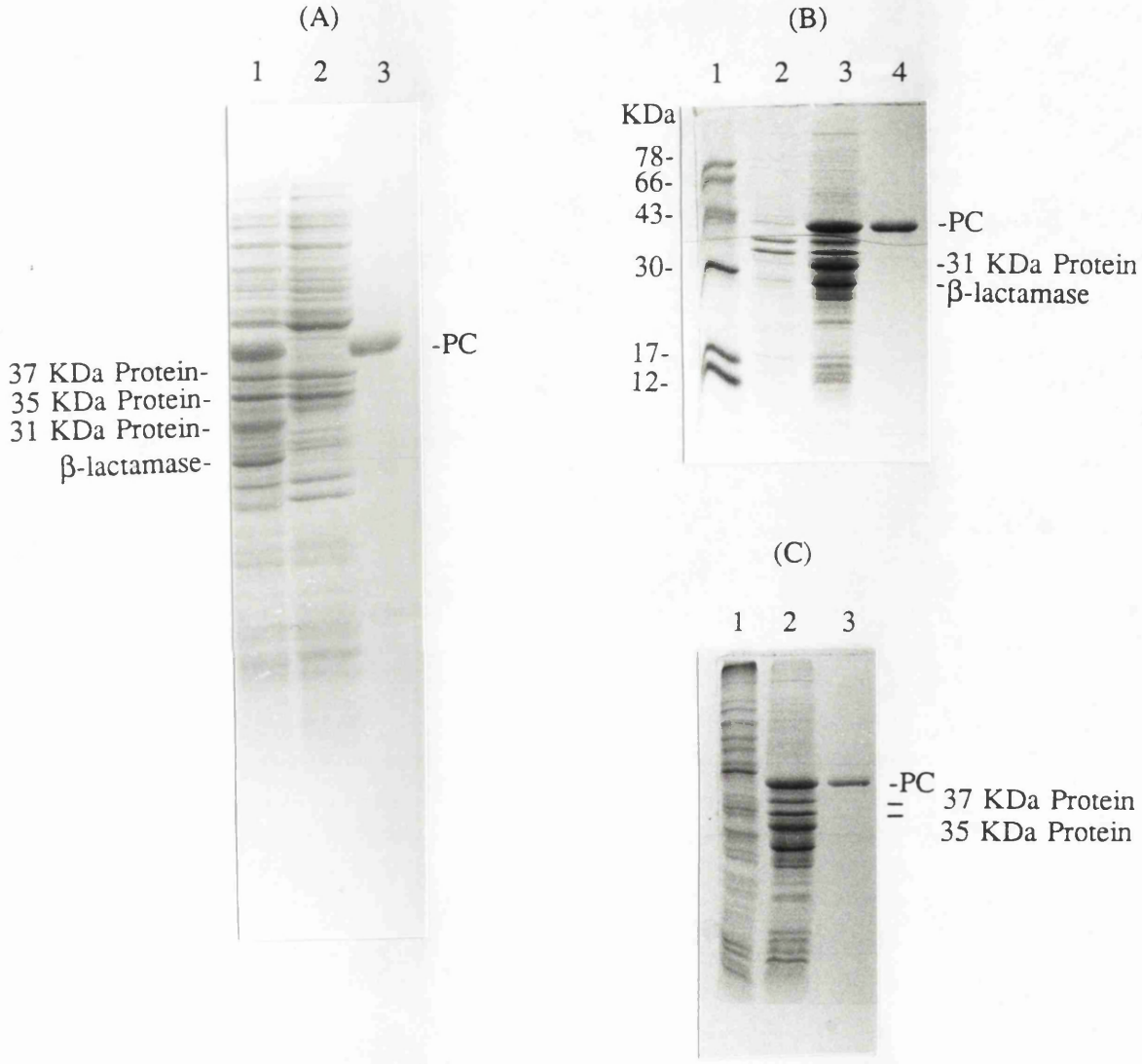

(A) total cell proteins before (Lane 2) and after (Lane 1) induction; prochymosin standard (Lane 3)

(B) protein marker (Lane 1) ; sedimented cell debris proteins (Lane 2); total sedimented cell proteins, *i.e.* cell debris + inclusion bodies (Lane 3); prochymosin standard (Lane 4)

(C) total unsedimented (Lane 1) and sedimented (Lane 2) cell proteins; prochymosin standard (Lane 3)

All the sedimented cell proteins migrating below β-lactamase (29 KDa) (Lane 3 in Figure 3.4.3(B)) are common to both induced and uninduced whole cells (Lane 1 & 2 in Figure 3.4.3(A)) and are therefore unlikely to be inclusion body proteins. However, they are absent from the sedimented cell debris fraction. For convenience, these low molecular weight species are therefore defined as class II cell debris proteins to distinguish them from class I types *i.e.* 37 and 35 KDa sedimented cell debris contaminants. This will be further discussed in section 4.4.1.

Figure 3.4.3(C) shows SDS-PAGE analysis of total unsedimented and sedimented proteins from induced cells. No prochymosin exists in the soluble protein fraction (Lane 1) and all of it is confined to inclusion bodies (Lane 2). Furthermore, there are very few bands in common between the unsedimented and sedimented cell homogenate fractions.

The identification of the inclusion body and cell debris proteins in the cell homogenate is summarised in Table 3.4.2.

Table 3.4.2 Identification of the inclusion body and cell debris proteins in the cell homogenate

Inclusion body proteins	Prochymosin, 41 KDa
	β-lactamase, 29 KDa
	31 KDa species
Cell debris proteins	Class I, 37 & 35 KDa species
	Class II, species below 29 KDa

Calculation of recoveries of individual protein species (listed in the above table) in each fraction (the inclusion body fraction and the cell debris containing supernatant fraction) following the lab centrifuge separation was done using data obtained from BCA protein assays and SDS-PAGE analysis followed by scanning laser densitometry of the gels. The results are listed in Table 3.4.3. Following centrifugation at 2000 xg for 26 minutes, 9% of prochymosin still remained in the supernatant, while 47% of the cell debris co-sedimented with the inclusion bodies.

Table 3.4.3 Recoveries (%) of protein species following lab centrifugal fractionation

Protein species	Protein species (%) in inclusion body fraction	Protein species (%) in supernatant fraction containing cell debris
prochymosin	91	9
β-lactamase	78	22
31 KDa protein	90	10
whole inclusion body proteins	86	14
class I cell debris	8	92
class II cell debris	79	21
whole cell debris	47	53

The calculation procedures are as follows:

Individual protein species (%) in supernatant = $100 \times A_i(s)/A_i(h)$

Individual protein species (%) in the inclusion body fraction = $100 - 100 \times A_i(s)/A_i(h)$

Whole inclusion body proteins or whole cell debris (%) in supernatant = $100 \times \Sigma A_i(s)/\Sigma A_i(h)$

Whole inclusion body proteins or whole cell debris (%) in the inclusion body fraction

$$= 100 - 100 \times \Sigma A_i(s)/\Sigma A_i(h)$$

where $A_i(s)$ - peak area of each protein species in Lane 2 (supernatant sample) of Figure 3.4.3(B);

$A_i(h)$ - peak area of each protein species in Lane 3 (cell homogenate sample) of Figure 3.4.3(B);

$\Sigma A_i(s)$ - the sum of relevant protein peak areas (inclusion bodies or cell debris) in Lane 2 (supernatant sample) of Figure 3.4.3(B);

$\Sigma A_i(h)$ - the sum of relevant protein peak areas (inclusion bodies or cell debris) in Lane 3 (cell homogenate sample) of Figure 3.4.3(B);

3.4.4 Chromatography of the inclusion body fraction

Recently, analytical reverse phase HPLC has been tested in this laboratory for the separation of prochymosin standard from synthetic mixtures of pure proteins - with a view to monitoring the production and recovery of prochymosin (Salt and Turner, 1991; in preparation). The most attractive advantage of reverse phase HPLC over SDS-PAGE analysis for determination of prochymosin is that of speed, and consequently attempts to apply reverse phase HPLC to quantitation of prochymosin were initiated.

Prochymosin standard and the inclusion body fraction from lab centrifuge separations were dissolved in solubilisation buffer containing 8M urea and 50 mM KH_2PO_4 and applied to reverse phase HPLC analytical and semi-preparative columns packed with PLRP-S 300 (15 - 25 μm), as detailed in section 2.6.4. When prochymosin standard was developed on reverse phase HPLC with an eluant pH of 10, one peak was observed (Figure 3.4.4, bottom panel). However, when the inclusion body fraction was developed under identical conditions, the peak previously observed for the prochymosin standard disappeared and was replaced by two peaks - one on either side of the original peak for prochymosin (see Figure 3.4.4, middle panel). Analysis of these peak fractions from semi-preparative HPLC by SDS-PAGE revealed that prochymosin was primarily associated with the second peak (see Figure 3.4.5). However, both peaks contained a number of other components. Tentative identification of these contaminants are: in peak 1 - the 37 KDa cell debris class I protein; and in peak 2 - the 31 KDa inclusion body protein.

Varying the pH value of the eluant had little or no effect on chromatographic resolution of the double peaks (refer to Table 3.4.3). This suggests that electrostatic complex formation between prochymosin and the other peak components is unlikely.

Because of the uncertain results from HPLC analysis, and the lack of time available, only SDS-PAGE analysis was applied to the large-scale separation study in the next step.

Table 3.4.4 Effect of eluant pH value on chromatographic resolution of the double peaks

Column	Sample	pH 10.0	8.0	7.0
Analytical	pure prochymosin	13.84		
	Inclusion body fraction	13.37/13.93	11.77/12.33	12.71/13.33

*Elution time in minutes.

Figure 3.4.4 Reverse phase HPLC analysis of the inclusion body fraction from lab centrifuge separation

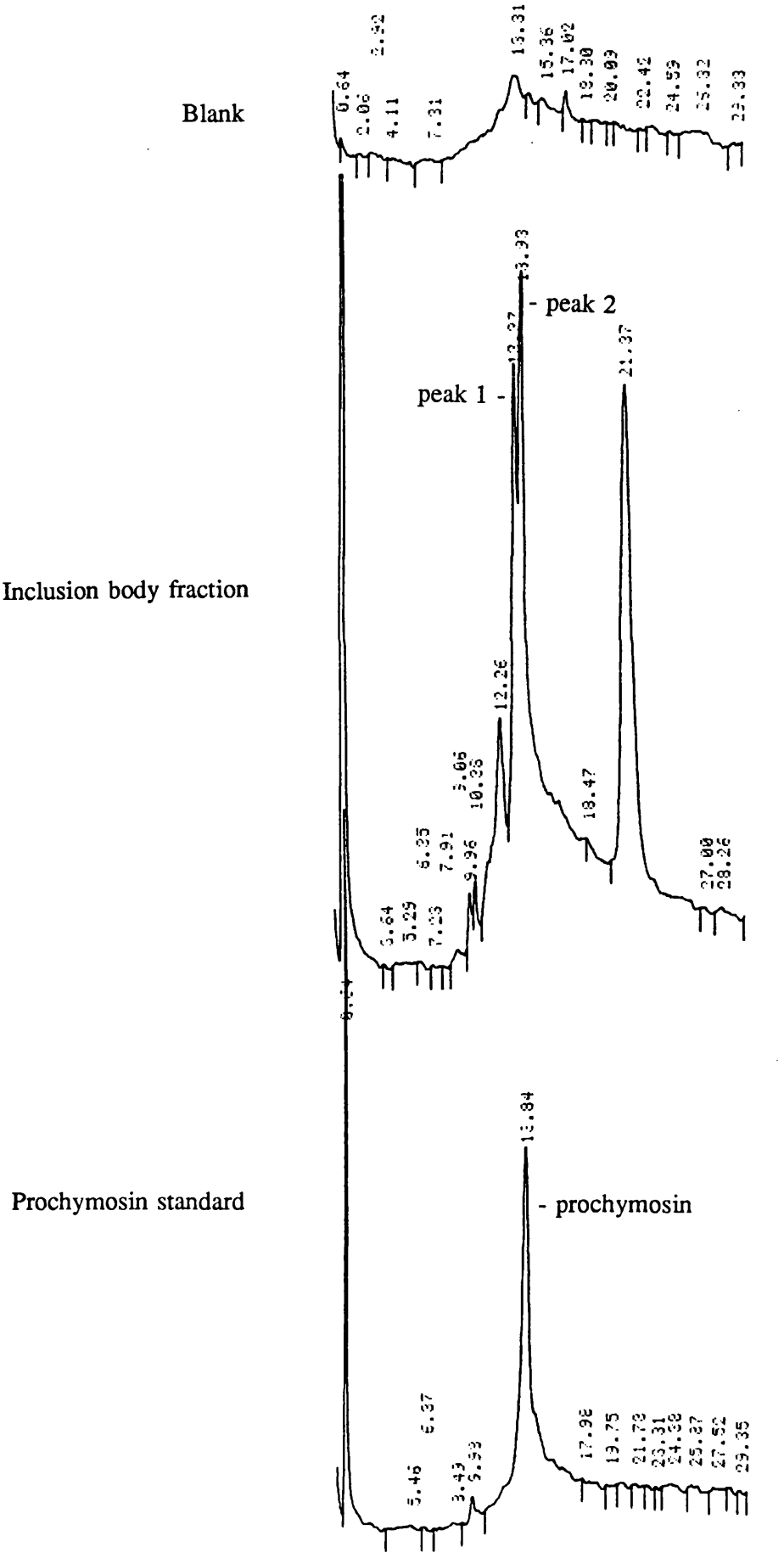

Figure 3.4.5 SDS-gel analysis of the double peaks eluted from the semi-preparative HPLC of the inclusion body fraction

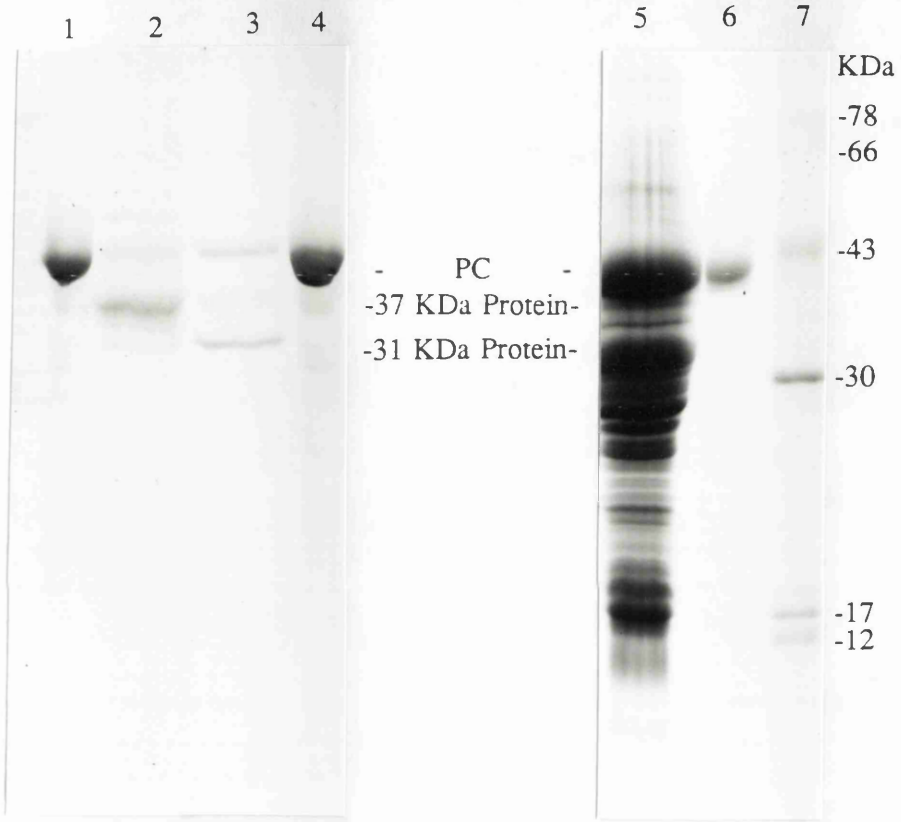

Lane 1 : Prochymosin standard

Lane 2 : Eluted fraction corresponding to peak 1

Lane 3 : Eluted fraction corresponding to peak 2

Lane 4 : Prochymosin standard

Lane 5 : Inclusion body fraction

Lane 6 : Prochymosin standard

Lane 7 : Protein marker

3.5 Inclusion body fraction separation for *E. coli* HB101 pMG168 in an industrial disc stack centrifuge

An industrial disc stack centrifuge (CSA-8-06-476 disc centrifuge) was employed for studies of the separation of the inclusion body fraction from the cell debris. Full experimental details are discussed in section 2.5.2.

3.5.1 Relationship between supernatant turbidity and feed flow rates

As discussed in section 3.4.2, the larger refractile inclusion body particles would appear to scatter light at 600 nm more effectively than smaller cell debris particles. This explanation was used to account for the higher ratio (OD_{600nm}/OD_{420nm}) of the cell homogenate containing inclusion bodies compared to that of the cell debris in the supernatant following lab-scale centrifugation.

Performance of the disc centrifuge was examined using a variety of feed flow rates. Increasing the flow rate reduced performance of the disc centrifuge - the recovery of inclusion bodies by the centrifuge diminished and there were increasing numbers of inclusion body particles found in the supernatant.

Manual monitoring of the turbidimetric ratio at different flow rates should enable an estimate of disc centrifuge performance to be made. Olbrich's (1989) model predicts that the flow rate for optimal inclusion body recovery and removal of cell debris in the industrial disc stack centrifuge (BSB-7-476) is within the range of 100 - 500 L/h. Initial plans were to examine the performance of the Westfalia (CSA-8-06-476) disc centrifuge within this range because this apparatus has similar specifications to that of the instrument employed previously by Olbrich (1989). However, during the early stages of the experiment, deviations from Olbrich's prediction were observed (estimation from the ratio of OD_{600nm}/OD_{420nm}). When carrying out the first run at a flow rate roughly in the middle of the predicted range, *i.e.* 228 L/h (see Figure 4.1.1), turbidimetric ratio (OD_{600nm}/OD_{420nm}) measurements were considerably lower (0.31, see Figure 3.5.1(B)) than those obtained with the lab centrifuge (0.38, marked with a line in Figure 3.5.1(B)). This implied that high recovery of inclusion bodies were achieved by the disc stack centrifuge at this flow rate, but may not be as high as predicted

Figure 3.5.1 Relationship between supernatant turbidity and feed flow rates

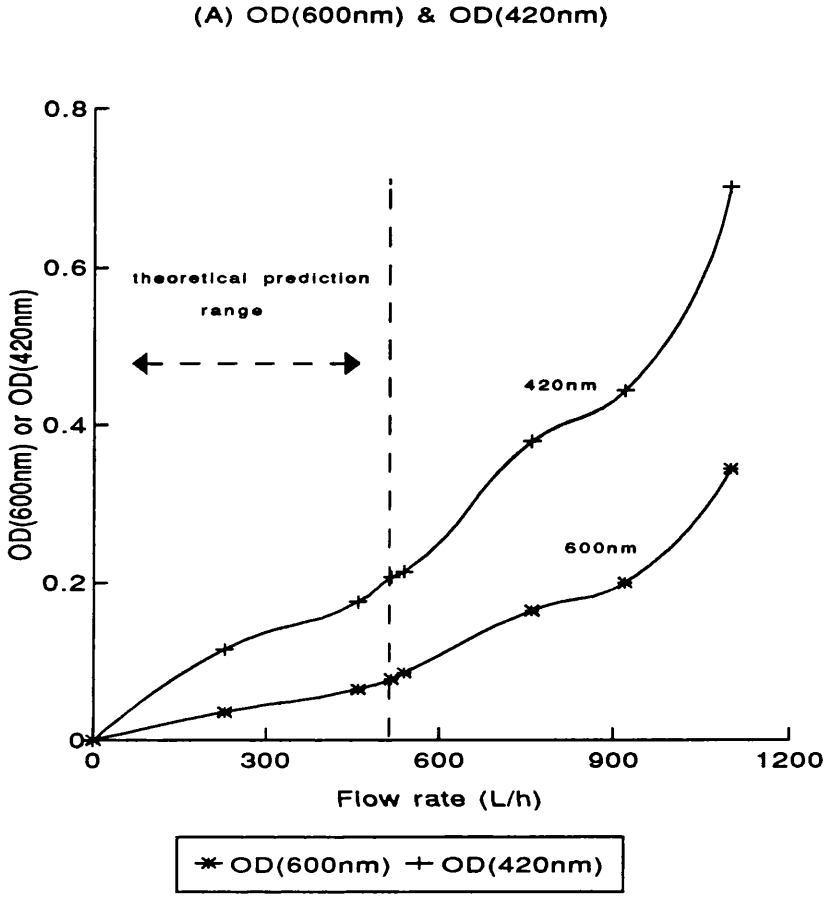

(see Figure 4.4.1 in section 4.4.1). On increasing the flow rate in the second run to a value at the top of the predicted range (518 L/h, marked with a line in Figure 3.5.1(A)), the turbidimetric ratio (OD_{600nm}/OD_{420nm}) was roughly equal to that obtained with the lab centrifuge (0.38), indicating that at this flow rate the recovery of inclusion bodies was still very high, and may be higher than that predicted (refer to Figure 4.4.1).

Increasing the flow rate further to observe deterioration of disc centrifuge performance was necessary in order to fully evaluate the true capabilities of this instrument. Subsequent flow rates were selected as a result of turbidimetric ratio measurements.

Figure 3.5.1(A) shows how the turbidity of the supernatant at 600nm and 420nm changes with increasing feed flow rate. Clearly, the amount of material retained by the centrifuge is reduced. The relationship between turbidimetric ratio and feed flow rate (Figure 3.5.1(B)) indicates that the proportion of inclusion bodies remaining in the supernatant rises with increase in feed flow rate as predicted above. However, information on the actual composition of the material in the flow through supernatant can only be obtained after detailed SDS-PAGE analysis.

3.5.2 SDS-PAGE analysis of inclusion body separation in an industrial disc stack centrifuge

SDS-PAGE analysis was carried out for three sets of samples taken after a volume passed of 30L, 60L and 90L respectively, and each set was composed of samples from 7 different feed flow rate, *i.e.* 228 L/h, 460 L/h, 518 L/h, 540 L/h, 760 L/h, 920 L/h and 1100 L/h plus the feed sample (section 2.5.2). The results are shown in Figure 3.5.2, in which pictures (A), (B) and (C) correspond to the sets of samples after a volume passed of 30L, 60L and 90L, respectively.

The identification of protein species for the cell debris and the inclusion body fraction was the same as discussed in section 3.4.3. The calculation results in terms of recovery or removal of the protein species listed in Table 3.4.2 were determined using data obtained from BCA protein assays (Table 3.5.1) and SDS-PAGE analysis followed by scanning laser densitometry of the gels (Figure 3.5.2).

Table 3.5.1 Concentrations of soluble and insoluble proteins in whole cell homogenate and from samples of supernatant obtained at different feed flow rates

Sample	Insoluble protein con. (μg/ml)	Soluble protein con. (μg/ml)
228 L/h	30	275
460 L/h	43	280
518 L/h	47	278
540 L/h	44	250
760 L/h	60	275
920 L/h	65	260
1100 L/h	96	285
whole homogenate	250	260

Figure 3.5.2 SDS-gel analysis of the supernatant samples from an industrial disc centrifuge

(A), (B) and (C) correspond to the sets of samples after a volume passed of 30L, 60L and 90L, respectively; the protein loading of each sample for SDS gel (13.5%) was based on the same sample volume.

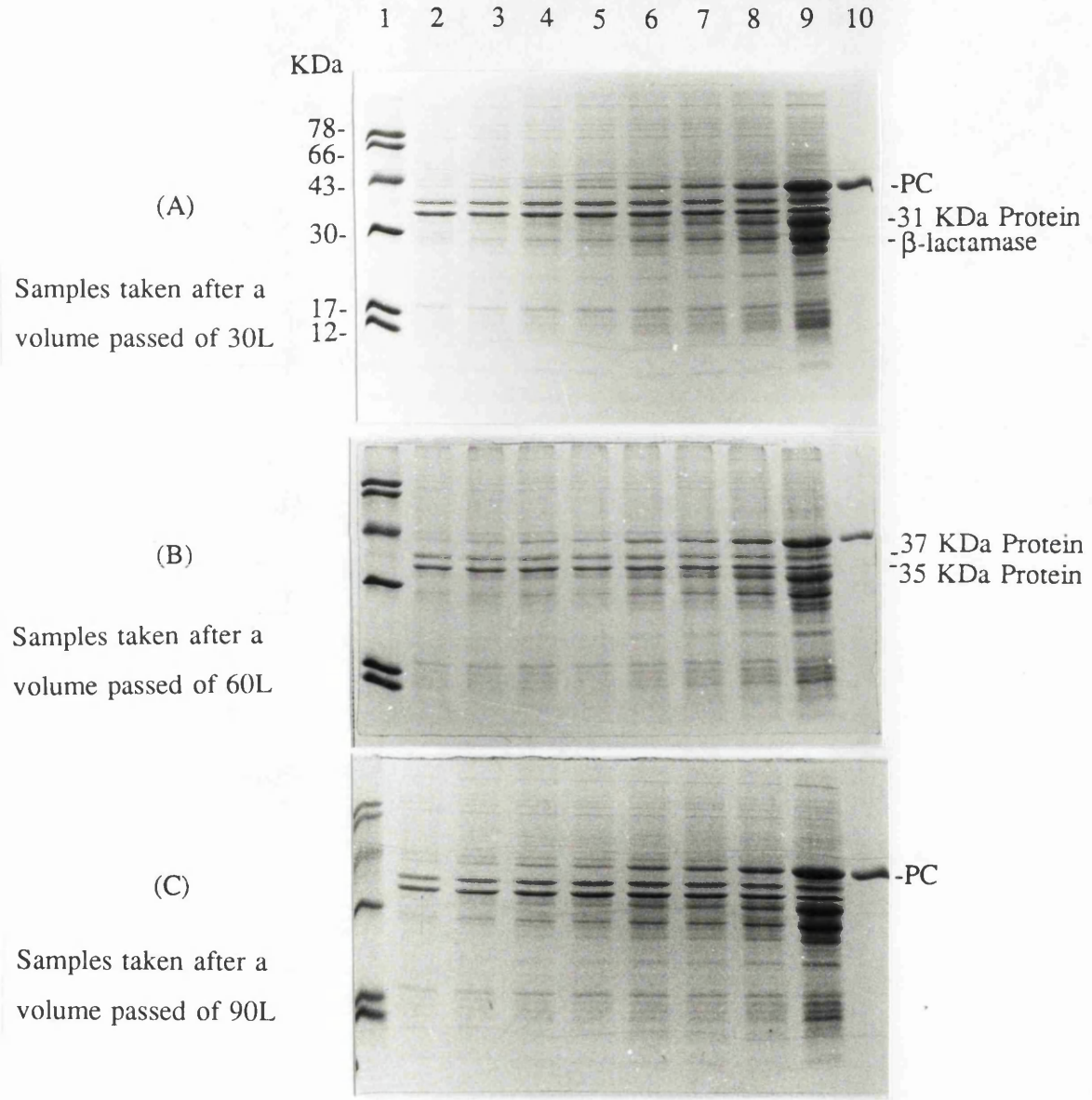

Lane 1 in (A), (B) & (C): Protein marker; Lane 2 - Lane 8 in (A), (B) & (C): insoluble proteins from the supernatant samples with a feed flow rate of 228 (Lane 2), 460 (Lane 3), 518 (Lane 4), 540 (Lane 5), 760 (Lane 6), 920 (lane 7) and 1100 L/h (Lane 8); Lane 9 in (A), (B) & (C): insoluble proteins from the whole homogenate; Lane 10 in (A), (B) & (C): Prochymosin standard.

Figure 3.5.3(A) gives the recovery (%) of individual inclusion body protein species, *i.e.* prochymosin (41 KDa), β-lactamase (29 KDa) and the 31 KDa protein, while Figure 3.5.3(B) shows the removal of individual cell debris protein species, *i.e.* class I (37 KDa and 35 KDa species) and class II cell debris (species below 29 KDa). The identification of these proteins is discussed in section 3.4.3, and summarised in Table 3.4.2. It was observed that these three inclusion body proteins had similar recovery curves, indicating that these three insoluble species either aggregated together or had similar sizes and size distributions. Class I cell debris (37 & 35 KDa protein species) was completely removed when the flow rate was increased to 500 L/h. In contrast, only 20% of class II cell debris was removed at this feed flow rate. This implied that class II cell debris either had larger sizes or formed aggregates. This will be further discussed in section 4.4.1.

Figure 3.5.4 presents the recovery of the whole inclusion body fraction (including these three inclusion body protein species, prochymosin, β-lactamase and the 31 KDa species) and the removal (%) of whole cell debris (including class I and class II). This figure will be use for comparison with the theoretical model developed by Olbrich (1989) in section 4.4.1.

As seen from both Figure 3.5.3 and 3.5.4, the recovery of the inclusion bodies or prochymosin decreased with the increase of feed flow rate, while the removal of cell debris or insoluble proteins increased. Therefore, a compromise has to be made when choosing the feed flow rate.

Figure 3.5.3 Recovery of individual inclusion body protein species and removal of individual cell debris protein species in an industrial disc centrifuge

(A) recovery of individual inclusion body protein species

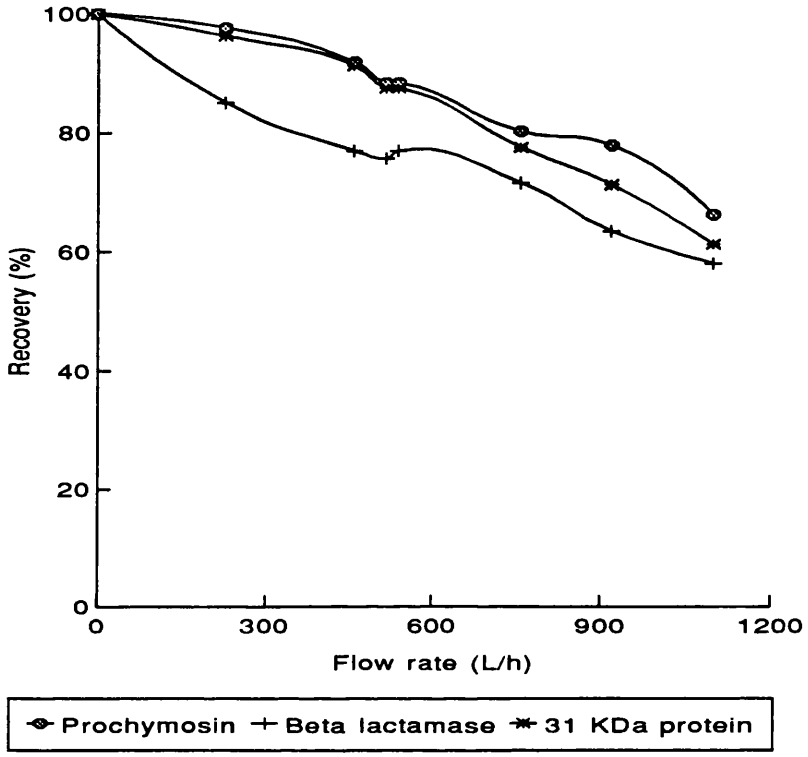

(B) removal of individual cell debris protein species

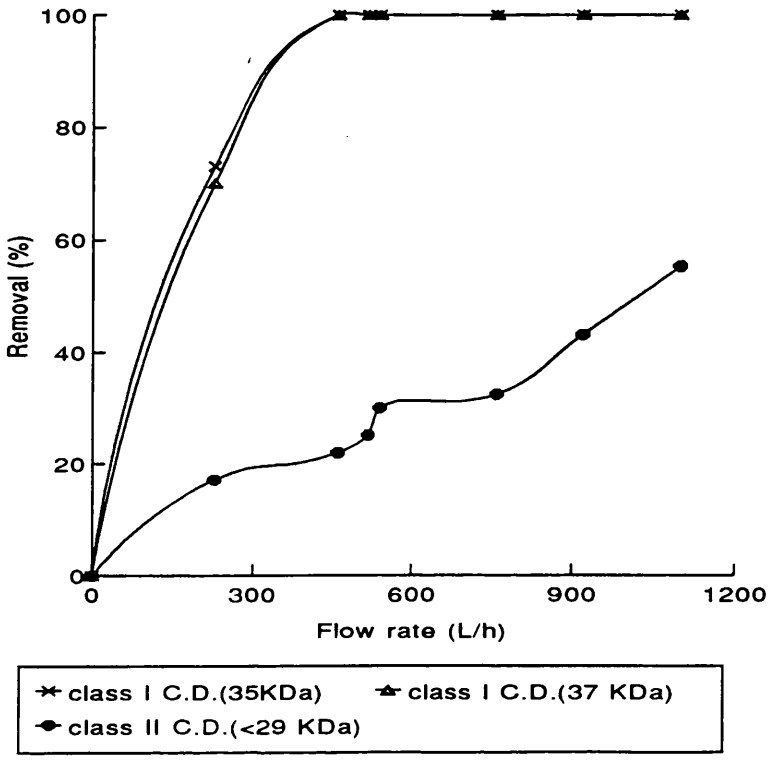

Figure 3.5.4 Recovery of whole inclusion bodies (I.B.) and removal of whole cell debris (C.D.) in an industrial disc centrifuge

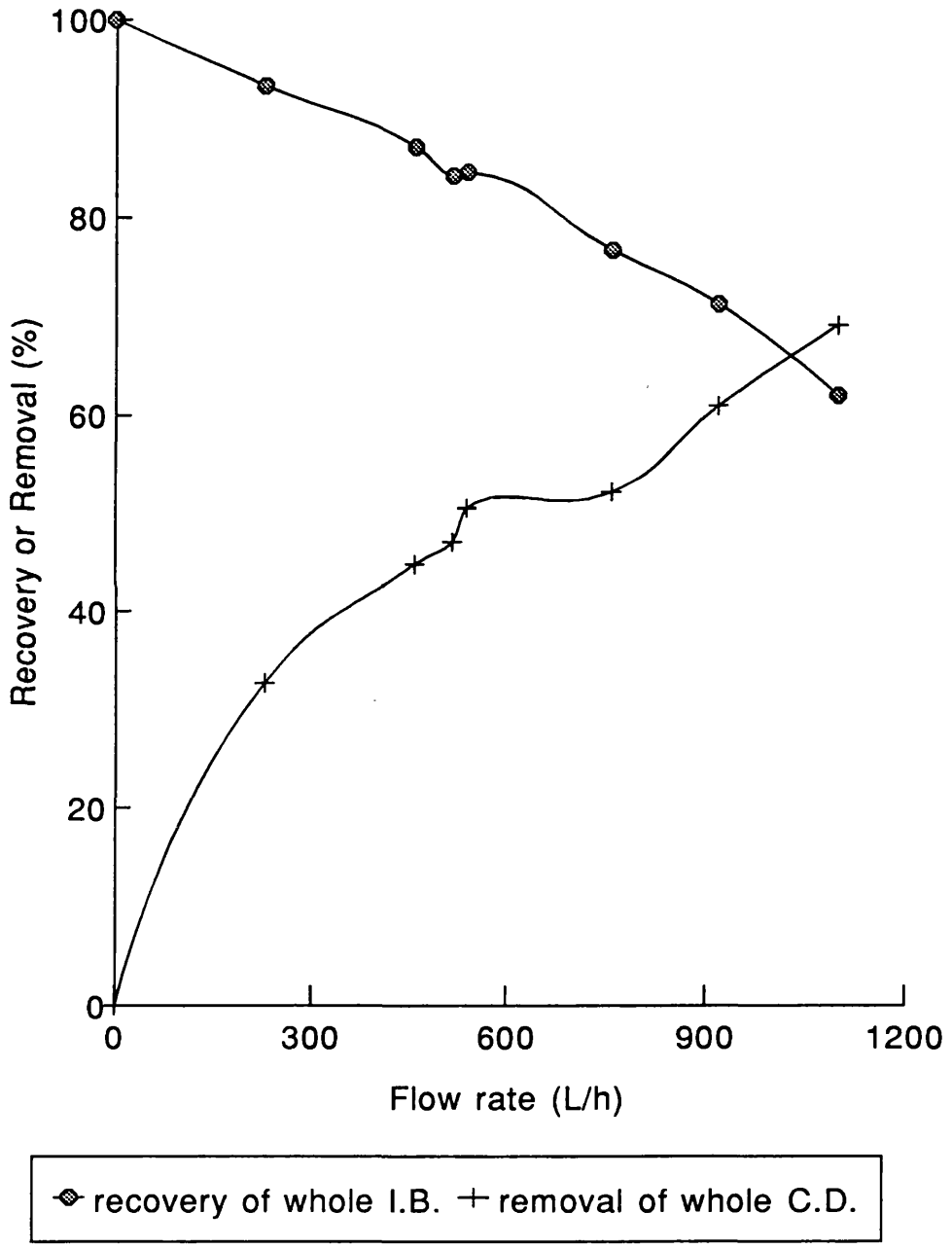

3.5.3 The relationship between the ratio of OD_{600nm}/OD_{420nm} and the separation of the inclusion body fraction from cell debris

As stated in section 3.5.1, manual monitoring of the turbidimetric ratio (OD_{600nm}/OD_{420nm}) for selecting feed flow rates was used in examining the disc centrifuge performance. This was based on the hypothesis that the larger refractile inclusion body particles would scatter light at 600 nm more effectively than smaller cell debris particles, thus the ratio (OD_{600nm}/OD_{420nm}) would increase with the increase of inclusion body particle numbers in the supernatant. By comparing the results of turbidity change (section 3.5.1) and the SDS-gel analysis (section 3.5.2), this hypothesis was confirmed.

Figure 3.5.5(A) combined the results from Figure 3.5.1(B), 3.5.3(A) and 3.5.4. It shows that on increasing the flow rate through the centrifuge, recovery of inclusion body particles is reduced and increasing numbers appear in the supernatant. This rise in inclusion body concentration in the supernatant is accompanied by a parallel increase in the ratio of OD_{600nm}/OD_{420nm}. Figure 3.5.5(B) shows this direct relationship between the recovery (%) of inclusion bodies or prochymosin and the ratio (OD_{600nm}/OD_{420nm}).

Earlier in section 3.5.1, it was estimated that at a flow rate of 518 L/h should yield the same % recovery of inclusion bodies as a lab centrifuge because of an identical OD_{600nm}/OD_{420nm} ratio value (0.38) of the supernatant. This was confirmed by the results shown in Figure 3.5.5(B). The recovery of inclusion bodies at 518 L/h was 84.2% compared to 86% for the lab centrifuge. Furthermore, the composition of the supernatant from 518 L/h was virtually identical to that obtained with the lab centrifuge, by comparison of Figure 3.5.3, 3.5.4, 3.5.5 and Table 3.4.3 (summarised in Table 3.5.2 below).

Because only prochymosin in the inclusion body proteins is the product of interest, the prochymosin concentration in the supernatants and the ratio of OD_{600nm}/OD_{420nm} obtained from different feed flow rates is shown in Figure 3.5.6(A). Figure 3.5.6(B) indicates that the extent of prochymosin loss can be determined from turbidimetric ratio measurements.

Table 3.5.2 Comparison of supernatant composition from the disc centrifuge operated at a feed flow rate of 518 L/h with that obtained by the lab centrifuge

Protein species	Protein species (%) in supernatant from the disc centrifuge at 518 L/h	Protein species (%) in supernatant from the lab centrifuge
prochymosin	11.6	9
β-lactamase	24.3	22
31 KDa protein	12.5	10
whole inclusion body proteins	15.8	14
class I cell debris	100	92
class II cell debris	25.2	21
whole cell debris	47.1	53

The calculation procedures refer to the notes of Table 3.4.3.

Figure 3.5.5 Relationship between turbidimetric measurements and percentage product recovery in an industrial disc centrifuge

(A) the change in recoveries of whole inclusion bodies (I.B.), prochymosin and the ratio of OD(600nm)/OD(420nm) with the feed flow rates

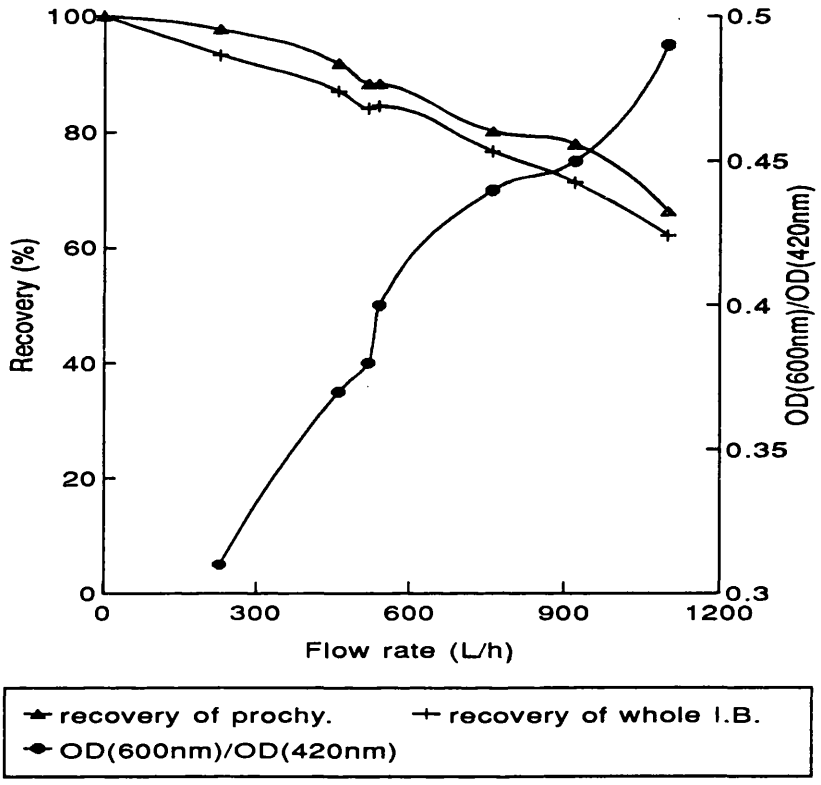

(B) relationship between the recovery of whole inclusion bodies (I.B.), prochymosin and the ratio of OD(600nm)/OD(420nm)

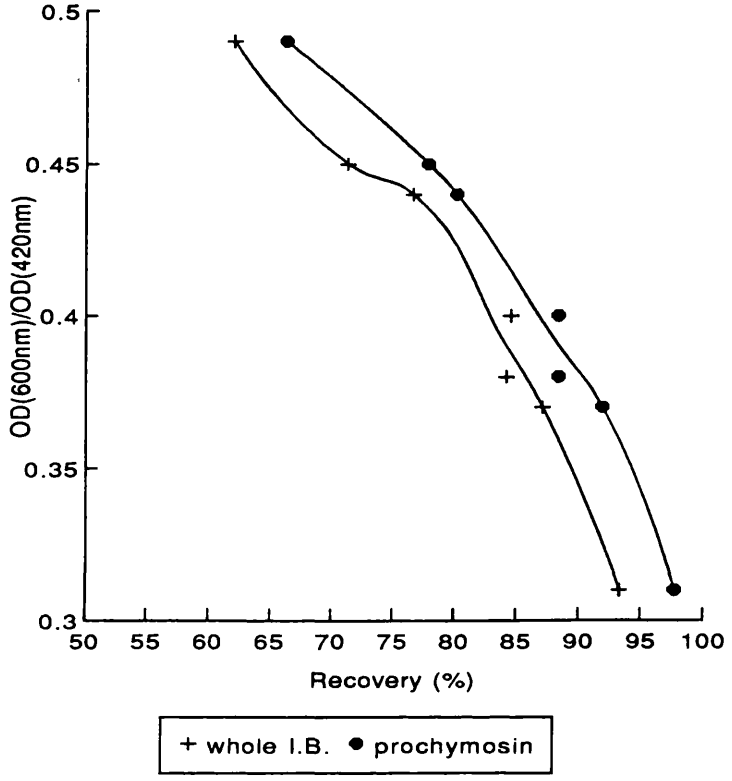

Figure 3.5.6 Relationship between turbidimetric measurements and the concentration of prochymosin in supernatants from the industrial disc centrifuge

(A) the change in prochymosin concentration in the supernatant and the ratio of OD(600nm)/OD(420nm) with the feed flow rate

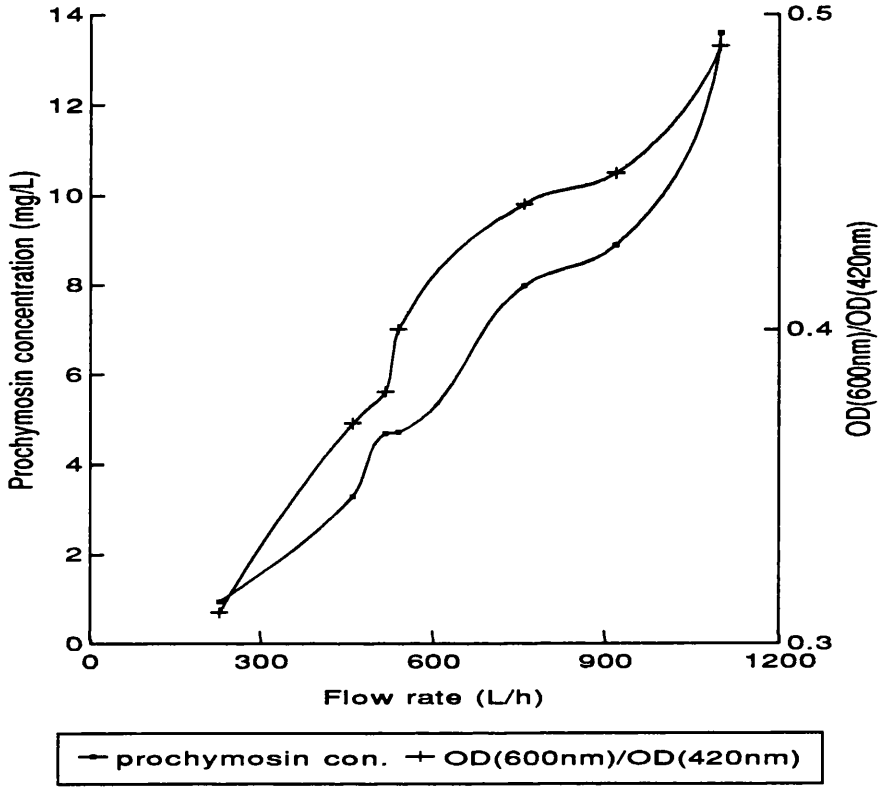

(B) relationship between the ratio of OD(600nm)/OD(420nm) and prochymosin concentration in the supernatant

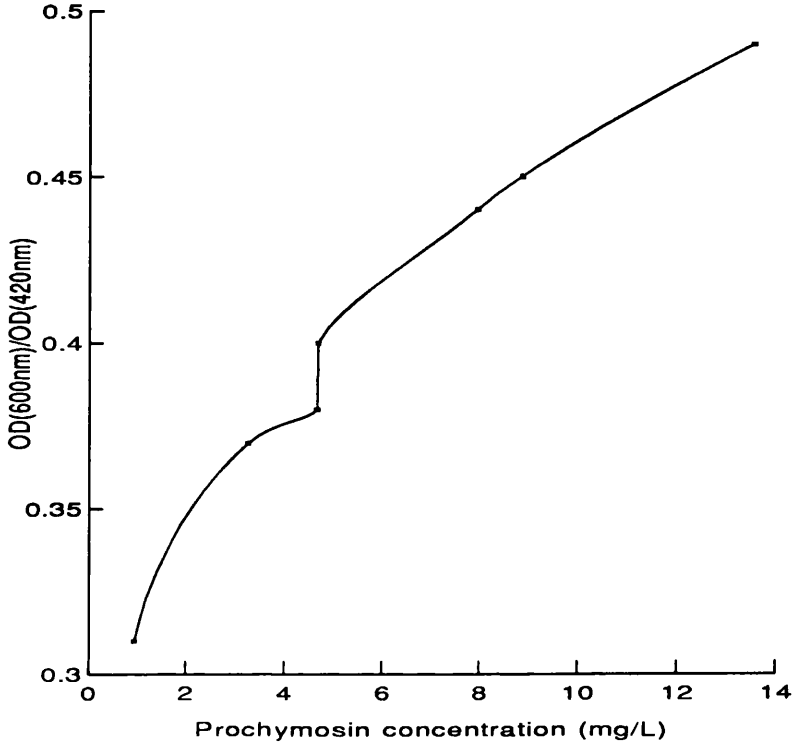

4. DISCUSSION

A general discussion of the results described in the previous chapter is made and suggestions for future work are presented.

4.1 Vector/host systems

4.1.1 Advantages and disadvantages of dual-origin plasmids amplified by thermal induction

Loss of plasmids in recombinant systems is related to expression of recombinant protein in host cells (Caulcott *et al.*, 1985). Thus the synthesis of foreign protein should be repressed before a sufficient cell mass is achieved. Regulated promoters, *e.g.* the tryptophan promoter, in high copy number plasmids can be difficult to control. For example, plasmid pCT70 (Emtage *et al.*, 1983), an intermediate copy number plasmid (40 - 60 copies each chromosome) carrying the prochymosin gene, has been shown to be unstable because of the inability of *trp* promoter to repress the synthesis of prochymosin even in the presence of tryptophan (Caulcott *et al.*, 1985). The problem of the instability of plasmid pCT70 was also found in the work of Gardiner (1988) and Olbrich (1989). This problem was solved by constructing a dual-origin plasmid (Yarranton *et al.*, 1984; Wright *et al.*, 1986), which was employed in this project (see section 1.7). The *trp* promoter was still employed for the control of foreign protein production. Because of a low copy number of plasmid in each cell before induction, the expression level was very low, as shown in gel pictures in section 3. This resulted in stable maintenance of plasmids even without antibiotic selection in the case of plasmid pMG168 (see section 3.2.2.2). Another advantage of this type of dual-origin plasmid is that thermal induction is cheap and can ease the subsequent downstream processing of protein product because it avoids the use of chemicals as inducer.

Thermal induction has some negative effects on host strains. For example, the rise of temperature results in a degree of cell death. This is explained in terms of temperature dependence of proteins and lipids for their structural stability and their activity. At high temperatures, proteins denature and lose their activity and structure (Pirt, 1975). This might explain the result obtained in this study, *i.e.* a lower cell density was achieved when cells

were induced at an earlier stage during growth. Many bacterial proteases, which are responsible for hydrolysing abnormal proteins, are formed in response to heat-shock so that this is a particular problem in such temperature-inducible expression system. Furthermore, such dual-origin plasmids amplified by thermal induction do not seem to have potential application in developing systems which are capable of producing soluble recombinant proteins. Thus, several studies have demonstrated that the solubility of recombinant proteins is temperature dependent, and that the lower temperature is favoured for formation of soluble recombinant proteins (Schein and Noteborn, 1988; Haase-Pettingell and King, 1988; Piatak, *et al.*, 1988). It has been suggested that the easiest way to obtain soluble recombinant protein is to use a lower growth temperature and avoid thermally induced plasmid vectors (Schein, 1989).

4.1.2 Selection of the *E. coli* host strain

As discussed in section 1.2.2, the formation of inclusion bodies was believed to provide protection from proteolysis in some cases (Cheng *et al.*, 1981). It has been reported that proteolytic attack on inclusion bodies does occur but it is dependent on the protein expressed (Goff and Goldberg, 1985). The phenomenon of proteases attacking unfolded, random structures better than native ones has also been reported (Schein and Noteborn, 1988). In consequence, it was desirable to select host strains which are protease deficient. *E. coli* CAG629 is a heat shock protease and *La* protease deficient strain, which was chosen by Field (1988) as the antibody fragments expression system. This system was used in this project (section 1.7.1.1). *E. coli* HB101 has been shown to give the lowest inclusion body yield among different strains, and the variation of inclusion body yields in different hosts may be due to differences in the levels of proteases or the levels of tRNA molecules recognising codons of eukaryotic genes (Kaytes *et al.*, 1986). The replacement of *E. coli* HB101 by *E. coli* B/r as the host for plasmid pCT70 resulted in a 4-fold increase in the amount of inclusion bodies (Schoemaker *et al.*, 1985). *E. coli* HB101 has been employed as host for plasmid pMG168 in this study, but it is also interesting to change host, for example, using *E. coli* B/r, to examine the effect on inclusion body yield in future study.

4.1.3 Selection of expression strategies

A major advantage of *E. coli* cytoplasmic expression of foreign proteins formed as inclusion bodies has been shown by the downstream processing study in this project, *i.e.* the separation of inclusion body products from cell debris achieved at large-scale (discussed in section 4.5). However, problems will arise in the denaturation and renaturation stages. These are: (1) Denaturants (usually urea or guanidinium) are unpleasant to work with and expensive, and they can cause irreversible modifications of protein structure (Marston, 1986); (2) Refolding usually must be done in very dilute solution and the protein must be reconcentrated (Marston, 1986; van Kimmenade *et al.*, 1988). The reconcentration step is complicated by proteolysis and further precipitation of the protein. Efforts have been made to study the cause of inclusion body formation in *E. coli* and ways of increasing the production of soluble recombinant proteins (Wilkinson and Harrison, 1991; Schein, 1989).

Another strategy is the functional expression of recombinant proteins by secretion into *E. coli* periplasm. This has been discussed in section 1.5 for antibody fragments production, and in section 1.6 for prochymosin production. There are several advantages to this expression system: (1) It directly leads to an assembled functional product without the need to refold the protein *in vitro*; (2) The problem of protease degradation is greatly diminished, as there are fewer proteases in the periplasm than in the cytoplasm , protection is also achieved by the oxidation of the disulfide bonds in the periplasm (Plückthun, 1991). However, this expression strategy can suffer lower expression level because of a finite volume in periplasmic space. The secretion of expressed product into the medium can bypass the problem of limited periplasmic space, but a large volume has to be processed in the downstream processing for product recovery.

4.2 Fermentation

4.2.1 Growth conditions for recombinant *E. coli*

Some published reports concerning the relationship between growth conditions and plasmid stability have been discussed in section 1.2.3. The results obtained in this study showed the influence of medium composition and thermal induction at a particular cell growth stage on the stability of plasmid and recombinant protein productivity.

Expression of antibody Gloop2 fragment V_L was achieved in the 20L fermentation using LB medium (section 3.1.2.1), but no expression was obtained in the 20L fermentation when using medium 1 (section 3.1.2.2). The main reasons for this are evidently the medium composition and cell induction point.

LB medium had a specific growth rate of 0.36 h^{-1}. In contrast, medium 1 had a much higher specific growth rate of 0.8^{-1}, because glucose was employed, which is a readily metabolised carbon source. Seo and Bailey (1985) employed different media, which gave different specific growth rates, to study the effect on recombinant system. They reported that a higher specific growth rate resulted in a lower copy number of plasmid and a lower recombinant product expression level. Therefore, the inability to achieve V_L expression in medium 1 may be related to its high specific growth rate.

The cell induction point may also affect V_L expression. In the batch with LB medium, cells were induced at a middle stage in the growth phase (Figure 3.1.4), while cells were induced at an early stage in the stationary phase in the batch using medium 1 (Figure 3.1.6), for the purpose of achieving a higher final cell density. From the results of shake flask cultures, expression of V_L was achieved when using LB medium, but no expression of V_L was achieved when using medium 1 (with only one exception) even with a similar induction point to that of LB medium (section 3.1.1.1 and 3.1.1.2). However, because of the difference between shake flask culture and fermentation (discussed in section 3.1.2), it was difficult to conclude that expression of V_L cannot be achieved in fermentations using medium 1 before more batches were performed with different induction points.

Originally, it was thought the inoculum strategy used in the antibody fragments expression system, *i.e.* the standard inoculum method, might cause the instability of the plasmids (section 3.1.2.2), explaining why no V_L expression was achieved in medium 1. However, the results from the prochymosin expression system, in which the type of plasmid was the same as that for carrying the antibody fragment gene (see section 1.7), showed that this type of dual-plasmid was stable even without antibiotic selection (section 3.2.2.2). Therefore, this explanation was unlikely.

In studies of the prochymosin expression system, efforts were put on medium modification to allow scale-up. Medium 2 (Table 2.2.4) contains casamino acids which is expensive, antibiotic (ampicillin) which not only has high cost but causes safety problems, and AnalaR chemicals which are expensive and not practical in large-scale production. Medium 4 (Table 2.2.5) overcomes these drawbacks and still enables expression of prochymosin to be achieved. Although the prochymosin yield achieved in medium 4 (0.3 g/L) was not as high as that obtained in medium 2 (0.4 g/L), the materials cost for producing the same quantity of prochymosin employing medium 4 was reduced to one fifth of that needed when using medium 2 (section 3.2.4). The reduction in the prochymosin yield when employing medium 4 was a result of both reduction in the expression level (as a % of total cell proteins) and in the final cell density. The reason for the reduction in the prochymosin expression may be a higher specific growth rate (0.52 h^{-1}) of medium 4 compared with that of medium 2 (0.37 h^{-1}), as discussed earlier. The decrease in final cell density may be caused by the poorer nutrition of Standard Yeatex in medium 4 compared to casamino acids in medium 2. Future work needs to be done to improve medium 4.

The effect of cell induction point on the production yield of prochymosin was also studied employing medium 4 in the prochymosin expression system (section 3.2.2.2.3). It was found that higher cell density was achieved when cells were induced at a later stage during growth, as explained in section 4.4.1. No expression was achieved in a 20L batch when cells were induced at an earlier stage in the stationary phase, evidently due to structural instability of plasmids. This result also suggested that the induction point was one factor which affected expression of the antibody fragment V_L in the fermentation using medium 1, as discussed earlier. Two 20L batches achieved the same prochymosin yield (0.3 g/L) when cells were induced at late stages in the growth phase (Figure 3.2.16). One potentially confirmatory

finding was that the expression level (as a % of total cell proteins) was not improved in a 100L batch when cells were induced at an earlier stage in the growth phase compared with the two 20L batch (Figure 3.2.17). Because of the reduction in cell density caused by the earlier induction, the prochymosin yield was consequently reduced (0.2 g/L). However, this result needs to be confirmed in a future study by carrying out fermentations at the same scale in order to obtain the optimal cell induction point.

Lower specific growth rates were observed for the media (medium 2 - 4) used in the prochymosin expression system compared with the medium (medium 1) for antibody fragments expression system. This was because glycerol was used as carbon source instead of glucose. It was reported that the cell growth rate was severely limited by allosteric inhibition of the rate-limiting enzyme, glycerol kinase (Lin, 1976). This seemed to be advantageous for recombinant systems, as discussed earlier. Another advantage of using glycerol is to reduce acetate excretion. As shown in Figure 3.2.9, the concentration of acetate was below 0.5 g/L before cell induction in the 100L batch using medium 2, where glycerol was employed as carbon source. It was reported that the acetate concentration could reach as high as 2 g/L if glucose was used for growing the same strain (Luli and Strohl, 1990). However, it was observed from Figure 3.2.9 that the acetate concentration was remarkably increased after cell induction (maximum 2 g/L). This may be explained as follows: (1) The thermal induction of cells resulted in an increase of plasmid copy number and the synthesis of prochymosin, this would change the relative levels of many cell proteins and ribosomal components in recombinant cells (Birnbaum and Bailey, 1991), thus there would be a change in the metabolic pathways of cells; (2) The thermal induction resulted in a quick fall in DOT, although stirrer speed and gas flow rate were increased to reduced the extent. It has been reported that oxygen deficiency caused acetate excretion (Konstantinov *et al.*, 1990), because of the possible interruption of cell metabolism, *e.g.* TCA cycle. One way to prevent the acetate excretion is to use fed-batch mode (discussed in section 1.2.4).

The DOT value was always controlled above 25% in fermentations performed in this study, because it has been shown that the deficiency in oxygen supply (DOT < 5%) resulted in the loss of plasmids even with antibiotic selection (Hopkins *et al.*, 1987). But the quick fall in DOT value during thermal induction could still cause the loss of plasmids to some extent.

As mentioned earlier, the increase of stirrer speed and gas flow rate cannot prevent the rapid fall in DOT. It would be interesting to find out that whether the supply of pure oxygen during the period of thermal induction to maintain a high DOT value can improve the expression level of recombinant protein. This might allow enhancement of plasmid stability and increase the final cell density because of the possibility of reducing acetate excretion.

4.2.2 Optimizing thermal induction method

The thermal induction procedure used during fermentations in this study mimics that used in shake flask culture, optimized by Wright *et al.* (1986). That is: a rapid temperature shift from 30°C to 42°C followed by immediate incubation at 37°C (section 2.2.6). It would be useful to investigate the effect of the length for temperature shift on expression of recombinant proteins. A slow increase of temperature is easy to control but if a fast shift is necessary, it would lead to an increase in cost for a sophisticated controller to prevent temperature overshoot in large-scale production. In the work of Wright *et al.* (1986), expression of a recombinant protein from the same type of dual-origin plasmid was also achieved by simply raising the temperature to 37°C, avoiding the shift to 42°C, but with a lower expression level compared with the previous one. This procedure remains of interest for future work, because it diminishes the risk of temperature overshoot and higher cell density could be achieved by avoiding the dominance of cell death rate at high temperature (Pirt, 1975), thus the recombinant protein yield could be less affected even if the expression level is reduced.

4.3 Cell disruption

4.3.1 The measurement of cell disruption in homogenisation

The degree of cell disruption is usually obtained by measuring the soluble protein release from microorganisms. A limitation in measuring the disruption by measurement of soluble protein release is the inability to define the extent of cell wall disintegration. This is a concern when the desired product is formed as inclusion bodies. In such instance, the parameters of interest are not only the release of soluble protein, for obtaining the information on cell breakage, but also the size distributions of cell debris and inclusion body particles achieved, which is crucial in subsequent separation of inclusion bodies from cell debris. Hence, particle sizing techniques were employed in this study, for monitoring cell disruption process, combined with soluble protein assay. This approach extends a previous study of the characteristics of cell debris and inclusion body particle sizes, using various particle size analysis techniques (Olbrich, 1989). This has been discussed in section 1.4.2.1.

It has been reported that centrifugal disc photosedimentation (CPS) has been used to quantify the disruption of recombinant *E. coli* (inclusion body producing system) during homogenisation (Middelberg *et al.*, 1991), as an alternative for soluble protein assay. The value of disruption was expressed as the percentage of cells disrupted, obtained by analyzing particle size distribution curves of both homogenate and cell suspension.

4.3.2 Effect of repeated homogenisation on cell debris and inclusion body size reduction

By combining the soluble protein assay and particle sizing techniques, it was shown that the disruption of recombinant *E. coli* HB101 pMG168 cells was complete after 3 discrete passes under the homogenisation condition used, *i.e.* 550 barg at 5^{0}C (Figure 3.3.1). Further disruption up to 5 discrete passes resulted in continued reduction in cell debris particle size with no measurable reduction in inclusion body particle sizes (Figure 3.4.1). This has also been observed by Olbrich (1989), and he found that cell debris sizes did not decrease further after more than 5 passes, and some breakup of inclusion body particles happened after 7 passes, but not significantly. This was the reason for using repeated homogenisation up to 5 passes for preparation of cell homogenate, which was subjected to subsequent separation

of inclusion bodies from cell debris in this study.

The mechanism of cell debris size reduction by homogenisation up to 5 passes seemed to be divided into two phases, as suggested by Olbrich (1989). The first phase was the breaking open of the bacterial cell wall, releasing the cytoplasmic contents. The second phase was the breakage and particle size reduction of the large cell debris into small cell debris. Olbrich (1989) only considered class I cell debris, and the results on cell debris size reduction shown in Figure 3.4.1 also concerned class I cell debris only. This was because of the inability to separate class II cell debris from inclusion bodies (the identification of cell debris is discussed in section 3.4.3). With the aid of SDS-PAGE analysis, the characteristic of class II cell debris should be capable of definition. This will be discussed in section 4.4.1.

4.3.3 Factors affecting cell disruption

In this project, cell homogenisation was performed under constant pressure (550 barg), constant temperature (5^{0}C) and constant feed concentration (20 g CDW/L). The disruption results were described by equation 3.3.2 (*i.e.* ln [Rm/(Rm - R)] = K'N^b, see section 3.3). This description does not have a first-order dependency on the number of passes, deviating from the disruption model developed by Hetherington *et al.*(1971), *i.e.* ln [Rm/(Rm - R)] = KNP^a, with a first-order dependency on the number of passes. The modified disruption model, ln [Rm/(Rm - R)] = KN^{b}P^a, was first introduced by Sauer *et al.* (1989) and supported by the work of Middelberg *et al.* (1991). In both of their studies, examination of the disruption by changing the homogenisation pressure and the feed concentration has also been performed. It remains of interest to study the effects of homogenisation pressure and feed concentration on the size distribution of cell debris and inclusion body particles in the system used in this project for future work.

Comparison of the disruption of recombinant cells and versus wild type cells has been made in several studies. Olbrich (1989) stated that the disruption of host cells (*E. coli* HB101) resulted in larger cell debris particle sizes compared with the recombinant cells (*E.coli* HB101 pCT70). Middelberg *et al.* (1991) reported that the disruption of recombinant *E. coli* JM101 cells containing inclusion bodies exhibited a higher disruption rate than the equivalent uninduced cells. In the work of Olbrich (1989) and Middelberg *et al.* (1991), cells were

obtained from batch fermentations. However, Sauer *et al.* (1989) claimed that higher disruption of the recombinant *E. coli* NM989 cells, compared with the wild type *E. coli* HB101 cells, was only achieved when both of these two types of cells were obtained from continuous cultures. If batch culture was used, no appreciable difference was observed. This was explained by the long residence time of cells in batch mode, resulting in repair of cell wall defects. They also reported that both recombinant cells and wild type cells were disrupted more readily from the continuous culture with a higher specific growth rate. An explanation for this was that a greater specific growth rate tends to produce cells having weaker walls.

Cell disruption was also strain dependent, according to Middelberg *et al.* (1991) after comparing several previous studies in which different *E. coli* strains were employed.

The same type of cells from different batches exhibited a difference in the maximum soluble protein release, according to Gardiner (1988) and Olbrich (1989). This was also observed from cell disruption results in this study (Figure 3.3.1). The reasons for this were not clear, but protein assay errors could be one of them.

Much remains to be done to fully define the disruption of recombinant cells by high pressure homogenisation. However, the present study has added to the knowledge required to conduct efficient scale-up and to recover the resulting product.

4.4 Separation of inclusion bodies from cell debris at a large-scale by employing an industrial disc centrifuge

4.4.1 Comparison of the true performance of an industrial disc centrifuge and the theoretical prediction

The centrifugal throughput (feed flow rate) is a centrifugal variable that can be practically altered. The throughput affects the performance of centrifuge, particularly the recovery efficiency for solids. Figure 4.4.1 shows the experimentally obtained performance curves for an industrial disc centrifuge (from Figure 3.5.4) and the theoretical prediction described by Olbrich (1989). Deviations were observed for both the inclusion body recovery and the cell debris removal curves.

By comparing the inclusion body recovery curves, the recovery rate was overpredicted within the feed flow rate range of 0 - 300 L/h; and the recovery rate was underpredicted in the range from 300 - 500 L/h.

The predicted cell debris removal curve did not match the real curve. The reason for this was the identification of different cell debris protein species in Olbrich's model and that used in this study. As discussed earlier in section 3.4.3, cell debris protein species were identified into two types: class I and class II (see Table 3.4.2). Class I cell debris was composed of the 37 KDa and 35 KDa protein species, which can be removed from inclusion bodies completely after the feed flow rate reaches 400 L/h in the large-scale separation study (see Figure 3.5.3(B)). Class II cell debris was composed of protein species with molecular weights below 29 KDa. It was found to co-sediment with inclusion bodies, because it did not appear in the supernatant from lab-scale centrifugal separation (see Figure 3.4.3 (B)). It behaved like inclusion bodies in the large-scale separation in an disc centrifuge, *i.e.* the amount in the supernatant increased with feed flow rate and cannot be completely removed from inclusion bodies even at the feed flow rate as high as 1100 L/h. In the theoretical prediction, cell debris identified by Olbrich (1989) was only equivalent to class I cell debris described in this study, thus gaving a higher removal rate of cell debris compared with the true removal of cell debris including class I and class II (Figure 4.4.1). The prediction suggested that class I cell debris cannot be completely removed in the range of 0 - 500 L/h.

Figure 4.4.1 Comparison of the theoretically predicted and experimentally obtained performance of an industrial disc centrifuge

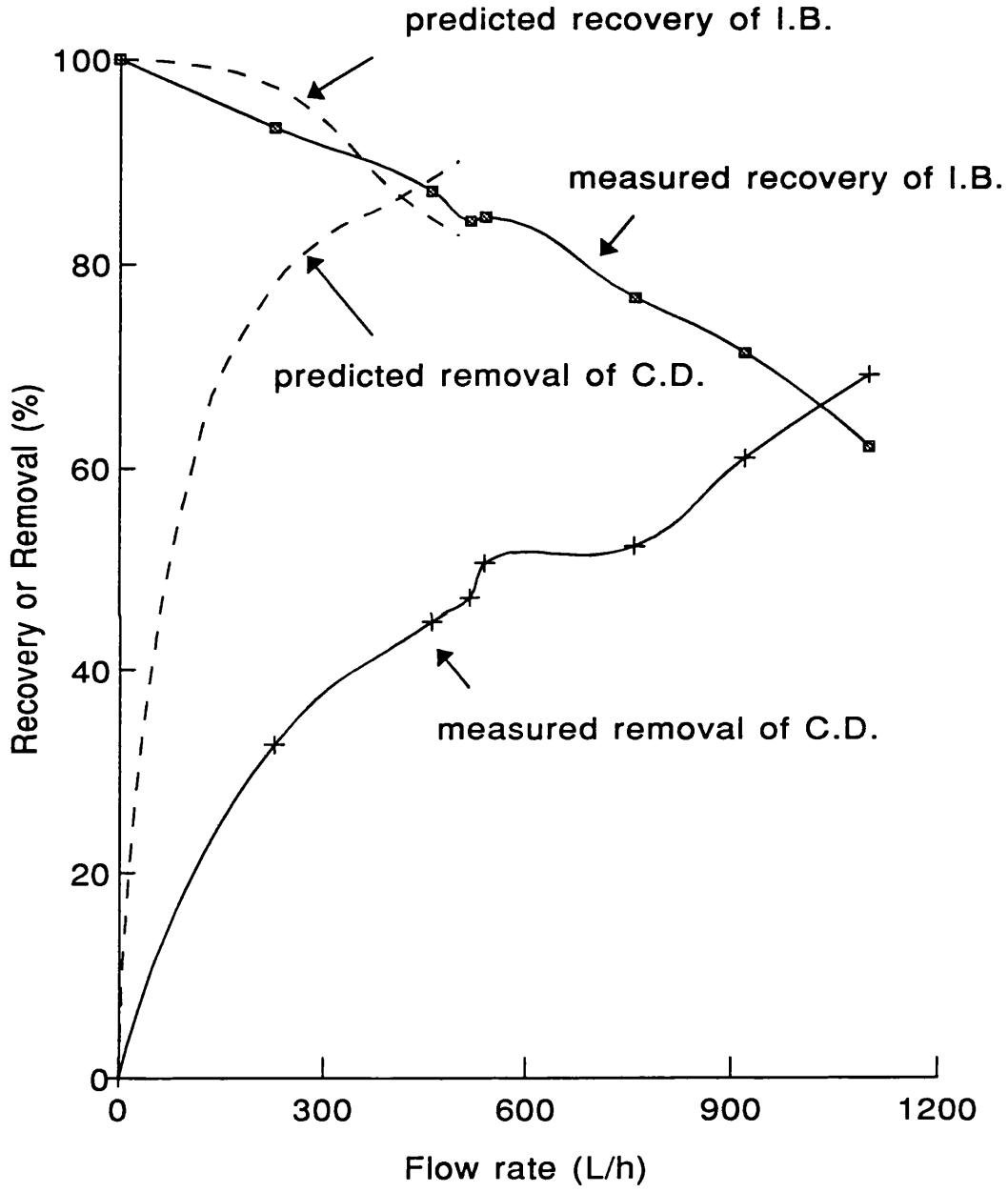

I.B. = inclusion bodies

C.D. = cell debris

However, this was not the case in practice. It can be completely removed when the feed flow rate was increased to 400 L/h, as mentioned earlier (see Figure 3.5.3(B)).

At this stage, it was not possible to determine whether class II cell debris co-sedimented with inclusion bodies because of an intrinsically larger size (compared with class I cell debris) or because of it formed aggregates. However, this can be determined by using uninduced cells (not containing inclusion body proteins) as control sample. Uninduced cells are subjected to the same disruption procedure and subsequent centrifugal separation conditions as induced cells and a supernatant sample subjected to SDS-PAGE analysis. If class II cell debris does not appear, as in the case of induced cells, this suggests that these cell debris particles are of a larger size. If however they do appear in the supernatant, the suggestion is that the particles are not large enough to be spun down, and the reason for their absence in the supernatant sample from induced cells can then be assumed to be that they are trapped in the inclusion body particles.

This distinction is important because if class II cell debris co-sedimentation is due to larger sizes, the number of discrete passes or the pressure during homogenisation may be increased to ensure further reduction in cell debris particle sizes, as long as there is no significant reduction in inclusion body particle sizes. Therefore, the removal of cell debris can be improved.

Both the theoretical prediction and experimental results suggests that it is not possible to achieve high purity of inclusion body products while achieving high recovery rate. An optimal recovery rate will be decided by the product purity requirement at the particle classification stage. Removing cell debris to achieve product purity is often desired because the bacterial cell debris have potential pyrogenic and immunological effects. These are potentially hazardous if they are allowed to be processed in the subsequent downstream processing operations such as solubilisation and renaturation. Given this requirement, lower recovery rate of inclusion body product may be tolerated.

The feed homogenate used in this study was highly-diluted as stated in section 3.4, thus the viscosity was significantly reduced. The performance of the disc centrifuge obtained in this study cannot be generalised to more concentrated feed homogenate required in practice.

Deterioration in performance will be expected to happen as the result of increased viscosity, and the extent of which has also been predicted by Olbrich (1989).

4.4.2 A method for monitoring the performance of an industrial disc centrifuge and its potential application

As discussed in section 3.5.3, the turbidimetric ratio (OD_{600nm}/OD_{420nm}) value increases with the increase of inclusion body particle numbers in the supernatant, thus has direct relationship with the recovery level of inclusion bodies (Figure 3.5.5 (B)) or the loss of inclusion body product - prochymosin (Figure 3.5.6 (B)). This correlation suggests that the turbidimetric ratio measurement can be used as a monitoring method during the inclusion body separation process in a disc centrifuge. Because the turbidimetric ratio measurement is rapid and reliable, this method has potential application in developing an automatic controlling system for optimal recovery of inclusion bodies. The simplified automatic process control may be as follows: An optimal recovery rate of inclusion body product is defined. This depends on the requirement of product purity at this stage (discussed in the last section). The quantitative correlation between the ratio of OD_{600nm}/OD_{420nm} and the recovery rate of inclusion body product is invoked (shown in Figure 3.5.5 or Figure 3.5.6), then a value of the ratio corresponding to the optimal recovery rate is determined. This turbidimetric ratio value can be programmed as a setpoint in a controller, which is connected to a spectrophotometer. During the separation process, an automatic sampling system directs the supernatant samples to the spectrophotometer where the ratio of OD_{600nm}/OD_{420nm} is measured and the value is sent to a microprocessor for comparison with the setpoint. If the measured ratio value is bigger than the setpoint, indicating the recovery rate has dropped, the feed rate will be reduced by controlling the feed pump; if the measured ratio value is smaller than the setpoint, the feed rate will be increased. This process control system is being developed.

It has been reported that a particle size analysis method, centrifugal disc photosedimentation (CPS), has been developed for process control of inclusion body separation from cell debris in an disc stack centrifuge (Thomas *et al.*, 1991). This is a direct monitoring method, because the deterioration of the centrifuge performance when increasing the throughput is reflected by the appearance of larger particle sizes in the size distribution curve of

supernatant samples. However, it is difficult to obtain a quantitative correlation between the inclusion body product recovery/cell debris removal and the particle size distribution of supernatant samples, thus this method is not easily developed for process control. Furthermore, it was not possible to obtain the size distribution of cell debris particles by using this technique (section 3.4.1.2). This suggested that it is not possible to apply the CPS technique for monitoring removal of cell debris in this system.

4.5 Problems of quantitative protein assay methods used in this study

Qualitative examination of protein species by SDS-PAGE analysis is a basic analytical tool, which has been extensively used in this study. It is always desirable to quantitate the amount of protein in particular bands on a gel. In this project, it is crucial to determine: the prochymosin expression level at different stages during fermentation, the expression level affected by cell induction point, the recovery of inclusion body proteins and the removal of cell debris proteins during particle classification stage. Densitometric scanning following SDS-PAGE analysis is perhaps the most common method for quantitative protein assay (Fishbein, 1972), and it has been employed in this study together with BCA protein assay (section 2.6.3). The scanning method suffers from various limitations. The scanning procedure is subject to errors arising from physical imperfections in the gel and distortions of the protein bands such as curvature and varying lane widths. A method for quantitative assay of protein species in the gel, which relies on extraction of Coomassie blue R from stained bands and spectrophotometric measurement of the eluted dye, has been reported (Ball, 1986; see section 2.6.6.4). This method can overcome the problems concerning with the physical imperfectation in the gel and distortions of protein bands and it was also tried in this study (see Appendix 1). However, common to both the scanning method and the elution dye method is the problem of variable dye uptake by different proteins. Furthermore, the quantitative assay methods based on SDS-PAGE analysis are time-consuming.

Chromatographic peak areas have been used extensively to quantify compounds. Reverse-phase HPLC is a rapid technique with a high selectivity (see section 1.3.4 and 1.4.4). It has been used for the separation of polar molecules, including peptides and proteins. However, it proved to be unsuccessful for chromatographic separation of prochymosin from other protein contaminants under the conditions used in this study (see section 3.4.4), though these conditions had been successfully used to separate pure prochymosin from a number of other protein standards (Salt and Turner, 1991). Effort needs to put on modifying this system before reverse phase HPLC technique can be used as a rapid and accurate quantitative assay method for monitoring the production and recovery of prochymosin.

5. CONCLUSION

In this final chapter, the results from fermentation, cell disruption and inclusion body separation are summarised and these findings are related to the design of economic fermentation process and the control of inclusion body recovery.

5.1 Shake flask culture and fermentation with antibody fragments expression system

Expressions of antibody Gloop2 V_L and V_H genes in *E. coli* CAG629 pMG LF9 and *E. coli* CAG629 pPW HF2 were achieved in shake flask cultures when LB medium was employed (Table 2.2.1). Expression of V_L was also obtained in a 20L scale fermentation using LB medium, indicating that the thermal induction method during fermentation (section 2.2.6), mimicking that for shake flask culture, was efficient. This cell induction procedure was used in the subsequent fermentations at different scales. The problem with LB medium is that only low cell density can be achieved.

When employing fermentation medium 1 (Table 2.2.3) for achieving high cell density, expression of V_L was only obtained in one shake flask culture, the result of which was not repeatable. One fermentation at 20L scale, in which cells were induced at an early stage in the stationary phase, was also carried out for expression of V_L by applying medium 1, but no expression was achieved. The reasons for not achieving expression of V_L might be due to the composition of medium 1 which gave a high specific growth rate, correlated with reduction in plasmid copy number and expression level (Seo and Bailey, 1985). The late stage of cell induction in this 20L fermentation using medium 1 may also cause the failure of V_L expression. The results from the study of the prochymosin expression system suggest that the standard inoculum method used in this antibody fragments expression study is unlikely to be the reason for not achieving V_L expressin.

5.2 Shake flask culture and fermentation with prochymosin expression system

Initial scale-up work was performed for production of prochymosin in *E. coli* HB101 pMG168 by employing medium 2 (Table 2.2.4), which was from a published report.

Expression of prochymosin was achieved in both shake flask cultures and fermentations up to 100L scale. During fermentation, cells were induced after the mid-point of the growth phase in order to obtain both expression of prochymosin and high cell density. A yield of 0.4 g/L of prochymosin was achieved in a 100L scale fermentation using medium 2.

However, medium 2 has two drawbacks: its cost is high (using an expensive nitrogen source) and it has a safety problem (containing antibiotic). Therefore, it was modified to give medium 4 (Table 2.2.5), in which a cheap nitrogen source and chemicals were used and antibiotic was removed to ease scale-up (the modifications were based on results from literature, see section 3.2.2.1 and 3.2.2.2). A series of batches was performed with different induction points over a wide range of cell growth times in order to establish the performance of medium 4 and to examine the effect on prochymosin yields. It was found that a higher prochymosin yield of 0.3 g/L was achieved when cells were induced at late stages in the growth phase. Prochymosin yield was reduced to 0.2 g/L when cell were induced at an earlier stage in the growth phase and no expression of prochymosin was obtained when cells were induced at an early stage in the stationary phase (refer to Figure 3.2.14). Based on fermentation results, the cost for producing the same quantity of prochymosin when employing medium 4 was calculated to be one fifth of that when using medium 2. It was concluded that the dual-origin plasmid pMG168 used in this project has potential application in industrial scale production of prochymosin because of its characteristics: before cell induction, it is maintained at low copy number and the expression level of prochymosin is very low, thus it is stable even without antibiotic selection; it is amplifiable (through thermal induction) to achieve expression of prochymosin when the cell density is fairly high, and this is required in order to obtain high yields of prochymosin; furthermore, it allows the use of cheap nutrient sources.

It was found that inclusion body formation affected the turbidity of the cell to a greater extent than cell dry weight (CDW), suggesting that the ratio of OD/CDW is a good indicator of inclusion body formation. The ratio of OD_{600nm}/CDW increased with the increase of expression level of prochymosin in this system, but it was not possible to derive a quantitative correlation. The respiratory quotient (RQ) was not found to increase after cell induction and synthesis of recombinant prochymosin as predicted in some of the literature for recombinant systems. Therefore, RQ could not be used as an indicator for formation of

prochymosin in this system.

5.3 Cell disruption

In this project, the disruption of *E. coli* HB101 pMG168 cells at constant pressure (550 barg) in an industrial homogeniser (APV Manton Gaulin Lab60) can be described by the following equation:

$$\log[Rm/(Rm - R)] = 0.83\ N^{0.43}$$

where R = soluble protein release

Rm = maximum soluble protein release

N = number of passes

The combination of protein release assay and particle size analysis showed that although cell breakage was complete at 3 discrete passes, the homogenate required 5 discrete passes to effect further particle size reduction of cell debris without significantly altering that of the inclusion bodies. This approach can ease subsequent centrifugal separation of the inclusion body fraction from cell debris.

5.4 Separation of inclusion bodies from cell debris for *E. coli* HB101 pMG168

Studies of separation of inclusion bodies from cell debris were carried out both at lab-scale (using a MSE 21 lab centrifuge) and large-scale (employing an CSA-8-06-476 industrial disc centrifuge).

5.4.1 Lab-scale separation

Centrifugal conditions for separation of the inclusion bodies from cell debris at lab-scale were previously determined by Olbrich (1989). These conditions (*i.e.* 2000 xg, 26 minutes, 5^{0}C) were verified by SDS-PAGE analysis, which enabled identification of typical protein species of cell debris and the inclusion body fraction. The results showed that 14% of the inclusion bodies were still remaining in the supernatant, while 47% of cell debris co-sedimented with the inclusion bodies under these centrifugal conditions (Table 3.4.3).

Turbidimetric measurements of the cell debris supernatant and cell homogenate at two wavelengths (600nm and 420nm) revealed an interesting finding. The ratio of OD_{600nm}/OD_{420nm} was significantly higher for the cell homogenate containing inclusion bodies than that for the supernatant containing cell debris. It was evident that the larger refractile inclusion body particles scatter light at 600nm more effectively than smaller cell debris particle, and manual monitoring of the turbidimetric ratio could enable estimates of the performance of the industrial disc centrifuge in the subsequent large-scale separation study.

Chromatography of the inclusion body fraction using a reverse phase HPLC column proved to be unsuitable for quantitative assay of prochymosin, because a single peak of prochymosin separated from other contaminants was not achieved.

5.4.2 Large-scale separation

Large-scale separation of the inclusion body fraction from cell debris was examined in an industrial disc centrifuge (CSA-806-476) within a wide range of feed flow rates (200 L/h - 1100 L/h). The relationship obtained between the inclusion body recovery/cell debris removal and the feed flow rate suggests that it is not possible to achieve a high purity of inclusion body product while retaining high recovery rate (Figure 3.5.4). By combining the results from turbidimetric ratio measurement (OD_{600nm}/OD_{420nm}) and SDS-PAGE analysis of the supernatant samples from different feed flow rate, it was confirmed that the ratio of OD_{600nm}/OD_{420nm} increased with the increase of inclusion body particle numbers in the supernatant. The direct relationship between inclusion body recovery rate and the ratio of OD_{600nm}/OD_{420nm} makes the turbidimetric ratio measurement an efficient monitoring method in inclusion body separation process (Figure 3.5.5(B)). Furthermore, this method may have potential application in developing automatic controlling system for optimal recovery of inclusion bodies in industrial disc centrifuges. It remains to be established whether this is applicable to other proteins and the conditions of growth may lead to changes in inclusion body size which would interfere with this method.

By comparing the theoretical prediction (Olbrich, 1989) and the true performance of an industrial disc centrifuge examined in this study, deviations were found for both the inclusion body recovery curve and the cell debris removal curve (see Figure 4.4.1). Further

understanding of such differences will throw light on modelling of bioparticle-liquid separation.

6. FUTURE DIRECTIONS

6.1 Quantitative protein assay

Polyacrylamide gel electrophoresis is one of the most sensitive techniques available for separating proteins. Densitometric scanning of Coomassie blue stained polyacrylamide gels is commonly used for quantitating individual protein species in a mixture. These methods have been extensively used in this study (detailed in section 2.6.6) to determine the expression level of recombinant protein during fermentation and the recovery of inclusion body proteins in an industrial disc stack centrifuge. The major sources of error in quantitative densitometry may be: (1) variation in the amount of dye bound from one protein to another; (2) physical imperfections in the gels as well as distortions of the protein bands; (3) baseline selection and peak-splitting procedures whenever there is no baseline segment between peaks.

The first problem cannot be avoided in this study because of the existence of heterogeneous protein species in samples. The second problem is absent if one properly operates SDS-PAGE (section 2.6.6), especially in the aspects such as the preparation of samples (see section 2.6.6.3) and the selection of protein loading amounts (avoiding overloading). If the protein bands are well separated on gel, there is no difficulty in baseline estimation and no need for peak-splitting. This suggests the use of standard gel system (dimension 20x16x0.075 cm) rather than mini-gel system (dimension 7.3x8x0.075 cm) for whole cell protein extracts analysis, because of the large number of protein species contained in samples. However, mini-gel has shown some advantages like low cost and less time-consuming when dealing with insoluble proteins samples such as inclusion bodies and cell debris, which contain less protein species.

In order to improve the accuracy further in quantitation of protein species of interest by densitometric gel scanning in future work, it would be necessary to apply multiple gel analysis for the same protein sample with different loadings. It would be also necessary to have "blind test" procedures, *e.g.* using different people for performing gel scanning. The accuracy of gel scanning is crucial in determining the derived recombinant protein yields (refer to Table 3.2.12) and the recombinant protein recovery in the disc stack centrifuge (see Figure 3.5.4).

6.2 The method of optical density ratio measurement (OD_{600nm}/OD_{420nm}) for monitoring the recovery of inclusion body proteins in an industrial disc centrifuge

The differences in optical density at OD_{600nm} and OD_{420nm} which have been observed may have several explanations. Mannweiler (1989) has shown that extinction coefficients vary as a function of particle diameter for polyvinyl acetate particles at wavelengths ranging from 400 - 700 nm. For particles below 3 μm diameter, the extinction coefficient rises rapidly with increasing particle diameter. For shorter wavelengths, *e.g.* 400nm, the maximum extinction coefficient is shifted towards smaller particle diameters whereas for longer wavelengths, *e.g.* 600nm and 700nm, the maximum extinction coefficient is shifted towards larger particles diameters. The inclusion bodies are known to be particularly refractile and this may have a bearing. Finally the optical density of the fine debris at 420nm may be enhanced by the presence of cytochromes. The precise cause needs further investigation but it seems likely that whichever cause dominates the method might allow monitoring and thereby control of the separation process. In future work, it remains to be established whether this method can be applied to other inclusion body proteins. Furthermore, it will be important to examine whether different fermentation conditions will interfere with this method. This is because the variation in growth conditions (*e.g.* different media, different cell induction points or methods) may lead to changes in inclusion body size distribution. Therefore, the preliminary step in developing automatic controlling system is to examine the ratio readings (OD_{600nm}/OD_{420nm}) of different cell homogenates (either from different batches or from different expression systems) and their supernatants containing cell debris obtained by lab centrifugation (detailed in section 3.4).

6.3 Further comparison of the true performance of the disc centrifuge and the theoretical prediction

As discussed in section 4.4.1, the deviation between the measured cell debris removal curve and the predicted one was due to the difference in identification of cell debris. Cell debris identified by Olbrich (1989) was equivalent to class I cell debris described in this study. There is a good agreement between the class I cell debris removal curve and the one predicted by Olbrich (1989), although class I cell debris seems to be completely removed at the flow rate of 400 L/h, while this is not the case in the prediction (see Figure 6.1).
It is suggested that the prochymosin inclusion body proteins contain two contaminants, *i.e.*

Figure 6.1 Comparison of the theoretically predicted and experimentally obtained performance of an industrial disc centrifuge

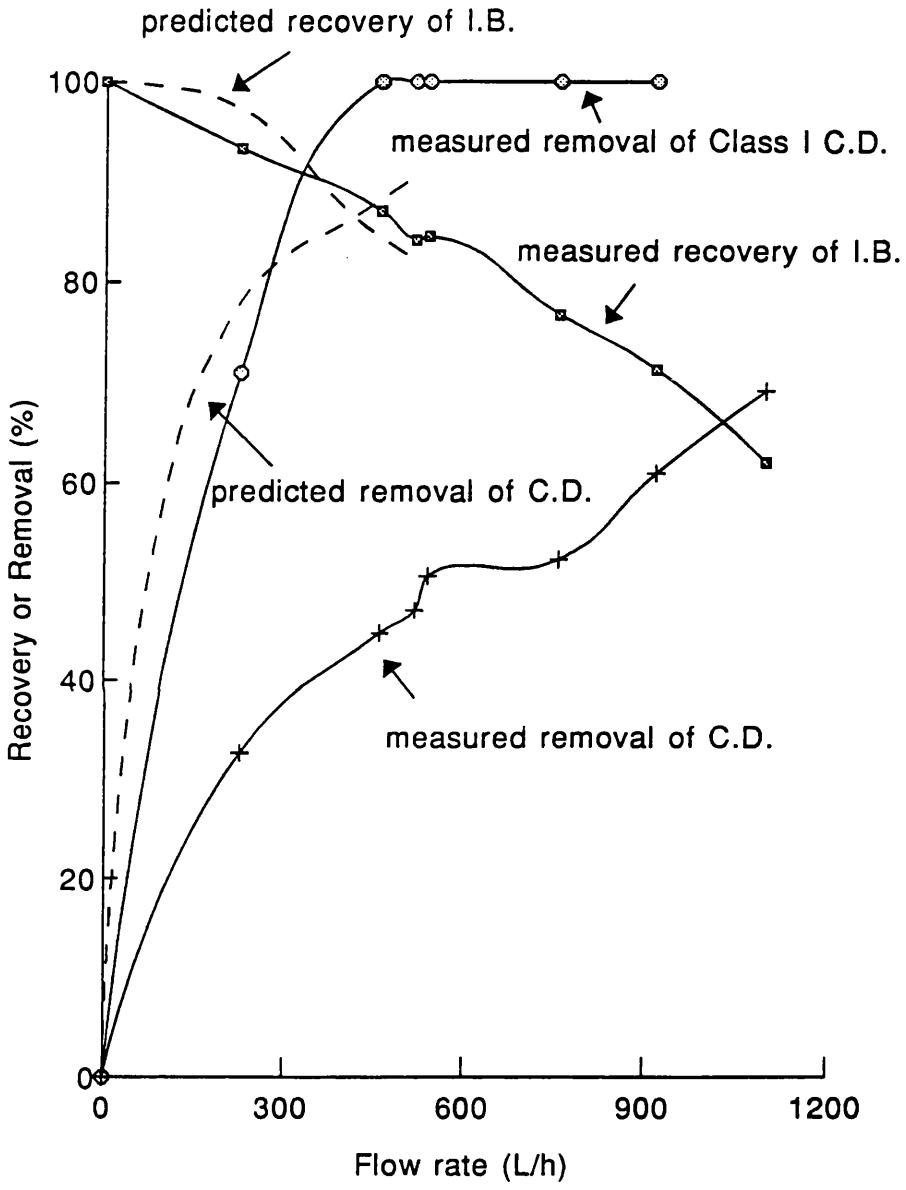

I.B. = inclusion bodies

C.D. = cell debris

3.2.9). The possible reasons for this have been explained in section 4.2.1, however, it remains of interest to find out whether the synthesis of foreign protein induced after temperature shift causes the acetate production. In order to examine this, host cells should be used for control batches, in which the thermal induction is performed as in the experiments with recombinant cells. It has also been found that the ratio of OD_{600nm}/CDW is a good indication of the formation of recombinant inclusion bodies (section 3.2.3). However, further data analysis should be carried out to illustrate the change of this ratio before and after cell induction. For example, linear regression may be performed for the ratio before induction (should be a constant) and after induction, with the corresponding error analysis.

In the production of recombinant proteins, not only a high expression of the target protein is important but also a high cell density. In this study, cell densities achieved from batch fermentations are fairly low. In future work, it will be necessary to develop a fed-batch mode. The fed-batch technique is usually employed in cultivations to obtain final high cell density since it is necessary to restrict growth due to limitations in oxygen transfer. Oxygen limitation leads to the formation of fermentative by-products that will inhibit growth and decrease yield. As discussed in section 4.2.1, oxygen limitation also causes the instability of plasmids. In the fed-batch mode, it is also possible to avoid restrictions in growth due to initially high concentrations of substrate or the formation of inhibiting by-products such as acetic acid, formed from excessive glucose consumption (refer to section 1.2.4).

6.5 Future work on recombinant cell disruption by homogenisation

In this study, it has been found that the disruption model of the recombinant *E. coli* cells (*i.e.* $\log[Rm/(Rm-R)] = KN^bP^a$, equation 3.3.1 in section 3.3) does not have a first-order dependency on the number of passes (discussed in section 4.3.3). However, the exponent value of b was not constant for each run (refer to Figure 3.3.2). This might be due to the variation of cells from different batches, different storage time and/or to protein assay errors (Figure 3.3.1). Future work needs to be carried out to verify this relationship by using cells from the same batch, with the same storage and each sample should be subjected to multiple measurements (protein concentration) instead of just duplicated. Furthermore, it remains of interest to study the effects of homogenisation pressure and feed concentration on cell disruption for future work, to complete the description of the disruption model (equation 3.3.1 in section 3.3), and to examine the effects on the size distribution of inclusion bodies

and cell debris. It is also interesting to perform disruption of relevant host cells obtained from the same fermentation conditions as recombinant cells, in order to compare the difference, and thus add to the knowledge of recombinant cell disruption.

Appendix 1

Gel elution methods for purification and quantification of prochymosin standard

The method of elution of proteins from SDS-Polyacrylamide gels was used to purify prochymosin standard in this project (detailed in section 2.6.6.5). Prochymosin standard was loaded on a preparative SDS-gel (13.5%) with dimensions 20x16x0.15 cm. The result of SDS-PAGE analysis of prochymosin standard is shown in Figure A.1.

Figure A.1 SDS-PAGE analysis of prochymosin standard
The arrow points out the major band excised from the gel.

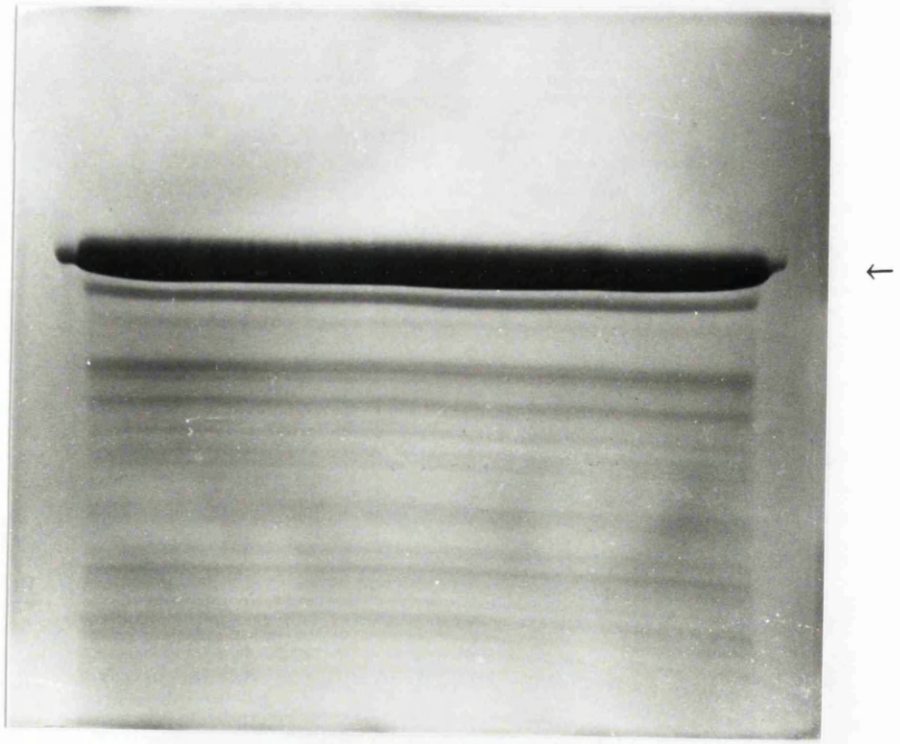

It is observed that original prochymosin standard is not pure, containing other protein species or degradation products. It is difficult to identify these tiny bands because of the lack of the prochymosin antibody. The major band (marked with an arrow in Figure A.1) was excised and protein was eluted as described in section 2.6.6.5. The eluted prochymosin was analyzed by a mini SDS-gel (13.5%) for purity. The result is shown in Figure A.2. A single band was achieved (Lane 7 - 10), suggesting the efficiency of the protein elution method for purification. In order to quantify prochymosin standard by the dye elution method, a set of known amounts of BSA protein standard was loaded on the gel for obtaining calibration curve (detailed in section 2.6.6.4). The amounts of prochymosin in Lane 7 and Lane 8 were quantified as 1 μg respectively, and those in Lane 9 and Lane 10 were 0.5 μg (BSA equivalency).

Figure A.2 Quantitation of purified prochymosin standard

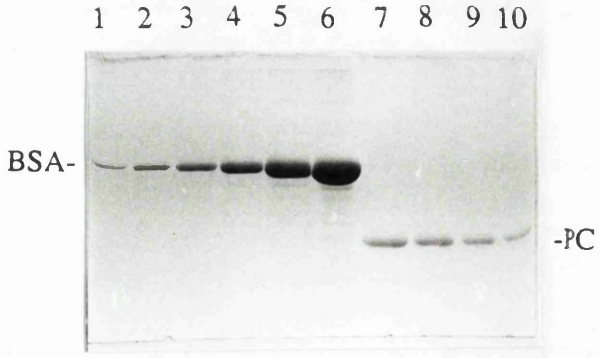

Lane 1 - 6: BSA protein standard, 0.25, 0.5, 1.0, 2.5, 5.0, 10 μg respectively.

Lane 7 - 10: Purified prochymosin standard.

Appendix 2

Addresses of equipment and chemical suppliers

APV Ltd., Manor Royal, Crawley, Sussex.

BCS Ltd., South Bank Technopark, London Road, SE1

BDH Ltd., Parham Drive, Boyatt Wood Industrial Estate, Eastleigh, Hants., S05 4NU

BioRad Laboratories Ltd., Greenhill Crescent, Haywell Industrial Estate, Watford, Herts..

Boehringer Corporation Ltd., Bell Lane, Lewes, East Sussex, BN7 1LG.

Bovril Foods Ltd., Wellington Road, Burton-on-trent, DE14 2AB.

Brookhaven Instruments Corporation, 750 Blue Point Road, Holtsville, New York 11742, USA.

Celltech Ltd., 216 Bath Road, Slough, Berks., SL1 4EN

Chemap AG, Switzerland.

Difco Laboratories, East Molesey, Surrey.

Fisons Scientific Apparatus, Bishop Meadow Road, Loughborough, Leics., LE11 ORG.

Gelman Ltd., 10 Harrowdene Road, Brackmills, Northampton, Northants., NN4 OEZ.

LH Fermentation Ltd., Bells Hill, Stoke Poges, Slough, Bucks., SL2 4EG.

Malvern Instruments Ltd., Spring Lane South, Malvern Worcestershire WR14 1AQ.

Millipore (U.K.) Ltd., Winster House, Heronsway, Chester Business Park, Wrexham Road, Chester CH4 9QR

Milton Keynes, Bucks, U.K.

MSE Scientific Instruments Ltd., Manor Royal, Crawley, Sussex, RH10 2QQ.

New brunswick Scientific Ltd., 6 Colonial Way, Watford, Herts, WD6 4PT.

Pall Process Filtration Ltd., Europa House, Havant Street, Portsmouth, Hants..

Pennwalt Ltd., Tower Works, Doman Road, Camberley, Surrey.

Perkin Elmer, Post Office Lane, Beaconsfield, Bucks.

Pharmacia Ltd., Pharmacia House, Midsummer Boulevard, Central Milton Kenes, Bucks., MK9 3HP.

Pierce Warriner (U.K.) Ltd., 44 Upper Northgate Street, Chester, Cheshire, CH1 4EF

Rheodyne, P.O. Box 996, Cotati, California 94928, U.S.A.

Shandon Southern Products Ltd., Runcorn, Cheshire, U.K.

Sigma Chemical Co. Ltd., Farcy Road, Poole, Dorset, BH17 7NH.

Silverson Machines Ltd., Waterside, Chesham, Buckinghamshire, HP5 1PQ

Turbo AG, Germany

VG Gas Analysis Systems Ltd., Aston Way, Holmes Chapel Road, Middlewich, Cheshire, CW10 OHT

Westfalia Separator AG, 4740 Oelde, Germany.

Westfalia separators (U.K.) Ltd., Habig House, Wolverton, Bucks..

Whatman Labsales Ltd., Unit 1 Coldred Road, Parkwood, Maidstone, Kent, ME15 9XN.

Appendix 3

Abbreviations

ACS	antigen combining site
APS	ammonium persulfate
CDR	complementary determining regin (antibody)
CDW	cell dry weight
CPS	centrifugal disc photosedimentation
DOT	dissolved oxygen tension
DTT	Dithiothreitol
EDTA	ethylenediamine tetraacetic acid
OD	optical density
PCS	photon correlation spectroscopy
RCF	relative centrifugal force
RQ	respiratory quotient
SDS	sodium dodecyl sulphate
TEMED	N,N,N',N'-tetramethylethylenediamine
Tris	tris (hydroxymethyl) aminomethane
trp	tryptophan

Appendix 4

Nomenclature

barg	bar guage
d	particle diameter
d_c	criticle particle diameter
d_{50}	value of particle size at which 50% of the population is greater than that diameter
Fv	antibody variable domain
g	gramme
xg	x gravity; average centrifugal force
h	hours
N	pass number
OD_{600nm} and OD_{420nm}	optical density at 600nm and 420nm
P	pressure
rpm	revs per minute
Re	reynolds number
Rm	maximum protein release
V_H	antibody heavy chain variable subdomain of Fv
V_L	antibody light chain variable subdomain of Fv

Bibliography

Ahmed, A. K., Schaffer, S. W., & Weltaufer, D. B. (1975). Nonezymic reaction of reduced bovine pancreatic ribonuclease by air oxidation and by glutathione oxidoreduction buffers. *J. Biol. Chem.*, 250, 8477-8482.

Alber, T., Dao-pin, S., Nye, J. A., Muchmore, D. C., & Matthews, B. W. (1987). Temperature-sensitive mutations of bacteriophage T4 lysozyme occur at sites with low mobility and low solvent accessibility in the folded protein.
Biochemistry, 26, 3754-3758.

Allen, B., & Luli, G. W. (1987). A gradient-feed process for *E. coli* fermentation.
Biopharm. Manuf., 1, 38-41.

Allen, T. (1981). Particle size measurement, 3rd edition.
ISBN 0-412-15410-2, Chapman and Hall.

Alm, R. S., William, R. J. P., & Tiselius, A. (1952). Gradient elution analysis I. A general treatment.
Acta Chemica Scandinavica, 6, 826-836.

Anderson, K. W., Grulke, E., & Gerhardt, P. (1984). Microfiltration culture process for enhanced production of rDNA receptor cells of *E. coli*.
Bio/Technology, 2, 891-896.

Austin, P. (1989). Will dAbs challenge mAbs?
Nature, 341, 484-485.

Baker, T. A., Grossman, A. D., & Gross, C. A. (1984). A gene regulating the heat shock response in *Escherichia coli* also affects proteolysis.
Proc. Natl. Acad. Sci. USA, 81, 6779-6783.

Ball, E. H. (1986). Quantitation of protein by elution of Coomassie brilliant blue R from staned bands after sodium dodecyl sulfate-polyacrylamide del electrophoresis.
Anal. Biochem., 155, 23-27.

Becker, T., Ogez, J. R., & Builder, S. E. (1983). Downstream processing of proteins.
Biotech. Advs., 1, 247-261.

Bell, D. J., Hoare, M., & Dunnill, P. (1983). The formation of protein precipitates and their centrifugal recovery.
Adv. Biochem. Eng. Biotechnol., 26, 1-72.

Benedek, K., Dong, S., & Karger, B. L. (1984). Kinetics of unfolding of proteins on hydrophobic surfaces in reverse-phase liquid chromatography.
Journal of chromatography, 317, 227-243.

Bentham, A. C. (1990). The formation, separation and dewatering of aggregated biological materials. Ph.D. thesis, University College London, U.K.

Bernard, H. U., & Helinski, D. R. (1980). Bacterial plasmid cloning vehicles.
Genet. Eng., 2, 133-167.

Better, M., Chang, C. P., Robinson, R. R., & Horwitz, A. H. (1988). *Escherichia coli* secretion of an active chimeric antibody fragment.
Science, 240, 1041-1043.

Bird, R. E., Hardman, K. D., Jacobson, J. W., Johnson, S., Kaufman, B. M., Lee, S. M., Lee, T., Pope, S. H., Riordan, G. S., & Whitlow, M. (1988). Single-chain antigen-binding protein.
Science, 242, 423-426.

Birnbaum, S., & Bailey, J. E. (1991). Plasmid presence changes the relative levels of many host cell proteins and ribosome components in recombinant *Escherichia coli*.
Biotechnol. Bioeng., 37, 736-745.

Boss, M. A., Kenten, J. H., Wood, C. R., & Emtage, S. J. (1984). Assembly of functional antibodies from immunoglobulin heavy and light chains synthesised in *E.coli*.
Nucl. Acids Res., 12, 3791-3806.

Brems, D. N., Plaisted, S. M., Dougherty Jr, J. J., & Holzman, T. F. (1987). The kinetic of bovine growth hormone folding are consistent with a framework model.
J. Biol. Chem., 262, 2590-2596.

Brown, S. W., Meyer, H. P., & Fiechter, A. (1985). Continuous production of human leukocyte interferon with *E. coli* and continuous cell lysis in a two stage chemostat.
Appl. Microbiol. Biotechnol., 23, 5-9.

Brunner, K. H., & Molerus, O. (1979). Theoretical and experimental investigation of separation efficiency of disc centrifuges.
Ger. Chem. Eng., 2, 228-233.

Brunt, J. V. (1987). Host system pointers.
Bio/Technology, 5, 664.

Brunt, J. V. (1986). Improving human and hybrid monoclonals.
Bio/Technology, 4, 392-393.

Builder, S. E., Belmont, J. R., & Ogez, S. M. (1986). Purification and activity assurance of precipitated heterologous proteins.
U.S. patent 4,620,948.

Burgess, K., & Shaw, M. (1983). Dairy.
in Industrial Enzymology, T. Godfrey and J. Reichelt (eds.).
The Nature Press, New York. 260-265.

Cabilly, S., Riggs, A. D., Pande, H., Shively, J. E., Holmes, W. E., Rey, M., Perry, L. J., Wetzel, R., & Heyneker, H. L. (1984). Generation of antibody activity from immunoglobulin polypeptide chains produced in *Escherichia coli*.
Proc. Natl. Acad. Sci. USA, 81, 3273-3277.

Caulcott, C. A., Lilley, G., Wright, E., Robinson, M., & Yarranton, G. T. (1985). Investigation of the instability of plasmids directing the expression of met-prochymosin in *Escherichia coli*.
J. Gen. Microbiol., 131, 3355-3365.

Cheng, Y. S. E. (1983). Increased cell buoyant densities of protein overproducing E. coli cells.
Biochem. Biophy. R. Commun., 111, 104-111.

Cheng, Y. E., Kwoh, D., Kwoh, T. J., Soltvedt, B. C., & Zipser, D. (1981). Stabilization of a degradable protein by its overexpression in *Escherichia coli*.
Gene, 14, 121-130.

Chisti, J. A., & Moo-Young, M. (1986). Disruption of microbial cells for intracellular products.
Enzyme Microb. Technol., 8, 194-204.

Chothia, C., Novotny, J., Bruccoleri, R., & Karplus, M. (1985). Domain association in immunoglobulin molecules: The packing of variable domains.
J. Mol. Biol., 186, 651-663.

Coakley, W. T., Bater, A. J., & Lloyd, D. (1977). Disruption of micro-organisms.
Adv. Microb. Physiol., 16, 279-241.

Cohen, S. A., Benedek, K., Tapuhi, Y., Ford, J. C., & Karger, B. L. (1985). Conformational effects in the reverse-phase liquid chromatography of ribonuclease A.
Anal. Biochem., 144, 275-284.

Cohen, S. A., Benedek, K. P., Dong, S., Tapuhi, Y., & Karger, B. L. (1984). Multiple peak formation in reverse-phase liquid chromatography of papain.
Anal. Chem., 56, 217-221.

Coll, H., & Searles, C. (1986). Use of density gradients in a disk centrifuge.
Journal of colloid and interface science, 110, 65-72.

Crea, R., Kraszouski, A., Hirose, T., & Itakura, K. (1978). Chemical synthesis of genes for human insulin.
Proc. Natl. Acad. Sci. USA, 75, 5765-5769.

Creighton, T. E. (1990). Protein structure - a practical approach.
ISBN 0-19-963001-1, Oxford University Press.

Davies, D. R., & Metzger, H. (1983). Structural basis of antibody function.
Annu. Rev. Immunol., 1, 87-117.

de la Paz, P., Sutton, B. J., Darsley, M. J., & Rees, A. R. (1986). Modelling of the combining sites of three anti-lysozyme monoclonal antibodies and of the complex between one of the antibodies and its epitope.
EMBO, 5, 415-425.

deBoer, H. A., Comstock, L. J., & Vasser, M. (1983). The *tac* promoter: a functional hybrid derived from the trp and *lac* promoters.
Proc. Natl. Acad. Sci. USA, 80, 21-25.

Dostalek, M., & Häggstrom, M. (1982). A filter fermenter - apparatus and control equipment.
Biotechnol. Bioeng., 24, 2077-2086.

Dunnill, P., & Lilly, M. D. (1975). in Single Cell Protein II. S.R. Tannenbaum and D.I.C. Wang (ed.).
MIT Press, Cambridge MA, U.S.A., 179-207.

Dwivedi, C. P., Imanaka, T., & Aiba, S. (1982). Instability of plasmid-harboring strain of *E. coli* in continuous culture.
Biotechnol. Bioeng., 24, 1465-1468.

Emtage, J. S., Angal, S., Doel, M. T., Harris, T. J. R, Jenkins, B., Lilley, G., & Lowe, P. A. (1983). Synthesis of calf prochymosin (prorennin) in *Escherichia coli.*
Proc. Natl. Acad. Sci. USA, 80, 3671-3675.

Engler, C. R. (1985). in Comprehensive Biotechnology, Moo-Young, M. (ed.).
Pergamon Press, Oxford & N. Y., 2, 305-324

Engler, C. R., & Robinson, C. W. (1981). Disruption of *Candida utilis* cells in high pressure flow devices.
Biotechnol. Bioeng., 23, 765-780.

Engler, C. R., & Robinson, C. W. (1979). New method of measuring cell-wall rupture.
Biotechnol. Bioeng., 21, 1861-1869.

Fahey, R. C., Hunt, J. S., & Windham, G. C. (1977). On the cysteine and cystine content of proteins: Difference between intracellular and extracellular proteins.
J. Mol. Evol., 10, 155-160.

Field, H. (1988). On production of recombinant immunoglobulin variable domains.
D. Phil. thesis. Oxford University, U.K.

Field, H. (1990). Recombinant immunoglobulin variable domain production - feasibility, progress and directions.
Chimica*oggi*, September(1990), 33-36.

Fieschko, J. C. (1989). Fermentation technology using recombinant microorganisms.
Biotechnology, 7b, 118-140.

Fieschko, J., & Ritch, T. (1986). Production of human alpha consensus interferon in recombinant *Escherichia coli.*
Chem. Eng. Commun., 45, 229-240.

Fieschko, J., Ritch, T., Bengston, D., Fenton, D., & Mann, M. (1985). The relationship between cell dry weight concentration and culture turbidity for a recombinant *E. coli* strain producing high levels of human alpha interferon analogue.
Biotechnol. Prog., 1, 205-208.

Fish, N. M., & Hoare, M. (1988). Recovery of protein inclusion bodies.
Biochem. Soc. Trans., 16, 102-104.

Fish, N. M., & Lilly, M. D. (1984). The interactions between fermentation and protein recovery.
Bio/Technology, 2, 623-627.

Fishbein, W. N. (1972). Quantitative densitometry of 1 - 50 ug protein in acrylamide gel slabs with Commassie Blue.
Anal. Biochem., 46, 388-401.

Flamm, E. L. (1991). How FDA approved chymosin: a case history.
Bio/Technology, 9, 349-351.

Foltmann, B. (1970). Prochymosin and chymosin.
Methods Enzymol., 19, 421-436.

Gardiner, S. A. M. (1988). Process design for recombinant protein recovery from inclusion bodies. Ph.D. thesis, University of London, U.K.

Ghelis, C., & Yon, J. (1982). Protein Folding.
Academic Press, New York.

Godwin, D., & Slater, J. H. (1979). The influence of the growth environment on the stability of a drug resistance plasmid in *Escherichia coli* K12.
J. Gen. Microbiol., 111, 201-210.

Goeddel, D. V., Heyneker, H. L., Hozumi, T., Arentzen, R., Itakura, K., Yansura, D. G., Ross, M. J., Miozzari, G., Crea, R., & Seeburg, P. (1979b). Direct expression in *Escherichia coli* of a DNA sequence coding for human growth hormone.
Nature, 281, 544-548.

Goeddel, D. V., Kleid, D. G., Bolivar, F., Heyneker, H. L., Yansura, D. G., Crea, R., Hirose T, Kraszewski A, Itakura, K., & Riggs, A. D. (1979a). Expression in *Echerichia coli* of chemically synthesized genes for human insulin.
Proc. Natl. Acad. Sci. USA, 76, 106-110.

Goeddel, D. V., Yelverton, E., Ullrich, A., Heyneker, H. L., Miozzari, G., Holmes, W., Seeburg, P. H., Dull, T., May, L., Stebbing, N., Gross, M., Familletti, P. C., & Pestla, S. (1980). Human leukocyte interferon produced by *E. coli* is biologically active.
Nature, 287, 411-416.

Goff, S. A., & Goldberg, A. L. (1985). Production of abnormal proteins in *E. coli* stimulates transcription of *lon* and other heat shock genes.
Cell, 41, 587-595.

Gray, P. D., Dunnill, P., & Lilly, M. D. (1972). in Fermentation Technology Today, G.Terui (ed.).
Society of Fermentation Technology, Japan, 347-351.

Gribskov, M., & Burgess, R. R. (1983). Overexpression and purification of the sigma subunit of RNA polymerase.
Gene, 26, 109-118.

Grossman, A. D., Erickson, J. W., & Gross, C. A. (1984). The *htpR* gene product of *E. coli* is a sigma factor for heat-shock promoters.
Cell, 38, 383-390.

Haase-Pettingell, C. A., & King, J. (1988). Formation of aggregates from a thermolabile *in vivo* folding intermediate in P22 tailspike maturation. A model for inclusion body formation.
J. Biol. Chem., 263, 4977-4983.

Hager, D. A., & Burgess, R. R. (1980). Elution of proteins from sodium dodecyl sulfate-polyacrylamide gels, removal of sodium dodecyl sulfate, and renaturation of enzymatic activity: results with sigma subunit of *Escherichia coli* RNA polymerase, wheat germ DNA topoisomerase, and other enzymes.
Anal. Biochem., 109, 76-86.

Hames, B. D., & Rickwood, D. (1987). Gel electrophoresis of proteins - a practical approach.
ISBN 0-904147-22-3, Oxford University Press.

Hashimoto-Gotoh, T., Franklin, F. C. H, Nordheim, A., & Timmis, K. N. (1981). Specific-purpose plasmid cloning vectors; low copy-number, temperature-sensitive, mobilization-deficient pSC101-derived containment vectors.
Gene, 16, 227-235.

Hetherington, P. J., Follow, M., Dunnill, P., & Lilly, M. D. (1971). Release of protein from baker's yeast *Saccharomyces cerevisiae* by disruption in an industrial homogeniser.
Trans. Inst. Chem. Eng., 49, 142-148.

Hoare, M., & Dunnill, P. (1989). Biochemical engineering challenges of purifying useful protein.
Phil. Trans. R. Soc. Lond. B, 324, 497-507.

Hochman, J., Inbar, D., & Givol, D. (1973). An active antibody fragment (Fv) composed of the variable portions of heavy and light chains.
Biochemistry, 12, 1130-1135.

Holland, I. B. (1989). Secretion of *Escherichia coli* haemolysin.
Biochem. Soc. Transact., 17, 323-325.

Holms, W. H. (1986). The central metabolic pathways of *Escherichia coli* relationship between flux and control at a branch point, efficiency of conversion to biomass, and excretion of acetate.
Curr. Top. Cell. Reg., 28, 69-105.

Hopkins, D., Betenbaugh, M. J., & Dhurjati, P. (1987). Effects of dissolved oxygen shock on the stability of recombinant *Escherichia coli* containing plasmid pKN401.
Biotechnol. Bioeng., 29, 85-91.

Howard, G. A., & Martin, A. J. P. (1950). The separation of the C12-C18 fatty acids by reverse-phase partition chromatography.
Biochem. J., 46, 532-538.

Huber, R. (1986). Structural basis for antigen-antibody recognition.
Science, 233, 702-703.

Huston, J. S., Levinson, D., Mudgett-Hunter, M., Tai, M. S., Novotny, J., Margolies, M. N., Ridge, R. J., Bruccoleri, R. E., Haber, E., Crea, R., & Oppermann, H. (1988). Protein engineering of antibody binding sites: recovery of specific activity in an anti-digoxin single-chain Fv analogue produced in *Escherichia coli.*
Proc. Natl. Acad. Sci. USA, 85, 5879-5883.

Hwang, S. O., & Feldberg, R. S. (1990). Effect of inclusion body production on culture turbidity and cell dry weight in growing bacterial cultures.
Biotechnol. Prog., 6, 48-50.

Jones, S. A., & Melling, J. (1984). Persistence of pBR322 - related plasmids in *Escherichia coli* grown in chemostat cultures.
FEMS Microbiol. Lett., 22, 239-243.

Kane, J. F., & Hartley, D. L. (1988). Formation of recombinant protein inclusion bodies in *Escherichia coli.*
TIBTECH, 6, 95-101.

Kassenbrock, C. K., Garcia, P. P., Walter, P., & Kelly, R. B. (1988). Heavy-chain binding protein recognizes aberrant polypeptides translocated *in vitro.*
Nature, 333, 90-93.

Katzenstein, G. E., Vrona, S. A., Wechsler, R. J., Steadman, B. L., Lewis, R. V., & Middaugh, C. R. (1986). Role of conformational changes in the elution of proteins from reversed-phase HPLC columns.
Proc. Natl. Acad. Sci. USA, 83, 4268-4272.

Kawaguchi, Y., Shimizu, N., Wishimori, K., Uozumi, T., & Beppu, T. (1984). Renaturation and activation of calf prochymosin produced in an insoluble form in *Escherichia coli.*
J. Biotechnol., 1, 307-315.

Kaytes, P. S., Theriault, N. Y., Poorman, R. A., Murakami, K., & Tomich, C. C. (1986). High-level expression of human renin in *Escherichia coli.*
J. Biotechnol., 4, 205-218.

Kennedy, J. F., Rivera, Z. S., & White, C. A. (1989). Minireview: The use of HPLC in biotechnology.
J. Biotechnol., 9, 83-106.

Keshavarz, E. (1990). Studies of cell disruption in high pressure homogenisers.
Ph.D. thesis, University of London, U.K.

Klausner, A. (1986). 'Single-chain' antibodies become a reality.
Bio/Technology, 4, 1041-1043.

Klotz, L. C. (1983). Office of technology assessment: Genetic technology.
Ann. N.Y. Acad. Sci., 413, 1-11, Boulder, CO, Westview Press.

Köhler, G., & Milstein C. (1975). Continuous cultures of fused cells secreting antibody of predefined specificity.
Nature, 256, 495-497.

Konstantinov, K., Kishimoto, M., Seki, T., & Yoshida, T. (1990). A balanced DO-stat and its application to the control of acetic acid excretion by recombinant *Escherichia coli.*
Biotechnol. Bioeng., 36, 750-758.

Kula, M.-R. (1985). Recovery operations.
Biotechnology, 2, 727-760.

Lambert, P. W., & Meers, J. L. (1883). The production of industrial enzymes.
Phil. R. Soc. Lond., B, 300, 263-282.

Lang, K., & Schmid, F. X. (1988). Protein-disulphide isomerase and prolyl isomerase act differently and independently as catalysts of protein folding.
Nature, 331, 453-455.

Langley, K. E., Berg, T. F., Strickland, T. W., Fenton, D. M., Boone, T. C., & Wypych, J. (1987). Recombinant-DNA-derived bovine growth hormone from *Escherichia coli*: 1. Demonstration that the hormone is expressed in reduced form, and isolation of the hormone in oxidized, native form.
Eur. J. Biochem., 163, 313-321.

Lewis, R. V., Fallon, A., Stein, S., Gibson, K. D., & Udenfriend, S. (1980). Support for reverse-phase high-performance liquid chromatography of large proteins.
Anal. Biochem., 104, 153-159.

Lin, E. C. (1976). Glycerol dissimilation and its regulation in bacteria.
Annu. Rev. Microbiol., 30, 535-578.

Liu, A. Y., Robinson, R. R., Hellström, K. E., Murray, E. D., Chang, C. P., & Hellström, I. (1987). Chimeric mouse-human IgG1 antibody that can mediate lysis of cancer cells.
Proc. Natl. Acad. Sci. USA, 84, 3439-3443.

Lowe, P. J., Angal, S., Marston, F. A. O, & Schoemaker, J. A. (1984). A process for the production of a protein.
U.K. patent application, GB 2, 138004A.

Luli, G. W., & Strohl, W. R. (1990). Comparison of growth, acetate production, and acetate inhibition of *Escherichia coli* strains in batch and fed-batch fermentation.
Appl. Environ. Microbiol., 56, 1004-1011.

Mannweiler, K. (1989). The recovery of biological particles in high speed continuous centrifuges with special reference to feed-zone break-up effects.
Ph.D. thesis, University College London, U.K.

Marston, F. A. O. (1986). The purification of eukaryotic polypeptides synthesized in *Escherichia coli.*
Biochem. J., 240, 1-12.

Marston, F. A. O, Lowe, P. A., Doel, M. T., Schoemaker, J. M., White, S., & Angal, S. (1984). Purification of calf prochymosin (prorennin) synthesized in *Escherichia coli.*
Bio/Technology, 2, 800-804.

Meacock, P. A., & Cohen, S. N. (1980). Partitioning of bacterial plasmids during cell division: a cis-acting locus that accomplishes stable plasmid inheritance.
Cell, 20, 529-542.

Meek, J. L. (1980). Prediction of peptide retention times in high-pressure liquid chromatography on the basis of amino acid composition.
Proc. Natl. Acad. Sci. USA, 77, 1632-1636.

Meyer, H. P., Kuhn, H. J., Brown, S. W., & Fiechter, A. (1984). Production of human leukocyte interferon by *E. coli.* in Proceedings of the Third European Congress on Biotechnology, 1,
Verlag chemie GmbH, Weinheim, Federal republic of Germany, 499-505.

Middelberg, A. P. J, O'Neill, B. K., & Bogle, D. L. (1991). A novel technique for the measurement of disruption in high-pressure homogenisation: studies on *E. coli* containing recombinant inclusion bodies.
Biotechnol. Bioeng., 38, 363-370.

Milburn, P., Bonnerjea, J., Hoare, M., & Dunnill, P. (1990). Selective flocculation of nucleic acids and colloidal particles from a yeast cell homogenate by PEI, and its scale up.
Enzyme Micro. Technol., 12, 527-532.

Miller, J. H. (1972). Experiments in molecular genetics.
Cold Spring Harbor Laboratory, Cold Spring Harbor, New York.

Mitraki, A., & King, J. (1989). Protein folding intermediates and inclusion body formation.
Bio/Technology, 7, 690-695.

Morrison, S. L. (1985). Transfectomas provide novel chimeric antibodies.
Science, 229, 1202-1207.

Morrison, S. L., Johnson, M. J., Herzenberg, L. A., & Oi, V. T. (1984). Chimeric human antibody molecules: Mouse antigen-binding domains with human constant region domains.
Proc. Natl. Acad. Sci. USA, 81, 6851-6855.

Murooka, Y., & Mitani, I. (1985). Efficient expression of a promoter-controlled gene: Tandem promoters of lambda P_R and P_L functional in enteric bacteria.
J. Biotechnol., 2, 303-316.

Muth, W. L. (1984). Presented at American Chemical Society Meeting Philadelphia, 26-31 August.

Nagata, N., Herouvis, K. J., Dziewulski, D. M., & Belfort, G. (1989). Cross-flow membrane microfiltration of a bacterial fermentation broth.
Biotechnol. Bioeng., 34, 447-466.

Neuberger, M. S., Williams, G. T., Mitchell, E. B., Jouhal, S. S., Flanagan, J. G., & Rabbitts, T. H. (1985). A hapten-specific chimaeric IgE antibody with human physiological effector function.
Nature, 314, 268-270.

Neuberger, M. S., Williams, G. T., & Fox, R. O. (1984). Recombinant antibodies possessing novel effector functions.
Nature, 312, 604-608.

Nugent, M. E., Primrose, S. B., & Tacon, W. C. A. (1983). The stability of recombinant DNA.
Dev. Ind. Microbiol., 24, 271-285.

Olbrich, R. (1989). The characterisation and recovery of protein inclusion bodies from recombinant Escherichia coli.
Ph.D. thesis, University College London, U.K.

Patzer, E. J., Nakamura, G. R., Hershberg, R. D., Gregory, T. J., Crowley, C., Levinson, A. D., & Eichberg, J.W. (1986). Cell culture derived recombinant HBsAG is highly immunogenic and protects chimpanzees from infection with hepatitis B virus.
Bio/Technology, 4, 630-636.

Paul, D., Van Frank, R. M., Muth, W. L., Ross, J. W., & Williams, D. C. (1983). Immunocytochemical demonstration of human proinsulin chimeric polypeptide within cytoplasmic inclusion bodies of *Escherichia coli.*
European journal of cell biology, 31, 171-174.

Pearson, J. D., Lin, N. T., & Regniet, F. E. (1982). The importance of silica type for reverse-phase protein separations.
Anal. Biochem., 124, 217-230.

Pelham, H. (1988). Coming in from the cold.
Nature, 332, 776-777.

Piatak, M., Lane, J. A., Laird, W., Bjorn, M. J., Wang, A., & Williams, M. (1988). Expression of soluble and fully functional ricin A chain in *Escherichia coli* is temperature-sensitive.
J. Biol. Chem., 263, 4837-4843.

Pierce, J., & Gutteridge, S. (1985). Large-scale preparation of ribulosebisphosphate carboxylase from a recombinant system in *Escherichia coli* characterized by extreme plasmid instability.
Appl. Environ. Microbiol., 49, 1094-1100.

Pirt, S. J. (1975). Principles of microbe and cell cultivation 1st ed.
Blackwell.

Plückthun, A. (1991). Antibody engineering: advances from the use of *Escherichia coli* expression systems.
Bio/Technology, 9, 545-551.

Redfield, C., & Dobson, C. M. (1988). Sequential HNMR assignments and secondary structure of hen egg white lysozyme in solution.
Biochemistry, 27, 122-136.

Rees, A. R., & de la Paz, P. (1986). Investigating antibody specificity using computer graphics and protein engineering.
TIBS, 11, 144-148.

Robbins, P. F., Rosen E M, Haba, S., & Nisonoff, A. (1986). Relationship of V(H) and V(L) genes encolding three idiotypic families of anti-*p*-azobenzenearsonate antibodies.
Proc. Natl. Acad. Sci. USA, 83, 1050-1054.

Roberts, S., & Rees, A. R. (1986). The cloning and expression of an anti-peptide antibody: a system for rapid analysis of the binding properties of engineered antibodies.
Protein Engineering, 1, 59-65.

Rossmann, M. G., Arnold, E., Erickson, J. W., Frankenberger, E. A., Griffith, J. P., Hecht, H. J., Johnson, J. E., Kamer, G., Luo, M., Mosser, A. G., Rueckert, R. R., Sherry, B., & Vriend, G. (1985). Structure of a human common cold virus and functional relationship to other picornaviruses.
Nature, 317, 145-153.

Ryu, D. D. Y, & Siegel, R. (1986). Scale-up of fermentation processes using recombinant microorganism.
Ann. N. Y. Acad. Sci., 469, 73-82.

Salt, D. E., & Turner, M. (1990). Quantitative assay for unfolded prochymosin using reverse-phase HPLC. in preparation.

Sauer, T., Robinson, C. W., & Glick, B. R. (1989). Disruption of native and recombinant *Escherichia coli* in a high-pressure homogenizer.
Biotechnol. Bioeng., 33, 1330-1342.

Scarlett, B., Rippon, M., & Lloyd, P. J. (1967). Particle Size Analysis. Proceedings of Conference held at Loughborough University of Technology, 14-26 September 1966. Society for analytical chemistry, London_, 242.

Scawen, M. D., Atkinson, A., & Darbyshire, J. (1980). in Applied Protein Biochemistry. Grant, R. A. (ed.)
Applied Science Publishers, London, 281-235.

Schein, C. H. (1989). Production of soluble recombinant proteins in bacteria.
Bio/Technology, 7, 1141-1146.

Schein, C. H., & Noteborn, M. H. M. (1988). Formation of soluble recombinant proteins in *Escherichia coli* is favored by lower growth temperature.
Bio/Technology, 6, 291-294.

Schoemaker, J. M., Brasnett, A. H., & Marston, F. A. O. (1985). Examination of calf prochymosin accumulation in *Escherichia coli*: disulphide linkages are a structural component of prochymosin-containing inclusion bodies.
EMBO, 4, 775-780.

Schoner, R. G., Ellis, L. F., & Schoner, B. E. (1985). Isolation and purification of protein granules from *Escherichia coli* cells overproducing bovine growth hormone.
Bio/Technology, 3, 151-154.

Scott, M. G. (1985). Monoclonal antibodies - approaching adolescence in diagnostic immunoassays.
TIBTECH, 3, 170-175.

Sen, J., & Beychok, S. (1986). Proteolytic dissection of a hapten binding site.
Proteins, 1, 256-262.

Seo, J. H., & Bailey, J. E. (1985). Effects of recombinant plasmid content on growth properties and cloned gene product formation in *Escherichia coli*.
Biotechnol. Bioeng., 27, 1668-1674.

Sharon, J., & Givol, D. (1976). Preparation of Fv fragment from the mouse myeloma XRPC-25 immunoglobulin possessing anti-dinitrophenyl activity.
Biochemistry, 15, 1591-1594.

Skerra, A., & Plückthun, A. (1988). Assembly of a functional immunoglobulin Fv fragment in *Escherichia coli*.
Science, 240, 1038-1043.

Skvortsov, L. S. (1984). A study of separation in the settling space of a centrifugal cleaner-separator.
Theoretical Foundations of Chemical Engineering, 3, 226-233.

Smith, R. A., Duncan M J, & Moir, D. T. (1985). Heterologous protein secretion from yeast.
Science, 229, 1219-1224.

Smith-Gill, S. J., Mainhart, C., Lavoie, T. B., Feldman, R. J., Drohan, W., & Brooks, B. R. (1987). A three-dimentional model of an anti-lysozyme antibody.
J. Mol. Biol., 194, 713-724.

Sokolov, V. I., & and Dolzhanova, G. A. (1972). Influence of the angular velocity of centrifuge and separator rotors on separation efficiency.
Theoretical Foundations of Chemical Engineering, 45, 1063-1066.

Staehelin, T., Hobbs, D. S., Kung, H.-F., & Pestka, S. (1981). Purification of recombinant human leukocyte interferon (IFLrA) with monoclonal antibodies.
Methods Enzymol., 78, 505-512.

Svarovsky, L. (1977). Solid-liquid separation.
Chem. Eng. Series. Butterworth, London.

Szoka, P. R., Schreiber, A. B., Chan, H., & Murthy, J. (1986). A general method for retrieving the components of a genetically engineered fusion protein.
DNA, 5, 11-20.

Tacon, W. C. A, Bonass, W. A., Jenkins, B., & Emtage, J. S. (1983). Expression plasmid vectors containing *Escherichia coli* tryptophan promoter transcriptional units lacking the attenuator.
Gene, 23, 255-265.

Tartaglia, J., & Paoletti, E. (1988). Recombinant vaccinia virus vaccines.
TIBTECH, 6, 43-46.

Taub, R., Gould, R. J., Garsky, V. M., Ciccarone, T. M., Hoxie, J., Friedman, P. A., & Shattil, S. J. (1989). A monoclonal antibody against the platelet fibrinogen receptor contains a sequence that mimics a receptor recognition domain in fibrinogen.
J. Biol. Chem., 264, 259-265.

Taylor, G., Hoare, M., Gray, D. R., & Marston, F. A. O. (1986). Size and density of protein inclusion bodies.
Bio/Technology, 4, 553-557.

Thatcher, D. R. (1990). Recovery of theraputic proteins from inclusion bodies: problems and process strategies.
Biochem. Soc. Trans., 18, 234-235.

Thomas, J. C., Middelberg, A. P. J, Hamel, J. F., & Snoswell, M. A. (1991). High-resolusion particle size analysis in biotechnology process control.
Biotechnol. Prog., 7, 377-379.

Tsuji, T., Nakagawa, N., Sugimoto, N., & Fukuhara, K. (1987). Characterisation of disulfide bonds in recombinant proteins: reduced human interleukin 2 in inclusion bodies and its oxidative refolding.
Gene, 26, 3129-3134.

Valuenzuela, P., Coit, D., and Kuo, C.H. (1985). Synthesis and assembly in yeast of hepatitis B surface antigen particles containing the polyalbumin receptor.
Bio/Technology, 3, 317-320.

van den Berg, J. A., van der Laken, K. J., van Ooyen, A. J. J, Renniers, T. C. H M, Rietveld, K., Schaap, A., Brake, A. J., Bishop, R. J., Schultz, K., Moyer, D., & Richman, M. J., R. (1990). *Kluyveromyces* as a host for heterologous gene expression: expression and secretion of prochymosin.
Bio/Technology, 8, 135-139.

van Kimmenade, A., Bond, M. W., Schumacher, J. H., Laquoi, C., & Kastelein, R. A. (1988). Expression, renaturation and purification of recombinant human interleukin 4 from *Escherichia coli*.
Eur. J. Biochem., 173, 109-114.

Vitetta, E. S., Fulton, R. J., May, R. D., Till, M., & Uhr, J. W. (1987). Redesigning nature's poisons to create anti-tumor reagents.
Science, 238, 1098-1104.

Ward, E. S., Güssow, D., Griffiths, A. D., Jones, P. T., & Winter, G. (1989). Binding activities of a repertoire of single immunoglobulin variable domains secreted from *Escherichia coli*.
Nature, 341, 544-546.

Ward, M., Wilson, L. J., Kodama, K. H., Rey, M. W., & Berka, R. M. (1990). Improved production of chymosin in *Aspergillus* by expression as a glucoamylase-chymosin fusion.
Bio/Technology, 8, 435-440.

Waxman, L., & Goldberg, A. L. (1982). Protease *La* from *Escherichia coli* hydrolyzes ATP and proteins in a linked fashion.
Proc. Natl. Acad. Sci. USA, 79, 4883-4887.

Weiner, B. (1984). Particle sizing using photon corelation spectroscopy.
ISBN 0-471-87-571-6, John Wiley and sons.

Weir, M. P., & Sparks, J. (1987). Purification and renaturation of recombinant human interleukin-2.
Biochem. J., 245, 85-91.

Weis, W., Brown, J. H., Cusack, S., Paulson, J. C., Skehel, J. J., & Wiley, D. C. (1988). Structure of the influenza virus haemagglutinin complexed with its receptor, sialic acid.
Nature, 333, 426-431.

Wilkinson, D. L., & Harrison, R. G. (1991). Predicting the solubility of recombinant proteins in *Escherichia coli*.
Bio/Technology, 9, 443-448.

Williams, G. (1988). Novel antibody reagents: production and potential.
TIBTECH, 6, 36-42.

Williams, W. V., Moss, D. A., Kieber-Emmons, T., Cohen, J. A., Myers, J. N., Weiner, D. B., & Greene, M. I. (1989). Development of biologically active peptides based on antibody structure.
Proc. Natl. Acad. Sci. USA, 86, 5537-5541.

Willus, C. A., & Fitch, B. (1973). Flow patterns in a disc centrifuge.
Chemical Engineering Progress, 9, 73-74.

Wright, E. M., Humphreys, G. O., & Yarranton, G. T. (1986). Dual-origin plasmids containing an amplifiable ColE1 *ori*; temperature-controlled expression of cloned genes.
Gene, 49, 311-321.

Yarranton, G. T., Wright, E., Robinson, M. K., & Humphreys, G. O. (1984). Dual-origin plasmid vectors whose origin of replication is controlled by the coliphage lambda promoter P_L.
Gene, 28, 293-300.

Zabriskie, D. W., & Arcuri, E. J. (1986). Factors influencing productivity of fermentations employing recombinant microorganisms.
Enzyme Microb. Technol., 8, 706-717.

Zastrow, J. (1976). Theoretical calculation of the performance of disc centrifuges.
International Chemical Engineering, 3, 515-518.

Zemel-Dreasen, O., & Zamir, A. (1984). Secretion and processing of an immunoglobulin light chain in *Escherichia coli*.
Gene, 27, 315-322.